Fire protection of surface coatings

by

Jennifer Rhodes

A thesis submitted in partial fulfilment for the requirements of the degree of
Doctor of Philosophy
at the
University of Central Lancashire
in collaboration with
Integra Coatings Ltd

February 2012

ABSTRACT

Multilayer paint is a significant fire hazard particularly concerning rapid spread of flame, smoke and toxic species production. Fire protective coatings are often employed to protect this unpredictably flammable substrate from ignition (for example resulting from arson attacks in the communal areas of multi-occupancy buildings). Literature shows a gap in the understanding of this problem, a lack of suitable flammability tests, and methods for screening new fire protective coatings required to address this problem.

This work investigates the factors affecting coating performance and develops screening test methods to estimate protection performance in standard fire tests. The dependence of these tests has been investigated with regard to substrate, coating thickness, composition of coating, thermal conductivity and rheological properties, to inform the development of modified coating formulations with enhanced fire safety.

Coating materials have been investigated using thermogravimetric analysis (TGA) in both air and inert atmospheres and their burning behaviour using the cone calorimeter (ISO 5660). Novel screening test methods also include a test adapted from BS EN 367 for measurement of thermal conductivity, a thermocouple embedded in cone samples to assess the temperature profile at the substrate-coating interface and BS 476: Part 6 (adapted) as a scaled down version of the standard fire test. The chemical changes occurring during burning of current coatings formulations were investigated using CHN analysis, pyrolysis gas chromatography coupled with mass spectrometry (pyGC-MS), inductively coupled plasma coupled with mass spectrometry (ICP-MS), diamond attenuated total reflectance coupled with fourier transform infra-red (dATR-FTIR), nuclear magnetic resonance (NMR) and scanning electron microscopy coupled with electron dispersive X-ray analysis (SEM-EDAX) to inform the development of novel formulations.

Generally, intumescent formulations tend to exhibit lower fire propagation indexes when assessed in the BS 476: Part 6, longer time to ignition and lower peak heat release rates in the cone calorimeter, as well as reduced thermal conductivity recorded in the BS EN 367. Results report mixed performance, suggesting that it is not only char residue formation that ensures a pass in the standard fire tests. Rheological properties of the coatings are crucial to performance, with softening temperature and reduction in viscosity coinciding with gas release of the fire retardant additive. Each screening test method assesses one particular aspect of flammability, they are dependent on the controlled conditions under which results are collected, and the limited correlation observed with the performance in the standard fire tests, do not conclusively predict performance in a real fire situation.

TABLE OF CONTENTS

INDEX OF FIGURES

INDEX OF TABLES

INDEX OF EQUATIONS

ACKNOWLEDGMENTS

ABBREVIATIONS

Analyses:

CHN	Carbon, Hydrogen and Nitrogen analysis
dATR-FTIR	Diamond Attenuated Total Reflectance – Fourier Transform Infra-Red
DTA	Differential Thermal Analysis
ICP-MS	Inductively Coupled Plasma - Mass Spectrometry
NMR	Nuclear Magnetic Resonance
pyGC-MS	Pyrolysis - Gas Chromatography - Mass Spectrometry
SBI	Single burning item
SEM-EDAX	Scanning Electron Microscope – Electron Dispersive X-Ray analysis
TGA	Thermogravimetric analysis

Materials:

APP	Ammonium polyphosphate
ATH	Aluminium hydroxide
CO	Carbon monoxide
CO_2	Carbon dioxide
DAP	Diammonium phosphate
M	Melamine
N_2	Nitrogen
NC	Nitrocellulose
PA6	Polyamide 6
PER or P	Pentaerythritol
PMMA	Poly(methyl methacrylate)
PVA	Poly vinyl alcohol
PVAc	Poly vinyl acetate
PVC	Poly vinyl chloride
PVDC	Poly vinylidene chloride
U	Urea
V	Vinyl resin

Vs	Dulux vinyl silk emulsion
W	Wickes vinyl emulsion
WBB	Warrington blue board

Terms:

FIGRA	Fire Index Growth Rate
HRR	Heat Release Rate
RRFSO	Regulatory Reform Fire Safety Order
THR	Total Heat Release
VOC	Volatile organic compound

Units:

A	Area
E	Energy
F	Force
G'	Storage modulus
G''	Loss modulus
h	Gap measurement
l	Fire propagation index
kW	Kilowatts
S_i, S_2, S_3	Sub-indices
S	Shear
T	Absolute temperature
v	Velocity
δ	Phase angle
τ	Shear stress
γ	Shear deformation
η*	Complex viscosity

TERMINOLOGY

For the purpose of this thesis the term 'paint' will be used to describe a non-fire retardant system or a coating of unknown origin and composition. The term 'coating' will be used to describe an outer layer having fire retardant properties thus reducing the surface flammability. The term substrate refers to the base material to which the paint is applied.

CHAPTER 1. INTRODUCTION

1. The problem – Fire Hazard of Multilayer Paint

Flammability of materials should be considered and precautions incorporated into building and construction products in order to maintain fire safety. There is much focus and research in this area in order to reduce the number of lives lost through the spread of fire. This may be achieved by reducing the heat release, controlling ignitability or the extent of flame spread across the surface of these materials. All of these factors allow a greater time for escape before the fire takes hold and as a result, more lives will be saved.

Protection is often required for cellulosic materials, such as textiles, plastics and wood to prevent ignition, whereas protection is required for steel structures to prevent catastrophic collapse in the event of fire. Steel is vulnerable under fire conditions, not due to flammability but as structure and rigidity become compromised under heat and pressure, as experienced during the collapse of the World Trade Centre.[1]

Certain buildings, particularly those open to public access, require regular redecoration as part of scheduled maintenance and to cover graffiti, dirt and other markings. In particular, access routes within multiple-occupancy social housing, corridors in schools, stairwells and other enclosed walkways, normally regarded as "safe refuge areas" may consequently have an excessive build-up of paint.

Paints are used widely for both decorative and protective purposes; they all contain combustible material that will burn to a greater or lesser extent depending on their type.[2] In many situations this is a fire risk, in particular in the communal and access areas and corridors in local authority buildings such as schools, hospitals, prisons and multi-occupancy buildings. These communal areas are also prime targets for arson attacks or vandalistic fires. In 2007, 47 % of all deliberately started fires were in multi-occupancy buildings,[3] and this figure has remained stable for several years. For this reason it is important to understand the way in which painted surfaces may contribute to fire hazard.[4]

While a single layer of paint poses almost no hazard, build-up of multiple layers over a number of years can present significant hazards. The specific hazards are summarised:

1. Paint build-up can cause rapid flame spread, taking a source of ignition to an otherwise flame-free area.

2. Sufficient paint build-up could result in unpredicted ignition of a supposedly non-flammable substrate.

3. In enclosed areas, smoke, and possible toxic gas build-up may hinder escape, potentially leaving people trapped when escape should have been possible as well as preventing access to emergency service teams.

The problem is exacerbated by the uncertainty surrounding the multilayer build-up. If any of the surfaces are not adequately cleaned prior to re-decoration, blistering will often occur and result in greater ease of ignition and flame spread; different binders and finishes have different ageing and flammability characteristics; and flaking paint has a higher risk of ignition than that properly adhered onto a normally thermally conductive substrate. As normal building upkeep and maintenance means redecoration occurs regularly, the issue of multilayer paint flammability must be considered and methods of protection devised to reduce loss.

There is a well documented history of the fire risk in communal living and local authority buildings such as schools, hospitals and flats. These are outlined in section 1.12. The first UK fire regulation followed the Great Fire of London, 1666, after which the King decreed that all buildings be made from non-combustible materials.[5] Regulations have progressively tightened, and for buildings in the UK are focused around Approved Document B[6] and the Regulatory Reform (Fire Safety) Order (RRFSO) 2005[7] (discussed later in section 1.14.). The aim of these regulations is to increase fire safety and the time allowed for escape in the case of fire.

Building occupiers wishing to demonstrate that their building is adequately maintained are likely to redecorate every few years. Generally paint is applied over the top of existing paint layers, even though these may be severely weathered or deteriorated. Over-coating is favoured over stripping current paint layers, softening processes (by heat or solvents) are costly, time-consuming and a risk to personal health (if fumes are inhaled by labourers or occupants where no extraction of affected areas is possible). There is an increasing fire risk as more layers of paint are added. The build-up of dirt between layers will adversely affect the adhesion of subsequent layers and promote delamination (de-adherence of the top layers from underlying layers), where, detached from the substrate (which acts as a heat sink) they will be more readily ignitable.

Figure 1 Images of communal areas after an arson attack

It is unfortunate that the area most likely to cause risk due to the build-up of paint layers, such as communal and access areas (in schools, hospitals, blocks of flats and prisons),[8] are also more likely to fall victim to arson attacks and would also be the main egress routes in case of a fire, examples are shown in Figure 1.

The aim of this thesis is to provide the understanding necessary for the development and formulation of a coating to protect paint layers, in order to pass standard fire tests. Various parameters will be investigated to establish the effect on burning behaviour. An understanding of the fire tests, and their limitations, will aid the development of screening test methods which will enhance determination of the optimum formulation to pass standard fire tests.

1.1. Basic paint components

The problem is made worse by the wide variety of surface coverings, all of which are classified as 'paints', varying considerably in type and loading.[9] A generic paint formulation will include a solvent, resin and pigments. The main components of formulation and their affect on burning behaviour are discussed in section 1.5.3.The solvent is the liquid portion of the paint that suspends the solid pigments and resins. The solvent allows the paint to be spread from the brush to the wall and then evaporates to leave the paint film on the substrate as shown in Figure 2.

Solvent

'Volatile Vehicle'
Resin and solvent

Substrate
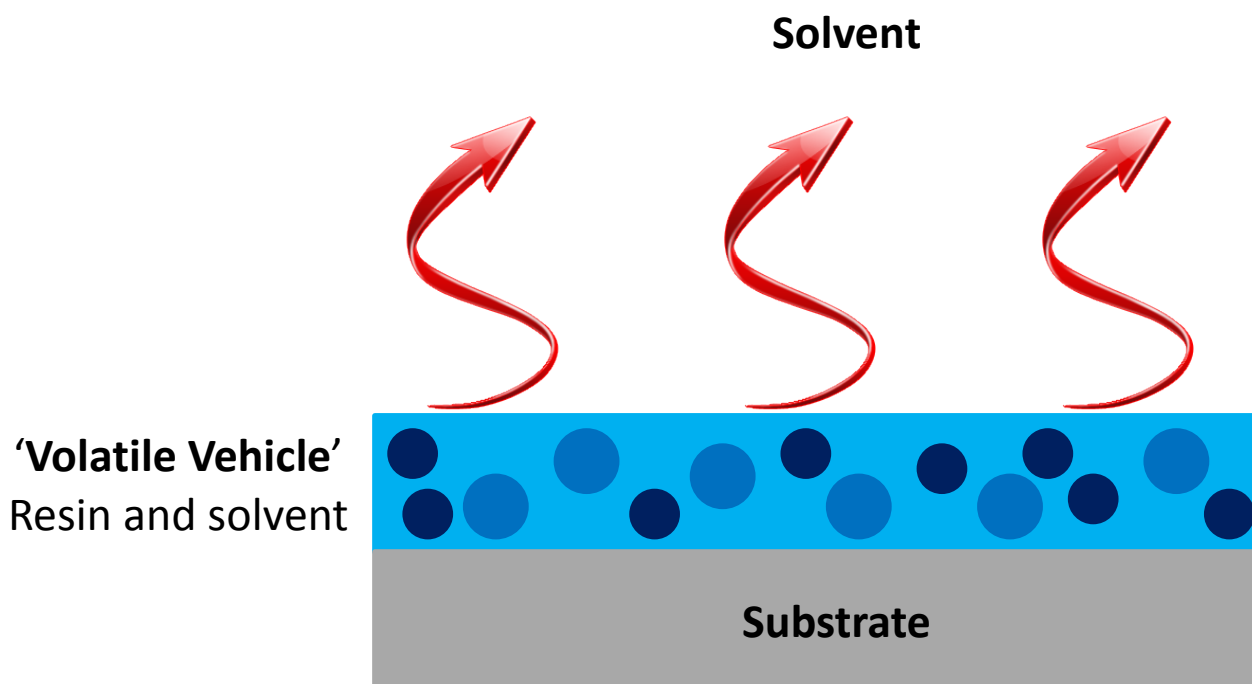
Figure 2 Schematic diagram of paint components

Water is a common solvent used for latex paints however mineral spirits can also be used for oil based alkyd paints. Once "dried" the polymer or "resin" makes up the combustible fraction of the paint film. These polymers are carefully selected during manufacture to optimise their functionality depending on the application of the system. Characteristics such as weatherability, gloss, toughness and flow can be optimised. If a multitude of properties are needed that are not available from one polymer system then a combination of polymers or 'copolymer' can be used. Additional functional groups or atoms can be added onto the bulk polymer to further optimise final properties. The chemical structure and uses of these different resins are described later in this thesis (section 1.5.3.). Resins are the film forming component of the paint, they allow paint to adhere to substrates. The combination of the resin and solvent is often referred to as the paint's 'volatile vehicle' as it allows the paint to be successfully applied and spread onto the substrate. Rheological properties of resin systems are therefore crucial, imparting flow properties, stability, softening temperature and viscosity.

Most pigments are not flammable and so will retard combustion; unless systems incorporating organic pigments and fillers are utilised which will burn. Conventional white paint reflects about 30 % of the radiated energy from fire and most coloured paints reflect less.[10] However, additives such as aluminium flake pigments[11] or other pigments optimised for IR reflectance have reflectance in excess of 80 %. Pigments include: talc, clay, chalk and silica. Additives can be incorporated into the formulation to optimise performance, however, the type and extent to which they are used will depend on the final application of the product. Additives include

extenders, fillers, wetting agents, thickeners and de-foamers. Varnishes and lacquers are often used on top of the paint layer to give a high sheen finish or properties such as anti-graffiti and good wear resistance, but may be more flammable.[12] Some of the basic ingredients mentioned above have fire retardant properties and flame inhibiting action. For example, mineral fillers are often incorporated and have an inherent fire retardant nature; one example is Gypsum.

Paints are mixed to ensure all of the components are adequately incorporated. This is done by high speed, high shear mixing. The samples formulated and investigated during this research were mixed using a Dispermat high shear mixer. These machines consist of a mixing blade attached to a rotary motor which produce a vortex within the liquid portion of the sample (the solvent and resin). This vortex continually moves the mixture enabling incorporation of the solid portion (fire retardant additives). The entire sample is involved in the mixing process preventing sedimentation of any additives and as coating samples are often shear thinning (experience a reduction in viscosity when subjected to shear) mixing is rapid and dissolution of additives complete.

1.2. Multi-coat systems

Paint systems are rarely applied in one coat. Even for decoration purposes at least two coats are required to provide even coverage. In the majority of cases a series of several layers is applied in order to give the overall system a greater range of properties and improved effect.

In the case of commercial coatings the initial layer is a primer (basecoat) which prepares the substrate for the subsequent application of further coatings. The primer may be an off white colour as it will not be seen when additional coatings are applied. An intermediate layer may be applied next, pigmented to the required colour; this layer is the bulk of the coating system and should impart the majority of the required action. The upper layer (top coat) will either be pigmented to the required colour or transparent. This coating will impart the required finish such as gloss, abrasion resistance, anti-graffiti etc.

Manufacturers must compromise between a paint system made up of numerous layers which would be time consuming to apply (therefore labour expensive) and a system with reduced performance when applied as a single layer thin film coating.

1.3. Fire retardant coating systems

There are several options available to the occupier or building owner when considering redecoration of interior walls. The flow chart in Figure 3 outlines the decision making process that should be considered to ensure the highest level of fire safety of such walls is maintained. If stripping and methods of encapsulation (covering the substrate in a non-combustible

material; these methods might include cladding or rendering) are not appropriate in a given circumstance then a fire retardant system might be preferred that upgrades the fire rating of the surface. Fire ratings are further discussed in section 1.9.4.1., Class 0 is the least flammable.
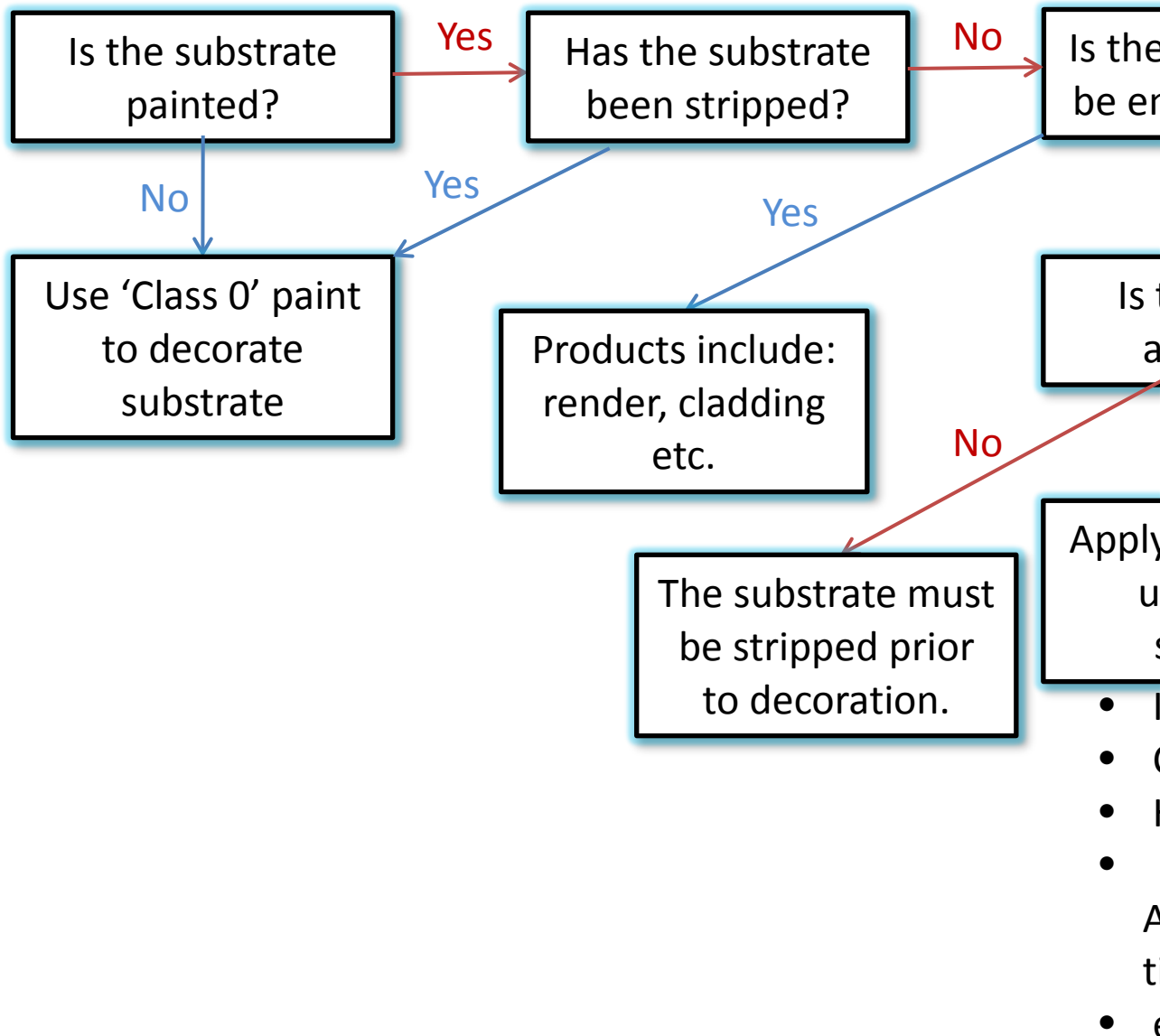
Figure 3 Selection procedure for fire safe redecoration of internal, previously painted surfaces

Cost and health implications of stripping methods, such as heat stripping and chemical solvent stripping, mean that removal of previous paint layers is often undertaken as a last resort. Both stripping methods produce large enough quantities of toxic vapours to require isolation and ventilation systems to protect labourers and occupants during this process. Hazard is increased as the composition of the paint layers is rarely fully understood, in some cases paint build-up may be 20 layers thick with the base layers being old and maybe based on less conventional components.[13] In these situations it is often preferable to use an 'upgrading system' to cover the walls as the other alternative could involve demolition and re-building. These types of

products aim to 'upgrade' the existing coating of high fire and flame spread risk (class 4) to a low risk fire retardant level (class 1 or class 0).

To reduce the fire hazard and enhance performance a protective coating may be applied.[14] Often a relatively thin film, of only a few microns thickness, is required to protect a large amount of fuel (a polymer, fabric or multilayer paint). In these situations films must be highly tailored to suit their end use application. Intumescents are preferred for steel substrates, while halogenated or char promoting additives may be used for textile and cellulosic materials. Intumescents are used due to the rapid and extreme expansion (sometimes up to 200 times) which reduces the thermal conductivity of the coating, preventing heat transmission to the flammable material. Other fire retardant systems are often ruled out due to the high loadings of fire retardant additives required to achieve the required level of fire protection for a sustained period of time, allowing protection of the bulk material from pyrolysis. High loadings cause loss of functionality of coatings, compromising properties such as flow, stability and finish.

Upgrading systems are often the chosen method of protection in the case of multilayer paint systems. The specific level of protection required and the nature of the substrate will determine which fire retardant mechanism would be best suited for each case. The various fire retardant additives and their mechanisms are discussed in section 1.15. Coatings can be applied in many ways such as by brush or roller, spray coating or dipping. These coatings can then be: dried by evaporation; cured by the addition or formation of another substance, acting as an agent to harden the coating by cross-linking; or cured by baking in an oven (more common for the application of intumescent coatings onto steel substrates). Factors affecting coating performance include: adhesion, substrate, thermal conductivity etc. All of which are outlined in section 1.11.

Specialist companies have formulated fire protection coatings which reduce the fire hazard of multilayer paint surfaces. These act in several ways.

By cooling – during decomposition of polymers water molecules may be liberated therefore cooling the system and preventing further pyrolysis of the substrate. Endothermic reactions act as a 'heat sink' to absorb extra heat within the reaction system thus delaying the time to ignition.

By diluting – inert gases may be emitted during the decomposition stages, reducing the concentration of flammable gases available for ignition.

By forming a protective layer – decomposition gives rise to the formation of a protective char layer, this coats the substrate and prevents further degradation of the substrate as well as reducing the transfer of heat and combustible gases through the layer, so inhibiting flame.

Conventionally coatings were formulated by physically blending flame retardants into the other coating components. This was not ideal as the high concentration of flame retardants needed to achieve the required level of protection leads to difficulty in curing and promotes degradation unless a lower loading can be used without compromising efficiency. Another more costly solution is the chemical bonding of flame retardant molecules to the backbone of the polymer. Reactive-type flame retardants have many advantages over their additive counterparts, reduced leaching of additives being the primary advantage. By promoting condensed phase mechanisms - particularly those exhibited by phosphorus and nitrogen containing flame retardants, which decompose at lower temperatures due to unstable bonds - protective char layers are formed during heating which occurs prior to any decomposition of the unburned polymer. Nitrogen containing species decompose producing incombustible gases without toxic smoke which dilute the flammable gases and oxygen in the flame zone. Trapped decomposition gases can form voids within the residual char which reduce thermal conductivity and provide superior barriers against flame and heat. Secondly, extended longevity is expected from reactive-type flame retardants as they will not be released from the polymer matrix during processing, use or ageing. Finally the mechanical properties of the polymer remain unaffected which is an important consideration for some applications.[15]

1.4. Environmental Safety

Coating manufacturers must not only deliver performance but must ensure safety by optimising environmentally friendly products therefore reducing the use of halogens such as chlorinated species which though highly effective fire retardants, form toxic hydrogen chloride species when combusted. The toxicity and hazard rating of the coating must also be as low as possible to meet the growing demand for environmentally friendly and halogen-free systems that yield non-toxic products during combustion.

1.5. Structure of polymers

Polymers may be classified into different groups according to their polymerisation reaction. Addition polymers are formed from monomers, adding to chain ends increasing the chain length without the loss of any atoms. Condensation polymers are formed when two or more molecules react together, with the loss of a smaller molecule (most commonly water). An example of a condensation reaction is shown in Figure 4.
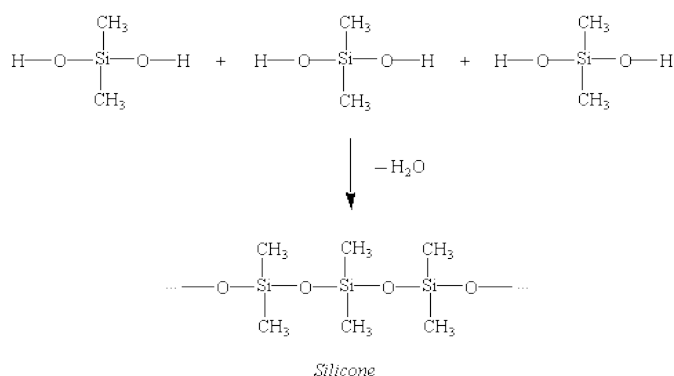
Figure 4 Example of a condensation reaction - polymerisation producing silicone

Polymers may also be classified according to their reaction to heating. Thermoplastic polymers soften and 'melt' during heating but harden when cooled. These are the most widely used polymers for rapid manufacturing as this softening process can be repeated. Thermosets are polymers that harden when formed because of cross-links between the polymer chains forming a 3-dimensional matrix. They cannot be softened again by heating, instead they will decompose.

1.5.1. Polymer decomposition

Heating causes organic polymers to fragment into shorter length chains until monomers are liberated in the form of volatile products and solid residues. This process is able to proceed in both gas and solid phase reactions. The process of polymer decomposition by application of heat is called pyrolysis and is responsible for the breaking down of 10 000 – 100 000 carbon atom chains into volatile species. There are many ways in which the chain can be broken down into smaller sections.

'End-chain scission' describes the liberation of groups from chain ends (also known as 'unzipping') where monomer units are the primary pyrolysis product. In some cases the chain breaks at random points along its length (known as 'random chain scission') producing a mixture of volatile fragments of varying length. The removal of side chain molecules from the polymer backbone is termed 'chain stripping'. Chain stripping leaves double bonds which may cross-link, which often prevents the polymer backbone from undergoing further scission, promoting carbonisation, resulting in char formation.[14] These mechanisms may occur in isolation or a combination may contribute to the overall decomposition reaction.

Properties such as volatile composition, rate of formation and reactivity of the volatiles can provide considerable information about the combustion behaviour of the polymeric material. Thermal stability of the polymer can also be calculated using data such as the temperature dependence of decomposition.

1.5.2. Structural effects on decomposition rate and behaviour

Polymer structure will significantly affect the rate and mechanism of decomposition - some common factors are explained below.[16]

Chain abnormalities, such as branching sites are the most reactive area on an otherwise un-reactive polymer. During thermal decomposition these points are the first to break, initiating a chain reaction of decomposition. Polymers with a large number of these sites will react more rapidly than those with less. Structures with double bonds and oxygen present in the polymer backbone also provide active sites for initiation of chain reactions.

Aromatic ring structures are highly stable and increase the rigidity of the chain when present in the polymer backbone. This increases the melting temperature of the polymer due to a reduction in entropy (disorder) and leads to a reduction in the rate of pyrolysis as the majority of the material is protected by surface layers.

Where the polymer decomposes by end-chain scission, this propagates at the end of polymer chains as the terminating groups are held by one bond only. The more of these end groups the polymer has, the faster the rate of pyrolysis will be, therefore high molecular weight molecules have a reduced pyrolysis rate.[17]

Cross-linking reduces decomposition and pyrolysis rates of polymers as fewer molecules are available at the material surface for pyrolysis. Cross-linking prevents melting as a larger number of bonds must be broken for this to take place, heat and fuel transfer through materials is also reduced.

Chemical bond strength also effects polymer decomposition. The stronger each individual bond and the more common the strong bonds within the polymer, the higher the decomposition temperature. Average bond dissociation energies aid prediction of the temperature at which the bonds will undergo a general breakdown. Knowledge of the bond strength and number of bonds help to explain the required temperature for decomposition and composition of fuel. For example, halogens (chlorine and bromine - Cl and Br) are the most suitable fire retardants for use in the gas phase as they are liberated at similar energies as the breakage of C-C and C-H bonds. Other bonds break as the temperature increases (C-O) however more than one of these bonds (C-C, C-H and C-O) must be broken for volatile fuel to be released.

1.5.3. Decomposition of polymers

Typical decomposition mechanisms of some common paint components are outlined below. Decomposition is greatly affected by many factors and so varies depending on the conditions under which polymer decomposition occurs.

1.5.3.1. Polyacrylics

'Acrylic' resins are polymers and copolymers of methacrylic and acrylic acid esters polymerised by free-radical initiators. The methacrylic monomer structure (Figure 5) combines to form polyacrylics such as Poly(methyl methacrylate) (PMMA) shown in Figure 6.
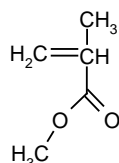
Figure 5 Acrylic monomer structure
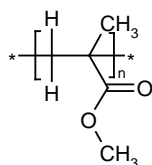
Figure 6 Poly(methyl methacrylate) structure

Acrylics are difficult to hydrolyse, producing good weather resistance [18] and are widely utilised for coating applications due to their outstanding outdoor durability. They are recognised for excellent properties such as toughness, flexibility, resistance to chemical fumes, acids, alkalis and water as well as gloss retention.[19] In the case of coatings these polymers are primarily made in emulsion or solution. One disadvantage of the methacrylates is the poor compatibility with other substances.

Solid PMMA decomposes almost solely to the monomer and displays a very steady burning rate and is widely used as a standard material in fire research. Decomposition temperatures of polyacrylics are greatly affected by the method of polymerization. Free-radical polymerised PMMA decomposes at a lower temperature than anionically produced PMMA, due to the decomposition being initiated only at chain ends due to the lack of double bonds in the latter. At higher temperatures end- and random-chain scission occurs, breaking down the polymer into monomer units.

Conversely PMA decomposes via random chain scission and very few monomer units are yielded. This is because there are no methyl groups to block intra-molecular hydrogen transfer destabilising the radical chain which propagates the decomposition in PMMA.[20]

1.5.3.2. Polyhalogens – vinyl-substituted polymers

The term 'vinyl resin' is usually used for polymers based on vinyl chloride, depicted in Figure 7, which are some of the most widely used polymers alongside polyethylene and polypropylene. Poly vinyl chlorides (PVC) are popular for use in coatings due to their good colour, flexibility, chemical resistance, and quick drying that is not temperature dependant. Drawbacks for vinyl resins include susceptibility to degradation under heat, UV radiation and exposure to oxidising agents which lead to the formation of hydrogen chloride. Stabilisers can be added to improve these qualities, but due to increased environmental pressures, the use of PVC resins has become restricted in coating applications.[19]
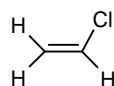
Figure 7 Vinyl chloride structure

Heating induces chain-stripping which evolves hydrogen chloride gas as the chlorine is stripped from the polymer backbone. Dechlorination rate depends on: molecular mass, crystallinity, oxygen and hydrogen chloride gas concentration which is autocatalytic to the chain stripping process. Greater oxygen concentration correlates to an increase in dechlorination as main chain scission takes precedence over cross-linking processes. At elevated temperatures hydrogen gas is produced due to carbonisation following cyclisation. Cross-linking develops a fully carbonised residue, which at higher temperatures in air oxidises completely leaving no residue.[20] Alternatives to chlorinated species are being sought to reduce the evolution of hydrogen chloride gas during combustion as more is understood about its toxic and corrosive effects in fire situations.

Other vinyl substituted polymers exist, with only one substituted group instead of a hydrogen atom on the basic repeat unit, these include: poly(vinyl acetate), poly(vinyl alcohol) and poly(vinyl bromide). All decompose following a similar mechanism to that of poly(vinyl chloride). Though chain-stripping of these polymers occurs at different temperatures the outcome remains the same, all aromatize by hydrogen evolution at roughly 450 °C.[20]

1.5.3.3. Epoxies
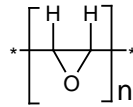
Figure 8 Epoxy polymer structure

The epoxy polymer is shown above in Figure 8, however the more widely used - in the paint and coating industry - epoxy resin structure is shown below in Figure 10. Epoxies are formed by reacting alkylene oxide groups in the presence of a catalyst (carboxylic acid anhydrides or amines) and are highly versatile.[14,21] The strained bonds in the cyclic C-O-C ring make this a highly reactive functional group which enables curing at low temperatures - even room temperature. The C-O-C ring opens to incorporate the reactive OH end of a bisphenol A molecule producing a single molecule and a cured resin.
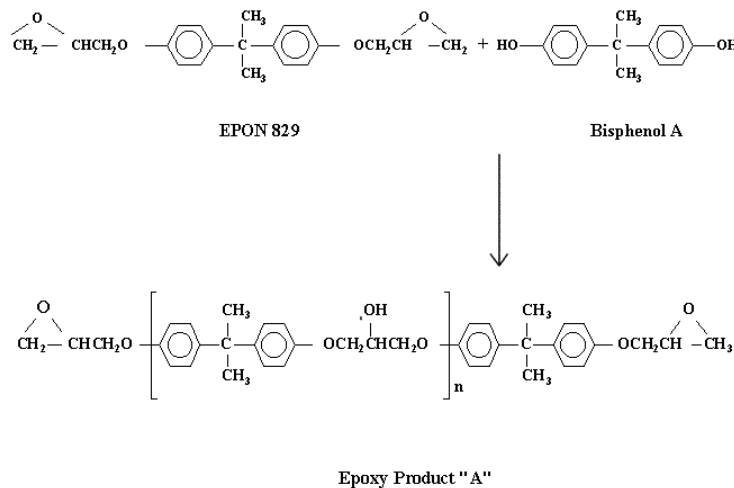
Figure 9 Epoxy resin curing mechanism[22]

Once cured, the high level of cross-linking results in reduced permeability. This form of cross-linking makes the epoxy coating tough and highly heat and chemical resistant as there are no double bonds for further reactions to occur.
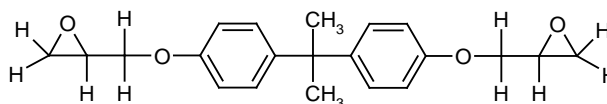
Figure 10 Epoxy resin monomer structure

Epoxy resins are successful in coating formulations due to their high processing mobility which allows rapid thorough wetting of surfaces. The high reactivity of the epoxy group with curing

agents such as amines and anhydrides enables easy conversion from the liquid form (monomers) to the highly cross-linked, high-molecular weight materials. The curing process is generally done via addition reactions so there is reduced production of volatile condensation by-products. Epoxies are utilised in a wide range of coatings due to the variation of functional groups in the chemical structure; hydroxyl, aromatics, aliphatics and ethers, producing a range of hydrogen-bonds and polarities resulting in adherence to a varied selection of surfaces.[23]

Decomposition of epoxy resins takes place in several steps and is very complex. Decomposition initiates at approximately 240 °C and continues to upwards of 450 °C. Principal decomposition products include: CO, CO_2, propylene and ethylene.[14] One suggested decomposition process begins with the evolution of water forming unsaturated structures, these are unstable at high temperatures and the decomposition proceeds with the scission of the weak allylic bonds. Cyclic products may be found in either the residue or the volatile fraction or both due to this mechanism.[24] Erickson[25] suggests that the major mechanism for decomposition of epoxies involves the bond scission between the bisphenol A moiety within the epoxy. Further scission occurs at similar rates at the isopropyl group and the carbon-oxygen bond opposite to the aromatic rings. This mechanism evolves products such as water, CO_2, and a range of phenol species.

Epoxies are expensive due to the use of epichlorhydrin and the removal of salt as a waste by-product. Epoxy resin formulations are not well suited to exterior applications. Glossy topcoats will fade and chalk with exposure to UV light[21] for this reason epoxies are more widely to be used as primers. Epoxy resins demonstrate good heat resistance, rapid drying, hardness, abrasion resistance, low volatile organic compound (VOC) release and easy 'water' clean-up but are not widely used for fire retardant coating systems due to the cost. Efforts are being made to improve the char forming attributes of epoxy resins.[26]

1.5.3.4. Polyurethanes

A Polyurethane structure is shown below in Figure 11. Polyurethane polymers are formed by reaction of di-isocyanates and a polyol. The carbonyl carbon of the isocyanate reacts with the oxygen atom of the alcohol molecule creating a urethane.[27] This then polymerises via an addition reaction to become polyurethane. In practice many different types of linkage and cross-linkage maybe present within a polyurethane structure.
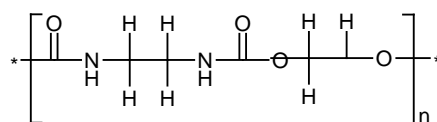
Figure 11 Polyurethane structure[21]

Decomposition of polyurethane does not usually occur below 200 °C and slows in the presence of air.[20] The decomposition mechanism is very complex occurring via many different reactions. Erickson[25] suggests that the decomposition is controlled by endothermic processes and the reactions involving the urethane functional group, these are dependent on the type of polyurethane being considered. The major mechanism is the scission of the polyol-isocyanate bond formed during polymerization. The isocyanate functional group is highly reactive aiding polymerization as well as casting and curing. The N-H bond is also reactive and is important in the polymerization and cure of polyurethane resins.[27]

Polyurethanes are used to exploit their good mechanical properties; flexibility, abrasion and chemical resistance, and toughness.[21] Limitations include poor processing, high cost and poor light stability which mean that polyurethanes used in coating formulations are used indoors only.

1.5.3.5. Polyolefins – Alkyds
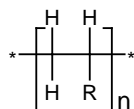
Figure 12 Polyolefin structure

Figure 12 depicts the polyolefin structure. Alkyd is a polyester resin formed via a reaction of alcohol (polyols) and acid anhydride. It is a highly cross-linked polymer matrix displaying rigid properties. Decomposition leads to minimal monomer production and instead a large number of small - mostly hydrocarbon - species are observed. Thermal stability is affected by branching. More branching correlates to a reduction in stability. The presence of oxygen significantly affects both mechanism and rate of decomposition. In the presence of oxygen the decomposition products are mainly ketones.[20]

1.5.3.6. Polycarbonates

Polycarbonate polymers (an example of which is depicted in Figure 13) yield substantial amounts of char on combustion. Decomposition begins at approximately 370-460 °C and is initiated by the scission of the weak $O-CO_2$ bonds - producing 35 % by mass of carbon dioxide.

Mixed mechanisms of random chain scission and cross-linking result in the evolution of products including bisphenol A and phenol.[20]
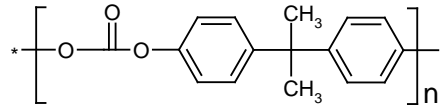
Figure 13 Polycarbonate structure

1.5.3.7. Cellulosics

Thermal decomposition occurs above 140 °C, facilitated by moisture.[14] Decomposition of cellulosic polymers occurs via four processes in addition to desorption of physically bound water:

1) Cross-linking of cellulose chains, yielding water (dehydration)

2) Unzipping of cellulose chains producing laevoglucosan from the monomer unit

3) Decomposition of the dehydrated (dehydrocellulose) product producing char and volatile products

4) Laevoglucosan further decomposes to produce tars and carbon monoxide.[20]

Char yields depend on heating rate with very high temperatures yielding no char, this occurs because the char production reaction is dependent on low-temperature dehydration reactions.

Alkali solutions force swelling of cellulose structures allowing water molecules to penetrate.

1.6. Requirements for testing and screening

Areas of fire testing are shown in the flow diagram in Figure 14.

```
                              ┌─────────────────────┐
                              │    Fire Testing     │
                              └──────────┬──────────┘
                    ┌────────────────────┴────────────────────┐
                    ▼                                          ▼
         ┌─────────────────────┐                   ┌─────────────────────┐
         │   Fire Resistance   │                   │  Reaction to Fire   │
         └──────────┬──────────┘                   └──────────┬──────────┘
                    │                          ┌──────────────┴──────┐
                    ▼                          ▼                     ▼
         ┌─────────────────────┐    ┌─────────────────────┐   ┌──────────
         │     Products        │◄───│    Flammability     │   │    Fire
         └─────────────────────┘    └──────────┬──────────┘   └──────────
                                               ▼
                                    ┌─────────────────────┐
                                    │     Materials       │
                                    └─────────────────────┘
```
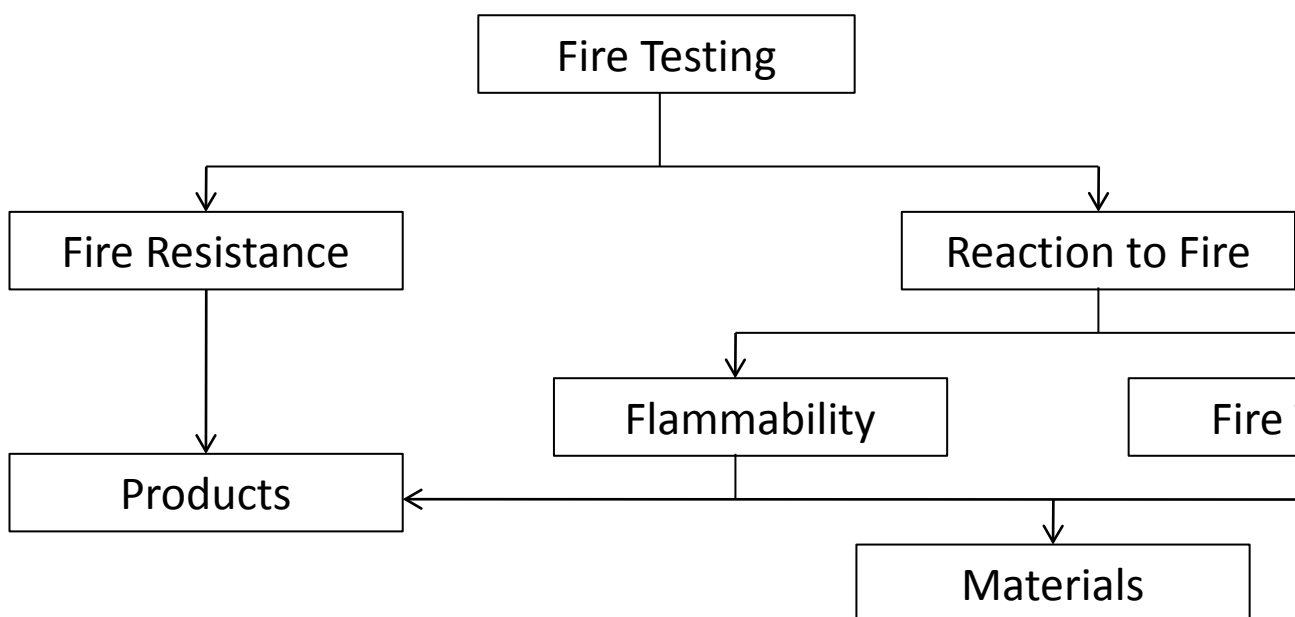
Figure 14 Areas of Fire Testing[28]

Fire tests aim to assess either the fire resistance of a material or the burning behaviour in a fire scenario. Both involve assessment of the time to ignition, peak and total heat release rates as well as flame spread. The material must be representative of the final product and end use application; therefore, several specific fire tests have been developed for specific materials and adapted for analysis of particular applications. Two standard test methods which in combination assess all of these factors are the BS 476: Part 6[29] and the BS 476: Part 7,[30] which are outlined and discussed later in this thesis (sections 1.9.3. and 1.9.4. respectively).

As the burning behaviour of multilayer paint is so unpredictable because of its unknown composition and unknown adhesion, regulatory agencies have assumed a worst case scenario in all situations. This has lead to the development of a highly flammable 'class 4' rated test substrate, onto which all coatings must be applied for assessment in standard fire tests. This substrate known as Warrington Blue Board (WBB) is discussed further in CHAPTER 3.

Standard fire tests are expensive to run requiring specialist apparatus, trained personnel and often large sample sizes; even the standard test substrate is expensive. In addition, certificated fire tests are typically more expensive than indicative tests (increased by a factor of 3). For this reason it was necessary to screen novel formulations prior to assessment in standard fire testing apparatus to optimise development. Screening test methods must assess factors crucial to performance (as listed above) as well as give some idea of the outcome of the standard fire test assessment.

Screening test methods considered as part of this research assess the contribution of the coating to fire load. The extent of fire retardant action is quantified with respect to heat

release rate, time to ignition and fire effluent gas production in the cone calorimeter. Polymer decomposition was investigated using thermogravimetric analysis (TGA) in air and inert (nitrogen) atmospheres and is discussed in the next section. Rheological properties such as flow, viscosity and softening temperature of the resin as well as complete formulations were investigated to estimate performance. Thermal conductivity of coatings was estimated using an embedded thermocouple within cone calorimeter samples (at the substrate-coating interface) and during exposure to a naked flame in the BS EN 367 apparatus. Rate and extent of intumescence is recorded when exposed to the naked flame of a Bunsen burner and flame spread is also assessed. Finally, prediction of performance in the BS 476: Part 6 is assessed using an adapted version of the standard test method in order to estimate the extent of intumescent under a specific heating regime and adherence of the coating to a specific substrate. Screening test methods are further discussed in section 2.3..

1.7. Testing methods for decomposition

As mentioned in previous sections polymer decomposition is varied and complex. Thermogravimetric analysis (TGA) provides valuable information on these processes and aids determination of decomposition rate and identification of decomposition products. This technique provides quantitative decomposition information with regard to polymeric materials. Samples are subjected to a known heating regime (usually consisting of a constant heating rate) and continuously recorded mass. Mass loss occurs through drying, liberation of gases and volatiles, or mass may be gained by reaction of the polymer or pigments with the atmosphere in which the sample is tested. Significant mass loss (in air) during decomposition is often indicative of the ignition temperature of the sample at the point when sufficient fuel is released. Once ignition has occurred the mass loss profile in nitrogen is more representative of the fuel production rate, since the oxygen concentration under a flame is approximately 0 %.[31] Thermal stability can be deduced from the data obtained. Small sample sizes (maximum 10mg) ensure that no thermal gradient exists through the bulk of the sample.

Differential thermal analysis (DTA) involves the comparison of the sample with an inert reference sample with similar heat capacity. Both are subjected to the same heating regime. In the case of exothermic reactions the sample temperature will exceed that of the reference and in endothermic reaction situations the sample temperature lags behind that of the reference. Differential temperature is then plotted against either time or temperature.

Another method used for the qualititation and quantification of decomposition products is pyrolysis gas chromatography coupled with mass spectrometry (pyGC-MS). The pyrolyser can be programmed to a known heating regime (similar to that of the TGA) and due to reduced

sample size the temperature ramps can be much faster. Decomposition products are separated by gas chromatography before analysis of volatile species by mass spectrometer. This process can be set to take snapshots of specific stages of decomposition and yields structural information allowing semi-quantitative concentrations of products to be determined.

1.8. Polymer combustion behaviour

Being made up of predominantly carbon and hydrogen, polymers are highly combustible.[32] For a combustion reaction to take place two factors must be present: the combustible (reducing agent) and the combustive (oxidising agent) - usually oxygen in air. Combustion processes are initiated by an increase in temperature of the polymer from an external heat source causing bond scission. Volatile fractions (pyrolysis products) produced diffuse into the air above the polymer surface and mix with air to form a combustible gaseous mixture (fuel).

Ignition may occur spontaneously whereby the temperature is increased sufficiently for a concentration of free radicals to initiate flaming combustion known as auto-ignition. More commonly, ignition is initiated at a lower temperature (around 200 °C lower) when the combustible gases interact with a source of intense energy - a spark or flame - this is known as piloted ignition.9 After ignition occurs, the additional radiation from the flame pyrolyses more fuel and steady flaming may occur. The polymer propagates the fire and self sustaining combustion proceeds.[33] Either form of ignition leads to the liberation of further heat. [34] Figure 15 shows the thermal feedback of heat produced by combustion. This in turn leads to increased temperatures of volatile polymer fragments and non-combustible gases surrounding the flame, resulting in increased heat transfer through conduction. These gases then expand (increasing heat transfer by convection), heating the solid particles entrained into the flame which results in increased heat transfer by radiation.[35]

Pyrolysis

Polymer → Combustible and non-combustible gases

Polymer → Liquid products and tar

Polymer → Solid charred residue

Endothermic (+ΔH)

Thermal feedback from flame
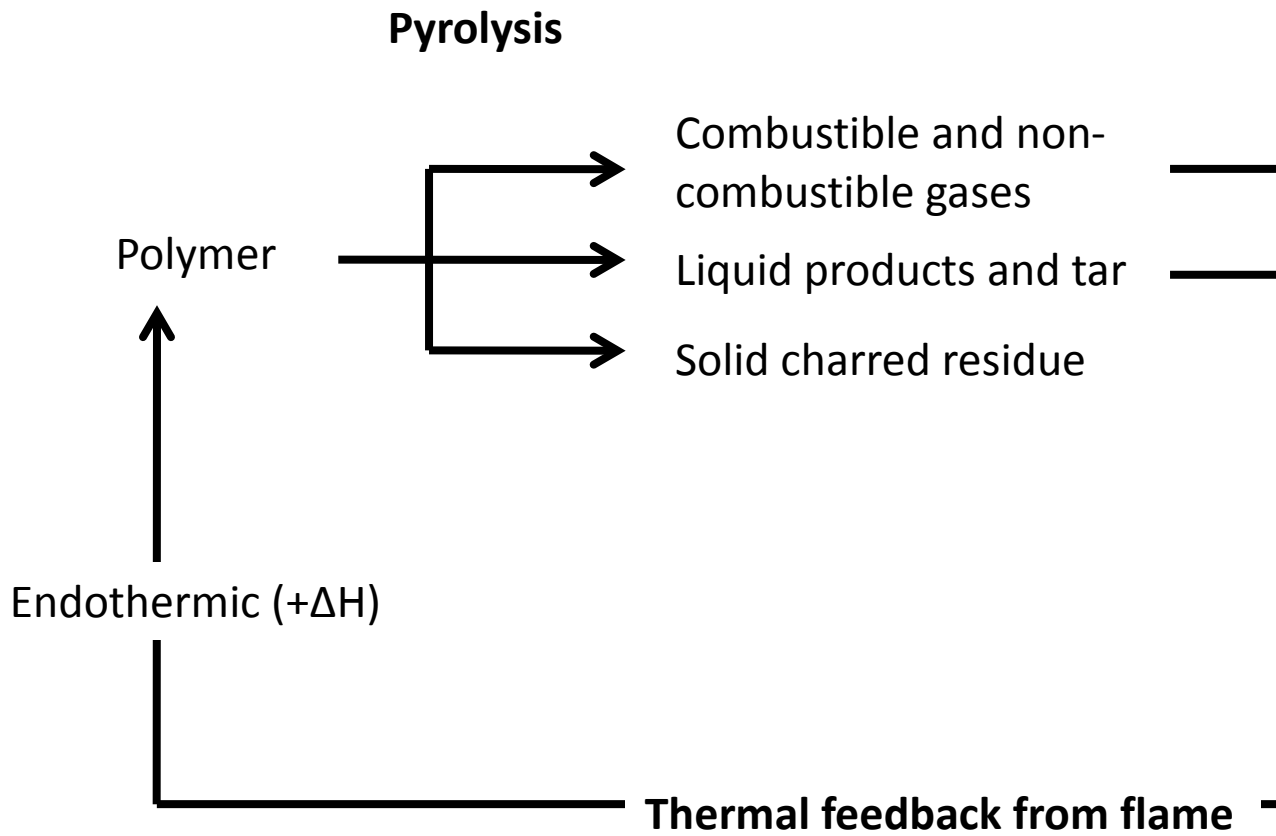
Figure 15 Schematic diagram of polymer combustion

The duration of combustion is dependent on the amount of heat evolved during fuel combustion. If a certain threshold of heat is produced then new decomposition reactions take place in the solid phase liberating more combustibles. The combustion cycle is maintained and is often referred to as the 'fire triangle' depicted in Figure 16.

HEAT

FIRE

Combustible
Reducing Agent
(Polymer)

Combust
Oxidising A
(Air)
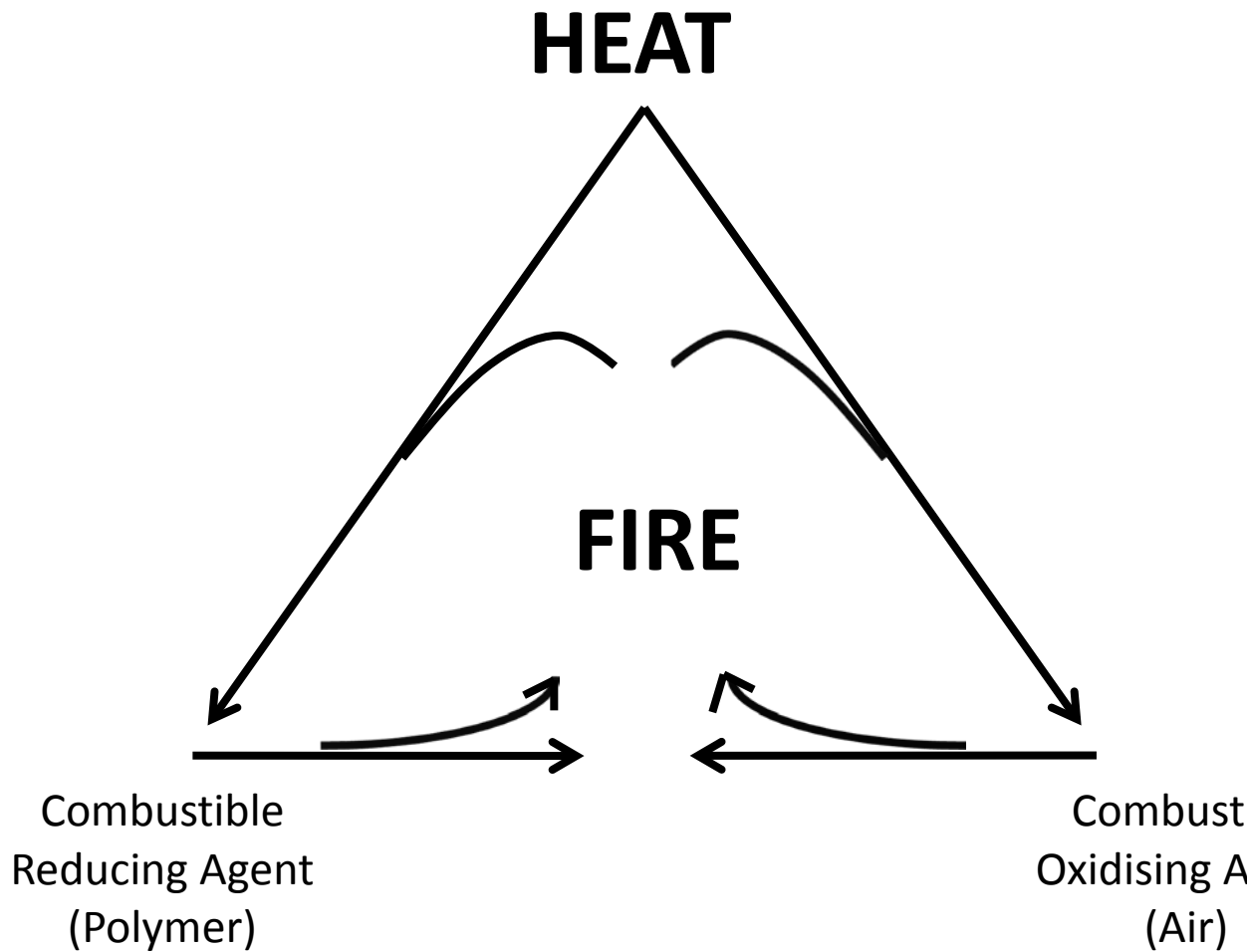
Figure 16 Schematic of the combustion cycle or 'fire triangle'

Flames are the light-emitting part of the combustion zone; the colour of the flame is dependent on the fuel being burned. Electrons are excited within transient reaction intermediates and light is emitted as excess energy is released. There are two types; pre-mixed and diffusion flames, each is shown in Figure 17.

Pre-mixed flames are formed when oxidiser and fuel are mixed prior to the flame front. Almost all modern fuel combustion for energy release involves pre-mixed flames - these are typically blue with efficient conversion of fuel to CO_2 and water, with little soot formation hence negligible radiant heat transfer. An example of a pre-mixed flame would be a Bunsen burner, with the air hole open.

Figure 17 Pre-mixed and diffusion flames

If the rate of combustion is determined by the rate of physical mixing between the fuel and oxidant then this is known as a diffusion flame. An example of a diffusion flame would be the burning of a candle where fuel and oxygen are transported from opposite sides of the reaction zone.[36] The reaction rate exceeds diffusion rate which results in continual fluctuations in product and reactant concentration throughout combustion. Almost all unwanted fires are diffusion flames. The poor mixing results in incomplete combustion, with higher yields of carbon dioxide and soot. The soot incandesces in a flame with the emission if radiation. This allows horizontal and even downward flame spread of flame, causing rapid fire growth.

Another classification of flame is through the position of the flame front. Stationary flames have a fixed flame front whereas propagating flames spread outwards spherically from the point of ignition, these flames will also spread in a linear fashion along a flammable surface.

1.9. Testing methods for burning behaviour

Flammability is a general word used to describe the reaction to fire behaviour of a material. It can be subdivided into many individual parameters including ignitability, flame spread and rate of heat release. It has been defined by the method used to measure it[37] but is most widely stated as the ease of which a material will ignite.[36] The purpose of any test is to meet a regulatory requirement or to demonstrate that the tested material will perform adequately in a fire scenario.[38]

Cone Calorimeter

The cone calorimeter is widely accepted as the best bench-scale method for determining flammability of materials due to its wide acceptance and the wide range of parameters it measures.[39]

Measured parameters include: -

- Ease of ignition

- Rate of flame spread

- Rate of heat release

- Ease of extinction

- Smoke and toxic gas evolution[40]

It is widely agreed that the most important of these factors is heat release rate.[41] There is limited literature on the interpretation of heat release rate curve data. Figure 18 shows the results of some work carried out to determine the typical heat release rate curves created by different materials.[42]
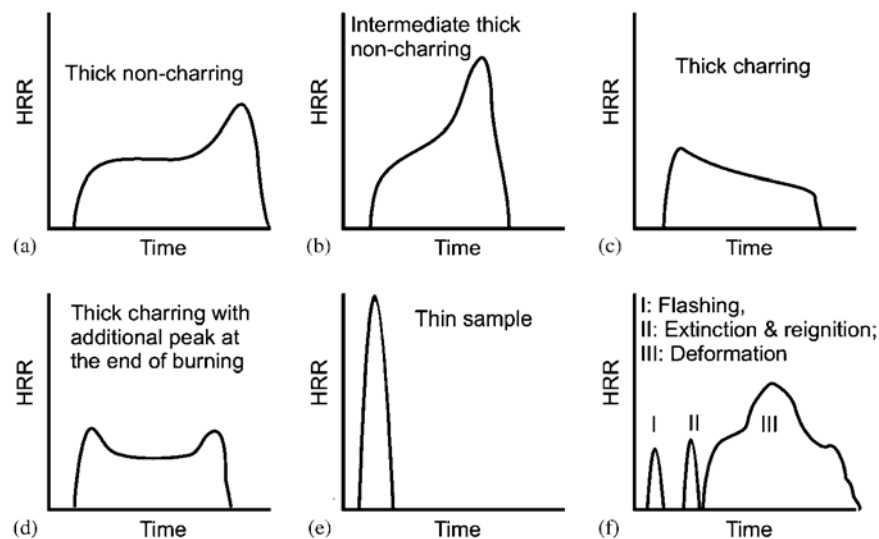
Figure 18 Heat release curves from various burning behaviours[42]

Heat release rate calculations rely on the net heat of combustion being proportional to the oxygen requirement for combustion. 13.1×10^3 kJ of heat are released for every kilogram of oxygen consumed.[43] Samples of size 100 mm x 100 mm and up to a thickness of 50 mm are exposed to a uniform radiant heat source that can be set to any value between 0-100 kWm^{-2}, during which time, oxygen concentration and exhaust gas flow rates are monitored. The radiant heat source and spark igniter apparatus in the cone calorimeter lend themselves specifically to the analysis of wall and ceiling scenarios where the ignition may not be by direct flame impingement but instead by thermal radiation from nearby flames.[44] The sample is constantly weighed during heating and smoke readings taken using a laser photometer,

further measurements include: heat release rate (HRR), mass loss rate and ignition properties. For the purposes of this thesis the cone calorimeter is arranged and operated following the standard ISO 5660-1: 1993.[45]

However the cone calorimeter does have its limitations; it is only able to simulate well-ventilated fires and results cannot be used to correlate to under-ventilated or post flash-over fires[46] although other versions of the cone calorimeter are being used to simulate these environments;[45] the cone heater contributes additional convective cooling by modifying the air flow around the sample and heat losses from the substrate and sides of the sample are neglected;[47] there is no direct flame impingement on the surface of the sample and so relies on the pyrolysis products being ignited by a spark; finally, samples are predominately tested in a horizontal orientation and sample sizes are small and so factors such as adhesion of paint layers and flame spread are ignored. Also the load cell sensitivity of ± 0.1 g is not suitable for paint layers.

Ultimately, full testing of coatings involves full scale testing of the coated construction,[48] involving much effort and cost. A brief history of flammability testing for thin film coatings is outlined below, though no standard screening test methods have been outlined. Many methods focus on coatings for the protection of steel substrates requiring a higher temperature range for intumescent action and therefore analysis.

1.9.1. ASTM Test Method for Fire Retardancy of Paints (Cabinet Method) D 1360.

This small-scale method measures, relative, fire retardant properties of coatings by determining mass loss and char index of coated wood panels exposed to flaming ethyl alcohol. This method provides good assessment under specified conditions. D1360 measures combustibility through mass loss rather than flame spread index and the precision of this method has not yet been determined.[49]

In 2003, a study of small-scale fire prediction was reported alongside numerical models used to assess coating performance.[50] This method involved coated steel being exposed to various heat fluxes in the cone calorimeter. Thermocouples were attached to the reverse of the steel plate to record the increase in temperature experienced by the steel plate thus establishing the level of protection afforded by the coating. Data was used to calculate a time dependant thermal conductivity and heat resistance of intumescent coatings. Limitations of this method were expressed as there is no assessment of the influence of direct flame impingement on coatings, vertical adherence of the coating was not considered as samples are horizontally orientated, and load and heat sink effects could not be determined (which is important when considering the impact on steel structures).

Further developments in 2005-2006 meant that the surface temperature of the intumescent coating could be measured using laser-induced phosphorescence.[51] Previously this measurement was thought to be impossible as any measuring device might affect or interrupt the swelling of the coating during heating. The use of thermocouples was eliminated as they could not be sustained on the surface of the coating due to limitations of weight and mechanical connection to the surrounding. A method was developed using a conical heater twice the size of that found in the cone calorimeter; to allow for the swelling of the intumescent coatings. Thermocouples were used to monitor the temperature increase of the reverse of the steel plates and a heat transfer model was developed to assess findings. Again this method ignored direct flame impingement effects and failed to monitor the adhesion of coatings but did provide more insight into the temperatures endured by the surface of the coatings and the protection given to the substrate below.

While these methods proved beneficial, allowing comparison and ranking of coating performance, there is limited correlation to the real fire scenario. "Real fire scenarios" are defined by standard fire curves, intended to represent the rate of temperature increase in a fire. The two of greatest relevance to this work are the hydrocarbon and cellulosic fire curves.

The cellulosic fire curve was developed to illustrate the temperature rise in residential or commercial buildings where the primary source of combustion is cellulosic in nature - wood, paper and furniture etc. This curve demonstrates the slow temperature rise to 927 °C after about 60 minutes.

The Hydrocarbon fire curve shows the rapid temperature rise indicative of hydrocarbon fuel such as oil or natural gas burning. This curve shows the rapid temperature increase to 1000 °C after about 4 minutes.

Fire curves have lead to a generation of fire retardant and protective coating formulations (particularly intumescents) tailored specifically to perform well under these test conditions, but which are untested under slightly varying situations which may be more typical of a real fire.

Several test methods have been developed for the analysis of steel protection.

1.9.2. UL 1709 Rapid Rise Fire Tests of Protection Materials for Steel Structures.
Intumescent formulations are coated onto steel and thermocouples attached to the reverse of the steel plate allowing measurement of temperature versus time. The failure temperature is outlined as 400 °C. The failure temperature of normally loaded steel structures is widely regarded as 550 °C whereas heavily loaded structures have a more conservative failure

temperature of 400 °C (this is the point when 60 % of the steel strength remains).[52,53] This method assumes the worst case scenario stating 400 °C as the temperature cut-off point. Samples are vertically orientated so adhesion of the coating is considered. Limitations of this method include a failure to correlate with the large-scale flame spread results; however, it is clearly of very limited applicability to highly flammable substrates such as multilayer paint.

The method above was further developed by Jimenez *et al.*[54] using an infra-red pyrometer to measure the surface temperature of the reverse side of the steel plate. This method focuses on the heat transfer through the coating and no failure temperature is assigned. Instead temperatures reached after a 20 minute period are compared and assessed when related to the temperature reached by an un-coated steel plate under the same conditions. This method demonstrates good correlation from small to large-scale tests for both hydrocarbon and cellulosic fire curves. The apparatus can also be adapted to analyse samples in both vertical and horizontal orientations.

Though this method appears to be the most promising there are no reported correlations between this and standard fire tests for coatings (outlined below) and no consideration for performance of coatings on inherently flammable substrates such as multilayer paint.

Standard fire tests for the assessment of the performance of coatings are BS 476 Part 6 - Method of test for fire propagation for products[29] and BS 476 Part 7 - Method of test to determine the classification of the surface spread of flame of products[30] which are outlined below.

1.9.3. BS 476: Part 6 - Method of test for fire propagation for products[29]

This method is primarily intended for internal wall and ceiling lining materials. The results of which are expressed as a fire propagation index (*I*), which provides a comparative measure of the contribution to fire growth by an essentially flat product. The apparatus consists of a non-combustible chamber containing two electric heating elements and a gas burner into which the sample is mounted. The gas burner is ignited and three minutes later the electric heating elements are switched on. Thermocouples mounted in the chimney record the temperature profile of fire gases throughout the analysis. Observations of burning behaviour such as heat release, time to ignition and adhesion to the substrate are recorded and fire propagation index (*I*) is calculated for each sample. These calculations are outlined and discussed in section 2.3.4. The resultant fire propagation classification then categorises the material according to Approved Document B.6

1.9.4. BS 476: Part 7 - Method of test to determine the classification of the surface spread of
flame of products[30]

This method provides data suitable for the comparison of end-use performances of essentially
flat materials, composites or assemblies which are primarily used as the exposed surfaces of
walls or ceilings. It measures the lateral spread of flame of a vertically orientated sample under
opposed flow conditions using a classification system based on the rate and extent of flame
spread. Samples are exposed to a radiant heat panel at 90° to the sample surface; this
produces a temperature gradient. An ignition source is introduced at the front end of the
sample and the rate and extent of flame spread are recorded as the flame passes markings
placed at intervals along the sample.
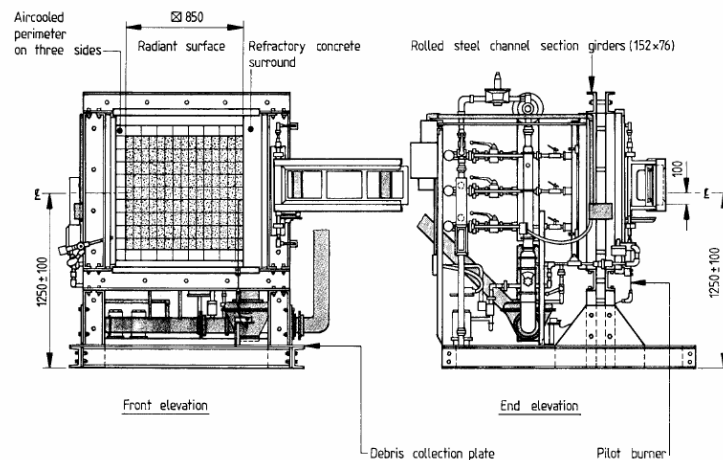
Figure 19 Schematic diagram of BS 476: Part 7 - Lateral spread of flame apparatus

Readings are taken which monitor the rate at which the flame front surpasses several markers
along the sample's surface. This then correlates to a rating of flame spread which when
combined with the result of the material in the BS 476: Part 6 gives a classification according to
Euroclass system or that used in Approved Document B.6

With the exception of the BS 476: Part 6 and BS 476: Part 7 methods, all analyses outlined
above neglect to assess coating performance on inherently flammable substrates. This is an
important consideration as the burning behaviour - and therefore the level of protection
provided - of a coating is highly dependent on the type of substrate onto which it is applied.
Thin protective films rely heavily on good adhesion to previously applied layers. Problems arise
as the current test methods test on highly flammable but well adhered substrate materials
whereas real fire cases require protection of poorly adhered and flaky substrate layers.

1.9.4.1. BS 476: Classification system

BS 476: Part 7 classifies products into Classes 1 to 4. Class 1 provides the highest level of protection against flame spread and Class 4 providing the least. Class 4 represents the worst case, highly flammable and rapid flame spread such as the un-protected Warrington blue board substrate material. To achieve the highest classification of a 'Class 0' products must not only achieve a 'Class 1' in the BS 476: Part 7[30] but also record a fire propagation index (I) value of less than 12 when applied over the Class 4 rated substrate material in the BS 476: Part 6.[29] (Calculations are described in section 2.3.4.). This is the standard to be met in order to pass the standard fire tests.

1.9.5. IMO Lateral Ignition and Flame Spread Test/Spread of Flame Apparatus ISO 5658

This method relies on a radiative heat source and pilot flame to measure time to ignition and lateral flame spread along a vertically orientated material. Samples are predominantly flat materials – wall composites and assemblies. After ignition horizontal progression of flame is measured and results expressed in terms of: flame spread in time, flame front velocity versus heat flux and critical heat flux at extinguishment, and average heat obtained from burning. The test method and assembly are carried out according to the standard ISO 5658-2:2006[55] and the apparatus is depicted in Figure 20.
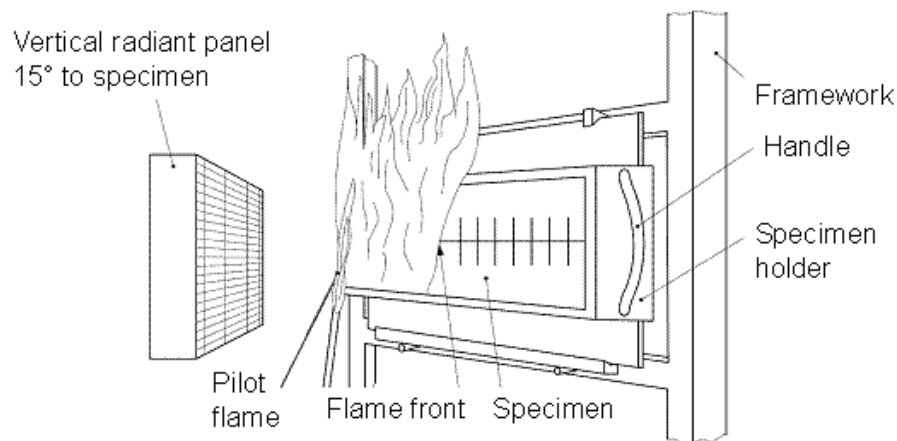
Figure 20 Schematic diagram of the IMO LIFT apparatus

The British standard methods (BS 476: Part 6 and BS 476: Part 7) are soon to be superseded by a European classification system and associated test methods. These are outlined below.

1.9.6. BS EN 13823:2002 Reaction to fire tests for building products – Building products
excluding floorings exposed to thermal attack by a single burning item (SBI)[56]

This test method is specific to wall lining products and determines the fire performance when exposed to a single burning item. A test specimen, consisting of two vertical wings forming a

right-angled corner is inserted into a test room and exposed to the flames from a burner placed at the bottom of the corner. Flames are obtained by combustion of propane gas, injected through a sandbox and calibrated to give a heat output of 30 ± 2.0 kW. Fire (as a diffusion flame) performance is evaluated over a 20 minute period and parameters include: heat production, smoke production, lateral flame spread and falling flaming droplets and particles. Measurements are taken from the gas exhaust which is equipped with sensors measuring: temperature, light attenuation, oxygen, carbon dioxide concentration and exhaust flow. These parameters are then used to calculate heat release rate (HRR), total heat release (THR) and smoke production rate. The fire index growth rate (FIGRA) - explained later in this section, is also calculated from this data. Visual observations are recorded to define lateral flame spread and falling flaming droplets. Limitations with this method include: large sample size and test apparatus (therefore higher cost), and calculation of heat release from oxygen concentration which may be skewed by use of nitrocellulose based substrates (discussed further in section 3.5.2.). This test method has not been utilised due to the limitations outlined above, particularly, time and sample resource restrictions, and expertise required to run this test. However, some work has been done to correlate the SBI data to cone calorimeter experiments under certain conditions.[57]

1.9.6.1 Euroclass grading system

The single burning item experiment is used to classify products into the classes listed in Table 1.[58]

Table 1 Explanation of Euroclass classifications

Class	Performance Description	Fire scenario and heat attack	
A1	No Contribution to fire	Fully developed fire in a room	At least 60 kWm^{-2}
A2	No Contribution to fire – products with a small amount of organic compounds	Fully developed fire in a room	At least 60 kWm^{-2}
B	Very limited contribution to fire	Single burning item in a room	40 kWm^{-2} on a limited area

C	Limited contribution to fire	Single burning item in a room	40 kWm^{-2} on a limited area
D	Acceptable contribution to fire	Single burning item in a room	40 kWm^{-2} on a limited area
E	Acceptable contribution to fire	Small flame attack	Flame height of 20 mm
F	No performance requirements	Small flame attack	Flame height of 20 mm

Classes B to E comprise all the combustible materials, describing decreased performance in the 'reaction to fire' experiments previously described however; 'Class B' is suitable for use in public places (including schools). Products obtaining a 'Class 0' in the BS 476 tests might be expected to obtain a 'Class B' in the Euroclass system. However, this must be confirmed by experiment as the majority of products tested in the new regime will fall into a lower class than would be expected using the BS 476 system. This is due to the parameters in which the products are analysed and means that a table of correlations between the new Euroclass and old BS 476 tests would be an over simplification.

Class A1 consists of all products which do not participate in the fire and Class A2 includes materials and products which contain components with a very limited participation in the fire. Further sub-classes are also defined for smoke (S1 to S3; S1 being the best and S3 the worst) and burning droplets (D0 to D2; D0 being the best and D2 the worst).

The revised Euroclass system requires products to be tested 'in application' which means that all products are to be tested in the manner in which they would be used as opposed to 'naked' or as placed on the market. This is especially important when considering paint and coating systems which perform very well when tested 'naked' (or in isolation on a non-combustible substrate) however when applied 'in application' (on a substrate made up of paint layers) performance is expected to be much worse.

Fire index growth rate (FIGRA) is used to determine the Euroclass rating. The concept is to classify the product based on its tendency to support fire growth. FIGRA is a measure of the biggest growth rate of the fire during a test; it is calculated as the maximum value of the function of heat release rate over the time taken for the test to take place and is reported in W s^{-1}.[59]
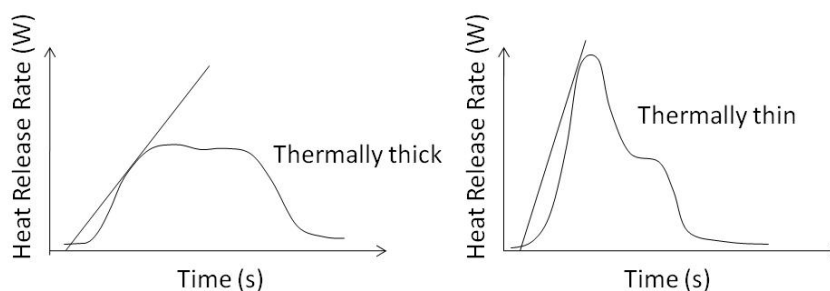
Figure 21 Diagram to demonstrate FIGRA

In the case of paint and coatings, the fire index growth rate (FIGRA) is usually regarded with caution as it unduly discriminates against products with a more combustible surface layer. FIGRA is increased due to a rapid burn off of this layer in the early stages of the analysis even though the product as a whole poses little fire risk and contributes minimally to the fire load. In these cases the total heat release (THR) is a preferred method of determining performance.

Test methods reveal a gap in the knowledge as there are no screening test methods defined for the development of thin film, low temperature, fire protective coating systems, on an inherently flammable substrate, which correlate to or estimate performance in the standard fire test methods.

1.10. Chemical analysis techniques

Chemical analysis of fire effluent material can divulge a great deal of information regarding decomposition processes. Techniques such as Nuclear Magnetic resonance (NMR), Fourier Transform Infra-Red (FT-IR) and Mass Spectrometry (MS) can be used to qualify and quantify the products of combustion.

During combustion a carbonaceous residue (or char) is formed, the structure and composition of can provide useful information about the level and mechanism of protection involved. Scanning Electron Microscope (SEM) can be used to assess the physical properties of the residue, which will have an effect on burning.[60] When coupled with the EDAX accessory, elemental analysis of the residue is also possible.

Further chemical analytical techniques allow determination of the composition of materials which allow determination of their fire retardant action or mechanism. These techniques include: Inductively Coupled Plasma Mass Spectrometry (ICP-MS) and diamond-Attenuated Total Reflectance (d-ATR-FTIR). Both processes provide information on the functionality and structure of the materials analysed.

1.11. Factors affecting coating performance

Performance factors of coatings are not only related to test methods, conditions and parameters measured, they are also reliant on the chosen formulation and physical coating properties. Some of the factors affecting coating performance for fire protection are outlined below.

1.11.1. Type of substrate

The type of substrate onto which the paint is applied will significantly affect the burning behaviour of the product. Physical properties such as the thickness, composition, thermal conductivity and heat capacity of the substrate material will affect the rate at which the paint layer increases in temperature when exposed to heat.4 A non-combustible substrate such as plasterboard, cement or brick which has good thermal conductivity will pose minimal threat when one coat of paint is applied. However, previously painted surfaces (especially when not correctly prepared) will exhibit greater flammability, most noticeably as a result of a reduction in thermal conductivity and a reduction in adhesion between paint layers. Similarly a highly insulating substrate will have a profound influence on the flammability of the paint layers.

1.11.2. Adhesion

A successful fire protective surface coating relies on cohesion between the film-forming substances and adhesion between the coating and the paint.

Where the paint film remains firmly adhered to the wall, with adequate heat sink properties, localised heat impingement onto one surface will be dissipated by the underlying substrate. Normally, combustion will only occur in the area of film that is ignited but will not rapidly spread heat across the attached surface.[61]

A failure in adhesion results in blistering and delamination of the coating, depicted in Figure 22. This produces two simultaneous effects. Firstly, delamination allows combustible gases to escape and become ignited,4 increasing the amount of heat released from the burning film. Secondly, the temperature of the exposed film will greatly increase, exceeding the ignition temperature. Trapped vapours below the surface of the film display a lower thermal conductivity ($k\rho c = 0.024$ $Wm^{-1}K^{-1}$) than the paint ($k\rho c = 0.74$ $Wm^{-1}K^{-1}$), therefore trapping heat, and the ignition temperature is rapidly exceeded.[62] Ignition causes the release of heat and the process will transfer along the surface. If the heat produced is sufficient to break down or delaminate the adjacent film, then the flame will be spread along its surface.[61]

Paint

$K\rho c = 0.74$ Wm^{-1} K^{-1}

Air
Lower thermal conductivity
$(K\rho c = 0.024$ Wm^{-1} K^{-1} $)$

Plasterboard

$K\rho c = 0.48$ Wm^{-1} K^{-1}
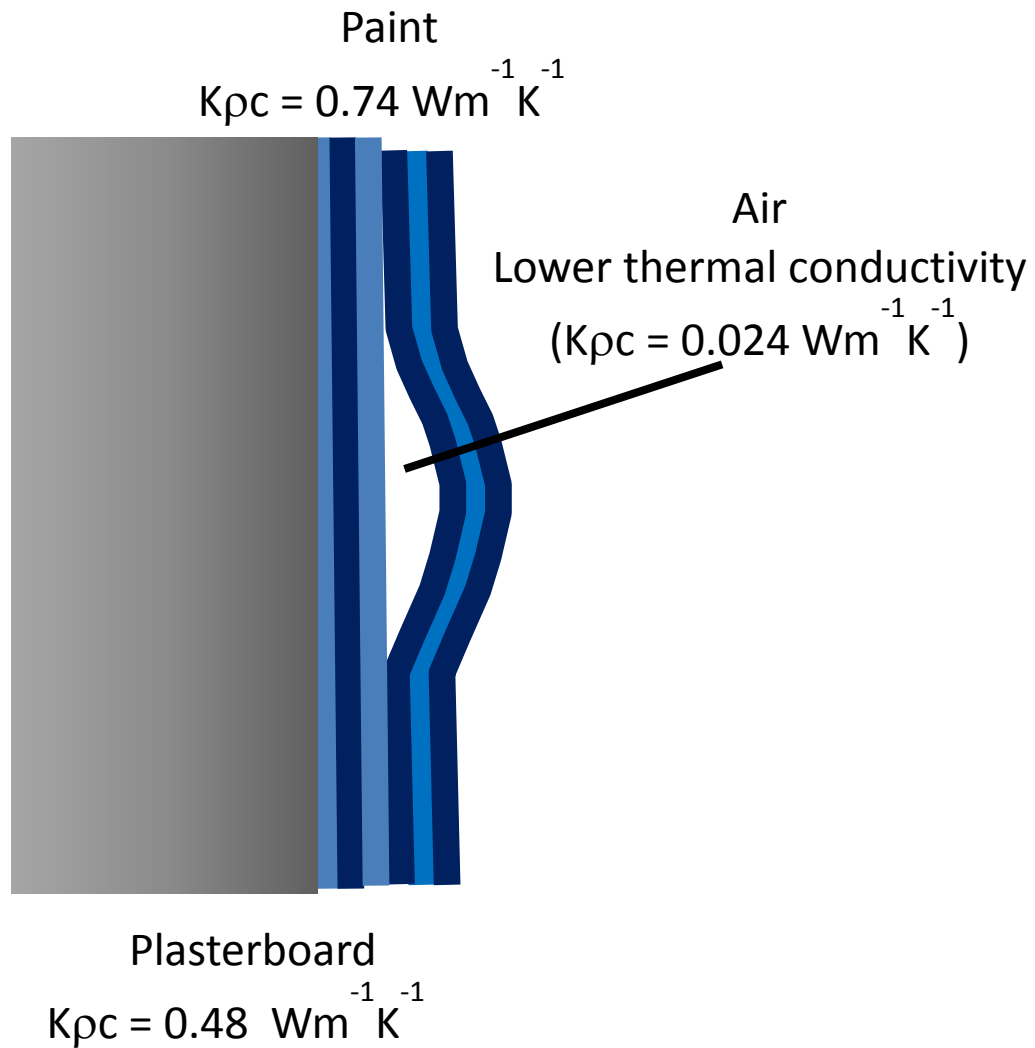
Figure 22 Schematic diagram of paint blistering

Behaviour of multilayer paint systems during heating is difficult to predict, however cases (described in section 1.12.) have shown that the softening, dripping and peeling of paint layers has even caused downward flame spread, igniting combustible materials below the initial flame. Ageing of paint layers between coats - trapping grime and moisture – promotes blistering when heated. The lack of a heat sink encourages ignition as previously described.[63] Research has been carried out to determine the effect of blistering on the time to ignition and flammability of painted Gypsum wallboard. It showed that blistering causes a reduction in time to ignition by a factor of 3 or 4 when compared to a sample with no blistering; surprisingly the burning duration remains unchanged.[64]

Application of a highly effective 'upgrading' fire retardant system over a well adhered substrate may still result in coatings which facilitate flame spread if previous paint layers have been applied over poorly prepared walls.[63]

There are several methods for adhesion testing used by product manufacturers to determine the level of protection required in individual cases. These methods determine the suitability of the existing substrate for over-coating or 'upgrading' with a fire protection coating system. The most common adhesion test is the 'cross method'.[65] This involves a cross being scored into the existing layers deep enough to reach the underlying substrate (e.g. Plasterboard or masonry) using a knife. The blade is then slipped under the paint layers - as close to parallel with the substrate as possible - and paint flakes are prised off the wall. This is repeated across both sides of the original cut in both directions. If paint layers are easily removed and form flakes then the substrate fails the test. Failure of adhesion tests suggest that even the most effective upgrading paint system would offer little or no protection. Underlying layers are likely to de-adhere prior to the activation of the fire retardant coating thus exposing the flammable substrate, maintaining the original fire risk. In these cases stripping of existing layers until a suitably adhered layer is reached is required prior to re-decoration. If no flakes greater than 10 mm can be removed then the substrate meets the minimum adhesion requirement for over-coating with an 'upgrading' fire protection system. Cross hatching and Sellotape methods are also used with a similar outcome.

1.11.3. Heat transfer

During a fire chemical energy is released as heat causing a temperature rise. The rate of heat transfer is measured in Kilojoules per second (kJs^{-1}) or Kilowatts (kW). In the absence of any heat losses, thermal energy is directly proportional to temperature. Heat transfer is an important factor in the analysis of fire as it explains the processes involved such as: vaporisation or pyrolysis of fuel, growth of the fire (propagation, flame spread and remote ignition) and its subsequent damage.[36]

There are several forms of heat transfer, which are described below. Perhaps the most important, with greatest influence on fire protective coating performance - is thermal conductivity.

1.11.3.1. Thermal conduction

Thermal conduction describes the movement of heat from high to low thermal energy regions with no net movement of the substance occurring. Transfer in this way continues until equilibrium is reached, reaching steady state conditions.[66]

Each substance has a thermal conductivity, determined by the composition and properties of the material. The high thermal conductivity of metals is due to the free movement of electrons present in the matrix. Collisions between these electrons allow transfer of thermal energy. In the case of lower thermally conducting solids, such as plaster or wood, heat manifests itself as

increased atomic vibrations which are transferred through the matrix. In the case of foams or intumescent systems, the multi-cellular matrix of voids prevents the transfer of movement of atoms and reduces collisions transferring energy between molecules thus reducing the thermal conductivity of the material. Figure 23 shows a comparison of temperature profiles collected from a high thermal conductivity material ('uncoated') and the reduced thermal conductivity of the same material when coated with two intumescent systems ('system A' and 'system B').

(a)
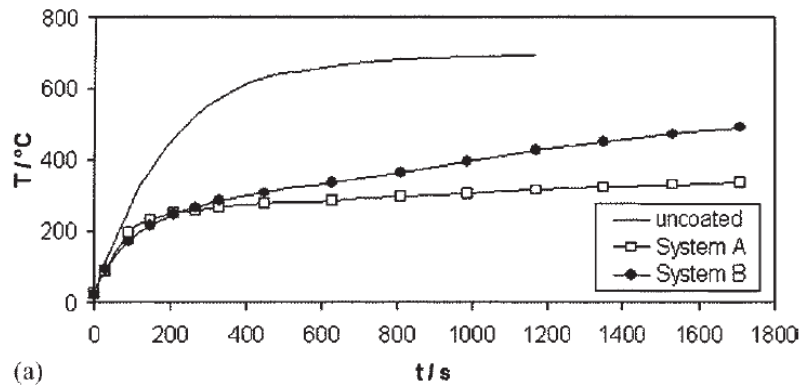
Figure 23 Temperature profiles for two commercial intumescent systems with an initial thickness of 1.0 mm and at a heat flux of 60 kWm^{-2}.[50]

(b)
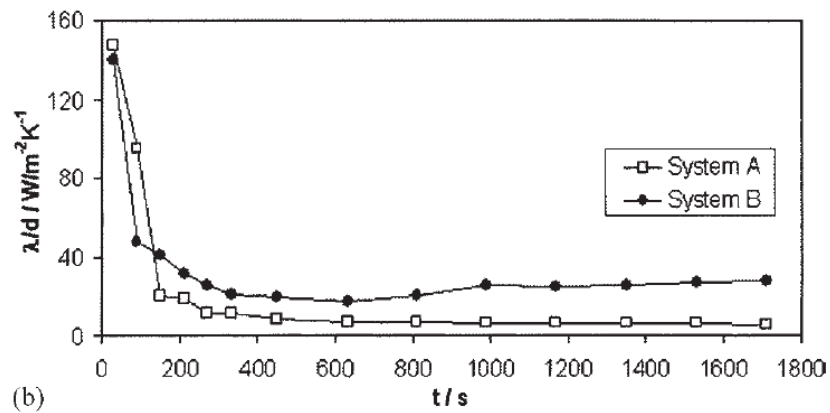
Figure 24 Effective thermal conductivity of the intumescent layer of System A and B with an initial thickness of 1.0 mm and at a heat flux of 60 kWm^{-2}.[50]

Figure 24 depicts the effective thermal conductivity of the two intumescent systems - A and B. The graph clearly shows that the thermal conductivity of the material is greatly reduced as the intumescent coating expands.

Increased temperature results in pyrolysis of polymers as molecules gain enough energy to break bonds and so become liberated from materials surface.

Layered materials are complex; each layer may have different thermal properties. Differences in thermal conductivity may cause unusual heating effects throughout the bulk of the material.

1.12.3.2. Thermal radiation

Thermal Radiation describes electromagnetic radiation (energy consisting of both electric and magnetic fields) that is emitted by a body exclusively in relation to its temperature. Radiation covers a continuous range of wavelengths; the allocation of energy between these wavelengths is dependent on the temperature of the emitter. Very hot objects emit within the ultraviolet spectrum (>2000 °C), but emissions are also present within the visible (glowing white, >700 °C, and red, >1000 °C, hot) and infra-red range.[36]

For fire gases or flames the emissivity is dependent on: flame thickness, radiation occurring from fuel, combustion products and soot particulates. For fire scenarios enclosure fires should be considered, however radiation within an enclosure is complex.[44] Stefan's radiation law states that the total radiation energy (E) per unit time by a black body of surface A is proportional to the fourth power of its absolute temperature as shown by the expression $E \propto T^4$.[67]

1.12.3.3. Thermal convection

The third type of heat transfer is convection. This involves heat transfer through a moving fluid, liquid or gas. The *Convective heat transfer coefficient* describes the ability of heat to be transferred from a moving fluid to a solid surface, for example the heat in the air being transformed to a wall in the case of a fire.

The rate of convection between fluids and solids is dependent on the temperature difference between the two areas. This phenomenon may lead to remote ignition as heat is transported to other areas of the compartment away from the original seat of the fire. Calculation of the heat flux to a target is very important in assessing potential fire damage.

As a fire develops, the small laminar flames give way to better mixed turbulent flames with greater rates of heat release. Under turbulent fire conditions the convective heat flux of a vaporising surface will be less than in the case of laminar flaming conditions due to the flow of fuel gases pushing the hot flame away from the surface. Conversely under laminar flame conditions the flames will be closer to the surface so these flames will display a higher heat flux to their originating surface than turbulent flames.[47]

Figure 25 shows the thermo-physical interaction of heat transfer within thermally thick and thermally thin materials. During combustion of thermally thin materials (such as delaminated paint) thermal feedback occurs from flames on the burning surface onto both surfaces of the exposed paint film, enhancing the burning rate by more than a factor of two. Paint will burn on both surfaces if peeled causing the flame to thicken, increasing the amount of heat transferred

to the fuel ahead mostly convective and radiative.[68] This significantly increases the fire hazard associated with the (two-sided) burning of a thermally thin material. Thermo-physical interactions of flames from either side of the burning material merge producing a uniform temperature throughout the bulk.[69] The higher heat release rate from combustion of such a material would enable rapid flame propagation as the next section of material is more rapidly heated to its ignition temperature, continuing the mechanism over the surface.
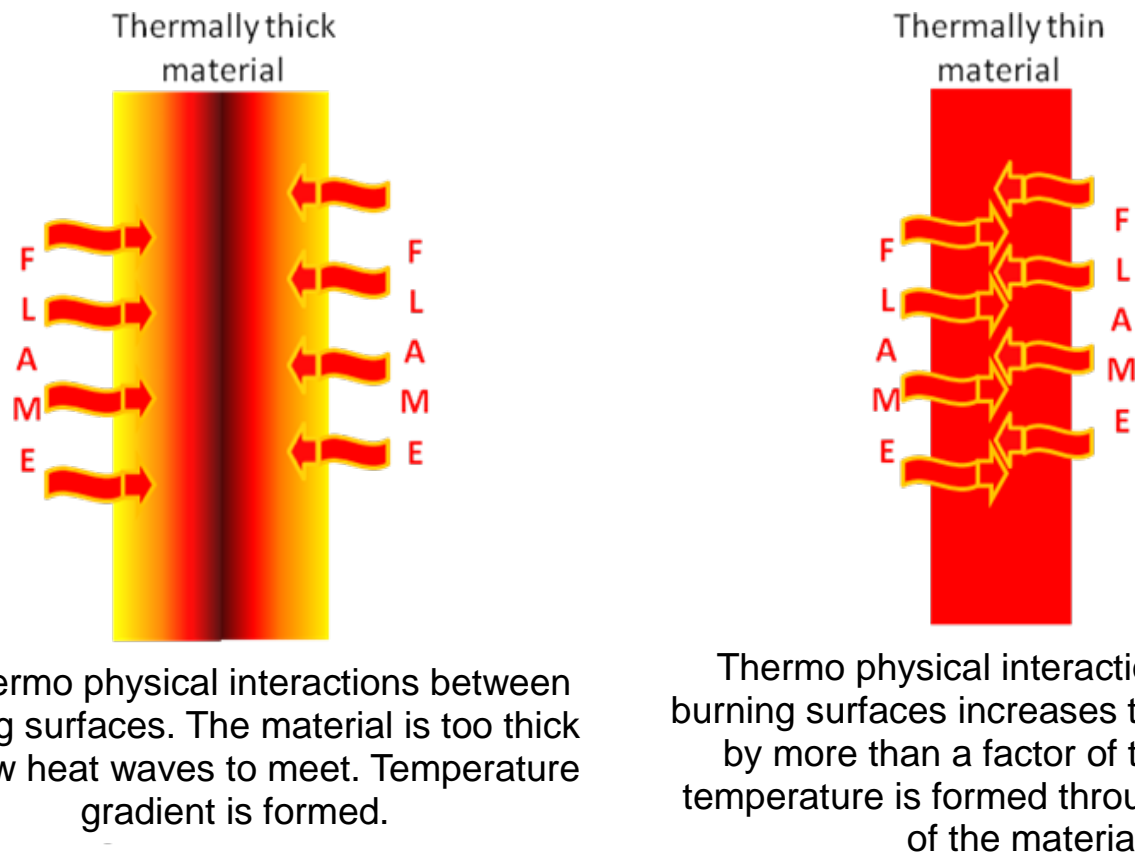
Figure 25 Thermo-physical interaction of heat transfer within thermally thick and thermally thin materials

Unpredictable burning behaviour, and its response to heat, requires coating systems to be performance tested in the same manner as their end use. Worst case scenarios are preferred for consideration even if these situations only occur when a failure of some initial bonding to a nominally protective second surface occurs.[69]

1.11.4. Mechanism of flame spread

Paint finishes on walls and ceilings have a significant effect on the rate and extent of fire development.[70] Individual layers of paint are not usually flammable. The presence of a thin film on a non-combustible substrate – with heat sink properties - does not readily ignite. In some cases the remaining char layer acts to further protect the underlying material.4 However

multiple layers of paint can increase the rate of flame spread across the surface of the wall or ceiling lining involving other compartments located away from the initial seat of the fire.9

Paint flammability is not only dependant on its composition but also the situation in which it is used and becomes ignited. For a flame to propagate temperatures must be reached which allow the material to thermally decompose, releasing combustible pyrolysis products, that are then ignited in the presence of a spark or flame. The flame is only able to be sustained and spread if the feedback of radiant heat to the adjacent material is sufficient to maintain a high enough concentration of combustible volatiles to support the flame. Auto-ignition of these gases is unlikely in domestic cases unless unusually high temperatures are involved (typically 200 °C above piloted ignition temperature).9 However in the presence of an external heat source - such as a small fire in the case of arson or other burning material in a room fire - combustible volatiles can easily become ignited allowing flame spread along any surface generating enough heat to release more volatiles.4

Horizontal flame spread can be considered as a series of repeated ignitions and is relatively slow when compared to vertical. This is due to the slow heating rate of the adjacent material via gas-phase conduction and minimal downward radiation from the flame. Upward flame spread is far more rapid as all three forms of heat transfer contribute as shown in Figure 26. This is the most prominent method of flame spread when considering multilayer paint surfaces.

Polymer

Next ignition zone

Pyrolysis zone

Radiative
Convective
Conductive

Heat transfer
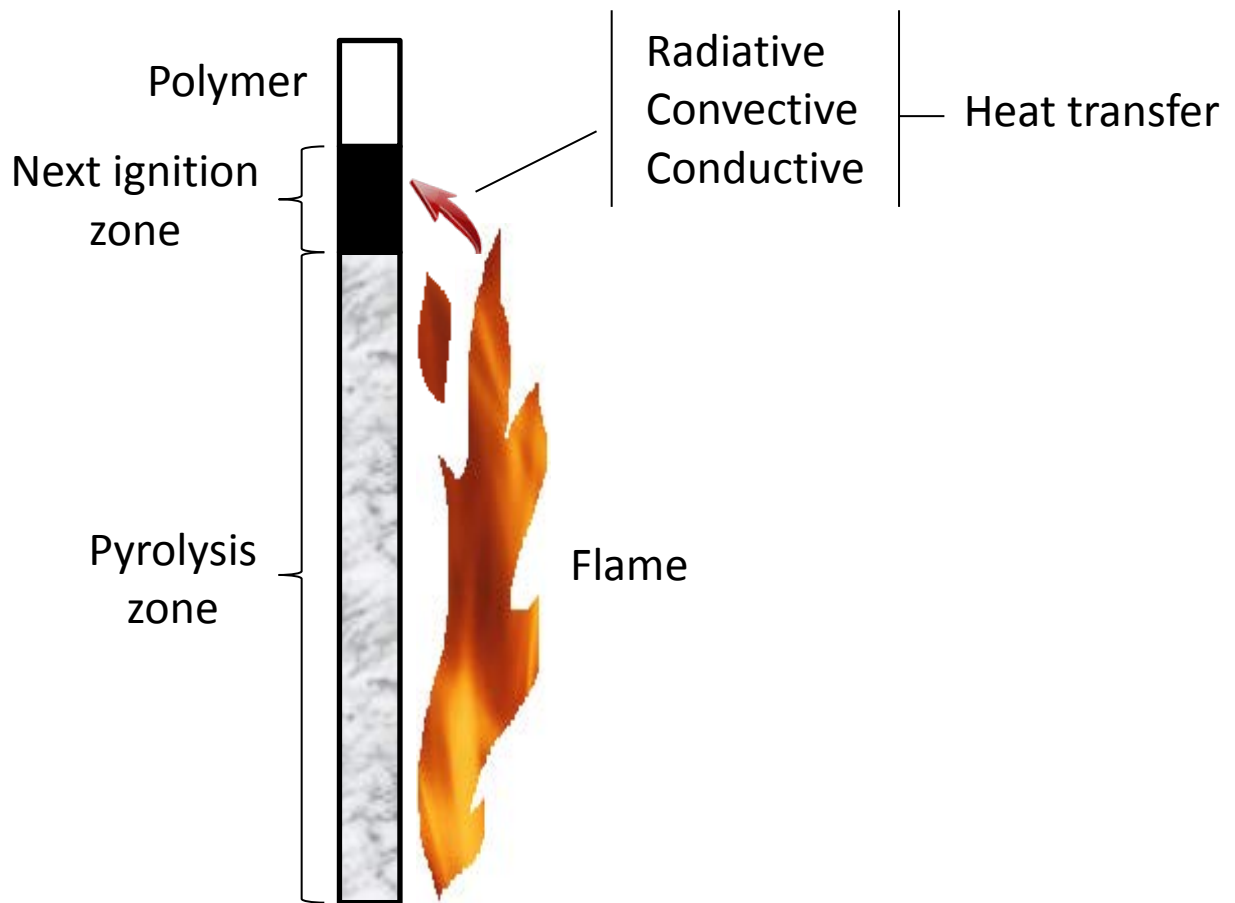
Flame

Figure 26 Schematic of vertical flame spread[31]

Fire investigators are sometimes able to determine the multilayer paint system as the main cause of flame spread due to the patterns of fire debris and smoke distribution on walls and ceilings after a fire of this kind. In such a case the paint displays a pattern, termed 'patching', as some of the paint layers may become loose and dislodged from the wall in the turbulence of the fire, whereas other more well-adhered areas of paint, may remain in situ. Peeled and curled edges of paint, still attached to the wall, increase the rapidity of flame spread due to the thermally thin burning behaviour displayed by such a film.

1.11.5. Temperature of decomposition

Each protective coating varies in mechanism and performance. The main factor determining fire retardant selection is decomposition temperature. For a fire retardant coating to be successful it must have an activation temperature that corresponds to the decomposition temperature of the substrate material it is designed to protect. For example a halogenated species must release the halogen free radicals in the early stages of flaming combustion otherwise the flames will be too big to quench, conversely early release results in wastage of stable free radicals (such as $Br\cdot$ or $Cl\cdot$) prior to the initiation of the flaming reaction. Intumescent formulations must also perform within a tight temperature window. The

softening of the resin must coincide with the decomposition of the spumific (material which decomposes to evolve gas which acts to expand the char e.g. melamine) - evolving the vapours which become trapped in the soft but tacky resin. Vapours must be released at a controlled rate to ensure maximum expansion with no eruption of the intumescent chambers. Carbonifics such as pentaerythritol are incorporated in the formulation to decompose to produce a mass of carbon. Catalysts must perform at the exactly the right moment (formulators often prefer to use auto-catalytic systems for this reason) and the resin must harden to ensure the voids remain trapped in the char residue. The char residue must remain stable at high temperatures ensuring continued protection after the intumescent reaction is complete.

1.11.6. Coating stability and finish properties

Compatibility of components is a big issue. Too many coatings have been proposed which have good fire retardant properties but which are inferior as surface coatings. Water-borne systems are especially difficult to stabilise due to the interaction of ions in solution. Changing one ingredient may lead to adverse effects for can stability, coating appearance, durability or handling.[14]

Physical properties of coatings (such as flow, stability and dispersion of additives) can be determined using rheology.[71,72,73] This method is the science of deformation and flow and is further described in the methodologies section. Rheology experiments reveal information about flow behaviour of liquids and the deformation behaviour of solids. Material behaviour relies on the combination of both the viscous and the elastic portion referred to as the viscoelastic properties. One rheological technique is the parallel plate rheometer, where the sample is forced to flow between stationary and oscillating plates.

There are a range of modes of rheological analysis. The base plate is most commonly flat with the option of the upper-plate being cone-shaped or flat - coining the term 'parallel plate' mode. Parallel plate rheometry was used to gain the results reported later in this thesis.

Parallel plate rheometry is used to define some fundamental parameters of coatings such as flow, viscosity and behaviour under shear. Figure 27 shows some parameters necessary to carry out calculations and analysis of samples. The upper plate with the area A is set in motion by a motor producing shear force F and the resulting velocity v is measured whilst the lower plate remains stationary. The distance between the plates (h) is monitored and the sample is placed between the plates in the gap. Readings can be recorded as long as two conditions are met:

1) The sample adheres to both plates and does not slide or slip along them

2) There are laminar flow conditions (i.e. flow in the form of layers) and no turbulence flow is occurring (i.e. no vortices).
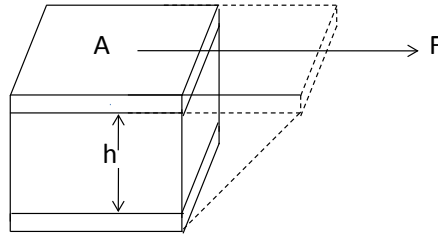
Figure 27 Shear stress schematic using the parallel plate model[74]

Shear stress is an internal force within a material, caused by an external force acting perpendicular to the material. This force makes adjacent molecules within a liquid slide past one another. Shear stress (τ) is given by the force (F) divided by the area (A) and shear deformation (γ) is given by shear (s) divided by the gap (h). Shear modulus (G) is calculated by dividing the shear stress (τ) by the shear deformation (γ).

Viscosity and more commonly reported 'complex viscosity' can be measured using rotational or oscillation tests. Rotational experiments involve the constant motion of the top plate in a single direction throughout analysis whereas oscillation experiments may involve the top plate rotating in one direction then the other.[74] This is the method adopted for this research and introduces a time factor. Shear stress in a time dependant system (τ_A) divided by the shear deformation in a time dependant system (γ_A) gives the complex shear modulus (G*). Phase angle (δ) demonstrate the solidity of the sample. 90° suggests liquid behaviour and 0° suggests solid properties. The rotational and oscillation methods record values including the storage modulus (G') and loss modulus (G") which combine to calculate the complex viscosity (G*) as shown below in Figure 28.
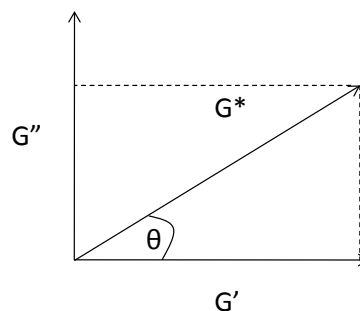
Figure 28 Vector diagram depicting G', G" and the resulting vector G*[74]

G' divided by G" gives the loss or damping factor (tan δ). When tan $\delta < 1$ the sample displays elastic behaviour when tan $\delta > 1$ displays viscous behaviour. All of these parameters can be analysed to assess the coating properties.

Products must also be marketable as commercial products and therefore be user friendly (easy to apply) as well as available in a wide range of colours and finishes which do not compromise the fire retardant properties of the coating.

1.12. Cases of flame spread across multilayer paint surfaces

Several cases have occurred where the mode of rapid flame spread was an unusual phenomenon which could not be explained by the characteristics of the building or its contents. Further investigation has since resulted in the attribution of the fire damage to flame spread across the build-up of multilayer paint. The details of a selection of these cases are outlined below.

1.12.1. King's Cross Underground station

The best known example of rapid flame spread involving multilayer paint finishes occurred on the 18th November 1987 in London's underground system, at King's Cross. The fire began under a wooden escalator and gradually grew in size. 31 people died in the tragedy as fire spread up the escalator shaft (trench effect) and ignited ceiling coverings spreading flame under the ceiling of the ticket hall. The fire took six hours to extinguish and this incident lead to Britain's largest public enquiry. Although several factors contributed to the devastation and much debate still surrounds the findings, examination of the ceiling showed there to be several layers of paint applied.[75] Multiple layers of paint supported rapid flame spread into the ticket hall and along the ceiling causing a fire-ball - described in witness accounts - as the wall and ceiling coverings became de-adhered. Falling debris would have hindered escape and prevented fire services entering. Since this tragedy all underground stations are lined with tiles or cementicious materials to reduce the fire load in such confined areas.

1.12.2. Moston Hospital

Fire hazards are of particular concern where the mobility and awareness of the occupants is impaired. Hospitals and residential care accommodation need to take additional precautions to guard against the risk and hazards of fire.

One of the first cases to highlight this issue was the Moston Hospital fire in the early 1970s. In this case the fire began in one of the patients' rooms at the end of the corridor. Flames had spread along painted walls and ceilings a distance of 50 metres (170 feet) in the three minutes it took the emergency services to arrive. Investigation of samples taken from the hospital corridors showed there to be up to 18 layers of paint which had a 'class 4' flame spread rating. There had been little or no structural damage in this case. While the surfaces of furniture had been scorched the contents were largely untouched by the fire by the time it had been

brought under control.[76] The subsequent investigation determined that in future all corridors and communal areas be treated with fire retardant paint in order to reduce the risk of such tragedies occurring again.

1.12.3. Multi-storey housing blocks

Multi-occupancy housing blocks are amongst the highest risk of rapid flame spread due to multilayer paint systems on stairwells and in communal areas. These areas are also highly susceptible to graffiti and therefore are likely to be re-decorated more frequently to maintain their appearance. They are also prime targets for arson, vandalism and rubbish build-up thus increasing the risk and hazard of ignition and flame spread.

One case illustrating this phenomenon is the Chelsea Gardens terrace flats in London which occurred on the 13th September 2007. The flats were built circa 1930; there were two flats on each floor accessible via a single stone staircase with a solid central stone wall. The fire was confined to the stairwell and fire damage was evident from the third floor upwards, involving wall and ceiling coverings as well as front entrance doors. It was believed that the cause of the fire was arson the fire originating from a metal drum outside one of the flats. Paint had burned off the walls - in some cases up to 15 coats of paint[77] - revealing the substrate; similar burn patterns were present on the ceiling. In this case there were no floor coverings so it was concluded that the rapid flame spread within the stairwell was due solely to flame spread across multilayer paint layers on the walls and ceilings.

Figure 29 depicts an image collected from the scene during the investigation. The wall and underlying paint layers where delamination has occurred are clearly shown. The green paint layer is exposed in areas of better adhesion whilst overlaying layers delaminated and fell away during the fire. Areas of blistering are evident where moisture trapped between layers is heated at a rapid rate causing the paint to be pushed off the substrate rather than being allowed to be slowly expelled through the top layers.

Figure 29 Image of paint build-up

A similar incident occurred in the 1990s when a settee was ignited at the base of a spiral stone staircase. In this incident the flame rapidly spread upwards and caused trapped victims to jump from third floor windows in an effort to escape. It was concluded that the rapid flame spread was due to the delamination of multiple layers of paint from the walls and ceilings,[78] causing the same 'patching' as in previous cases and depicted in Figure 30.

On the 13th November 1981 a fire broke out in one of the rooms of a multi occupancy building in which nurses - working at the Victoria Hospital, Fife - were resident. Flames were able to spread through ventilation ducts involving all but the ground and top floors. Limited information can be obtained from analysis of fire debris after such incidents due to the relatively thin layer of paint and because burning is so rapid and complete.[79] Investigation of replica ceiling panels demonstrated the effect of a burning film of paint, shown in Figure 30 below. Falling debris and burning materials caused localised ignition of paint on the corridor wall. Flames spread up to and along the ceiling consuming much of the paint at the top of the walls in the corridor.[80]

Figure 30 'Patching' of paint, characteristic burn pattern of this mechanism of flames spread

Kings Norton was the first identified case of fire spread across multiple layers of paint in the West Midlands. The fire was deliberately started outside the block of flats and was able to spread into the building via an open fire door. Flames spread up the main access stairwell of the three storey block. The flats had been recently renovated with fire doors and re-painting of the access hall and landing. The extent and range of flame spread was significantly reduced in this case accredited to the fewer coats of paint on the walls in the higher floors of the block. The mechanism of flame spread occurs by bubbling of the paint and lifting from the substrate material allowing the thin film that is exposed to be burned and propagate flame transfer along the wall; this is triggered by localised high temperature.[81]

Shropshire House was an arson case (9th September 1994), started by application of a naked flame to some paper debris. Flames were then able to spread up to and including the second floor by ignition of the paint layer in the stairway.[82]

There are many more cases of rapid fire spread in multi-occupancy buildings; Lambeth, London, (multi-storey apartment block); Birmingham, (low rise apartment block) and Edinburgh apartment block to name but a few.5 In each case the scenario is much the same. A fire is started in a stairwell or communal corridor and due to the build-up of decorative paint layers applied to maintain appearance flames are able to spread rapidly across the surface of the wall. This results in flame spread to other areas of the building and limiting chance for escape. Composition of such paints are unknown and not properly monitored therefore when

combustion occurs little is known about the flame spread, smoke released or toxicity of the fumes emitted during the fire and inhaled by people trying to evacuate.

1.12.4. Prisons

Another case where fire protection is of the utmost importance is within prison facilities where arson attacks are regular and the mode of escape must also be monitored so occupants are able to get to safety without escaping from the facility altogether. Regulations have been outlined specifying strict procedures in the case of a fire as well as precautions to be included during the construction of such facilities to maintain the highest level of protection possible.[83]

Ohio State Penitentiary held a total of 4,300 prisoners. A fire in 1930 killed 329 people. It was a possible arson case started in an adjacent scaffold. Fire rapidly spread onto the roof due to the interior finish on the walls. The guards were delayed in opening the cells allowing the prisoners to escape. The fire department arrived two minutes after the alarm was raised but on arrival some of the inmates attempted to cut the hose used to quench the flames. Most of the fatalities in this case were in the upper two tiers of the 6-storey prison.[84]

1.12.5. Ships

The high thermal conductivity of the steel bulkheads used aboard ships has in the past allowed the paint on the opposite side of the steel to be ignited spreading the fire between compartments. When several layers of paint have been allowed to build-up, flaking has aided the flame spread to lower levels. Another cause for concern is the use of aluminium paint on rusty iron as a corrosion inhibitor. Any physical impact upon such a surface has the risk of a violent thermite reaction occurring between the aluminium and ferric oxide. This releases a large amount of heat which could add to the severity of the flame or cause paint on the opposite side of a fire enclosure to ignite. Should this occur in an atmosphere containing combustible materials this could lead to ignition and/or explosion. 4

The SS Morro Castle was a luxury cruise liner built in the 1930s shipping passengers from New York City, USA to Havana, Cuba. On the 8th September 1934 a fire broke out in a storage locker. Fire rapidly spread and within half an hour the ship was engulfed in flames. A total of 137 fatalities were recorded making this incident a catalyst for improved shipboard safety. Ship design and crew practice were questioned. The lavish decorations caused a major fire hazard and produced a lot of thick black smoke when burned preventing passengers making a successful escape. Poorly trained crew became panicked and confused, even commandeering lifeboats without saving passengers first. One of the crewmembers said that it had been common practice to re-paint the ship to maintain its appearance and to occupy crewmen. It was these thick layers of paint that inevitably lead to the increased flammability of the ship.

Flammable strips were reported to have broken off during the fire thus aiding rapid flame spread.[85]

1.12.6. Nightclubs

In 1942, 492 lives were lost in a fire at the Cocoanut Grove nightclub, Boston, USA and further 160 were injured. Flames were reported to have spread so fast that some victims collapsed at their tables. The nightclub exceeded the safe maximum number of occupants allowed by more than 400 people. Fire doors were welded shut to avoid patrons leaving without paying and the main exit - a revolving door - became jammed trapping over 200 victims crushed in the rush. The National Fire Protection Association (NFPA) report claimed that "the interior, with its low ceilings, combustible wall and ceiling finish and flammable decorations was actually a death trap, but the building structure itself was 'fire proof'."[86]

1.12.7. Hotels

120 lives were lost in an early morning fire in the Winecoff Hotel in Atlanta, Georgia in 1946, 168 others were injured. The hotel was built in 1913 with no fire protection systems installed. The internal location of open stairway rapidly spread the flames aided by the coverings of paint and wallpaper. Window shutters prevented guests escaping, there was no fire escape, and the fire department notification was delayed allowing the fire to spread even further before it could be brought under control, and extinguished 6 hours later. This was reported to be the worst US hotel fire of the 20th century.[84]

1.13. Previous research into fire hazard of multilayer paint – Warrington Fire

After many cases of rapid flame spread due to multilayer paint had been reported, Warrington Fire Ltd undertook a study of the effect of multilayer paint on burning behaviour. It was reported that the spread of flame was far more rapid across surfaces made up of more than one type of paint. Layers which had been built up slowly over long periods of time rather than those applied at regular and frequent intervals increased flammability. Each specimen was prepared to have a build-up of 14 layers of paint prior to testing to BS 476: Part 6[29] and BS 476: Part 7.[30] Flame spread results are depicted in Figure 31. Increase in flame spread is attributed to the ageing of the paint layers and the build-up of dirt between subsequent layers. Delamination and deterioration is exacerbated by ageing between coats; exactly as would happen in routine maintenance decoration.2
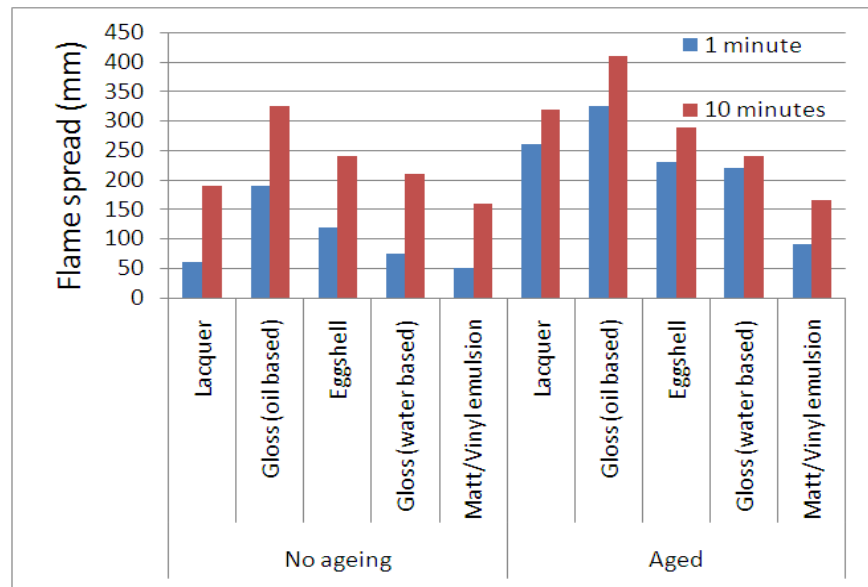
Figure 31 Multilayer paint flame spread, comparison of aged and non-aged samples[87]

1.14. Legislation and building regulations

The amount of fuel in a building before the contents and occupiers arrive is known as the 'fire load'. The factors considered when determining the level of fire protection required in a building are as follows:

- the size of the building

- the other fire hazards it contains

- the mobility and awareness of the occupants

- other fire systems within the building, such as sprinklers, fire doors etc.[88]

Building regulations and legislation are put in place to obtain a minimum level of fire safety in newly constructed buildings; these restrictions govern the design stage prior to occupation by any residents. Approved Document B states that the lining of a building should be able to resist the spread of flame over its surface.

Internal linings, referring to materials lining any partition wall, ceiling or other structure shall:

(1) Resist the spread of flame over the surface;

And

(2) if ignited, have a rate of heat release which is reasonable in the circumstance.6

The Regulatory Reform (Fire Safety) Order (2005)7 (RRFSO) is applicable to dwellings where rooms are rented. Through the use of risk assessments the RRFSO requires all fire hazards in a building to be identified and appropriate measures taken to reduce these risks. This reform places the responsibility on designers and contractors to communicate any fire risks to building

managers or owners. This requirement applies throughout the lifetime of the building – sustaining the fire protection - those failing to abide by the reform may face criminal prosecution.

1.15. Fire retardant additives and methods of protection

The type of fire retardant chosen and the mechanism by which it provides protection will significantly affect the coating performance. Optimum performance for specific applications can be ensured by careful selection of fire retardants included in the coating formulation. There are a wide range of fire retardants to choose from some of which are described in this section.

Bulk polymers are not usually inherently fire retardant and in some cases a more 'flammable' polymer is preferred due to other characteristics; fire retardant additives may be incorporated into the polymer to improve the fire retardant properties. There are several fire retardant technologies at the disposal of the chemist to achieve these results.

1.15.1 Intumescent – Ammonium polyphosphate and Diammonium phosphate

Intumescent coatings offer passive protection against heat and flame spread.[89] On heating an intumescent formulation swells 50 to 200 fold. A multi-cellular structure of low thermal conductivity voids is formed, which is an efficient heat barrier,[90] the outer surface of which comprises a charred layer acting as a physical barrier to the influx of radiant heat and oxygen. A reduction in the amount of flammable volatiles that can escape from the material's surface, as well as the amount of diffused oxygen to reach the materials surface, is recorded when these systems are used. In general intumescent formulations require three components.

1) An acid source, usually containing poly(phosphoric acid) or other acid which promotes char formation, these form an impermeable semi-solid vitreous layer during combustion such as ammonium polyphosphate (APP).

2) A carbonisation agent (carbonific), which is readily dehydrated by the acid initiating char formation such as pentaerythritol (PER).

3) A blowing agent (spumific) which decomposes, releasing a gas that expands the polymer and forms a swollen multi-cellular layer, such as melamine.[91] This swelling occurs due to the gases released following heating becoming trapped in the viscous fluid char layer and increasing the volume of the coating which must be tough enough to withstand the violent drafts arising in a fire.[14] The optimum intumescent formulation will react on heating to produce large amounts of predominantly non-combustible residue.

These systems have been widely used for protection of steel structures where it is essential to keep temperatures below 550 °C to prevent softening and collapse.[92,93]

Table 2 Examples of intumescent materials[94]

Acid release agents	Ammonium dihydrogen phosphate	Decomposition Temp 417 °C
	Ammonium polyphosphate	215 °C
	Melamine phosphate	300 °C
Carbonifics	Pentaerythritol	
	Starch	
Spumifics	Dicyandiamide	210 °C
	Melamine	300 °C
	Urea	130 °C

Additives with slightly altered properties can be substituted within the formulation to optimise performance. Some examples are listed in Table 2 and include urea which can replace melamine to improve water solubility. The resin system itself can be swapped or copolymerised to ensure the optimum softening temperature is achieved to coincide with the release of vapours from the decomposing material. Finally different fire retardant additives can be selected lowering the activation temperature of coatings. High activation temperatures will not protect multilayer paint substrates (or the Warrington blue board testing substrate – having an onset temperature of decomposition of only 170 °C) but there are some intumescent additives that cover much lower temperature ranges. Diammonium polyphosphate (DAP) is one such additive; it is a water-soluble ammonium salt that is produced by reacting ammonia with phosphoric acid; its formula is $(NH_4)_2HPO_4;$ and it has a decomposition temperature of 155 °C. DAP also acts to lower the pyrolysis temperature of materials (decreasing maximum mass loss rates) and increases the amount of residual char produced, this is especially useful in the protection against wildfires as these properties also have the effects of reducing the amount of fuel available, leading to the formation of a firebreak. For this reason DAP is a major component in popular outdoor fire fighting formulations. Early evolution of CO_2 at a high rate can act as a fire suppressant. In addition the production of volatiles at lower temperatures has a negative effect on the fire propagation.[95]

Decomposition reactions of diammonium phosphate are listed below.

$(NH_4)_2HPO_4$ (s) $\rightarrow NH_3$ (g) + $NH_4H_2PO_4$ (s)   (155-160 °C)

$NH_4H_2PO_4$(s) $\rightarrow NH_3$ (g) + H_3PO_4 (l)

$2 H_3PO_4$ (l) $\rightarrow H_2O$ (g) + $H_4P_2O_7$ (l)   (170-190 °C)

$H_4P_2O_7$ (l) $\rightarrow 2 H_2O$ (g) + P_2O_5 (s)[96]
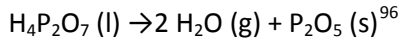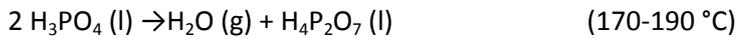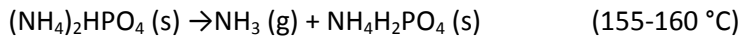
Studies have also shown that encapsulation of DAP allows more successful incorporation into polymer matrices. [97] Research suggests synergism with other fire retardants such as magnesium hydroxide where heat release rate, total heat release and total mass loss were all significantly reduced. Smoke production was also lowered as the level of fire retardants used increased.[98]

Thermo-analytical studies show that DAP decomposes at 87 °C into $(NH_4)H_2PO_4$ which further decomposes at 145-167 °C into phosphoric acid and ammonia (NH_3). At 216 °C the decomposition continues into final products P_2O_5 and H_2O. In the process of flame retardancy of wood the phosphoric acid esterifies polysaccharidic parts of the wood and water is released. Phosphates promote the dehydration reaction of wood and increase the char residue.[98]

However several intumescent paints are commercially available but there are many compromises to be made. Intumescent action may be compromised to ensure optimal coating properties or vice versa. The high loadings required to achieve the necessary level of performance (leading to viscous paints and textured finishes) and the water soluble nature of these agents (cannot be used on external surfaces without sealing) restricts their use until a more suitable formulation can be devised.[14]

1.15.2. Char promoters - phosphorus

Char promoting additives have also been incorporated into protective coatings. The formation of char on the surface of a substance protects the material from the harsh fire environment. The char can re-radiate heat transmitting less to the bulk material or substrate. It acts as a barrier inhibiting the diffusion of oxygen to the surface of the material and the diffusion of pyrolysis volatiles into the flame zone. This effect is often achieved using phosphorus additives which decompose to produce phosphoric acid. The main consideration to be assessed when using these products is the structure of the char. A weak or brittle char will simply fall off the substrate in the fire turbulence whereas a stable char - if predominantly organic - will only be stable up to 500 °C, where a residue with significant inorganic content may exist up to 1000 °C. Pore size also affects the level of protection offered by the char layer. Char promoting additives include ammonium polyphosphate (APP), nitrogen based additives whose

advantages include low smoke yield,[105] such as melamine cyanurate, and expandable graphite and elemental phosphorus.

1.15.3. Silicon

Fumed and precipitated silica are often used as reinforcing fillers, however they do not display chemical fire retardancy as they do not decompose to evolve water or carbon dioxide or promoting cross-linking acids etc. Instead research has shown that they act to lower heat release and mass loss rate in the condensed phase.[99,100,101] Schmauks[99] suggests a positive interaction of silicon dioxide and glass fibre in PA6 and EVA and Gardelle et al.[102] have done work utilising polysilazanes (silicon-nitrogen backbone polymers) in coatings.

1.15.4. Halogenated fire retardants – Bromine and Chlorine

Another approach includes incorporation of substances that produce flame quenching radicals during decomposition. These are examples of fire retardants acting in the gas phase whose mechanism are further described in Figure 32. Halogenated materials incorporated into materials decompose at similar temperatures as the bulk material[103] to release free radicals (Cl· and Br·) at the same time as the pyrolysis products are undergoing fission. This leads to the formation of highly reactive radicals ($CH_3\cdot$, H· and OH·). These radicals are taken up by more stable atoms, Cl or Br which escape from the flame zone unreacted, therefore preventing the branching chain reaction of the flame and aiding flame extinguishment.[104] Limitations include increased smoke production and toxic product evolution and persistence in the environment resulting in environmentalists arguing for the elimination of halogenated flame retardants.

$$CH_4 + X\cdot \rightarrow HX + CH_3$$
$$H\cdot + HX \rightarrow H_2 + X\cdot$$
$$OH\cdot + HX \rightarrow H_2O + X\cdot$$
$$\ddot{O} + HX \rightarrow OH + X\cdot$$
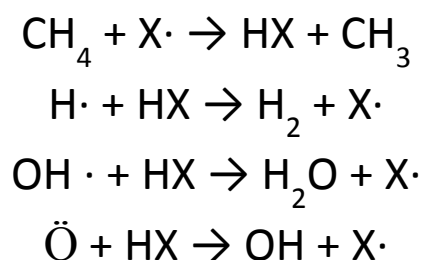
Figure 32 Free-radical flame quenching mechanism

Additives are also available which synergise with halogenated fire retardants to promote the transition of halogens into the gas phase - the most prominent of which is antimony oxide. Antimony oxide also acts as a char promoter and is a very successful fire retardant synergist.[14] The primary limitation remains the price (£9 per kilo), ecotoxicity and production of toxic gas during combustion which means their use in today's market is diminishing as more environmentally friendly, less toxic additives are sought.

1.15.5. Nitrogen

Nitrogen compounds are widely used and growing in popularity due to their environmental benefits over other systems. Nitrogen fire retardants decompose to yield non-combustible and poorly burning vapours. When incorporated with phosphorus compounds this is coupled with a high char yield action. This synergism results in a very promising system whose efficiency is higher than other fire retardant additives in the same loading - particularly metal hydroxides - as measured by the cone calorimeter.[105] In a fire nitrogen compounds display low toxicity provided that conditions do not lead to HCN formation (under-ventilated) - due to the absence of dioxin and halogen acids, as well as reduced smoke evolution. They are also widely used because of their compatibility with other formulations; they do not interfere with stabilisers incorporated into many materials. Melamine phosphates and dicyandiamide compounds are used in intumescent paints however their high decomposition temperature may limit their use for the application discussed in this thesis.

1.15.6. Inorganic fire retardants – Metal hydroxides

Magnesium and aluminium hydroxide make effective fire retardant fillers due to their endothermic decomposition mechanism releasing water (shown below in Figure 33) which has both a cooling and diluting effect. These additives are also smoke suppressants and are a popular choice as they are ecologically and environmentally friendly - there is no evolution of hazardous by-products. Problems arise using these additives in coatings as relatively high loadings (50-60 %) are required to achieve the desired level of fire retardance which is likely to compromise the mechanical properties of the coating during manufacture and reduce the quality of the decorative finish.

$$Mg\,(OH)_2 \rightarrow MgO + H_2O$$
$$2Al\,(OH)_{3\,(s)} \rightarrow Al_2O_{3\,(s)} + 3H_2O_{\,(g)}$$
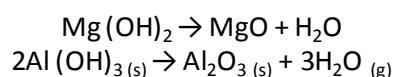
Figure 33 Decomposition products of metal hydroxide fire retardants

Aluminium hydroxide (ATH) is a popular fire retardant due to this multi-facetted action. Decomposition leads to a 35 % mass loss of water with an endotherm of 1170-1300 J g^{-1}. Applications are restricted due to the low temperature of decomposition - around 180-200 °C - which makes it unsuitable for many polymers due to their high processing temperatures. Polymers must also decompose at similar temperatures to ensure that the water is released simultaneously alongside the decomposition products of the decomposing polymer.[106] Magnesium hydroxide finds a wider range of applications due to its slightly higher decomposition temperature (300-330 °C) but this is too high for use in fire protection over multilayer paint surfaces. Another magnesium carbonate mineral filler of interest is

nesquehonite ($MgCO_3 \cdot 3H_2O$). This gives off 71 % by mass as carbon dioxide and water with the slightly higher enthalpy of decomposition of 1750 Jg^{-1} but at the lower decomposition temperature of 70-100 °C.[107] This parameter has greatly restricted its use and development but means it is ideal for use in systems that must act prior to the decomposition of cellulose substrates (such as wood and paper) or multilayer paint surfaces.

Other minerals used as fire retardants include: hydromagnesite and huntite, which are available together as a naturally occurring mixture.[106,108]

1.15.7. Nanoparticles

Recently incorporation of nanoparticulate additives has been proposed. The major concern with these materials is dispersion. Particles are so small current methods of dispersion are too crude to ensure complete separation of particles. Sometimes materials using these additives produce a greater amount of smoke and it is not yet clear whether the nanoparticulates remain in the residual char or the inhalable soot particle fraction of fire effluent. Examples of such additives include montmorillonite, hectorite and saponite and carbon nantubes.

1.16. Anti-graffiti coatings

Anti-graffiti coatings are commercially available and provide easy-clean surfaces for use in local authority buildings where the risk of graffiti is high. These systems often have a high gloss finish of low surface energy to which nothing will adhere[109] allowing easy cleaning, and are solvent based so that cleaning with water is possible. Unfortunately it is these properties which also make the paint more flammable and likely to promote rapid flame spread.

There are several well-established mechanisms used to achieve an easy–clean surface without compromising the fire-retardance. The incorporation of silicon into the coating in the form of Si-C bonds, which are strong, makes these structures highly thermally stable.

Fluorine, when bonded to carbon has very low surface energy; this is the main reason for its use in stain-proof fabric and non-stick cooking utensils as well as anti-graffiti coatings. As Fluorine is the smallest and most electronegative of the halogens the C-F bond is very chemically stable, which outlines its success as a low flammability, anti-graffiti coating.[110] Disadvantages of using fluorine in this way are the toxic fumes, which include hydrogen fluoride gas, evolved during its decomposition or combustion.

Caution should be taken when incorporating anti-graffiti additives to a fire retardant system as the effect may be unexpected and even detrimental to the fire retardant performance. It may

be preferable to use a two part system of a fire retardant undercoat combined with an anti-graffiti topcoat to ensure optimum performance from both.

Building owners often want to impart several properties within one protective coating such as a high level of protection against fire with additional anti-graffiti properties. In such cases all required properties must be adequately combined into one coating; or a multi-coat system is adopted. The fire retardant coating used in conjunction with a low flammability anti-graffiti top-coat maybe providing a 'class 0' rating, which also allows graffiti to be removed.[61] A range of different systems with varying fire protection mechanism and fire retardant additives will be investigated and assessed using the screening test methods previously discussed in this thesis.

CHAPTER 2. METHODOLOGIES

This research endeavours to understand and ultimately protect multilayer paint build-up from preventing a fire hazard. However, complete corridors cannot be used for testing and therefore understanding of the thermal decomposition and burning behaviour of the paint layer build-up on a small-scale is required in order to successfully predict the hazard in a whole corridor. An understanding of flaming behaviour and its relation to thermal decomposition is needed, and in particular, knowledge of heat transfers during burning.

The main tools for such analyses used in this work are: repeatable sample preparation using high shear mixing equipment; thermogravimetric analysis to understand thermal decomposition of materials; cone calorimetry to investigate the burning behaviour with relation to heat release rate, time to ignition and length of burn time; Bunsen burner tests to investigate coatings properties such as spreading and adhesion as well as extent of fire protection performance on a wooden substrate; BS 367 (adapted) to investigate the thermal conductivity of materials and influence of exposure to a naked flame on coatings performance; BS 476: Part 6 to assess the performance in the standard fire test.

Test substrates were chosen which would accurately represent the final end-use application (Warrington blue board or plasterboard coated with two layers of nitrocellulose paint), or which would allow the optimum test measurement to be recorded (aluminium sheet substrate for thermal conductivity analysis or a wooden splint for Bunsen burner analyses).

Halogenated systems were investigated (FR120 and FR121) to assess the capability of halogenated systems to protect multilayer paint. Intumescent formulations were investigated due to their combined fire protective properties of preventing heat transfer to the substrate, reducing oxygen and pyrolysis product diffusion across the carbonaceous barrier thereby giving an increased level of protection. Intumescent systems are predominantly formulated for the fire protection of steel substrates but often activate at too high a temperature to protect multilayer paint, therefore systems designed for protection of cellulose materials were also analysed. Commercial samples provided a bench-mark with which other formulations must compete and provided a formulation which could be adapted to meet the fire protection performance required for multilayer paint build-up. The majority of the research into adapted coatings was aimed at substituting the APP for DAP to reduce the activation temperature of the intumescent action. However, this created problems with compatibility and stability so a variety of solvent systems were also assessed in an effort to reduce this effect.

Reproducibility was ensured by completing all tests in triplicate and reporting the average of the three results. Errors were reduced by using the same standard methods throughout this work and all unavoidable errors are reported in the data shown. During formulation and testing, one variable was changed at a time to establish its effect on the complete performance of the coating. Standard methods and best laboratory practices were adhered to in all possible instances.

2.1. Sample preparation

Samples were prepared in the same manner on each occasion to ensure consistency and reproducibility.

2.1.1. Existing formulations

Where possible, 'Pure Brilliant White' systems were used to reduce variation in results due to pigment interaction and loading. Formulations were thoroughly stirred prior to use to ensure no settlement of components. All samples were coated using the same type of roller and allowed complete drying time in a low temperature oven - at 30 °C for at least 2 days - to ensure loss of all solvents prior to further investigation.

2.1.2. Novel formulations

Calculations were done to determine the mass of additive needed to obtain the required loading. The solids content of the starting resin must be known, if not this must be determined by assessing the mass loss on drying. The expression used to determine the mass loss of solids in any given formulation is given by Equation 1.

Equation 1

$$S = \frac{m}{100} x\, Sc$$

Where:

S is mass of solids in unit volume of resin

m is the mass of unit volume of resin

Sc is the solids content of the resin, in %

Calculation of mass of additive to be added to gain given loading is given by Equation 2.

Equation 2

$$a = \frac{S}{100} x\, l$$

Where:

a is the mass of additive to be added

S is mass of solids in total volume of resin

l is the required loading, in %

An empty standard paint can was placed on a balance, tared and the required mass of resin added. Separately, the required mass of additive was weighed as calculated using the above expressions (Equation 1 and Equation 2). The resin portion was mixed using a Dispermat high velocity mixer whilst the required mass of additive was introduced. This was mixed continuously until complete dissolution or dispersion occurs. Each coating was subjected to preliminary testing; dispersion can be observed by spreading a thin layer of the coating onto a substrate (in this case a metal spatula). By thinly spreading the coating any lumps or areas of poor dispersion are apparent. Observations of coating properties are recorded including stability observation recordings. Poor stability is easily observed as the coating will clump, agglomerate, become gritty and separate out leaving water and sediment due to settling and incompatibility of components. Stability is of great importance as fire retardance is of limited use if the coating does not function primarily as a coating. Cans are then sealed and labelled.

2.1.2.1. PVDC resin plus fire retardant additives

The range of reported loadings for intumescent and fire retardant additives varies from 1 % to over 60 %.[111] The majority suggest loadings in the region of 10 % which provided the starting point for the majority of the novel formulations investigated. This would be altered in later experiments depending on the coating properties and protection performance. Exceptions include Laponite which was added to give a 1 % solid content loading due to its thickening properties.

PVDC resin was thought to be an optimal starting point due to its inherent fire retardancy (due to the chlorine content) and its compatibility with many additives due to its stability. Expandable graphite is an intumescent additive which swells on heating to produce a thick residual char layer; this layer was thought to provide a protective barrier to the substrate material if loadings could be reached which would yield sufficient intumescent activity without compromising flow properties or colour. Noflan and Bizon are currently used in coating and textile applications due to their flame inhibiting and char producing properties. Noflan is an organophosphorus material based on complex alkyl phosphonates. It acts as a flame inhibitor preventing ignition. Bizon is an example of a halogen-free organophosphorus material, which is expected to increase char stability of the residue when used in combination with other fire retardant additives. Urea, melamine, PVA and PVAc were selected due to their decomposition

mechanisms yielding stable carbonaceous char structures which would aid protection of the underlying material. Craftglue was selected for similar reasons however when combined with 1% borax solution also cross-links to form a more stable, yet water soluble, compound which was expected to further enhance char formation and stability therefore increasing protection. Laponite was thought to increase char stability at higher temperatures and so incorporated in small amounts to investigate action and compatibility.

Additives were sourced from various companies: PVDC from Integra Coatings Ltd, Expandable graphite (TEG 160 and TEG 315) from Minelco; Noflan (complex of Alkyd-Phosphonates) and Bizon (Ammonium Alkydphosphonate) from Firestop; Urea and Melamine formaldehyde were prepared in the laboratory; Laponite from Rockwood; PVA and PVAc from Sigma Aldrich; EVA based Craftglue from an arts and craft supplier.

The details of coating formulations are listed below in Table 3.

Table 3 Formulation information for PVDC resin samples

Sample	Loading	Resin	Resin Mass	Additive Mass
PVDC	0%	PVDC	0g	0g
Noflan	10%	PVDC	650g	39g
TEG 315	10%	PVDC	650g	39g
Melamine Formaldehyde	10%	PVDC	650g	39g
Bizon	10%	PVDC	650g	39g
Urea Formaldehyde_1	10%	PVDC	650g	39g
Urea Formaldehyde_2	10%	PVDC	650g	39g
EVA based Craftglue	10%	PVDC	650g	39g
Melamine Powder	10%	PVDC	650g	39g
PVA	10%	PVDC	650g	39g
PVA and Borax	10%	PVDC	650g	39g
PVAc	10%	PVDC	650g	39g
TEG 160	10%	PVDC	650g	39g
Laponite	1%	PVDC	650g	3.9%

2.1.2.2. DAP and APP based intumescent formulations

Intumescent systems were formulated based on a standard intumescent recipe shown in Table 4 - taken from Malucelli et al.[112] Adjustments were made to tailor this formulation for multilayer paint application. Attempts were made to lower the activation temperature of intumescence by making changes to the formulation.

Table 4 Standard intumescent formulation[112]

Ingredient	Amount in Formulation (%)
Water	18.0
APP	24.0
Melamine	8.0
Pentaerythritol	8.0
Resin	25.5
Titanium dioxide	11.5
Other	5.0

DAP, APP, melamine, urea and pentaerythritol were all sourced from Sigma Aldrich. Titanium dioxide and base resin systems were supplied by Integra Coatings Ltd with the exception of the Dulux and Wickes vinyl silk, matt and gloss paints which were purchased from B&Q.

Reduction in activation temperature was made by replacing APP with DAP and urea replaced melamine. Details of coating formulations are listed in Table 5 and Table 6. These samples were produced as described above with the resin being mixed at high speeds during the addition of the solids all of which are added simultaneously over a period of less than ten seconds.

Table 5 Formulation details for Dulux vinyl silk samples

Sample Name	VsAMP	VsAUP	VsDMP	VsDUP
Resin Type	Dulux vinyl silk	Dulux vinyl silk	Dulux vinyl silk	Dulux vinyl silk
Solids Content	37%	37%	37%	37%
Resin Mass	120g	120g	120g	120g
DAP Mass	X	x	48g	48g
APP Mass	48g	48g	X	x
Urea Mass	X	16g	X	16g
Melamine Mass	16g	x	16g	x
Pentaerythritol Mass	16g	16g	16g	16g

Dulux vinyl silk was the chosen resin system for these formulations as it is based on PVA copolymer emulsion which is listed as the resin of other successful intumescent formulations. Furthermore, as described earlier, PVA resins have favourable coating characteristics. By using a stable formulation as the base resin it was believed compatibility issues would be reduced and changes in behaviour can be directly related to the corresponding change in additives.

Table 6 Formulation details for Wickes vinyl silk and vinyl resin samples

Sample Name	WAMP	WAUP	WDMP	WDUP	VrAMP	VrDUP
Resin Type	Wickes Vinyl Silk	Wickes Vinyl Silk	Wickes Vinyl Silk	Wickes Vinyl Silk	Vinyl Resin	Vinyl Resin
Solids Content	50%	50%	50%	50%	50%	50%
Resin Mass	200g	200g	200g	200g	185.2g	185.2g
DAP Mass	x	X	30g	30g	x	72g
APP Mass	30g	30g	x	x	72g	X
Urea Mass	x	10g	x	10g	x	24g
Melamine Mass	10g	X	10g	x	24g	x
Pentaerythritol Mass	10g	10g	10g	10g	24g	24g

Wickes vinyl silk and vinyl resins were chosen as these use vinyl copolymer emulsions similar to those used in the more successful commercial system (Magma Prime (clear)). Vinyl resin contains no other additives such as fillers, pigments or stabilisers therefore the fire retardant action of the intumescent additives can be assessed in isolation.

2.1.2.3. Oil and solvent based formulations

Oil and solvent based samples were investigated due to stability problems with DAP in water-based formulations. Destabilisation of the emulsion causes separation of water and gelling of remaining components resulting in poor coating properties which are further discussed in section 5.3. Analysis of oil and solvent based samples also enables assessment of the suitability of the various screening test methods for non-water-based samples. The details of these samples are listed in Table 7.

DAP, APP, melamine, urea and pentaerythritol were all sourced from Sigma Aldrich.

Table 7 Formulation details for oil and solvent based samples

Sample Name	VDP	VDU	VDM	GDP	GDU	GPM
Resin Type	Varnish	Varnish	Varnish	Gloss	Gloss	Gloss
Solids Content	65%	65%	65%	65%	65%	65%
Resin Mass	200g	200g	200g	200g	200g	200g
DAP Mass	39g	39g	39g	39g	39g	39g
APP Mass	X	X	x	x	x	x
Urea Mass	13g	X	x	13g	x	13g
Melamine Mass	X	13g	x	x	13g	x
Pentaerythritol Mass	x	X	13g	x	x	13g

Clear varnish was chosen as the oil based sample and gloss as the solvent alternative. Identical intumescent formulations were used for comparison with the water-based examples allowing any variation in performance to be attributed to the alteration in resin system.

2.2. Characterisation methods

Characterisation of existing products provides a starting point on which to base new formulations and suggests possible solutions to common issues. There are many methods by which to characterise samples. Some are as simple as magnification to identify structures and properties of the samples (microscopy and SEM). Others rely on the decomposition of the sample and analysis of decomposition products (TGA analysis, GC-MS, pyGC-MS, ICP-MS and NMR). Some provide elemental analysis (EDAX and CHN analysis) whilst others identify functional groups (d-ATR). Those more specific to coatings investigate physical properties such as stability and flow (rheology).

2.2.1. Microscopy

The technique was used to view and compare samples with details too small to be seen with the naked eye, with digital camera attachment.

2.2.1.2. Sample

Warrington blue board samples were only available at excessive cost. Since the ultimate success of the project depends on being able to fire protect this coating, it was necessary to find out what its composition was, in order to prepare my own. Microscopy samples were prepared by removing flakes of paint from the two types of board and viewing through the microscope.

2.2.1.3. Procedure

Paint flakes were mounted vertically so that layer composition of paint flakes can be viewed using the microscope. A camera, attached to the top of the microscope, allows collection of images at 10 times magnification; these could then be compared to reference samples to determine the composition of the flakes.

2.2.2. Thermogravimetric (TGA) analysis

TGA analysis allows the investigation of decomposition mechanism, mass loss rate and amount of residual char after heating in air and inert atmospheres.

2.2.2.1. Instrumentation

A schematic diagram of a typical TGA set up is shown in Figure 34 and is made up of four main component parts: a furnace, an electro balance, a data acquisition device and a computer.

Balance

Gas in

Pivot

Suspension

Counter Weight

Furnace

Sample holder

Thermocouple

Gas out
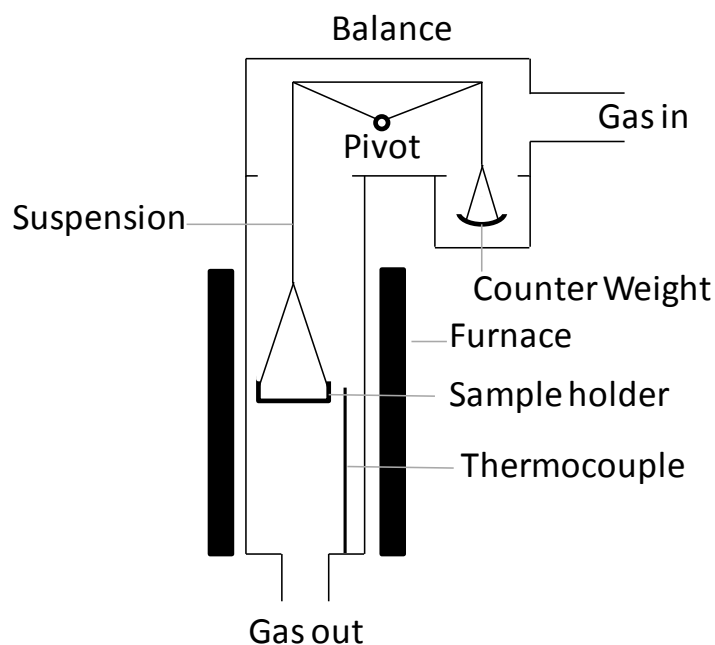
Figure 34 Schematic diagram of TGA apparatus

2.2.2.2. Calibration

Calibration can be carried out using known weights to confirm mass readings and standard materials to ensure temperature accuracy. Gases were controlled using a flow meter prior to each experiment, with flow verified using a calibrated gas burette.

2.2.2.3. Sample preparation

Samples were dried films and powders of mass 10 mg ± 0.5 mg. Film samples consisted of one piece of uniform size and thickness. In the case of highly intumescent samples mass was reduced to compensate for high expansion of the sample.

Samples included various fire retardant additives and resins as well as existing and novel formulations (made up of resin and additive mixtures). All samples were oven dried at 30 °C for at least two days to ensure loss of all solvents prior to experimentation.

2.2.2.4. Procedure

TGA experiments were undertaken in both air and nitrogen atmospheres using a Polymer Laboratories Ta 1000 (PL-TGA) apparatus. Temperature profiles ranging from 20 °C to 900 °C at heating rates of 2-10 °C min^{-1} were adopted. Experiments were carried out in triplicate to ensure repeatability.

2.2.3. d-ATR FTIR

Diamond attenuated total reflectance-Fourier transform infra-red (ATR-FTIR) is a technique for the analysis of surface materials. It relies on the passing of infra-red radiation through an infra-

red transmitting crystal, such as diamond, with a high refractive index. A schematic diagram of typical apparatus is shown in Figure 35.

Specimens are placed onto the stage over the diamond and pressure applied to ensure intimate contact with the crystal. Infra-red radiation is then passed through the crystal and penetrates the sample surface infinitely along with an evanescent wave; this is a penetrating electromagnetic field whose intensity quickly decays as it moves away from the source. This wave penetrates only a few microns (0.5 -5 µm) beyond the surface of the diamond into the sample surface. The evanescent wave is altered or attenuated in the region of the infra-red spectra coinciding with regions where the sample absorbs energy. This attenuated energy is passed back to the infra-red beam. At the output end of the ATR element the infra-red radiation is directed towards a detection source.
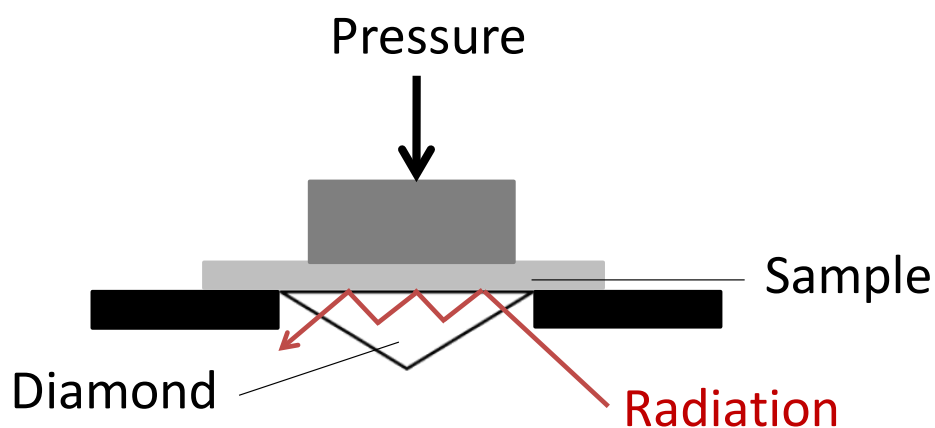
Figure 35 Schematic diagram of the ATR apparatus

2.2.3.1. Instrumentation

The apparatus consists of: ATR with diamond crystal and an FTIR.

2.2.3.2. Sample

Samples of the various coatings were dried into thin solid films using an oven at 30 °C. Additives were predominantly in powder form.

2.2.3.3. Procedure

Background data is collected with the gate (which holds the sample in place) closed but without the sample present. Sample data was collected by placing the sample film or powder over the diamond window in the centre of the stage and closing the sample gate. This is then secured in place to compress the sample and ensure maximum contact with the diamond. The software collects the data and subtracts the background signal to produce a transmittance

spectrum. Peaks are compared to library spectra to determine the functional groups present in the specimen.

2.2.4. SEM-EDAX

Scanning electron microscopy is a surface imaging technique and provides detailed images of physical properties and structures at a micron level. This technique exploits the shorter wavelength of electrons over photons to produce higher resolution images. The beam of electrons, channelled through electromagnetic lenses and focussed on the surface of the sample, on impact backscattered or secondary electrons are ejected and converted to a signal which produces an image. This process is carried out under vacuum to prevent the electron beam producing filament from burning out, gas molecules colliding with the electron beam, and the formation of other compounds as gas molecules interact with the electron beam.

Elemental analysis is carried out using energy dispersive x-ray (EDAX). During the period in which the electron beam is focussed on the sample surface, electrons are excited to a higher energy level leaving a gap in the electron shell. This gap is then filled by an outer shell electron. The difference in energy between the higher energy and lower energy shell is released in the form of an x-ray. This is then detected and analysed. X-rays are characteristic of the atom of the element from which they were expelled.

In combination, these two techniques provide a magnified image of the sample surface, as well as elemental composition (elements present and the ratios in which they occur).

2.2.4.1. Instrumentation

The SEM apparatus is shown in Figure 36 and consists of: an electron source, scanning electron microscope (SEM) and EDAX analyser.
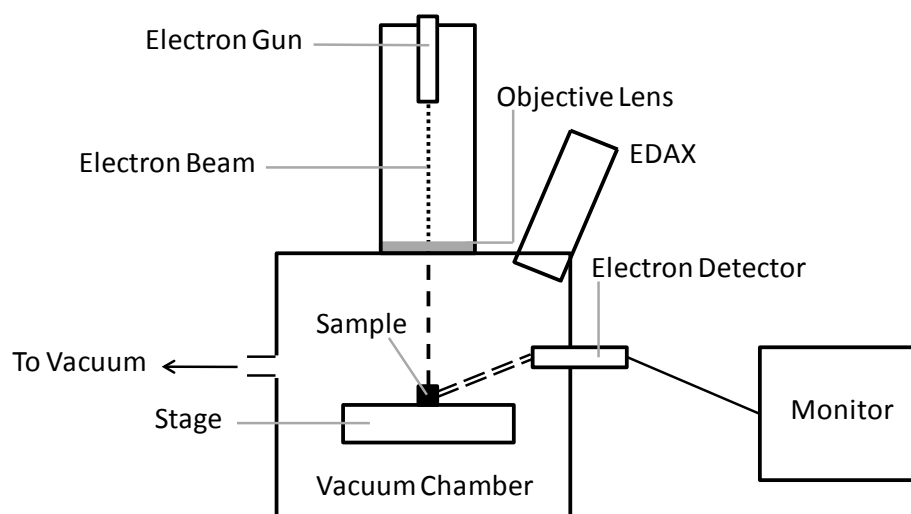
Figure 36 Schematic of SEM EDAX apparatus

2.2.4.2. Sample

Various forms of the Magma Prime (clear) sample were subjected to SEM analysis. Samples consist of: char residue collected from samples subjected to heating in the cone calorimeter at a heat flux of 35kW/m^2; dried films of resin samples; dried precipitate collected from the separation of commercial samples in water; residue samples.

2.2.4.3. Procedure

Samples were placed on a self-adhesive carbon pad, adhered to a peg and inserted into the sample stage. With the door closed the vacuum pump is switched on and the pressure within the chamber set to 0.5 torr. Once reached, the high voltage beam is switched on. The software allows focussing of the image in addition to contrast and brightness alterations. A snapshot tool allows the image to be recorded and saved. Once the beam is focussed, EDAX can then be used to collect a spectrum of elements within the sample. Peaks can be assigned and quantified using the 'quant' tool within the software and again these can be exported for use elsewhere.

2.2.5. CHN analysis

CHN analysis allows the carbon, hydrogen and nitrogen composition of samples to be determined and the ratios established.

2.2.5.1. Sample

A small sample of Magma Prime (clear) was oven dried at 30 °C into a film and then ground down into a fine powder using a pestle and mortar.

2.2.5.2. Procedure

This sample was sent away for analysis to the University of Manchester.

2.2.6. ICP-MS

Inductively coupled plasma mass spectrometry (ICP-MS) is a technique used for multi-element analysis at part per trillion levels. Samples are decomposed to individual atoms in high temperature argon plasma and analyzed based on their mass to charge ratios. An ICP-MS can be thought of as four main processes including: sample introduction and aerosol generation, ionization by an argon plasma source, mass discrimination, and detection.

2.2.6.1. Instrumentation

The ICP-MS apparatus is shown in Figure 37 and consists of: nebuliser, argon plasma "flame", vacuum pump, mass spectrometer and detector.
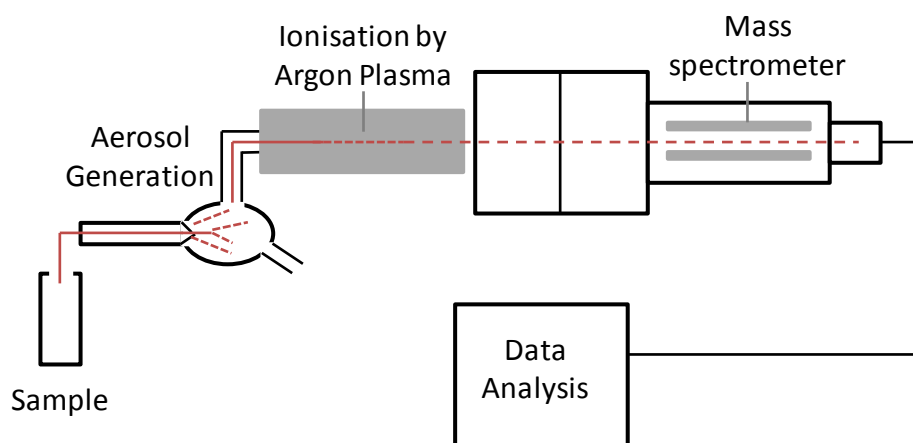
Figure 37 Schematic of ICP-MS apparatus

2.2.6.2. Sample

A sample of Magma Prime (clear) was digested in nitric acid in a microwave prior to analysis by ICP-MS.

2.2.6.3. Procedure

The sample is inserted into an analysis tube and inserted into the auto sampler. The software is then used to set the parameters of the analysis. The sample is run against several references in order to quantify the elements detected. Results are reported in the form of a graph and peaks can be assigned and quantified using the software package.

2.2.7. GC-MS/pyGC-MS

Gas Chromatography coupled with Mass Spectrometry (GC-MS) allows separation and analysis of a mixture of volatile compounds. When samples are pyrolysed prior to analysis using Pyrolysis GC-MS (pyGC-MS) decomposition products can be qualified and quantified. Knowledge of decomposition products provides information of decomposition mechanisms and assesses thermal stability of materials.

2.2.7.1. Instrumentation

The instrument consists of the three main components: a pyrolyser, a gas chromatograph and a mass spectrophotometer.
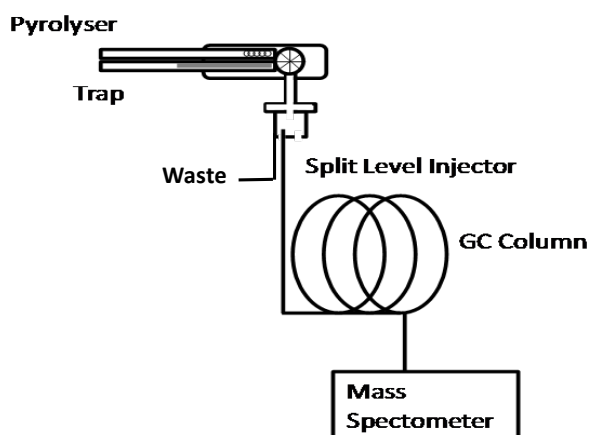
Figure 38 Schematic diagram of pyGC-MS apparatus[113]

A schematic of the pyGC-MS is shown above in Figure 38. All experiments reported in this thesis were carried out using a Perkin Elmer Turbo Mass GC/MS system coupled with a CDS pyroprobe 5200.

2.2.7.3. Sample

Samples were dried paint flakes of existing formulations - Magma Prime (clear) - oven dried for at least two days to ensure the loss of all solvents. Flakes were held in quartz tubes 25 mm long and 1.9 mm internal diameter with quartz wool plugs inserted at each end to prevent loss of sample during analysis.

2.2.7.4. Procedure

Quartz capillary tubes containing samples are inserted into the platinum heating coil within the pyroprobe. Heating rate and method are pre-selected. A temperature range was selected, determined by the decomposition mechanism investigated in the TGA analysis graphs reported in later chapters.

2.2.7.5. Interpretation

Identification of compounds and chemical structures of pyrolysis products is supported by the NIST library mass spectra.

2.2.8 Temperature Programmed Parallel Plate Rheology

This method is widely used in the paint and coatings industry to investigate physical properties of resin systems and formulations. Application of a constant force during heating allows assessment of material expansion by monitoring changes in gap measurement. By controlling

the amount of force applied and measuring the extent of deformation of the sample complex viscosity and softening temperature can be determined. Restrictions with this method include; lack of speed of the movement of the top plate being unable to keep up with the intumescent activity; constant force can restrict the amount of intumescence or crush residual char once intumescence is complete; heat supplied from the furnace creates a temperature gradient within the sample and therefore expansion is often sideways in preference of vertically; adhesion between solid samples and the parallel plates is often difficult to maintain causing fluctuations in the initial readings prior to the softening of the sample.

2.2.8.1. Instrumentation

The equipment is made up of three main components: motor, parallel plate geometry and a furnace. The apparatus is shown in Figure 39. All data reported in this thesis were collected using an AR200 rheometer from TA Instruments.
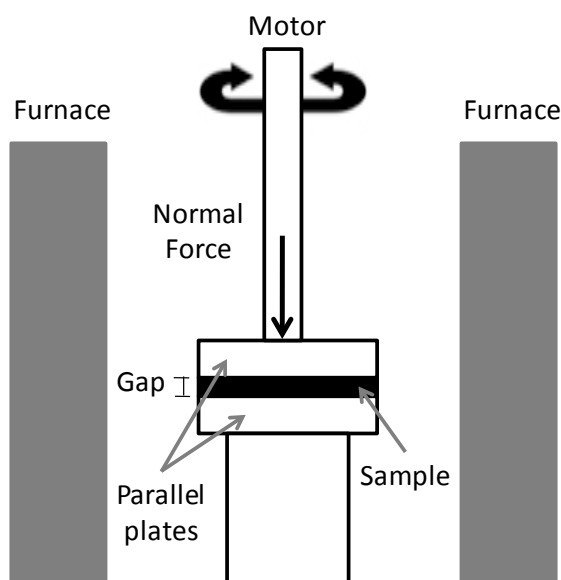
Figure 39 Schematic diagram of rheometry apparatus

2.2.8.2. Sample

Samples comprise of a solid disk of 25 mm diameter formed from the drying of base resin and formulation systems. Disk thickness varies depending on the viscosity of the material but cannot be in excess of 10 % of the diameter of the sample.

2.2.8.3. Procedure

Samples are inserted between the two parallel plates and the required method parameters set using the software. For resin samples, an oscillation method is selected using a temperature range determined by reported decomposition temperatures. For complete formulations an oscillation method was selected with a constant normal force to determine the changes in complex viscosity and gap measurement.

70

2.2.8.4. Interpretation

Parameters such as complex viscosity (η^*), gap measurement (μm), storage and loss modulus and delta (degrees) can be compared and assessed using the 'Rheology Advantage Data Analysis' software package.

2.3. Flammability screening test methods

As previously discussed, large-scale and standard laboratory tests are costly in terms of time and resources. Therefore, small-scale screening test methods are required to rapidly assess coating performance during formulation and prior to assessment in the standard fire tests. Screening test methods chosen for investigation and development in this thesis are outlined below.

2.3.1. Fire retardant action during exposure to a naked flame – Bunsen burner

This method was chosen as it is rapid, low cost, requires no specialist equipment and can be carried out directly after mixing. This method instantly gives an indication of performance regarding flame spread, adhesion and level of intumescence during exposure to a naked flame. However, it is merely a comparative observation technique and therefore rather subjective.

2.3.1.1. Instrumentation

Apparatus is set up as shown in Figure 40 and consists of: a Bunsen burner and wooden splints on which coatings are applied.
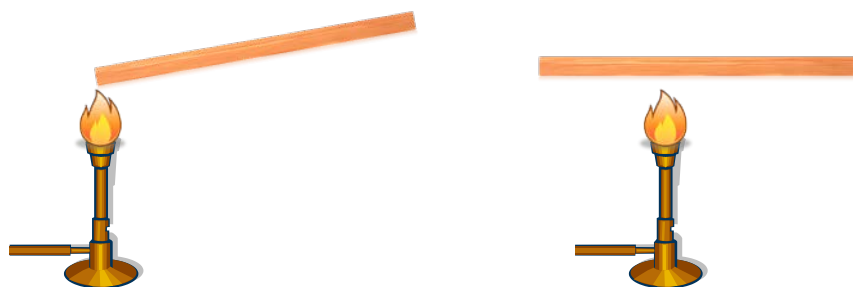
Figure 40 Diagram of Bunsen burner experiment apparatus

2.3.1.2. Sample

Wooden splints are coated in specimen formulations and excess removed to achieve an even coverage. Samples are oven dried at 30 °C to ensure all solvents are removed prior to exposure to the Bunsen burner flame.

2.3.1.3. Procedure

The Bunsen burner flame is set to a known and constant height of 10 mm ± 1 mm and applied to the end of the splint - angled at 20 °. Secondly the flame is moved to the centre of the horizontally orientated splint. Observations such as extent of flame spread, ignition of sample

or substrate, extent and nature of intumescence, adhesion of coating and char are recorded and compared between samples. Experimentation is carried out in triplicate to ensure repeatable results.

2.3.2. Cone calorimeter with embedded thermocouple

The second method is a more in-depth analysis of the burning behaviour and protection level given by the coating. The cone calorimeter is used as a radiant heat source and a type K thermocouple is embedded within the sample to record the temperature profile of the substrate-coating interface. Though important factors such as flame spread and adhesion properties are ignored this method will more accurately assess and quantify combustion parameters.

2.3.2.1. Instrumentation

The apparatus is shown below in Figure 41 and includes: a conical electric heater (10-100 kW m^{-2}), a load cell, spark ignition source, a paramagnetic oxygen analyser, specimen holder, a CO/CO_2 analyser, a heat flux meter, an exhaust gas system, gas sampling apparatus and data collection and analysis system.
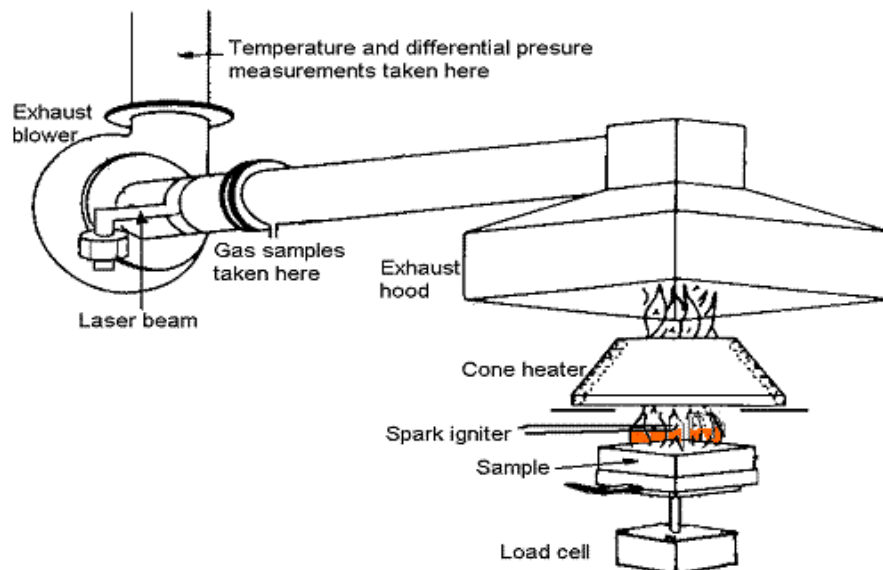
Figure 41 Schematic diagram of the cone calorimeter

2.3.2.2. Calibration

The cone colorimeter is calibrated each day before any tests are carried out. Initially the silica gel and soda lime drying columns are checked and replaced if any discolouration is observed. The refrigeration tap is opened to allow any collected water to drain out and this is returned to

the closed position prior to the start of the test. The 'Conecalc' software is initiated on the computer. Ensuring the extractor fan is turned off; the differential pressure transducer (DPT) and methane are set to zero. Next the load cell, cold trap, ignition and pump switches are all turned on. Air flow through the cone calorimeter is then set to 150 cm^3 s^{-1} and the fan is switched on and adjusted to a mass flow reading within the duct of 30 g s^{-1} and the volume flow at the orifice plate is 24 dm^3 s^{-1}. The Balston filter within the cone is checked to see if it needs replacing by allowing a short burst of nitrogen to pass through the fume duct, if the oxygen analyser responds within 30 s the filter does not need to be changed.

CO/CO_2 analyser – Ensuring that the pump and calibration gases are off, the CO/CO_2 "radio button" is selected on the computer. The calibration button (cal) on the front panel of the cone is pressed to automatically zero the apparatus before zero is selected on the computer. The CO/CO_2 calibration gas is switched on at a flow rate of 1.6 dm^3 min^{-1}. Once stabilized the calibration option is chosen and the CO component selected, when 'calibration ok' is displayed, the span button is selected on the computer, this displays an actual concentration which is stored by the software. Then the procedure can be repeated for CO_2.

Oxygen analyser – The air flow through the cone is manually reduced to zero using the flow meter regulator on the front panel of the cone. Nitrogen is passed through the cone at the flow rate of 150 cm^3 s^{-1} and a pressure no greater than 10 psi. Once the reading is stable the paramagnetic analyser and computer are set to zero. The nitrogen valve is switched off and air is once again allowed to flow through the cone at a flow rate of 150 cm^3 s^{-1}. Once stable the span is adjusted to read 20.95 %, span is selected on the computer and the readings are stored.

Laser Smoke Photometer – The opaque card is inserted into the laser side of the photometer and readings are allowed to stabilise, zero is selected on the computer. The card is removed and the shutter closed before selecting balance on the computer. Calibration is completed using a 0.8 and 0.3 optical density filter, once the readings have been checked, and the interference values are correct, calibrate is selected on the computer.

Orifice Flow Constant – The methane burner is inserted into the holder and the ignition arm positioned over the burner outlet (this should be sparking). High purity methane is passed through the cone at a pressure of about 10 psi and the valve on the cone switched on. The methane should ignite within 5 s. Once the flame is travelling through the cone heater adjust the flow of methane to 5 kW as the net heat of combustion of methane is 50 x 10^3 kJ kg^{-1}. Calibrate is selected on the computer allowing it to calculate the value of C (the orifice flow constant). This value should fall between 0.040 and 0.046 and therefore read between the two

73

red lines on the graph on the computer. After allowing time to equilibrate the green radio button is selected on the computer, thus storing the data.

Cone Heater Irradiance – Making sure that the shutters are closed and there is an insulating board protecting the load cell, the cone heater is turned on and temperature increased in stages of 200 °C until the required heat flux is obtained. For most experiments reported in this thesis a heat flux of 35 kW m^{-2} is used. Making certain the heat flux meter has water flowing through it (the back is cold to the touch); it is inserted into the holder with the meter in the centre of the radiant heat source. The shutters are opened to obtain a reading of the radiant heat flux; the temperature is then adjusted to get the required heat flux. This is allowed to stabilise and recorded by the computer.

Load Cell Calibration – Calibration of the load cell is carried out using known weights to determine if the cone and computer readings are comparable. Mass range is adjusted so the maximum is slightly above that of the heaviest sample (including the holder). "Menu" is selected on the load cell control panel until it reads OT.SC.OF. The 'min' button is pressed to obtain a Read 1 value of 0000. Next the menu button is selected to gain a reading of OUTPUT1; this should also have a value of 0000. Menu is selected again to alter the read 2 value to be the maximum mass. Press menu again to read OUTPUT2 which is adjusted to a value of 10.0 v. Pressing the menu button a final time will save any changes that have been made. This will be reflected in the readings on the computer.

PMMA Calibration – This calibration step should be carried out on a weekly basis using a standard sample of black PMMA. The temperature should be set to approximately 730 °C, to obtain an irradiance of 50 kW m^{-2}. If this irradiance is not obtained at this temperature then the temperature of the cone is altered until it is.

2.3.2.3. Sample

Samples were prepared on 100 mm x 100 m square plasterboard plaques of 12 mm thickness which are twice coated with blue nitrocellulose paint – this is to simulate the burning behaviour of the coating on the standard test substrate material (Warrington blue board). Samples are allowed to dry completely in a 30 °C oven for several days prior to analysis. The protective coating for analysis is then applied over the top of this flammable substrate. Three coats of protective coating were applied with two days drying time in between.

Samples include: reference paint systems, existing coating systems and novel formulations which are both intumescent and non-intumescent in nature.
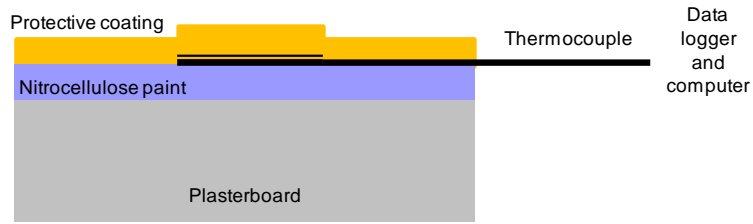
Figure 42 Schematic diagram of cone plaques with plate thermocouple mounted

Initially samples plaques were prepared with copper plate (type K) thermocouples mounted at the interface between nitrocellulose and protective coating layers. However, several problems arose. Firstly, even using the thinnest plate thermocouple available, the surface finish was raised in the location of the thermocouple as it was thicker than the protective coating layers applied as shown in Figure 42.
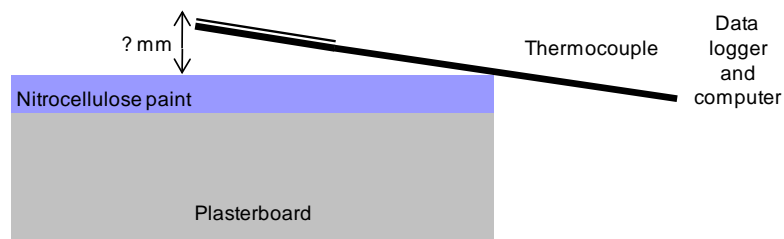
Figure 43 Schematic diagram of cone plaques with lifted thermocouple mounted

Secondly, once the protective coating had been completely combusted the plate thermocouple would lift off of the sample surface giving significant error as the temperature was recorded several millimetres above the sample surface, as shown in Figure 43.

This was overcome by mounting a spot-welded wire thermocouple through the centre of the plasterboard from beneath the sample as shown in Figure 44.
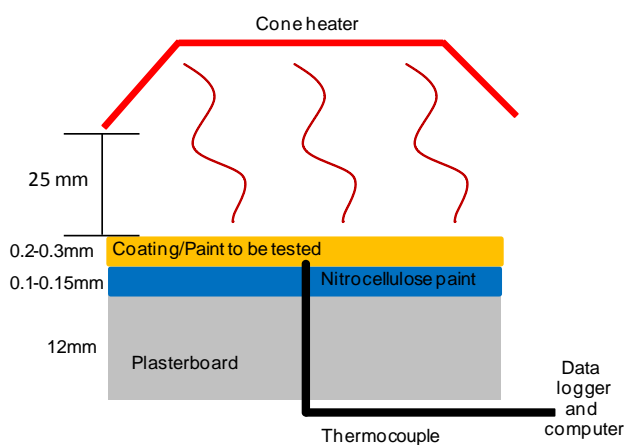
Figure 44 Schematic of sample prepared with embedded thermocouple

Plasterboard of thickness 12 mm was cut to size (100 mm x 100 mm) and edges were sealed by coating with 50:50 water: matt emulsion mix, then oven dried at 30 °C for at least two days prior to the recording of mass and thickness measurements. Boards were then painted with two layers of nitrocellulose paint (2 g wet film mass) and allowed to thoroughly dry in a 30 °C oven. A second set of mass and thickness measurements were taken. A 2 mm hole is drilled into the centre of each plaque and a type K thermocouple secured in place with the thermocouple tip level with the sample surface. Three layers of sample coating are applied; each allowed 24 hours drying time before subsequent layers are applied. The final mass and thickness recordings are taken before experimentation. A schematic of the sample composition is shown in Figure 44.

2.3.2.4. Procedure

To begin a new test, 'run' was selected on the computer and all test details were entered, including sample name, thickness, mass and cone heater irradiance. With the shutters firmly closed, the sample holder was inserted onto the load cell and once stabilised, 'tare' is selected to set the balance to zero. Then the coated plasterboard sample was placed into the holder as described above and the holder replaced on the load cell. Mass readings on the computer were compared to those recorded to ascertain accuracy. The igniter spark was positioned above the centre of the sample surface and a pre-run calibration was carried out automatically by the computer before the test run begins. Once the computer was ready, the test was initiated by opening the shutters and simultaneously pressing 1 on the handheld control panel (signifying the 'start of test') and the 'start' button on the data logger computer to begin temperature profile records. Button 2 was pressed at the point of 'sample ignition', button 3 allows the time to be recorded at points of interest throughout the test, to make note of any observations such as bubbling, swelling, char formation or sample deformation. Button 4 is pressed once the flame is extinguished to indicate 'end of test'. After a further 2 minutes of data is collected, button 1 is selected again to signify 'finish', this allows the input of any notes and the saving of the test data on the computer. The data is stored as a comma separated file which can then be imported into packages such as Microsoft Excel for further analysis.

2.3.3. BS EN 367 (adapted)

This method is taken from a European Standard specifying a technique for comparing the heat transmission through materials or material assemblies used in protective clothing.[114] It has been adapted for the analysis of the heat transmission through protective coatings allowing estimation of the thermal conductivity of coating samples. Specimens are ranked using the temperature profiles recorded under specific test conditions. These should not been

considered as a measure of protection time as conditions will vary greatly under actual use conditions.

The following major modifications have been made from the BS EN 367: 1992 standard:

1) Specimens are analysed on a 2 mm thick aluminium sheet substrate

2) Heat flux of exposure is reduced from the suggested 80kW/m^2 to within the range 30-40kW/m^2 and is regularly monitored by calibration between every few tests.

3) The specimen support frame has been discarded. The purpose of this was to prevent the shrinking and curling of fabrics but acts as an unnecessary heat sink in coating analysis so has been removed for these experiments.

4) Heat transfer index values were not calculated. Instead temperature profiles of the samples were compared and the time to reach 150 °C and 350 °C investigated.

2.3.3.1. Instrumentation

The apparatus was set up as depicted in Figure 45 and consists of: a gas burner, copper disc calorimeter, a calorimeter location plate, a support stand and data recording computer.

Key
1 Thermocouple
2 Calorimeter block
3 Specimen
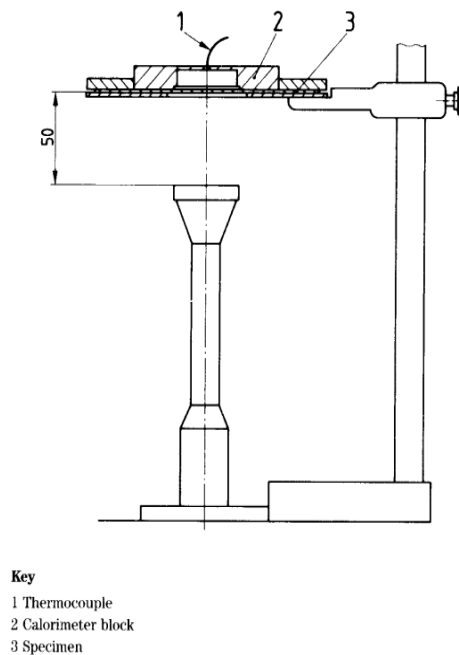
Figure 45 Schematic of BS EN 367 apparatus

2.3.3.2. Calibration

The copper calibration plate (of known mass) was exposed to the heat flux for 10 seconds. The temperature increase recorded and heat flux calculated using the expression in Equation 3.

Equation 3

$$Q = \frac{m \ x \ c\rho \ x \ R}{A}$$

Where:

Q is the heat release rate, in kW m^{-2}

m is the mass of the copper calibration disk, in kg

$c\rho$ is the specific heat capacity of the copper calibration disk 0.385 (kJ kg^{-1} °C)

R is the rate of temperature increase, in the linear region, in °C s^{-1}

A is the area of the copper calibration disk, in m^2

This should fall between 30-40 kW m^{-2}. This is repeated until two readings are taken that are within 5 kW m^{-2}. A reference is also tested which consists of an uncoated aluminium sheet being exposed to test conditions, this provides a bench-mark for all future samples to be compared against. The apparatus was calibrated and a reference recorded each day prior to testing and at several intervals throughout the day to ensure there is no drift in heat flux values.

2.3.3.3. Sample

Two layers of sample coatings were applied to 2 mm thick aluminium sheet (140 mm x 140 mm) of known mass and thickness and allowed at least 24 hours drying time in a 30 °C oven between each coat. Mass and dry film thickness of samples were recorded prior to experimentation to ensure consistency and repeatability.

2.3.3.4. Procedure

Samples were inserted into the apparatus as shown in Figure 45. The logger was started and ambient temperature recorded for 10 seconds before the gas burner was inserted under the sample. The temperature profile of the sample was recorded until a temperature of 350 °C was reached and the time to reach 150 °C recorded. All samples were analysed in triplicate and average taken. A graph of temperature profile was plotted and compared between samples to assess performance and level of protection given.

Initially water was used to cool the system quickly between analyses, however this caused problems with the temperature profile measurement. The calcium-silicate board used in the sample mounting absorbs the water used for cooling, and a plateau is observed in the temperature profiles (around 100 °C) which corresponds to the evaporation of the water

trapped in the calcium-silicate board. Two temperature profiles are shown in Figure 46, both collected from the same sample type however, one using the water logged calcium-silicate board and the other recorded using a dry board. This artefact was eliminated by using a second calcium-silicate mounting block. These were alternated for each test, allowing cooling between tests, whilst analyses continue.
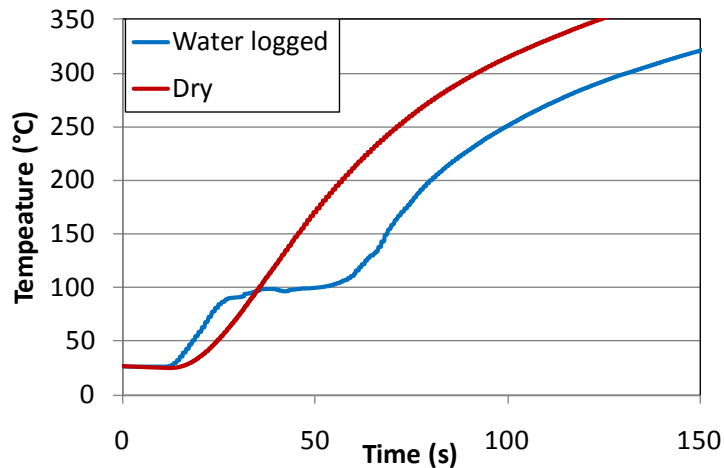
Figure 46 Comparison of water logged and dry calcium-silicate board

2.3.4. BS 476: Part 6 (adapted)

This is an adapted version of the BS 476: Part 6 method[29], the results being expressed as a fire propagation index (*I*) which provides a comparative measurement of the contribution to the growth of fire made by essentially flat materials or composites. Adaptations to this method include:

1) Use of methane in place of G112 gas. G112 gas is synthetic coal gas – predominantly hydrogen and carbon monoxide, used only to provide a pilot flame. The gas flow is reduced to compensate for the change in heat of combustion

2) Substrate material has 12 mm Gypsum plasterboard coated with two layers of nitrocellulose paint as the official Warrington blue board was not affordable

2.3.4.1. Instrumentation

The BS 476: Part 6 apparatus is shown below in Figure 47 and consists of: a combustion chamber, specimen holder, chimney and cowl, a gas burner, two electric heating elements, two thermocouples and data logging computer.
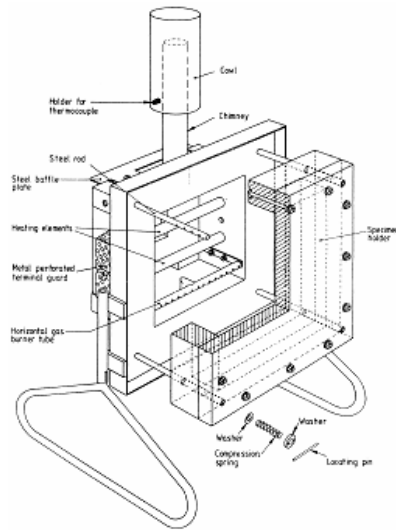
Figure 47 Schematic diagram of the BS476-6 apparatus

2.3.4.2. Calibration

The equipment was calibrated each day prior to testing. A square calibration sheet (225 mm x 225 mm) inserted into the apparatus at ambient temperature. The gas flow was set to 527.5 ± 10 W (0.4 L min^{-1} for methane gas) and vapours allowed to disperse. Two minutes of ambient temperature were recorded using the thermocouples. Then the gas supply was turned on and ignited; the test time was recorded from the time of ignition. 165 s after ignition turn on the electrical supply to give an indicated output of 1800 W; this was reduced to 1500 W 5 minutes after ignition. The temperature was recorded by the thermocouples at specific time intervals.

a)   0.5 minute intervals, up to and including 3 minutes from the gas ignition time

b)   1 minute intervals up to 10 minutes from the gas ignition time

c)   2 minute intervals up to 20 minutes from the gas ignition time

The temperature should fall between certain limits in order for the calibration to be considered valid; these limits are listed below in Table 8.

Table 8 Limits of temperature rise for valid calibration

Time from ignition of gas (min)	Limits for rise above initial temperature (°C)
3	27 to 39
5	85 to 110
10	175 to 205
20	230 to 260

Calibration C is calculated from the expression in Equation 4.

Equation 4

$$C = \sum_{t=0.5}^{t=3} \frac{\theta c}{10t} + \sum_{t=4}^{t=10} \frac{\theta c}{10t} + \sum_{t=12}^{t=20} \frac{\theta c}{10t}$$

Where:

θc is the actual temperature rise to the nearest °C

t is the time, in minutes, at the intervals specified above

The calibration value, *C,* (Equation 4) shall not differ more than 1.0 between consecutive calibrations.

2.3.4.3. Sample
Samples are prepared as outlined above.

2.3.4.4. Procedure
The same procedure was carried out as described above for calibration; however samples were inserted in place of the calibration sheet. Observations were recorded throughout the experiment taking special note of the following phenomena:

a) Intumescence or deformation of specimen which leads to the blockage of burner ports so the required gas flow is no longer maintained.

b) Melting or slumping of specimen resulting in escape through the air inlet hole or a reduction in the exposure to specific heating conditions

Results were expressed in the form of a fire propagation index for specimens, *S*, (Equation 5) which provides a numerical measure of the contribution to the growth of a fire made by a specimen. When tested in triplicate, these sub-indices can be used to calculate the fire propagation index (*I*) of products (Equation 9). This value is weighted so heat evolved in the initial stages is more heavily penalised than heat evolved in the later stages of the experiment. The fire propagation index, S, is calculated from three sub-indices, s1, s2 and s3, according to the respective temperature ranges; as follows:

Equation 5

$$S = s1 + s2 + s3$$

Where:

s1, s2 and s3 are given by Equation 6, Equation 7 and Equation 8 respectively.

Equation 6

$$s1 = \sum_{t=0.5}^{t=3} \frac{\theta s - \theta c}{10t}$$

Equation 7

$$s2 = \sum_{t=4}^{t=10} \frac{\theta s - \theta c}{10t}$$

Equation 8

$$s3 = \sum_{t=12}^{t=20} \frac{\theta s - \theta c}{10t}$$

Where:

θs is the actual temperature rise, at the intervals specified above, for flue gases during sample analysis

θc is the actual temperature rise, at the intervals specified above, for the calibration board

t is the time in minutes at the intervals specified above

The overall fire propagation index, I, for the product is calculated from the individual results of each specimen run, as follows:

Equation 9

$$l = i1 + i2 + i3$$

Where:

i1, i2 and i3 are given by Equation 10, Equation 11 and Equation 12 respectively.

Equation 10

$$i1 = \frac{1}{3}[(s1)A + (s1)B + (s1)C]$$

Equation 11

$$i2 = \frac{1}{3}[(s2)A + (s2)B + (s2)C]$$

Equation 12

$$i3 = \frac{1}{3}[(s3)A + (S3)B + (s3)C]$$

Where:

A, B and C represent individual specimens giving valid test results.

Experiments are deemed invalid for samples: which disrupt the gas flow rate by blocking gas burner ports, which melt or flow causing the loss of sample through the air inlet hole and which melt or flow leading to the reduction in heat exposure during the experiment.

All samples yielding a fire propagation index value (I) of less than 6 are regarded as a 'pass'. This is slightly reduced from the standard test method which accepts all systems with an I value of less than 12 as a 'pass'. This is due to the use of an alternative (less flammable) substrate for analysis in the adapted method.

CHAPTER 3. INVESTIGATION OF FACTORS AFFECTING COATING PERFORMANCE

Burning behaviour and coating performance is heavily influenced by parameters such as substrate type and thickness, coating type and thickness, level of adhesion and variations in heat flux as discussed in section 1.11. In order to ensure all experiments were carried out in appropriate conditions, some preliminary work was undertaken to determine the optimum parameters for each experiment and coating type.

3.1. Effect of substrate on burning behaviour

At the start of the project it was envisaged that paint films could be produced on non-stick substrates and then peeled off prior to analysis in the cone calorimeter however, this required an increased number of layers to be applied to enable removal. Many samples were warped and torn during peeling and when wrapped in aluminium foil for testing by cone calorimetry, air pockets formed producing large variation in time to ignition, heat release rate and burning behaviour observed. Paint layers were then applied directly onto thicker, catering grade aluminium foil. However, the foil wrinkled during roller application, producing a poor finish and non-uniform sample surface which also significantly effects performance and burning behaviour.

A substrate had to be found which allowed production of reproducible samples maintained constant weight but also mirrors burning behaviour on plasterboard substrate which is the substrate used in standard methods.

Experiments were carried out on samples prepared on aluminium sheet substrates of varying thicknesses (0.8 mm, 1 mm, 1.5 mm and 5 mm) and plasterboard (of thickness 12 mm) to determine the effect of substrate properties on the flammability. Samples were prepared by applying six coats of Dulux Pure Brilliant White Eggshell paint (2g wet mass which dries to approximately 50 microns, dry film thickness when applied over the 100 mm square sample plaque) to the substrate and exposing samples to an irradiance of 35 kW m^{-2}. The results are shown in Figure 48.
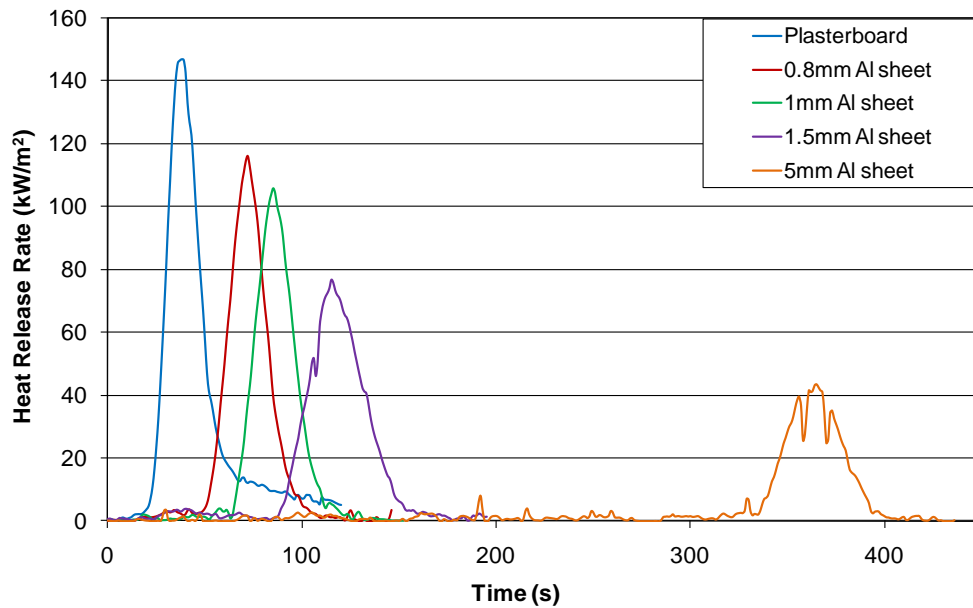
Figure 48 Heat release rate curves for 6 coats of Eggshell on various substrate thicknesses

Figure 48 shows that in the case of aluminium increased substrate thickness leads to increased time to ignition, a decrease in peak heat release rate and burning behaviour shifts from thermally thin to thermally thick. Time to ignition increases with substrate thickness as heat capacity increases. Aluminium acts as a heat sink dissipating heat away from the paint layers requiring more energy input for the paint to reach its decomposition and pyrolysis temperature leading to ignition. The thicker the aluminium substrate the more energy is required to reach this critical temperature.

Conversely plasterboard has insulating properties - preventing movement of heat through the material – and displays low thermal capacity. This promotes a build-up of heat at the upper surface of the substrate material causing earlier pyrolysis and ignition of paint layers. Burn time is brief as all fuel is utilised simultaneously to support the flame.

The substrate chosen to carry out paint thickness analysis (mass of paint or number of layers applied) was the 0.8 mm aluminium sheet. This material displayed behaviour closest to the plasterboard substrate and yet was much easier to work with when preparing samples. Difficulties arise as plasterboard samples are prone to mass loss from the (crumbling) freshly cut edges during sample preparation. The mass of such a loss would far outweigh the mass loss during the paint decomposition, invalidating results.

For later experiments where the test method and coating formulations provide the variables for analysis, samples were prepared on 12 mm gypsum plasterboard substrate. For cone calorimeter and BS 476: part 6 (adapted) experiments, a constant mass of coating was applied

and mass loss from the edges of the plasterboard was reduced as edges were sealed with a 50:50 mix of water and white emulsion paint. With mass loss issues overcome, it is preferable to use a substrate material which is representative of a real fire scenario and substrate used in standard fire tests. The aluminium substrate is only used in initial investigation of factors affecting burning behaviour, not for the assessment of coating performance or prediction of protection in standard fire tests as it displays much different thermal properties.

3.2. Effect of coating mass on burning behaviour

Experiments were carried out to determine the burning behaviour of various masses of paint (numbers of layers). These results not only investigate the fire risk of multilayer painted surfaces, but also begin to explain some of the combustion phenomena observed in real fire cases and aid development of a reproducible methodology for sample preparation. Two paint types were analysed to compare the effect on burning behaviour between sample types. These consisted of Dulux water-based 'brilliant white' eggshell (acrylic copolymer emulsion), and Dulux water-based 'brilliant white' gloss (alkyd). Pure brilliant white paints from the same manufacturer were chosen to try to reduce the influence of varying factors such as pigment type and loading.

Experiments were carried out for 1, 5, 10, 15 and 20 coats of Dulux Eggshell on the 0.8 mm thick aluminium sheet substrate and exposed at an irradiance of 55 kW m^{-2} in the cone calorimeter.
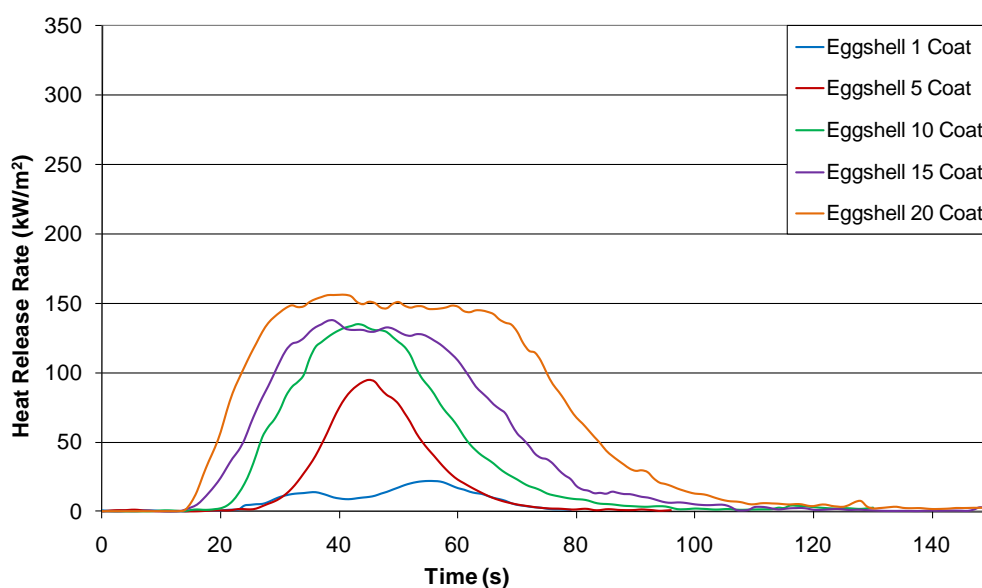
Figure 49 Heat release rate curves for various masses of Eggshell on 0.8 mm aluminium sheet substrate

Acrylic resins decompose primarily forming the monomer species promoting steady burning behaviour which is clearly observed in Figure 49. The graph in Figure 49 shows the rapid move

from the thermally thin burning behaviour - of the two and five paint layer samples - to the thermally thick burning behaviour as the number of coats of paint and therefore the amount of fuel present increases. This behaviour is characteristic of acrylic species. The time to ignition decreases as the number of paint layers increases, however, the peak of heat release rate reaches a plateau at approximately 150 kW m^{-2} for ten or more paint layers. For samples of more than 10 paint layers the length of burn time is increased due to the increase in the amount of fuel present.

Table 9 Eggshell sample cone calorimeter properties

Sample	t_{ig} (s)	PHRR (kW m^{-2})	tPHRR (s)	THR (kW m^{-2})
Eggshell (1 coat)	40 ± 8	38 ± 11	50 ± 9	640 ± 158
Eggshell (5 coat)	28 ± 2	96 ± 5	47 ± 5	1920 ± 87
Eggshell (10 coat)	24 ± 0	137 ± 3	44 ± 1	4292 ± 292
Eggshell (15 coat)	16 ± 2	138 ± 1	41 ± 5	5994 ± 439
Eggshell (20 coat)	17 ± 1	160 ± 3	42 ± 3	9134 ± 383

The reduction in time to ignition (listed in Table 9) shown by these samples may be explained by the heat flux attacking only the top layers of paint, causing ignition of the upper paint layers prior to thermal equilibrium being reached into the depth of the sample. As the upper most layers burn, thermal feedback from the flame pyrolyses deeper paint layers, the products of which support further combustion. Another explanation is that failure in the binding of adjacent layers causes layer by layer burning whereas, if only one very thick layer of paint had been applied, the burning behaviour observed would be very different.

Identical experiments were carried out for up to 20 coats of Dulux Gloss and the results shown in Figure 50.
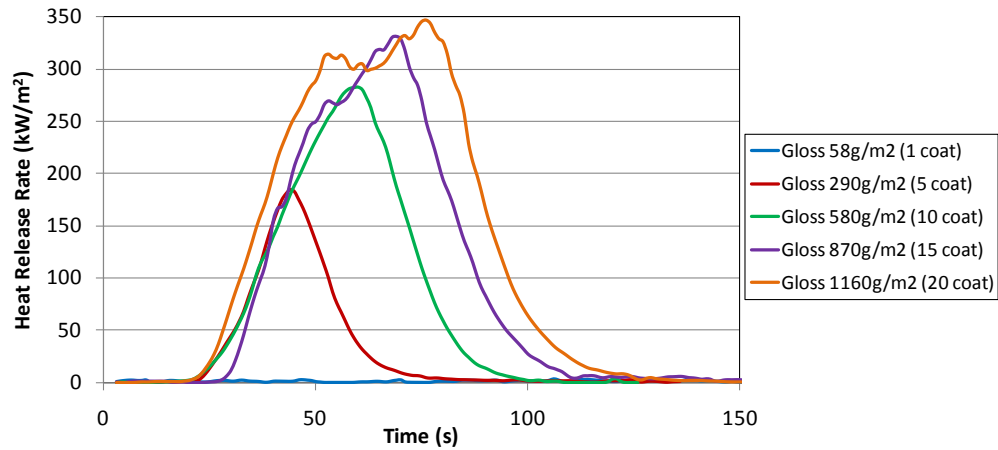
Figure 50 Heat release rate curves for various masses of Gloss on 0.8 mm aluminium sheet substrate

Time to ignition, listed in Table 10, remains largely unaffected by the increase in mass (number of layers) of gloss paint applied. All samples, with the exception of '58 g m^{-2} (1 coat)' and 870 g m^{-2} (15 coats)', have ignition times of approximately 20 seconds. This suggests that this type of paint displays higher thermal conductivity (rate of heat transfer through the layers) than observed in the eggshell samples above. Heat penetrates through the entire depth of the sample (without a temperature gradient being observed) and more rapidly reaches temperature equilibrium meaning that more mass (or thickness) of gloss is required before a temperature gradient can be developed and thermally thick burning behaviour is recorded. Peak heat release rate values for gloss paint are approximately 300 kW m^{-2} double the values recorded for the eggshell samples. This is further supported by the structural and decomposition information given above in section 1.5.3. Alkyds are highly cross-linked species. The formation of chains tightly held in position by cross-linkages promotes thermal conductivity via free moving electrons and the collision of high energy molecules. '58g/m^2 (1coat)' samples failed to ignite as heat was dissipated by the substrate, there was not enough fuel to support combustion and the energy input was not high enough to break the cross-linking bonds. This prevents the formation of monomers and instead produces short chain hydrocarbon pyrolysis products.

Table 10 Gloss sample cone calorimeter properties

Sample	t_{ig} (s)	PHRR (kW m^{-2})	tPHRR (s)	THR (kW m^{-2})
Gloss (1 coat)	0 ± 0	20 ± 7	581 ± 222	69 ± 65
Gloss (5 coat)	23 ± 1	178 ± 8	41 ± 1	4 ± 0
Gloss (10 coat)	23 ± 5	303 ± 7	56 ± 3	10 ± 0
Gloss (15 coat)	25 ± 1	338 ± 15	66 ± 1	14 ± 0
Gloss (20 coat)	19 ± 3	348 ± 8	73 ± 1	18 ± 0

The data shows that a greater mass of gloss paint is required to observe the move from thermally thin to thermally thick burning behaviour when compared to the eggshell samples. 15-20 layer thickness of gloss paint started to show thermally thick behaviour whereas only 10 layer thickness (half the mass) of eggshell paint shows such behaviour. This suggests that the fire hazard resulting from the use of gloss paint would be greater than eggshell due to the increased amount of heat released during combustion, promoting rapid spread of flame along a surface.

3.3. Effect of coating mass on burning behaviour of fire retardant systems

This work was extended to include commercially available fire retardant and anti-graffiti systems to investigate the relationship between coating thickness and fire protection performance. Two fire retardant, and one anti-graffiti system, were supplied by Integra Coatings Ltd and were investigated: FR120 - a halogenated system with good fire retardant properties; FR121 – moderate fire retardant properties; and ES500AG an anti-graffiti top coat with no fire retardant functionality. These systems were coated on the 0.8 mm thick aluminium sheet and exposed to a heat flux of 55 kW m^{-2} in the cone calorimeter. Burning behaviour in the cone calorimeter was investigated for one to six coats (the upper limit for successive layers of fire retardant paint through regular re-decoration and maintenance). Results are plotted using the same axis scaling for comparison purposes.

3.3.1. FR120
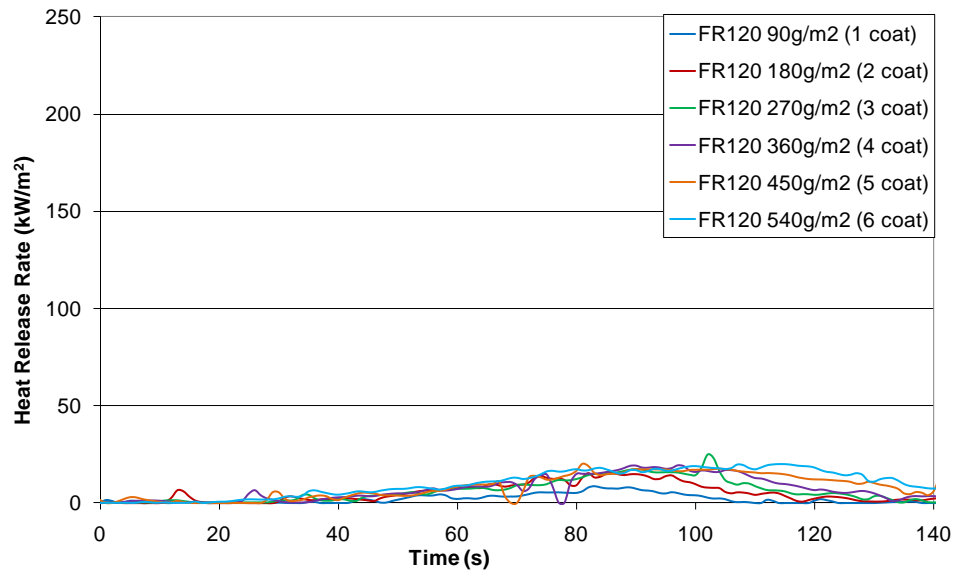
Figure 51 Heat release rate curves for various masses of FR120 on 0.8 mm Aluminium sheet substrate

The FR120 system showed no ignition as depicted in Figure 51 (even when tested at an irradiance of 70 kW m^{-2}), indicating good intrinsic fire retardancy. FR120 is based on a polyvinylidene chloride (PVDC) resin and contains brominated fire retardant additives. During decomposition vinyl chloride resins undergo chain stripping to yield hydrogen chloride (HCl) gas. The bromine held within the structure is also liberated as hydrogen bromide (HBr) species during pyrolysis. The temperature of radical liberation coincides with the decomposition of the residual organic material which will already have a high carbonaceous content. Chlorine and bromine free radicals act as flame inhibitors interrupting the flame process and quench highly reactive OH· and O· free radicals preventing ignition of the small amount of volatile fuel from occurring. Further heating promotes cross-linking reactions believed to produce a polycyclic char structure at approximately 450 °C. Only a slight increase in peak heat release rate was observed as the mass of coating (number of layers) increased. As the coating decomposes to residue and non-combustible pyrolysis products, there is little fuel available to support burning. The slight increase in heat release rate observed is due to the decomposition of the organic residue; the more coating present, the higher the heat release rate from decomposition even though no flames are present. A summary of burning behaviour is shown in Table 11.

Table 11 FR120 samples cone calorimeter properties

Sample	t_{ig} (s)	PHRR (kW m^{-2})	tPHRR (s)	THR (kW m^{-2})
FR120 (1 coat)	0 ± 0	10 ± 4	264 ± 193	347 ± 220
FR120 (2 coat)	0 ± 0	13 ± 3	74 ± 12	271 ± 52
FR120 (3 coat)	0 ± 0	15 ± 6	361 ± 99	283 ± 67
FR120 (4 coat)	0 ± 0	19 ± 1	97 ± 5	1158 ± 8
FR120 (5 coat)	0 ± 0	20 ± 3	81 ± 5	1607 ± 7
FR120 (6 coat)	0 ± 0	20 ± 2	114 ± 2	2155 ± 15

3.3.2. FR121

FR121 is also a brominated system but contains lower loadings of the bromine fire retardant additive and does not contain the PVDC resin. The FR121 system displayed a far greater variation of results when compared to the other systems investigated as shown above in Figure 52. This is associated with test conditions close to the critical heat flux of ignition.
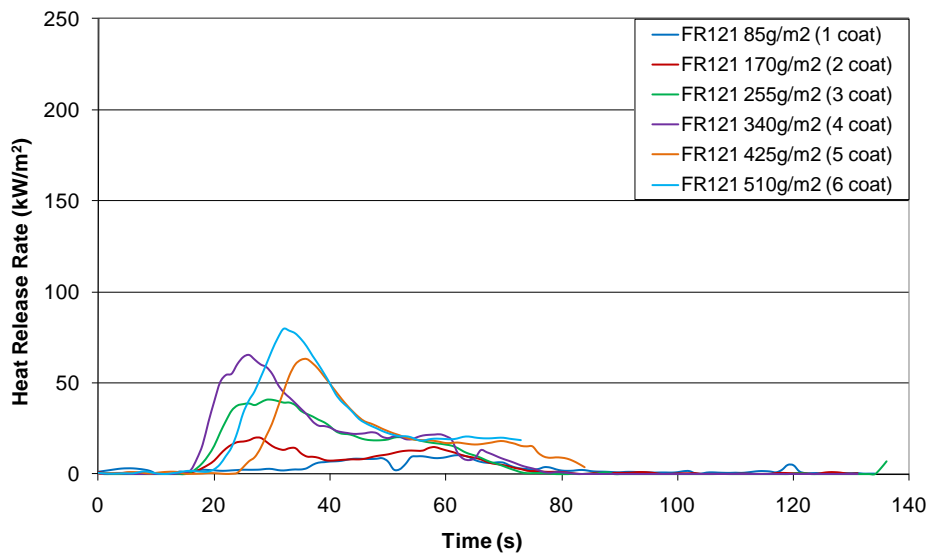
Figure 52 Heat release rate curves for various masses of FR121 on 0.8 mm Aluminium sheet substrate

Peak of heat release rate for these samples is around 70 kW m^{-2} and not significantly altered with the addition of coats in excess of four layers. This shows that the coating can provide its own fuel if sufficient numbers of layers are present. The peak of heat release for four to six coats is significantly higher than that recorded for one to three coats (presumably) due to the greater amount of fuel present. This suggests that the chlorine and bromine are inhibiting some of the flame reactions. This maintains a reduced peak of heat release rate but fail to prevent ignition for thicker layers. This could be due to inadequate halogen loadings for the fuel to be protected, or a failure to decompose at the optimum time to deliver effective protection.

Table 12 FR121 samples cone calorimeter properties

Sample	t_{ig} (s)	PHRR (kW m^{-2})	tPHRR (s)	THR (kW m^{-2})
FR121 (1 coat)	10 ± 2	4 ± 1	15 ± 1	53 ± 31
FR121 (2 coat)	2 ± 0	25 ± 8	12 ± 1	214 ± 59
FR121 (3 coat)	3 ± 1	36 ± 2	30 ± 5	323 ± 156
FR121 (4 coat)	17 ± 0	65 ± 1	26 ± 0	1598 ± 17
FR121 (5 coat)	27 ± 1	63 ± 2	36 ± 0	1434 ± 1
FR121 (6 coat)	25 ± 1	80 ± 1	33 ± 1	1873 ± 32

Time to ignition decreases as the number of coats increases from one to four coats suggesting low thermal conductivity of the coating forcing ignition of upper layers. However for five and six coats the time to ignition is significantly increased - to 20 and 24 seconds respectively (as shown in Table 12). This indicates that the increased loading of fuel associated with additional coating mass delays ignition as it requires more energy to be absorbed for fuel pyrolysis to occur.

3.3.3. ES500AG

ES500AG is an example of an anti-graffiti system with no fire retardant additives in its formulation.
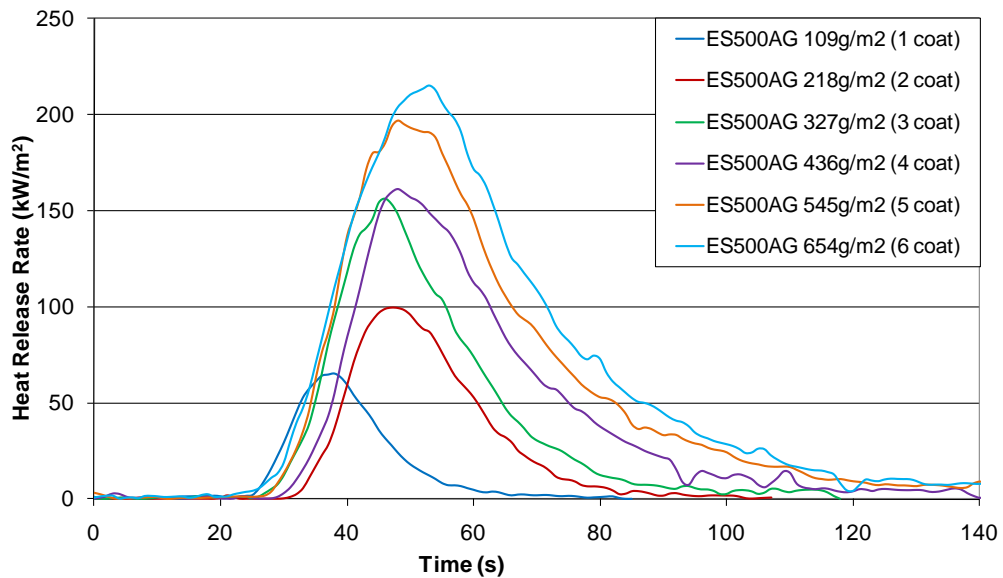
Figure 53 Heat release rate curves for various masses of ES500AG on 0.8 mm Aluminium sheet substrate

Analysis of the ES500AG system data showed an increase in peak and total heat release for each layer of coating added; this is simply due to the additional fuel present with each subsequent layer applied. As this system contains no fire retardant additives the flame is only restricted by the amount of fuel available in the sample.

Table 13 ES500AG sample cone calorimeter properties

Sample	t_{ig} (s)	PHRR (kW m^{-2})	tPHRR (s)	THR (kW m^{-2})
ES500AG (1 coat)	29 ± 1	68 ± 1	38 ± 2	1155 ± 41
ES500AG (2 coat)	26 ± 2	99 ± 2	47 ± 1	2341 ± 37
ES500AG (3 coat)	28 ± 1	156 ± 3	46 ± 1	3982 ± 36
ES500AG (4 coat)	32 ± 1	161 ± 5	48 ± 1	5171 ± 58
ES500AG (5 coat)	30 ± 2	197 ± 5	48 ± 2	7222 ± 59
ES500AG (6 coat)	30 ± 3	216 ± 6	53 ± 1	8479 ± 64

Ignition times fall between 26 and 32 seconds as listed in Table 13. This suggests that though the aluminium sheet acted as a heat sink – a similar amount of time is required for each of the coating systems to reach the ignition temperature. This suggests that ES500AG has a high rate of heat transfer. Peak heat release rate values increase with each additional layer and are very high in comparison with other non fire retardant systems analysed. A peak heat release rate of approximately 215 kW m^{-2} was recorded for six layers suggesting that this coating would significantly add to the fire load of a compartment actively promoting flame spread. These results suggest the possible presence of a highly cross-linked resin allowing increased thermal conductivity, perhaps a vinyl.

3.4. Effect of substrate flammability on burning behaviour

The same three fire retardant systems were tested in the cone calorimeter at a heat flux of 55 kW m^{-2} but this time on substrates of varying flammability to establish the effect on burning behaviour. Substrates included: gypsum plasterboard of thickness 12 mm; Warrington blue board substrate supplied for BS 476: Part 6 - Flame Propagation experiments; Warrington blue board substrate supplied for BS 476: Part 7 - Lateral Spread of Flame experiments. This analysis would also give an indication of the performance of these systems in the standard fire tests.
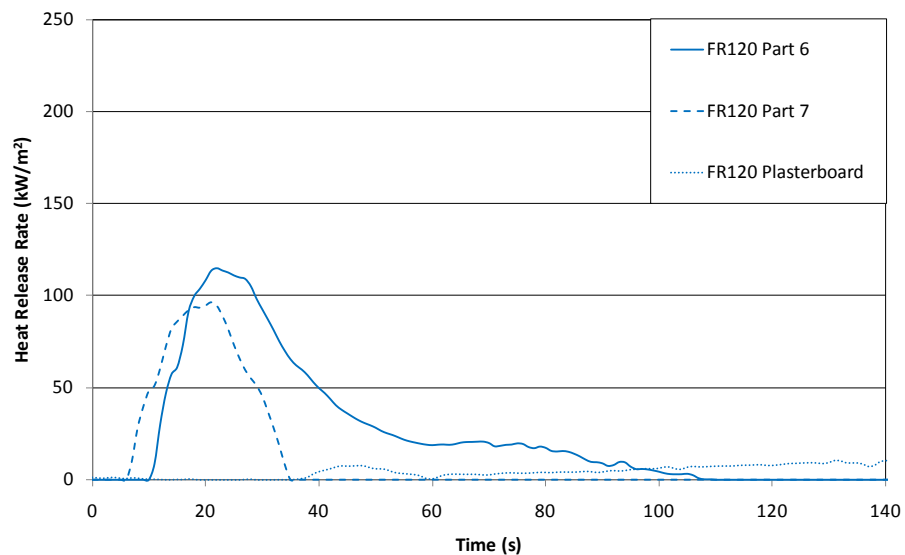
Figure 54 Comparison of heat release rate curves for FR120 tested on Warrington blue board Part 6, Warrington blue board Part 7 and Plasterboard substrates
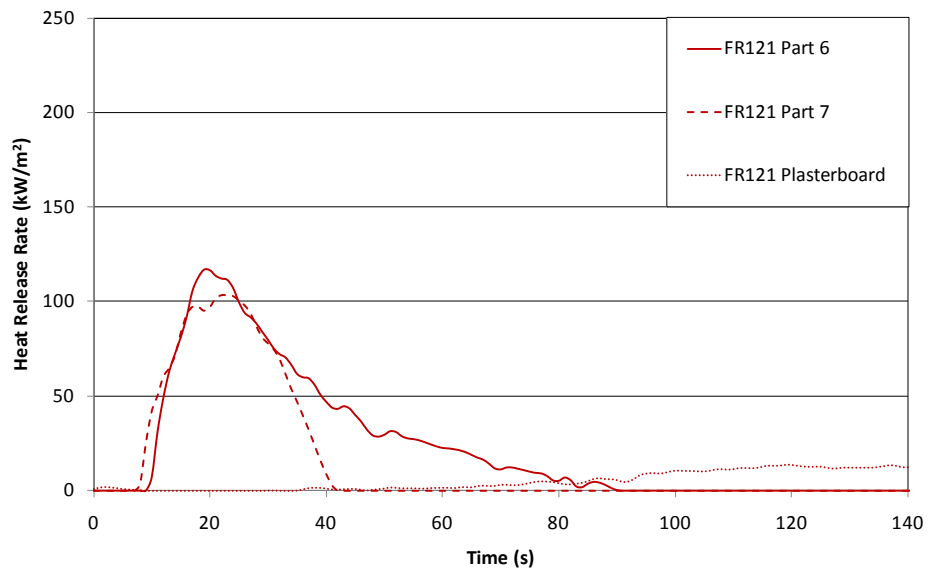
Figure 55 Comparison of heat release rate curves for FR121 tested on Warrington blue board Part 6, Warrington blue board Part 7 and Plasterboard substrates
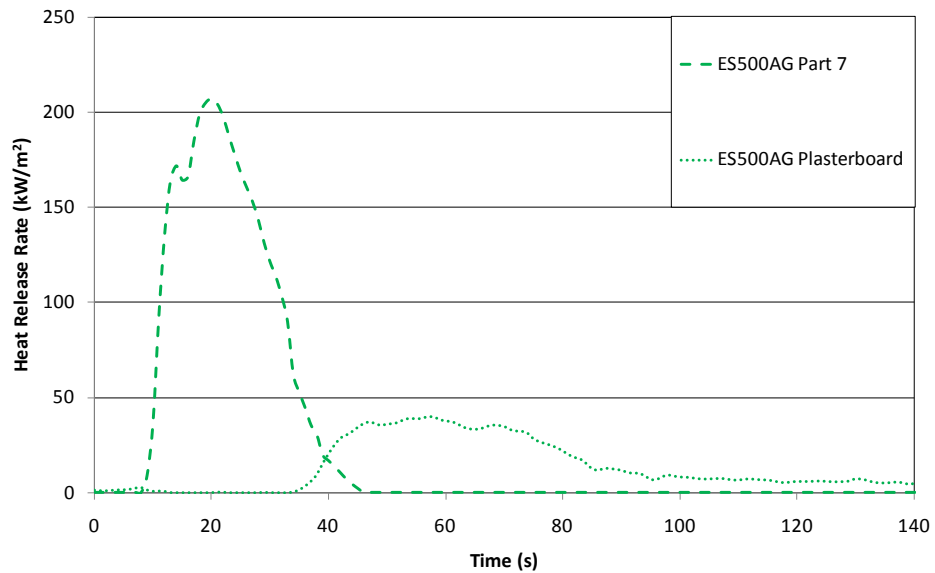
Figure 56 Comparison of heat release rate curves for ES500AG tested on Warrington blue board Part 6, Warrington blue board Part 7 and Plasterboard substrates

Results collected are depicted in Figure 54, Figure 55 and Figure 56. Burning behaviour varies not only between coating systems analysed but is also dependant on the type of substrate on which the system is assessed. All systems show the lowest peak of heat release when tested on the plasterboard substrate - maintained below 50 kW m^{-2}. This is due to the 'non-combustible' nature of the plasterboard which does not contribute any significant fuel to the fire load.

95

When assessed on the plasterboard substrate; the ESS500AG shows the highest peak of heat release (approximately 40 kW m^{-2}) and earliest time to ignition (approximately 35 seconds) suggesting that this is the most flammable coating system of the three investigated. The FR121 and FR120 systems exhibit heat release rate curves maintained below 23 kW m^{-2} with the FR121 system having a brief flaming period around 40 seconds; and the FR120 system failed to ignite and therefore appears to be the best system on this substrate.

When prepared on the Warrington blue board BS 476: Part 7 substrate (which itself contributes fuel) the ES500AG peak of heat release rate value is the highest recorded for all systems analysed in this group (more than 200kW/m^2), with an ignition time of approximately 10 seconds. The data for the FR120 and FR121 systems are more closely matched. Neither the FR120 nor the FR121 systems ignited on the plasterboard substrate, suggesting that neither contains enough combustible fuel to support flaming unless provided by the substrate. In the case of each system the peak of heat release rate is higher when considering the Warrington blue board BS 476: Part 6 substrate (around 120 kW m^{-2}) than the BS 476: Part 7 (100 kW m^{-2}). This suggests that the BS 476: Part 6 board is more flammable than the BS 476: Part 7 alternative.

The ignition time for Warrington blue board BS 476: Part 7 substrate sample is shorter (less than 10 seconds) than that displayed by the BS 476: Part 6 substrate samples (approximately 10 seconds). This evidence supports the theory that the two Warrington blue board substrates differ in composition and have different burning behaviours and properties. This will be reported further in section 3.6.

The data above shows that the FR120 and FR121 fire retardant systems exhibit similar burning behaviour when analysed on the Warrington blue board BS 476: Part 6 substrate suggesting a similar level of protection is offered in each case. However, when comparing the Warrington blue board BS 476: Part 7 substrates, the FR120 system is more effective, exhibiting a slightly reduced peak of heat release rate and reduced burn time.

The data discussed suggests that burning behaviour and coating performance are highly dependent on substrate properties such as heat release rate and time to ignition. Though the Warrington blue board is too expensive to use for all future tests a suitable alternative will be formulated which has similar burning behaviour and therefore will provide the best estimate of performance in the standard fire tests.

3.5. Standard test method substrate analysis: Warrington blue board (WBB)

As the Warrington blue boards provide the standard substrate on which all paints and coating systems are analysed, it is important to understand the burning behaviour and composition of this material itself. There is further ambiguity as results collected from previous experiments suggest variation in the burning behaviours of the Warrington blue board substrates issued for BS 476: Part 6 and BS 476: Part 7 analyses (though reports issued by the test facility report the composition of the boards to be identical). Assuming the regulators to be correct in their choice of the Warrington blue board as the appropriate substrate to represent multilayer paint build-up – the ability to protect this substrate will correspond to fire protection of multilayer paint. A better understanding of the test substrate will certainly aid determination of the best method of protection. Flammability and characterisation results are discussed below.

3.5.1. Flammability analysis

Warrington blue boards were supplied by Integra Coatings Ltd from Exova – Warrington Fire. These are specification boards on which all commercial products must be analysed in order to gain certification and a performance ranking. The boards in question are supplied for the BS 476: Part 6 - Method of test for fire propagation of products[29] and BS 476: Part 7 - Method of test to determine classification of the surface spread of flame of products[30] tests. Flammability experiments were carried out in the cone calorimeter and thermogravimetric (TGA) analysis was undertaken to analyse the thermal decomposition behaviour of the layers. Optical microscopy was later used to identify the layers.

Initial flammability experiments were carried out in the cone calorimeter at an irradiance of 55 kW m^{-2}. Averages calculated from three repeat experiments of each sample type were plotted on the same axes to compare data sets and results are shown Figure 57.
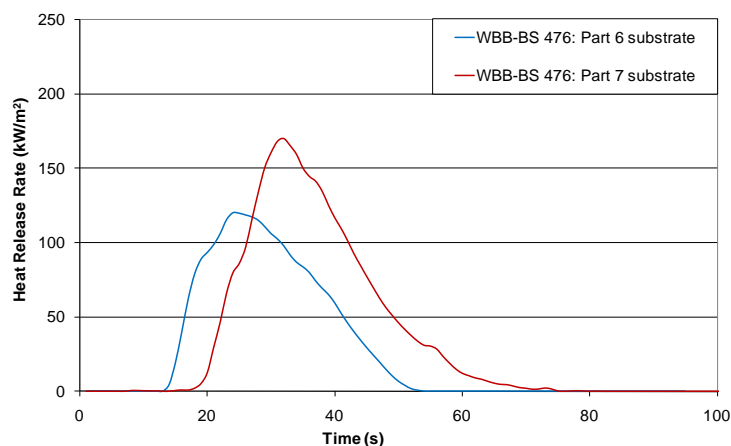
Figure 57 Comparison of WBB-BS 476: Part 6 and WBB-BS 476: Part 7 Warrington blue board heat release rate curves

The average heat release rate data collected suggests a significant difference between the two types of Warrington blue board supplied for flammability testing in the standard test apparatus. The WBB-BS 476: Part 6 substrate sample shows an earlier ignition time of 15 seconds - compared to an ignition time of 20 seconds for the WBB-BS 476: Part 7 substrate sample - and a lower peak heat release rate of 120 kW m^{-2} in contrast to a heat release rate of 170 kW m^{-2} recorded for the WBB-BS 476: Part 7 substrate sample. These results might be interpreted to suggest that the WBB-BS 476: Part 6 substrate demonstrates favourable flammability properties posing a lower fire risk. This is contradictory to visual observations recorded throughout experimentation which suggests that the WBB-BS 476: Part 6 substrate samples display more vigorous burning with a taller flame that yields more radiant heat. Images of the resulting char residues are shown in Figure 58.

Warrington Blue Board
BS 476: Part 6

Warrington Blue Board
BS 476: Part 7
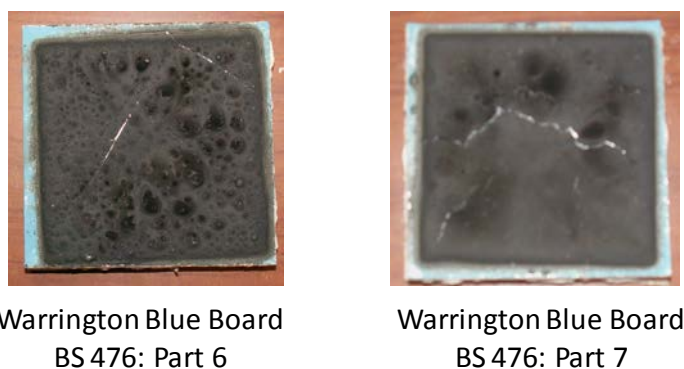
Figure 58 Images of Warrington blue board plaques after exposure to 55 kW m^{-2} in the cone calorimeter

The difference in residue properties can be clearly observed. The BS 476: Part 6 residual char is non-uniform with many small voids within the char structure. Conversely BS 476: Part 7 residue is uniform, forming one large chamber of vapours which was easily compromised (split in sample surface – right hand image in Figure 58).

3.5.2. Oxygen depletion calorimetry for determining heat release rate.

Further investigation of the substrate composition and informal discussions (discussed later in this section) reveals that the majority of the substrate comprises nitrocellulose paint. The structure of nitrocellulose is shown in Figure 59.
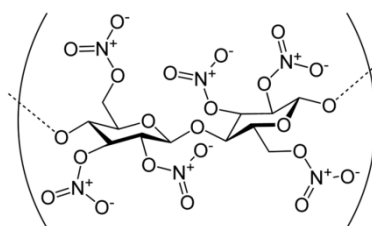
Figure 59 Nitrocellulose structure

Nitrocellulose is highly flammable due to the oxygen held within its structure. Oxygen atoms are bound to nitrogen as shown in the structure above (Figure 59). Combustion reactions lead to the release of oxygen, while nitrogen preferentially forms N_2 leaving oxygen available for the oxidation of the hydrogen and carbon within the structure, forming carbon dioxide and water. Further oxidation of the remaining residue, of empirical formula CH_2O, relies on the uptake of oxygen from the atmosphere.

In the case of nitrocellulose, the liberated oxygen is sufficient to support combustion of the material without any additional oxygen. This means that it can even burn under water! Nitrocellulose is therefore highly flammable as it requires only a source of heat or a spark to provoke combustion as both the fuel and oxygen are already present within structure. Once ignited, nitrocellulose burns very vigorously and coupled with its low melting point (around 170 °C) nitrocellulose is very difficult to fire protect. It is thought that halogenated and char promoting, fire retardant coatings will not provide the level of fire protection that an intumescent coating might, when applied over a nitrocellulose based substrate. Flame inhibiting fire protection coatings will not prevent ignition of the nitrocellulose (because of the oxygen in the structure), a better method would be to prevent heating of the nitrocellulose. This is the action an intumescent fire protection coating would display.

Variation in nitrocellulose composition between the two samples would explain the difference between heat release data collected in the cone calorimeter and the perception of heat release, as well as the difference in appearance of the two residual char samples. Warrington blue boards are made up of nitrocellulose based paint in order to simulate a worst case scenario, providing a 'class 4' rated substrate on which to test fire protection coatings. Problems arise as the cone calorimeter determines the heat release rate of a sample by oxygen depletion calorimetry. This is based on the assumption that the heat released from any given sample is proportional to the oxygen consumed during the combustion of the sample. The majority of materials do not have available oxygen within their structure, as nitrocellulose does. Furthermore the heat release can normally be quantified because 13.1 kJ of energy are released per gram of oxygen consumed.[43, 115] There are only a few exceptions to this generalisation and nitrocellulose is one. Nitrocellulose has oxygen bound within its structure. Oxygen bound to nitrogen atoms which during decomposition will preferably decompose to form N_2 molecules, liberating oxygen atoms for oxidation reactions. This freed oxygen is short lived due to its highly reactive nature and will therefore be preferentially used to create carbon dioxide and carbon monoxide in the decomposition of carbon within the sample before any oxygen is depleted from the atmosphere. This lack of atmospheric oxygen depletion leads to an underestimation of heat release value when calculated using oxygen depletion calorimetry

– as is the case with the cone calorimeter. For materials containing nitrocellulose lower peak heat release rate curve may indicate the presence of a larger nitrocellulose content within the sample rather than reduced flammability.

Varying nitrocellulose composition of the two samples also explains the variance in appearance of residual chars shown in Figure 58. 43 % of the WBB-BS 476: Part 6 and 30 % of the WBB-BS 476: Part 7 is attributed to nitrocellulose content; this is described in section 3.6. The low melting temperature of the nitrocellulose means the substrate is molten prior to the ignition temperature being reached. The greater the nitrocellulose content, the greater the molten proportion of the sample at lower temperatures. This traps the vapours earlier in the tests therefore producing a greater amount of smaller voids which are observed in the WBB-BS 476: Part 6 substrate sample, compared to the WBB-BS 476: Part 7 substrate sample.

In this situation, CO_2 production rate curves collected by the cone calorimeter give a more accurate estimation of heat release rate (as would be experienced in a real fire, or as recorded by a thermocouple) and therefore provide a better method than oxygen depletion calorimetry. This substitution can be made because the cone calorimeter is designed to simulate well-ventilated conditions thus promoting complete combustion. This assumes that all oxygen is converted into CO_2 during combustion and therefore a correlation can be drawn between the CO_2 production rate and the heat release rate. The greater the CO_2 production rate (g s^{-1}) the greater the heat release rate (kW m^{-2}).[116]
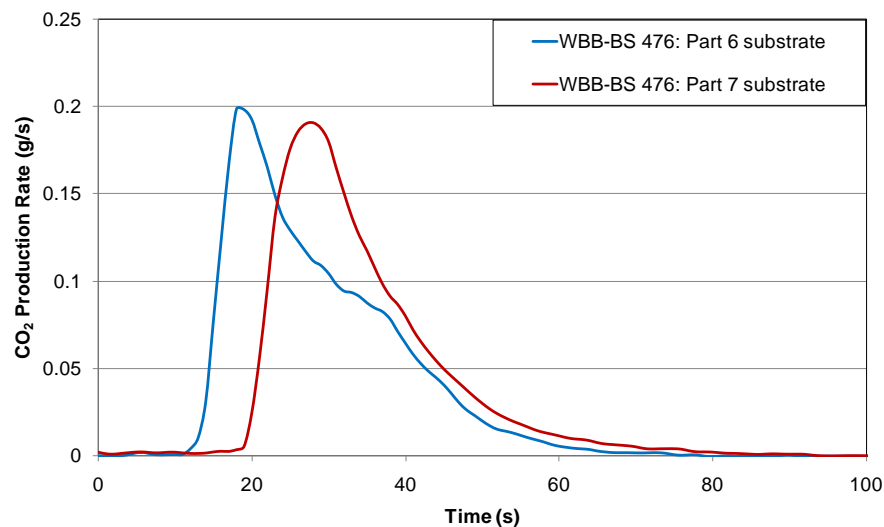
Figure 60 Carbon dioxide production rate curves for Part 6 and Part 7 Warrington blue boards

Figure 60 shows the CO_2 production rate curves recorded during the same experiments for which the heat release rate curves were reported above. The data shows a greater degree of agreement for the WBB-BS 476: Part 6 substrate and WBB-BS 476: Part 7 substrate materials

when considering peak CO_2 production rate - 0.2 g s^{-1} and 0.19 g s^{-1} respectively. This supports the suggestion that heat release rates for the two boards are in fact similar and it is an artefact of the oxygen depletion calorimetry that suggests otherwise. Interestingly, a greater discrepancy in oxygen depletion and CO_2 production rate data is recorded for the WBB-BS 476: Part 6 sample when compared to the WBB-BS 476: Part 7 supporting the conclusion that there is a greater amount of nitrocellulose paint present on the WBB-BS 476: Part 6 board causing a more significant under-estimation in the data. This is further supported by the earlier ignition time and longer burn time displayed by the WBB-BS 476: Part 6 samples. Nitrocellulose decomposes at approximately 170 °C resulting in very early time to ignition, other components may be more stable providing pyrolysis products or fuel to sustain burning at higher temperatures once the nitrocellulose is consumed.

When comparisons are made between the oxygen depletion data and the CO_2 production rate, discrepancies can be clearly viewed, these are tabulated in Table 14.

Table 14 O_2:CO_2 ratio comparison for Part 6 and Part 7 Warrington blue boards

Sample		Total O$_2$ Depletion %	Total CO$_2$ Yield kg/kg	Total O$_2$:CO$_2$ Ratio %:kg/kg
WBB BS 476: Part 6	1	1.3	204.67	0.635
	2	1.5	107.87	1.391
	3	1.6	231.35	0.692
WBB BS 476: Part 7	1	2.7	177.04	1.525
	2	2.5	159.79	1.565
	3	2.8	142.15	1.970

Though initial coating mass and dry film thickness measurements for all samples were within a range of ± 0.5g and ± 0.5µm respectively, the data suggests that though less oxygen is depleted from the atmosphere for the WBB-BS 476: Part 6 samples, almost double the amount of CO_2 is produced. Conversely the WBB-BS 476: Part 7 boards deplete twice as much O_2 from the atmosphere and only produce half as much CO_2, producing an O_2:CO_2 ratio of more than double that of the WBB-BS 476: Part 6 samples. This provides strong evidence that the amount of nitrocellulose paint present in the two test substrates differs, leading to disparity in burning behaviours and experimental results in fire tests. This suggests that different fire retardant mechanisms (or levels of protection) may be required for each substrate.

Repeat analyses were carried out on substrates obtained in previous years as well as currently supplied boards. Surprisingly there is no variation between old and new samples, suggesting that the composition of each board has not been altered but are instead manufactured to display different levels of flammability depending on the test to be undertaken, or a large number of samples were made and stored for the two different sizes required for the Part 6 and 7 tests.

3.5.3. Thermogravimetric Analysis

Thermogravimetric analysis of paint flakes taken from the two boards and analysed in both air and nitrogen atmospheres show similar decomposition curves. A constant flow rate of 50 cm^3 min^{-1} per minute and a heating rate of 10 °C min^{-1} over a temperature range of 25-900 °C were adopted and the results are shown in Figure 61.
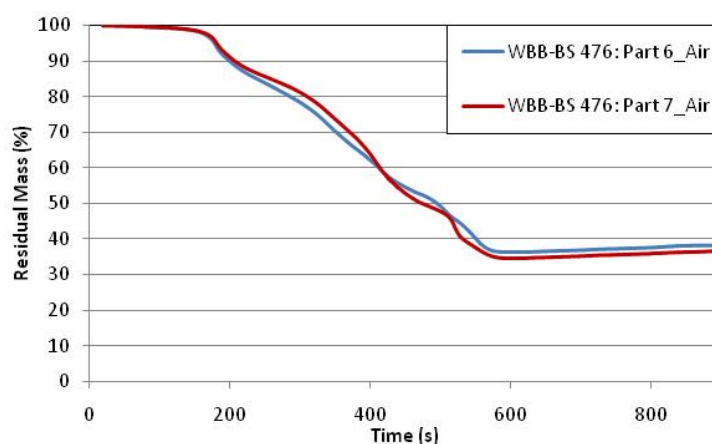
Figure 61 Decomposition curves for Part 6 and Part 7 Warrington blue boards in air atmosphere

Thermogravimetric analysis in air relays information about the oxidation, decomposition and mass loss of the sample. The almost linear thermal decomposition shown above for both samples is rarely observed. At very high temperatures (around 900 °C) there remains a residual mass of approximately 35 %. This suggests that the inorganic material content is similar for both samples, but slightly larger for the WBB-BS 476: Part 6 substrate and it is stable, avoiding oxidation or decomposition up to 900 °C. The increase in mass between 600 °C and 900 °C is believed to be an artefact of the TGA apparatus (or it may be due to the final residual char oxidising and increasing in weight as oxygen is incorporated into the structure). Another explanation would be that the gas expands as it enters the furnace chamber due to an increase in temperature, causing aerodynamic drag of the crucible. The effect is increased as the flow rate is increased and even occurs when an empty crucible is subjected to an identical heating regime. Thermal decomposition of nitrocellulose begins at approximately 160 °C. The mass loss at approximately 170 °C is assigned to the decomposition of the nitrocellulose portion of the

paint flake. [117] Mass loss coincides with the liberation of NO_2, [118] this is the initial stage of the decomposition reaction due to the weak nature of the $CO-NO_2$ bonds. Conversely at higher temperatures the principal oxide of nitrogen formed during pyrolysis is NO. [119]
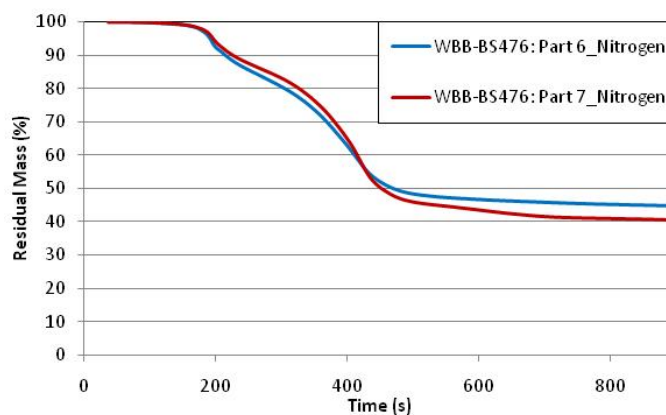
Figure 62 Decomposition curves for Part 6 and Part 7 Warrington blue boards in nitrogen atmosphere

Analysis of thermal stability in an inert atmosphere (such as nitrogen) provides information regarding spontaneous chain degradation, carbonisation, dehydration and other decomposition mechanisms. Experiments carried out under nitrogen conditions more accurately simulate conditions in a fire, where the oxygen concentration is close to 0 % under a flame. However, for samples with available oxygen present within the chemical structure of the sample the oxygen concentration will be greater than 0 % as it will be liberated from the structure and thus react with the oxidisible components. It can be assumed that any oxygen within the system has come from the sample itself and not from an external source. Figure 62 shows the decomposition mechanism in nitrogen is somewhat more stepwise process than in air though there are stronger similarities than normally observed for polymers in air and nitrogen. The decomposition curves are similar up to a temperature of 450 °C where no further decomposition is observed in the nitrogen conditions, instead a greater fraction of residual mass is remaining after the analysis. 40-45 % residual mass remains in the nitrogen atmosphere whereas in oxygen the residue is further oxidised and a residue mass of 35-40 % remains, probably because all the nitrocellulose has decomposed below 300 °C and therefore remaining decomposition is generally anaerobic.

3.5.4. Inverted samples

TGA analysis was undertaken on inverted samples placed into the crucible to determine if the thermal decomposition was altered by changing the orientation of samples. This investigated whether decomposition occurs throughout the bulk of the sample simultaneously or layer by layer. In this case a temperature gradient is formed throughout the bulk of the sample. Experiments were repeated in air and nitrogen for both WBB-BS476: Part 6 and WBB-BS 476:

Part 7 samples and the thermal decomposition behaviour is shown in Figure 63 and Figure 64 respectively with comparison curves also depicted.
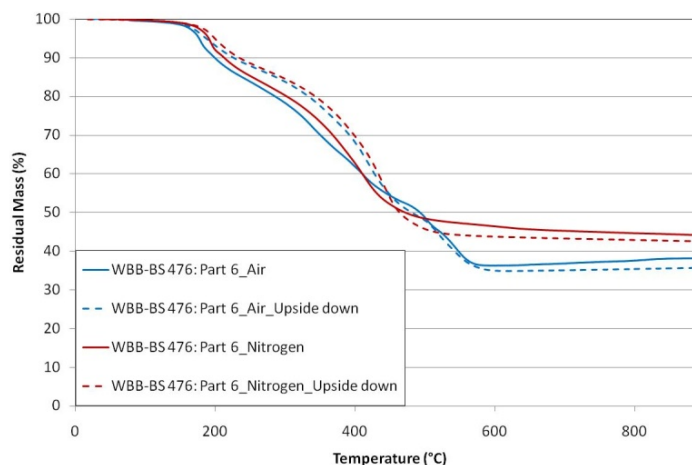
Figure 63 Decomposition curves for Part 6 Warrington blue boards, righted and upside down.

The data collected from the 'Upside down' samples for WBB-BS 476: Part 6 shown above in Figure 63 suggests some variation in the decomposition of the sample when analysed in a different orientation. Variations in thermal decomposition mechanism are most prominent between 250 °C and 450 °C. The curves follow a similar trend. However, 'Upside down' samples are stable to a slightly elevated temperature before decomposition occurs at a similar rate as observed for normal samples. The upside down samples are also less stable at elevated temperatures (>600 °C) leaving in each case approximately 5 % less residual char than their normal counterparts. Residue masses are dependent upon the condition in which the analysis takes place rather than the orientation of the sample when analysed. This data supports the suggestion that there may be a temperature gradient within the depth of the sample and decomposition occurs through each of the layers in sequence rather than decomposing the sample as a whole. Alternatively, and possibly more likely, there may be a protective effect of other layers, or an oxidising effect as O_2 from nitrocellulose passes through other layers of paint. As the rates of decomposition are relatively unchanged it may not be sequential decomposition but rather specific components decomposing earlier and others being more stable to higher temperatures, the variation in mechanism may be due to the positioning of these layers in the sample.
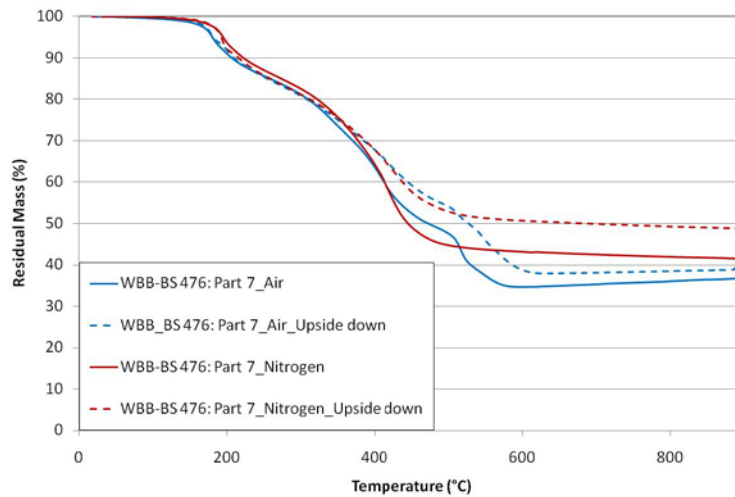
Figure 64 Decomposition curves for Part 7 Warrington blue boards, righted and upside down

Variation in decomposition mechanism for the WBB-BS 476: Part 7, shown in Figure 64, is most prominent for temperatures above 400 °C. Prior to this the decomposition curves are almost identical and suggest the atmosphere and orientation of the sample have limited affect on decomposition mechanism. Above 400 °C there is a notable difference in mechanism, dependant on orientation of sample. 'Upside down' samples are more thermally stable, preserving approximately 5 % more residual mass at higher temperatures in each atmosphere compared to that of the normal samples. This suggests that variation in this case is a factor of both atmosphere and orientation. These results suggest that heat effects the entire sample as a bulk up to a temperature in the region of 400 °C when the mechanism alters. Variation due to orientation is more prominent in the nitrogen atmosphere analyses.

In summary, the data collected shows a surprising lack of variation in the thermal decomposition of WBB-BS 476: Part 6 and WBB- BS 476: Part 7 Warrington blue board substrates when exposed to the TGA heating regime in each of the different atmospheres. Expected differences are observed during comparison of oxygen and nitrogen analyses, such as higher residual mass in nitrogen atmospheres. The sample orientation has a more prominent effect on the WBB-BS 476: Part 7 substrate samples in both atmospheres but most prominently in nitrogen. Results suggest that the thermal decomposition mechanisms for all samples are similar until approximately 400 °C, at which point the mechanism for 'Upside down' samples alters. Increased residual mass suggests that the samples are more protected in the 'Upside down' orientation. TGA analysis of the Warrington blue board does not strongly suggest a difference in board composition until analysed 'Upside down'. The thermal decomposition mechanism appears similar for both substrate boards in the correct orientation however, greater variation is observed in the 'Upside down' orientation suggesting variation in composition. For both substrate boards results suggest that the decomposition in the TGA may

not be as a bulk material but instead layer by layer – predominantly above 400 °C- perhaps not governed by position in the sample but more by the thermal stability of the component. Interestingly if the orientation of the sample has such a significant impact on the decomposition mechanism, this must also suggest a difference in composition.

3.6. Characterisation of Warrington blue boards

Heat release curves showed variation in the behaviour of the two test substrates suggesting disparity in composition, whereas the thermal decomposition analysis revealed inconclusive data. For clarification, characterisation of the two Warrington blue boards was completed to determine specific properties of the substrates and establish any variation between samples.

3.6.1. Microscopy

Optical microscope analysis of paint flakes taken from the two substrate materials was carried out to assess the differences between the samples at the microscopic scale. A magnification of 100 times was utilised to obtain a detailed image of all the composite layers of the material. To achieve optimum lighting (as the samples are opaque) an external LED light source was used to increase the amount of light hitting the sample from above improving the image recorded. The collected images are shown in Figure 65 and Figure 66 respectively below.
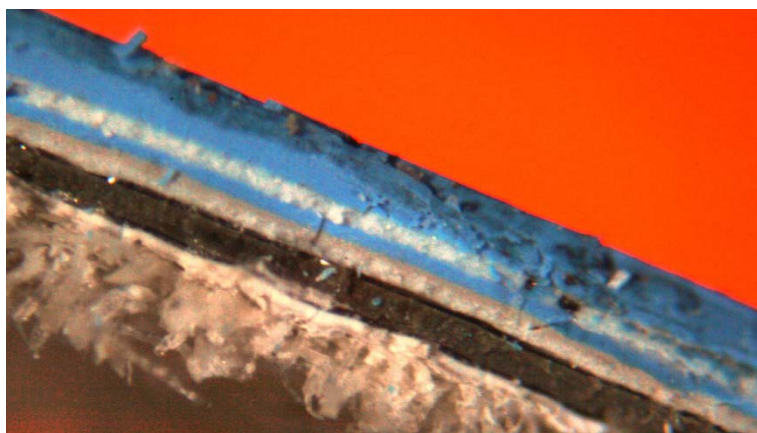
Figure 65 100 times magnified image of WBB-BS 476: Part 6 Warrington blue board

Figure 66 100 times magnified image of WBB-BS 476: Part 7 Warrington blue board

Visual comparison of the two images clearly shows a significant difference in composition of the two samples. The boards appear to be made of the same coloured materials applied in a different order and different ratios in each case. This supports the explanation of the variation in burning behaviour and conflicting thermal decomposition data of the two substrate materials observed in other analysis.

3.6.2. Assignment of layers and determination of thickness

The next stage of characterisation involves the identification and assignment of the layers within the blue board substrate material and estimating layer thickness. This should enable better determination of composition, better understanding of decomposition and allow re-creation of similar substrates for future experiments.

The individual components of the Warrington blue board have previously been identified[120] and are listed in Table 15. Some information from the original formulation of Warrington blue board indicated that its composition was likely to contain the following components.

Table 15 Components of the Warrington blue board

Material	Colour
MDF Primer	Off white
Nitrocellulose based gloss	Magnolia
Nitrocellulose based gloss	Grey
2 pack polyurethane	Clear
Commercial solvent based gloss	Dark grey
Nitrocellulose based gloss	Blue

To correctly assign these paints to layers observed under the optical microscope, samples were brush applied onto a plasterboard substrate and dried before microscopic analysis was carried out on the paint flakes. This allowed direct comparison between the appearance of the layers in the WBB-BS 476: Part 6 and WBB-BS 476: Part 7 substrates and the component paint from Table 15 under the same conditions.

3.6.3. WBB-BS 476: Part 6 substrate

Initially total coating thickness was measured using a micrometer and recorded. Using images captured through the light microscope, each layer could be identified (using comparison data from above) and layer thickness determined. Figure 67 and Table 16 show the WBB-BS 476: Part 6 board at 100 times magnification and the assignment of each layer's thickness and identity.

0.05 mm

0.5475 mm
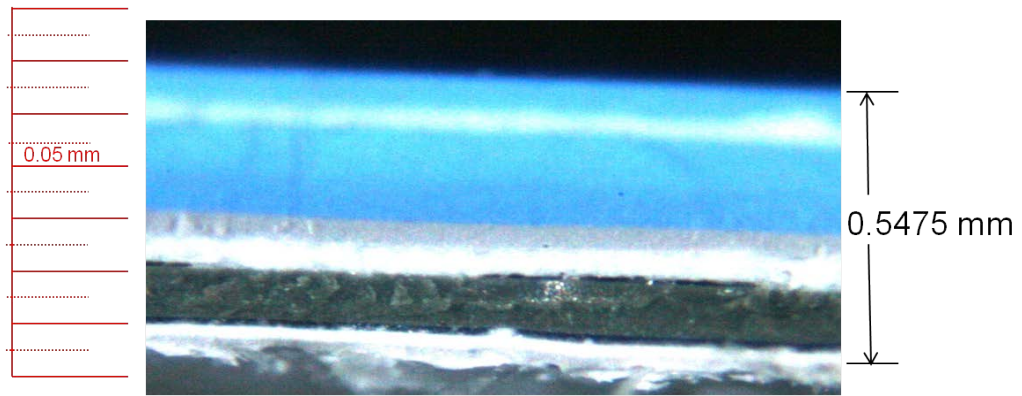
Figure 67 100 times magnified image of WBB-BS 476: Part 6 Warrington blue board with assigned layer thicknesses

Table 16 Layer assignment for WBB-BS 476: Part 6 Warrington blue board

Sample – Part 6	Measured thickness from Photograph	Calculation	Layer thickness
Blue NC gloss	9 mm	(0.05/6.5) x 9	0.069 mm
MDF Primer	6 mm	(0.05/6.5) x 6	0.046 mm
Blue NC gloss	23 mm	(0.05/6.5) x 23	0.177 mm
Magnolia NC gloss	5 mm	(0.05/6.5) x 5	0.038 mm
MDF Primer	8 mm	(0.05/6.5) x 8	0.062 mm
Dark grey gloss	1 mm	(0.05/6.5) x 1	0.008 mm
PU clear	14 mm	(0.05/6.5) x 14	0.108 mm
Dark grey gloss	2 mm	(0.05/6.5) x 2	0.015 mm
PU clear	4 mm	(0.05/6.5) x 4	0.031 mm
MDF primer	3 mm	(0.05/6.5) x 3	0.023 mm
Total	**70 mm**		**0.578 mm**

Table 16 shows that nitrocellulose based paint makes up 42.6 % of the total coating thickness.

3.6.4. WBB-BS 476: Part 7 substrate

The same was done for WBB-BS 476: Part 7 Warrington blue board samples and the details are shown below in Figure 68 and Table 17 respectively.
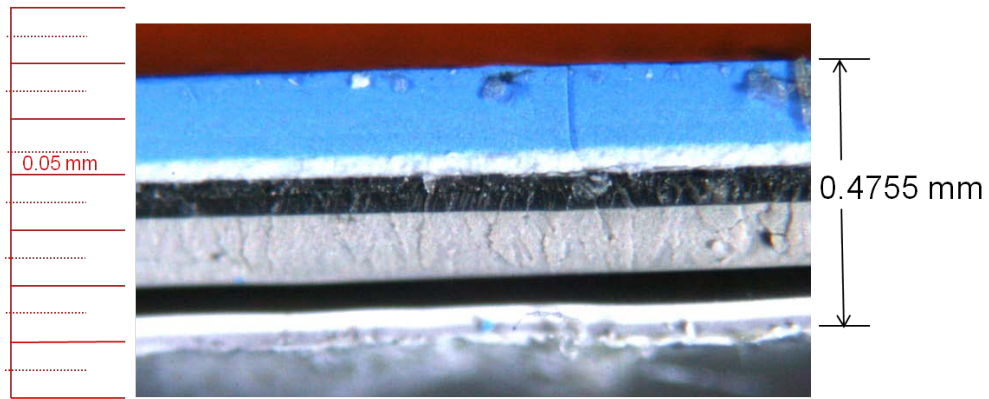
Figure 68 100 times magnified image of WBB-BS 476: Part 7 Warrington blue board with assigned layer thicknesses

Table 17 Layer assignment for WBB-BS 476: Part 7 Warrington blue board

Sample – Part 7	Measured thickness from Photograph	Calculation	Layer thickness
Blue NC gloss	23 mm	(0.05/8) x 23	0.144 mm
MDF Primer	7 mm	(0.05/8) x 7	0.044 mm
PU Clear	9 mm	(0.05/8) x 9	0.056 mm
Dark grey gloss	19 mm	(0.05/8) x 19	0.119 mm
PU Clear	8 mm	(0.05/8) x 8	0.05 mm
Grey NC gloss	6 mm	(0.05/8) x 6	0.0375 mm
Magnolia NC gloss	4 mm	(0.05/8) x 4	0.025 mm
Total	**76 mm**		**0.4755 mm**

In contrast to the WBB-BS 476: Part 6 results nitrocellulose makes up only 30.3 % of the WBB-BS 476: Part 7 coating thickness, as shown in Table 17. This supports the variation in heat release rate data collected. WBB-BS 476: Part 6 has a higher CO_2 production rate combined with a lower oxygen depletion value which further suggests a higher concentration of nitrocellulose is present in these samples.

Results reported above clearly suggest that although the component paints of the two boards are the same, the order and thickness in which they are applied is different. This leads to variation in burning behaviour and conflicting thermal decomposition data of the two substrates; as a result different methods of fire protection may be necessary. It also explains the different response to inverse orientation in thermogravimetric analysis.

3.6.5. Warrington blue board component analysis

Investigation was then carried out on the component paints of the Warrington blue board substrate using TGA analysis to determine the thermal decomposition mechanism of the individual components. Results were then compared to the data collected from experiments on the WBB-BS 476: Part 6 and WBB-BS 476: Part 7 paint flakes, to ascertain the extent of any interaction between layers. Individual decomposition curves (for each component of the blue board) were combined to create a 'calculated' TGA curve. This was then compared to the actual TGA curve recorded and any synergism or antagonism between layers assessed. The calculated and actual curves for each sample are depicted below in Figure 69 and Figure 70 respectively.

3.6.4.1. WBB-BS 476: Part 6
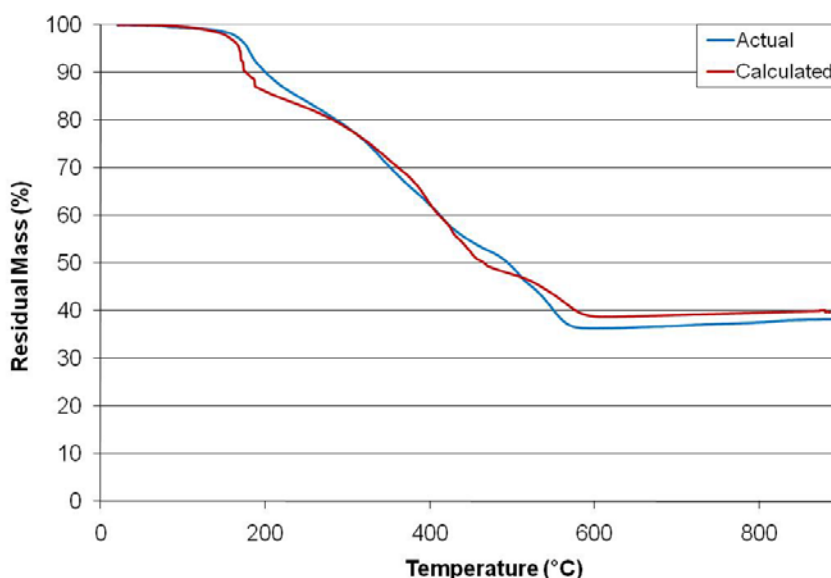
Figure 69 Calculated and actual TGA curves for Part 6 Warrington blue board

The calculated TGA curve closely mirrors the actual curve, suggesting there is very little interaction between the component layers of the blue board during decomposition. The initial variation between the two curves is observed at 200 °C. The actual curve is more stable than the calculated one. This suggests antagonistic decomposition behaviour. This recurs at approximately 450 °C. The final residual mass is slightly overestimated suggesting that the actual residue is less thermally stable. It is not surprising that the actual coating does not behave the same as the sum of the composite parts, when analysed in the TGA. This is due to the samples being made up of several different components, layered in a sample. Most TGA samples consist of only one material; therefore decomposition can be more easily predicted and reproduced. This is further supported by the results previously reported, where samples of

the Warrington blue board were tested in various orientations in the TGA. Each sample displayed a variation in thermal decomposition because of the layered nature of the sample.

3.6.4.2. WBB-BS 476: Part 7
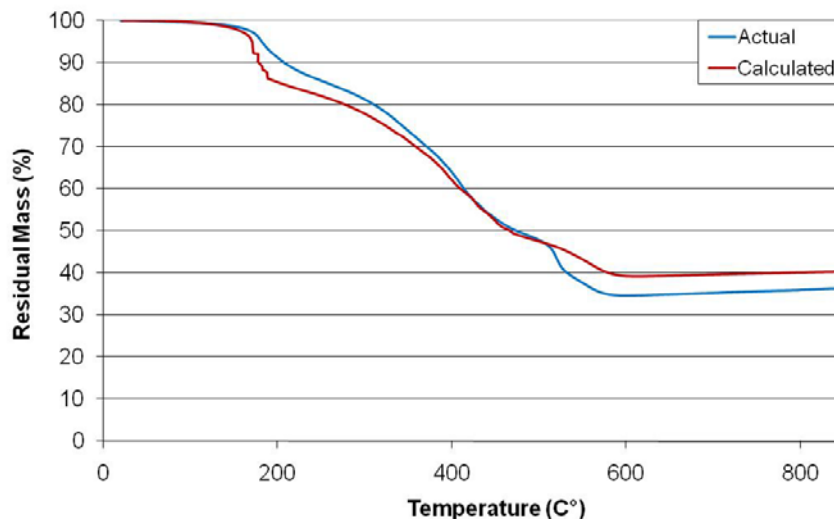
Figure 70 Calculated and actual TGA curves for Part 7 Warrington blue board

Greater discrepancies are observed in the actual and calculated decomposition curves for the WBB-BS 476: Part 7 sample. The most prominent of these starts at 200 °C and continues until 400 °C. The second is the final residue mass, this is significantly overestimated (by approximately 5 %), and again the actual residue is less stable than the expected. This supports the suggestion that the layered composition of the sample causes variation in decomposition mechanism that would not be present in single component samples.

No significant synergism or antagonism is observed between layers during decomposition of the samples.

3.6.5. Reproduction of the Warrington blue board

To establish the mass of paint needed to achieve the required dry film thickness of each layer within the Warrington blue board, investigations of wet and dry film mass and thickness were undertaken. This was carried out by measuring a known thickness of wet paint onto a substrate of known thickness. This was then allowed to dry and the dry film thickness was measured. This was repeated for all six paints that make up the Warrington blue board substrate. The results are listed in Table 18.

Table 18 Solvent content of Warrington blue board components

Can	Sample	Wet Film thickness	Dry Film thickness	% Loss [Solvent content?]
1	MDF Primer	0.8 mm	0.25 mm	31%
2	Nitrocellulose gloss (magnolia)	0.8 mm	0.66 mm	82.50%
3	Nitrocellulose gloss (grey)	0.8 mm	0.25 mm	31%
4	2 pack PU (clear)	0.8 mm	0.77 mm	96%
5	Standard gloss (dark grey)	0.8 mm	0.76 mm	95%
6	Nitrocellulose gloss (blue)	0.8 mm	0.23 mm	28.70%

With this data collected and the mass loss during drying the mass of paint to be applied to achieve the required thickness can be determined. The reproduction of the blue boards can then be assessed to ensure a similar burning behaviour and heat release rate.

However, reproduction of the Warrington blue board is highly labour intensive and material costly as many paint layers have to be built up with complete drying time allowed in between. While these would replicate the exact test conditions they were deemed too expensive a substrate for basic formulation work. Therefore, it was decided that all future experiments would be carried out on a plasterboard substrate with two coats of nitrocellulose paint applied. This would reduce labour and material costs but also maintain the most awkward properties of the Warrington blue board, such as the low melting point, oxygen within structure and high flammability.

3.7. Heat flux

The heat flux to which samples are exposed will have a significant impact on the action of the coating. Various systems particularly intumescents have been optimised for specific conditions, therefore a slight alteration in the heat flux can produce a disproportionate variation in the rate and extent of fire retardant action – particularly for intumescent systems. Heat flux is very important for the cone calorimeter, BS EN 367, and BS 476: Part 6 (adapted) fire tests,

therefore the effect of heat flux on the samples was investigated prior to any flammability analysis.
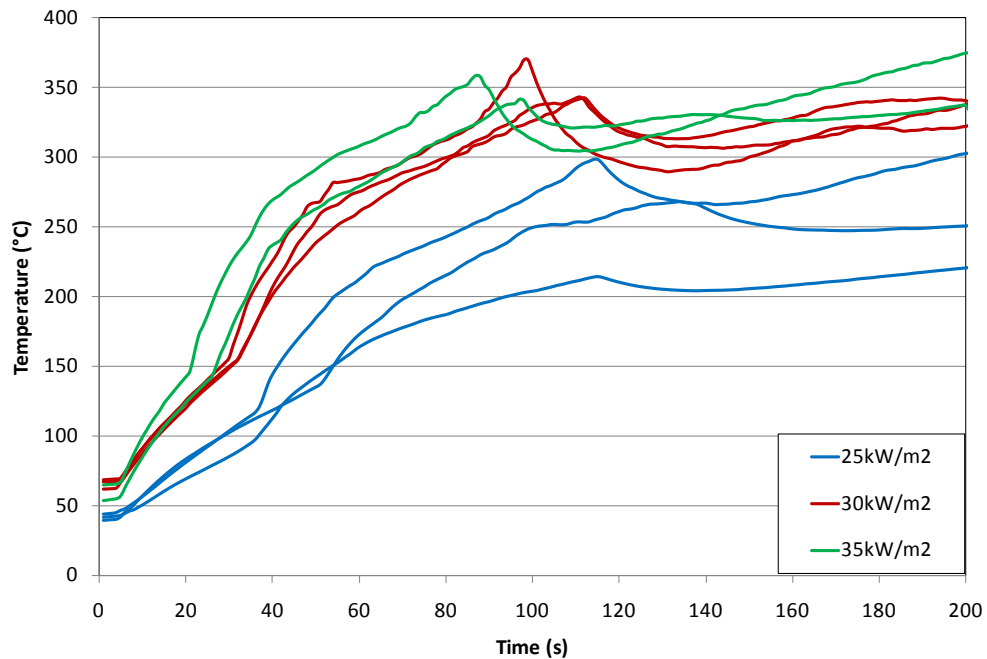
Figure 71 Analysis of gloss paint at various heat fluxes

Figure 71 shows heat release rate curves collected from analyses of 3 coats of gloss paint on a nitrocellulose substrate at various heat fluxes. The results show limited variation between 30 and 35 kW m^{-2}. Conversely 25 kW m^{-2} produces a far lower heat release rate and a far larger scatter in results. The heat flux must exploit the fire retardant properties of a system highlighting the difference between a protective and non-protective coating as well as measuring the efficiency of a range of similar fire retardant systems. A balance must be found between lack of ignition (particularly for fire retardant systems at lower heat fluxes) and too rapid burning (of non-fire retardant systems at higher heat fluxes). Therefore 35 kW m^{-2} was chosen for future analysis as this induced ignition for all but the most protective fire retardant systems whilst also maintaining long enough burn time to gather all the detail in the data and reducing scatter. This heat flux could then be simulated in the BS EN 367 experiments and would be fairly representative of the temperature profile of the early stages of the BS 476: Part 6 (adapted) analysis.

Heat flux measurements in the BS EN 367 are only reported within a range of 30-40 kW m^{-2} due to the drift observed within any given experimentation session. Though the heat flux is monitored throughout any testing period it cannot be reported as an exact figure and instead is maintained within a range of 30-40 kW m^{-2}.

3.8. Softening temperature, viscosity and window of expansion

The heat flux of exposure leading to the softening and decomposition of the resin is vital to the performance of intumescent coatings. The rate and extent of resin decomposition ensures that the optimal level and structure of intumescence is achieved. This requires an understanding of the changes in viscosity during the intumescent process. Results obtained using the rheometer accurately record the viscosity of the coating but this method is not designed for the measurement of the extent of intumescence. For any paint or coating, the initial viscosity should be such that the coating has good stability so the shelf-life is acceptable and prevents settling of additives, it should be such that the flow allows application of the coating without sagging or cracking. For intumescent fire protective coatings, it is important for the resin to soften and decompose under the application of heat such that the bubbles formed during the decomposition of the spumific can be contained within the residual char. However, it should not be so runny that the bubbles escape from the foamed layer, or so that the coating falls off the substrate. An increase in viscosity should then occur, to stabilise the char and prevent loss of the protective barrier layer.

The extent of intumescence is highly dependent on the interaction of the components within the formulation. The softening temperature of the resin must coincide with the activation of the blowing agent and the resin must harden to maintain a stable char residue. The complex viscosity (η^*) is widely accepted as a measure of the viscosity of a paint product prior to application. However, analysis of the complex viscosity also enables prediction of the temperature window of intumescence of a system as well as the extent of expansion expected.

Commercial products - steel intumescent and Magma Prime (clear) - were analysed using the rheometer to estimate the magnitude of reduction in complex viscosity required to produce the maximum amount of intumescence.
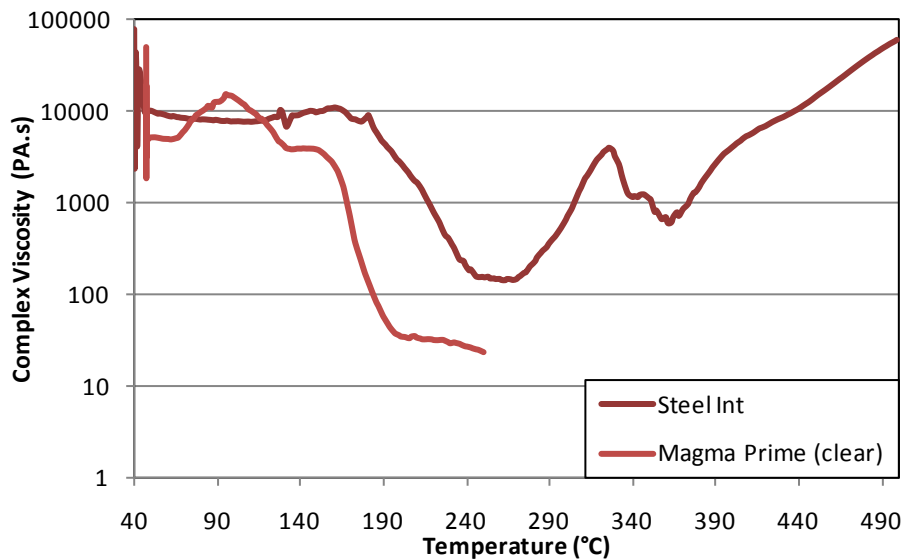
Figure 72 Complex viscosity measurements from commercial intumescent systems

Figure 72 shows that a reduction in complex viscosity of more than two orders of magnitude is typical for samples of this type. Resins should also be selected with similar properties. At the softest point, the steel intumescent sample maintains a complex viscosity greater than that of the Magma Prime (clear) sample. This may aid explanation of the reduced expansion of the Magma Prime (clear) sample (shown in Figure 73). If the sample becomes too runny it will fail to trap any of the vapours produced from the decomposition of the spumific. The steel intumescent system appears to display the optimum complex viscosity to allow the maximum level of expansion, but this occurs at a higher temperature than needed to protect nitrocellulose or possibly other multilayer paint build-up.

The rheology method consisted of a normal force of 2N constantly applied throughout analysis. This allows analysis of the gap measurement to estimate the amount and temperature of onset of expansion. As vapours are formed and escape from the sample, it applies pressure to the geometry increasing the gap.

Figure 73 is a comparison of gap measurement collected from the two systems, commercial steel intumescent and a lower temperature intumescent system probably designed for timber. The graph clearly depicts the earlier onset of intumescence displayed by the Magma Prime (clear) sample at approximately 120 °C. Conversely the steel intumescent has two periods of expansion, the first at 240 °C and the latter at 340 °C protecting the substrate over a greater temperature range. The two phases of intumescence may occur due to a stagger in the decomposition of the components, caused by the heat penetration through the depth of the coating.
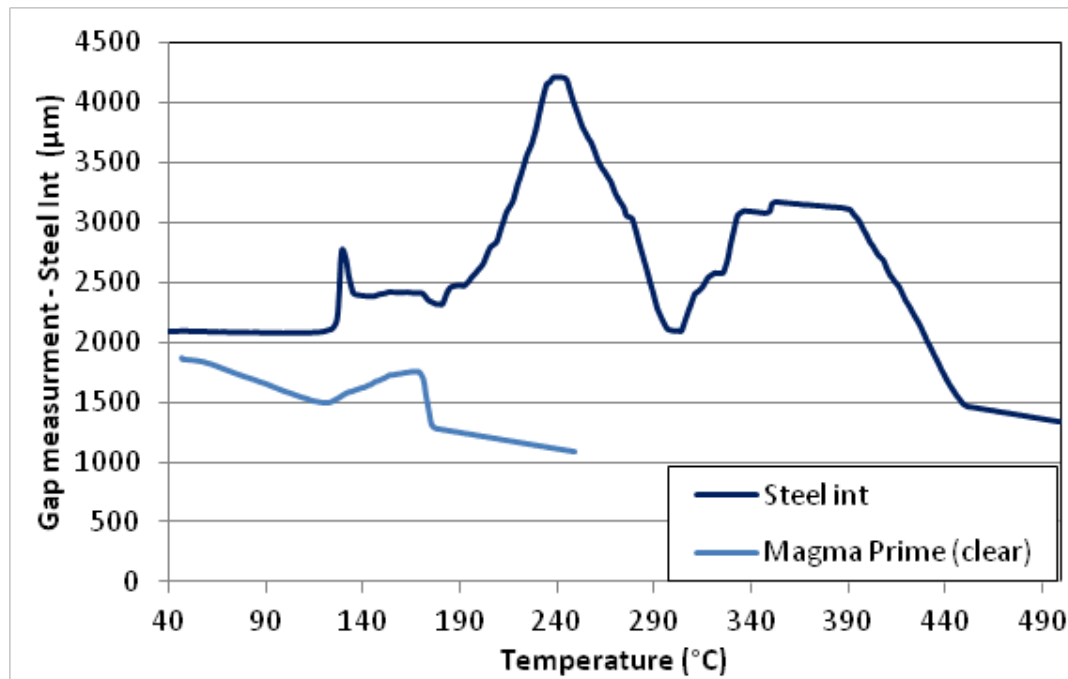
Figure 73 Gap measurements from commercial intumescent systems

Magma Prime (clear) sample analyses are terminated at 250 °C due to the excessive expansion of the sample which reaches the inner wall of the furnace chamber. This suggests that the gap measurements shown in Figure 73 under-estimate the level of expansion of the cellulose system as most of the expansion occurs sideways in preference to upwards. This is because the heat from the furnace attacks the edges of the samples rather than the centre, inducing intumescence sideways rather than upwards. It should be noted that both systems are compressed continuously at 2N throughout the analyses and so the expansion will be limited to some extent. The top geometry is unable to move rapidly enough to maintain the required normal force when the intumescent reaction occurs.

Softening temperature of some commonly used (halogen-free) resin systems was undertaken to assess the magnitude of reduction of the complex viscosity and temperature at which this occurs. This determines the most appropriate combination of resin and fire retardant additive with respect to thermal stability. Resins selected for analysis are listed in Table 9.

Table 19 Identity of resin samples selected for viscosity analysis.

Sample name	Sample
Resin 2	Vinyl acrylic copolymer PVDC
Resin 6	PVA
Resin 7	Styrene acrylic dispersion
Resin 18	Acrylic copolymer dispersion
Resin 19	Vinyl acetate Veovaio Acrylic copolymer dispersion
Resin 24	Acrylic dispersion
Resin 25	PVA
Resin 26	Vinyl acetate Veovaio copolymer dispersion
Resin 27	Vinyl acetate Veovaio copolymer dispersion
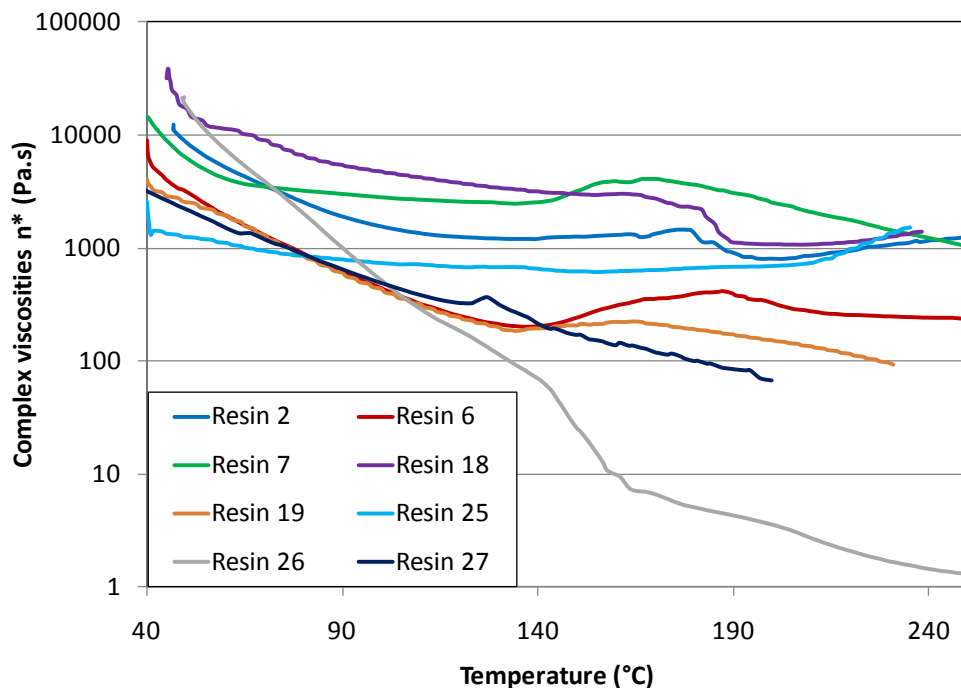
Figure 74 Comparison of complex viscosity from resin samples listed in Table 19

The vinyl acetate resins (Resins 6, 19, 26 and 27) all display reduction in complex viscosity within the range of around two orders of magnitude similar to the reduction shown by the steel intumescent and Magma Prime clear formulations (Figure 72). All of these resins are vinyl acetate compounds suggesting that intumescent formulations would benefit from being based on this resin type. All other resin systems analysed, failed to show the required reduction in complex viscosity and therefore were excluded from further trials.

The four resin systems were then combined with 10 % loading of DAP to determine any change to the complex viscosity characteristics of the material. The results are shown below in Figure 75, Figure 76, Figure 77 and Figure 78 respectively.
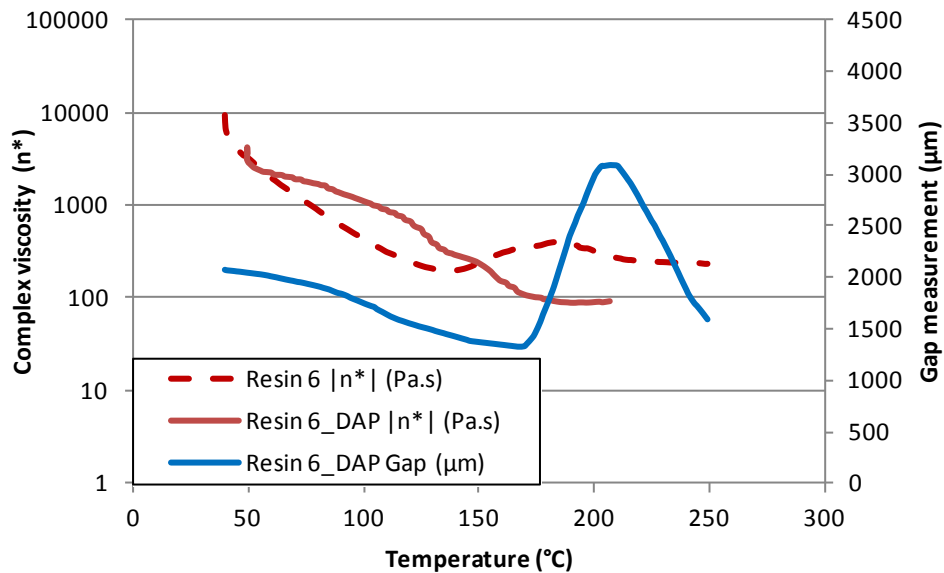
Figure 75 Analysis of complex viscosity and gap measurement of Resin 6 with added DAP

Figure 75 shows that complex viscosity of the resin decreases at a slower rate and at a higher temperature, with the incorporation of the DAP. Increase of gap measurement is observed at approximately 175 °C suggesting the occurrence of intumescence even without the incorporation of the additional additives. For these reasons this appears to be a promising system.
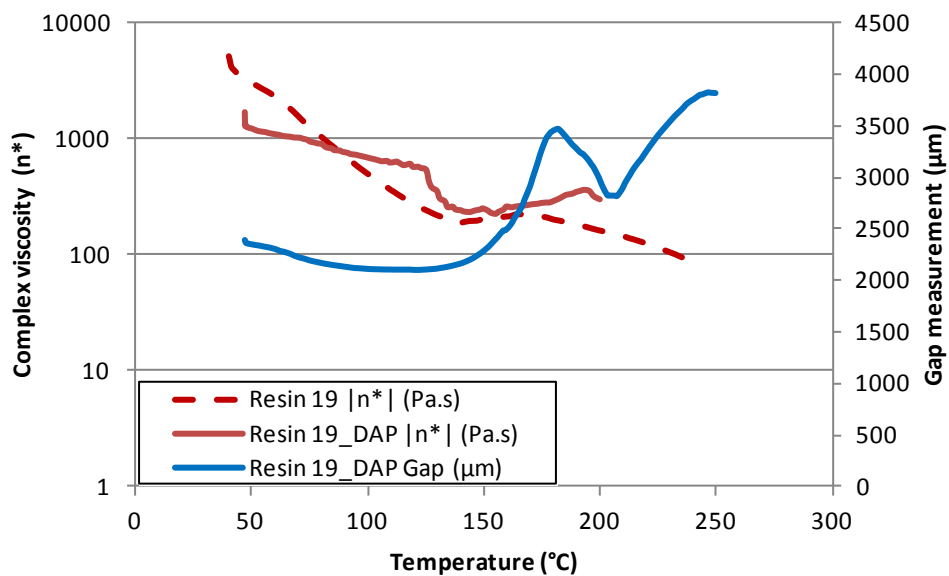
Figure 76 Analysis of complex viscosity and gap measurement of Resin 19 with added DAP

Similar observations are recorded for resin 19 and are depicted in Figure 76. In this case far more intumescence is observed as the gap increases in two stages, firstly beginning at 150 °C and secondly at 220 °C. This is similar behaviour as observed in the commercial steel intumescence system and is promising. On the other hand the complex viscosity does not

reduce as much. Normally this might indicate lower expansion however; in this case the expansion appears to be good.
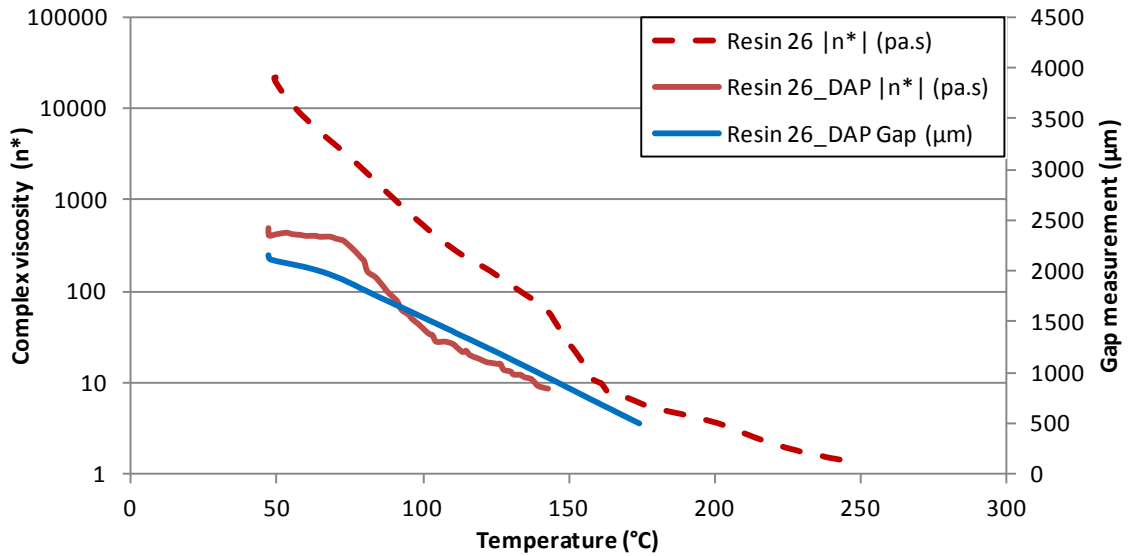
Figure 77 Analysis of complex viscosity and gap measurement of Resin 26 with added DAP

Resin 26 shows no increase in gap measurement, and there is limited evidence to suggest that the DAP has any effect on the complex viscosity measurement. Observations of this sample after analysis suggest that softening is too extensive. The sample runs out from between the two plates within this temperature range thus removing it from the measurement zone. At this viscosity the material is unable to trap any vapours produced from the intumescent action and furthermore may even drip or run off of the substrate to which it is applied.
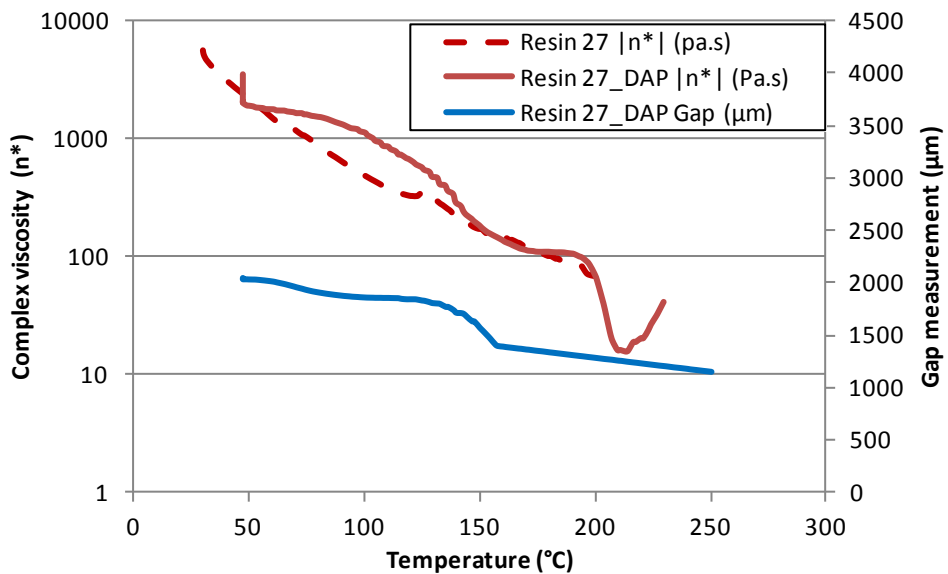
Figure 78 Analysis of complex viscosity and gap measurement of Resin 27 with added DAP

119

Figure 78 shows that complex viscosity of resin 27 (with added DAP) is prolonged to a higher temperature; however the rate of reduction remains unchanged. No gap increase is observed.

Analysis was then carried out on some novel formulations based on commercial steel intumescent systems (VrAMP) see section 5.2. with additional additives to aid fire retardance such as Noflan (to hinder ignition) and silica fume (to increase char stability and reduce fuel loading).
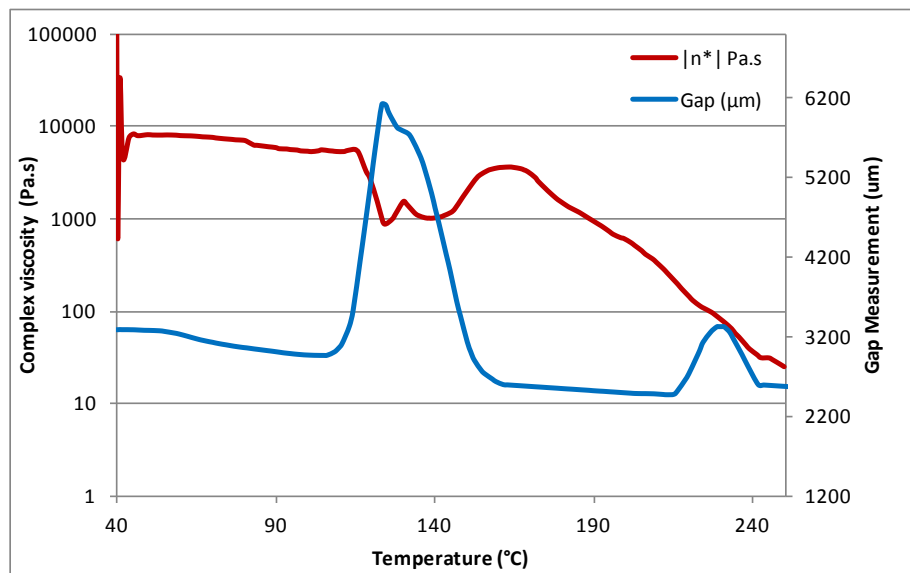
Figure 79 Complex viscosity and gap measurement analysis of VrAMP

Initial reduction in complex viscosity coincides with the intumescent action producing a significant increase in gap measurement at approximately 120 °C (shown in Figure 79). Vapours are lost due to the lack of resin hardening once the voids are trapped leading to a complete loss of intumescent residue. A second gap increase is recorded at 220 °C which is approximately a quarter of the initial increase and again is lost due to the lack of stiffening of the resin. The normal force allowing assessment of gap increase will also act to crush any resultant char suggesting that more protection would be offered in a fire situation were this system to be used.

10 % loadings of Noflan and silica fume were added independently to this base formulation and the results are shown in Figure 80 and Figure 81. Noflan is an organophosphorus fire retardant additive which acts to prevent ignition and silica fume is added to stabilise char without increasing the viscosity of the paint.
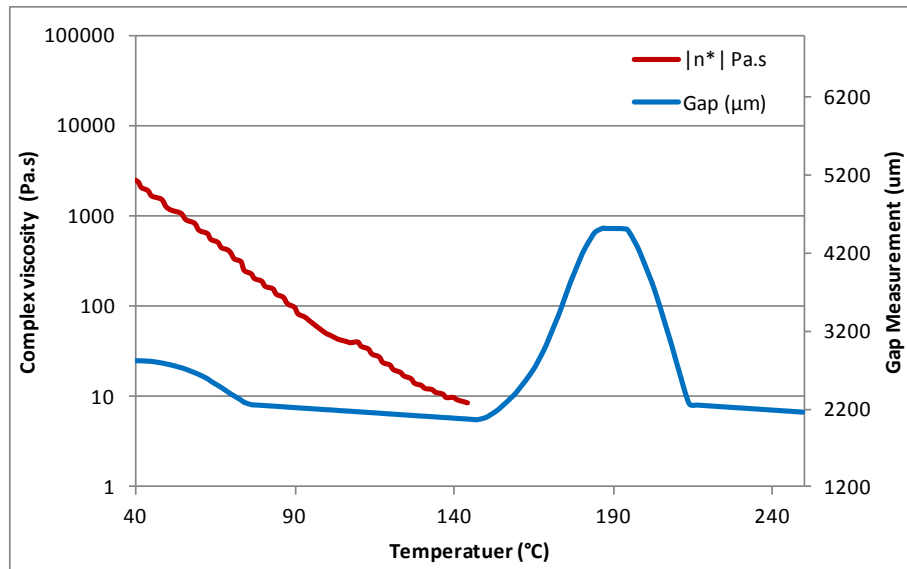
Figure 80 Complex viscosity and gap measurement analysis of VrAMP_Noflan

An initial fluctuation in complex viscosity, due to lack of adhesion between the sample and parallel plate has been removed from the figures. This effect is reduced by increasing the normal force however this increase also destroys any char residue formed. In this case the normal force is set to 2N; this allows best adhesion and still records intumescent action even though the resultant char is mostly destroyed. Figure 80 shows intumescent action around 150 °C which is again lost due to the lack of hardening. This suggests that the influence of the Noflan is to delay the intumescent action to a higher temperature. The reduction in complex viscosity remains unchanged, suggesting that Noflan reduces gas production inhibiting intumescence.
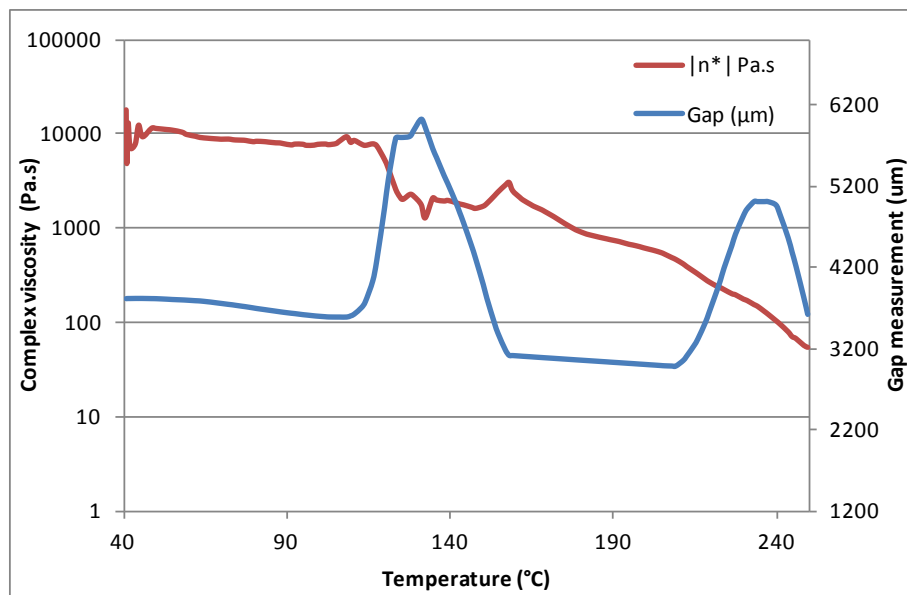
Figure 81 Complex viscosity and gap measurement analysis of VrAMP_Silica

With the addition of silica fume, the sample mirrors the behaviour of the unchanged formulation (Figure 81 and Figure 79). This suggests that the silica fume does not affect complex viscosity or rate, temperature and extent of expansion. However, it may have other effects not measured in this method. These may include strengthening char structure and increasing radiative heat reflected from the char surface.

The rheology equipment was only available for use in the later stages of this research and though only a few analyses were possible it is already clear how much information can be gathered from sample analysis. These results suggest which resin systems should go forward for further analyses, and those which can be discounted. Resins can be discounted due to the rate and amount of reduction of complex viscosity and the temperature range in which this occurs. Stiffening of the resin is also crucial and though not analysed in the results reported above, would be critical to the intumescent formulation. Results also determine the window of opportunity for intumescence when the resin is soft enough and the intumescent action takes place. Though the equipment cannot measure the extent and rate of expansion (due to the restricted speed of geometry movement – it is too slow to keep up with the intumescent action) it can provide comparison between samples under the same conditions.

SUMMARY

Preliminary analyses of the factors affecting coating performance have shown that several factors contribute to the overall performance of a protective coating system. Firstly, the type and thickness of the substrate material, including properties such as its intrinsic flammability and heat transfer properties at various heat fluxes. Burning behaviour of multiple layers of paint has been investigated and is shown to be significantly altered by the application of additional coats, even when frequently applied, independently of whether the system is an example of a fire retardant coating or not. Variation in the heat flux in the cone calorimeter also influences factors such as heat release rate, time to ignition of samples and extent of data scatter. Secondly, adhesion of the coating to the substrate material and cohesion of layers within the substrate material is vital to performance. Standard test substrates' characterisation and flammability assessment in the cone calorimeter establish a significant difference between their burning properties and the reason for these differences. Finally, rheological properties of base resins and complete formulations are defined, in order to determine the influence of physical parameters such softening temperature, complex viscosity, extent and window intumescent action on the coating performance and test result. All are shown to be valuable factors for consideration and provide a basic understanding which provides the foundation for future analyses. However, it is noted that rheometry is not the optimum method for analysis of

the extent of intumescence as the temperature regime is not representative of a real fire or that experience in the standard fire tests. Also, the gap measurement is not an accurate measure of intumescent action because the normal force crushes any char residue formed, and the top geometry cannot move rapidly enough to allow char growth during the intumescent process.

These investigations most clearly outline the variation in laboratory based testing and real case scenarios. Results are so highly dependent on minute and un-controllable factors that a slight variation in testing conditions can result in a disproportionate discrepancy in result. This underlines the significance of not extrapolating laboratory results to other conditions and scenarios. Not least in the testing of fire protective coatings, where the target substrate is a highly flammable well-adhered substrate, however, in a real scenario the substrate for protection is likely to be of lower intrinsic flammability but flaky and not well-adhered increasing the fire hazard.

CHAPTER 4. EXISTING FORMULATIONS

Screening test methods designed to assess various flammability parameters were carried out on existing fire retardant formulations to determine the effect of each of the parameters outlined in section 1.11. on coating performance. This would aid determination of current successes and limitations of commercial products by predicting performance in standard fire tests and enabling optimisation.

4.1. FR120 and FR121

Existing fire retardant coatings were analysed using the screening test methods outlined in section 2.3.

4.1.1. Assessment of fire retardant action

FR120   FR121

Figure 82 FR120 and FR121 sample after the Bunsen burner experiment

Figure 82 depicts FR120 and FR121 samples after exposure to a Bunsen burner flame. FR120 appears to leave no char residue and some of the wooden substrate is sacrificed however, the FR121 system shows small signs of bubbling and perhaps some intumescence. The green tinge on exposure to the flames suggests the presence of copper.

4.1.2. Assessment of thermal decomposition - Thermogravimetric (TGA) analysis

Analysis was carried out in air and nitrogen from ambient temperature to 900 °C at a heating rate of 10 °C min^{-1} and a gas flow rate of 50 cm^3 min^{-1}. Three repeats of each sample were analysed and averages calculated. Results are shown in Figure 83 and Figure 84.
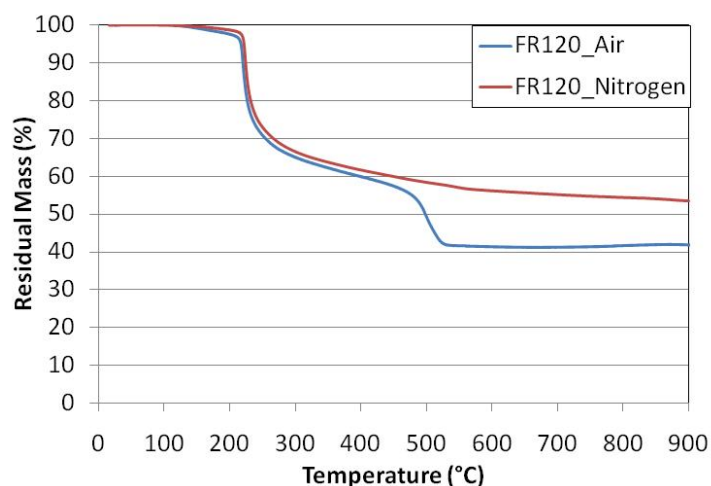
Figure 83 Decomposition curves for FR120 in air and nitrogen; ambient to 900 °C, at a heating rate of 10 °C per minute

The initial mass loss (between 150–225 °C) in Figure 83 is attributed to loss of HCl though this could be quantified using TGA-FTIR. The next stage of decomposition is a rapid decomposition step at approximately 230 °C, auto-catalysed by the release of hydrogen chloride from structure. A carbonaceous material is formed at approximately 230-240 °C which constitutes roughly 60 % of the residual mass which undergoes another decomposition stage in air to leave slightly more than 40 % residual mass but remains fairly stable in nitrogen.
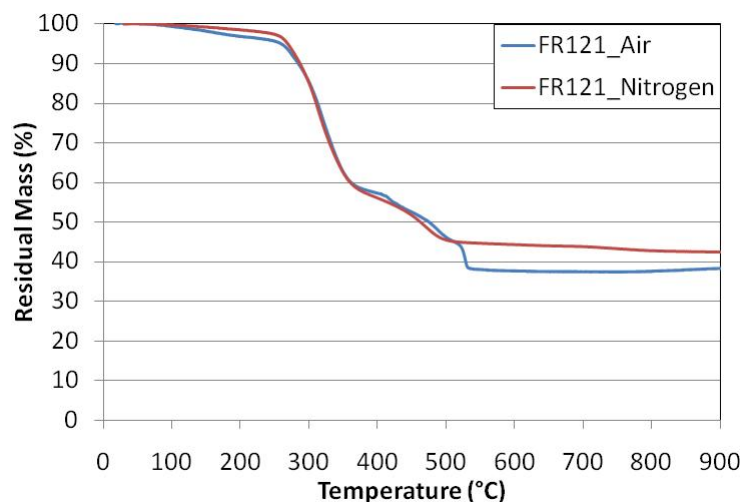
Figure 84 Decomposition curves for FR121 in air and nitrogen; ambient to 900 °C, at a heating rate of 10 °C per minute

The thermal decomposition of FR121 is shown in Figure 84 and is more complex; starting with a rapid (but not auto-catalysed) decomposition stage occurring at 275 °C and finishing at 350 °C leaving a 58 % residual mass. This undergoes another slower step to leave a 45 % residual mass in both atmospheres. This remains stable in nitrogen but is further oxidised in air to leave a final residual mass of 38 %.

125

4.1.3. Assessment of cone calorimeter properties

Average heat release rate curves, calculated from three repeat experiments of each of the systems on nitrocellulose substrate, were compared to assess fire protection performance. Samples were prepared three layers thick as it is unlikely that in a real situation there would be any more than three coats of fire retardant paint applied in succession to the same wall. Samples were prepared on a substrate of 0.8 mm aluminium sheet and exposed to an irradiance of 55 kW m^{-2} in the cone calorimeter. The comparison is shown below in Figure 85.
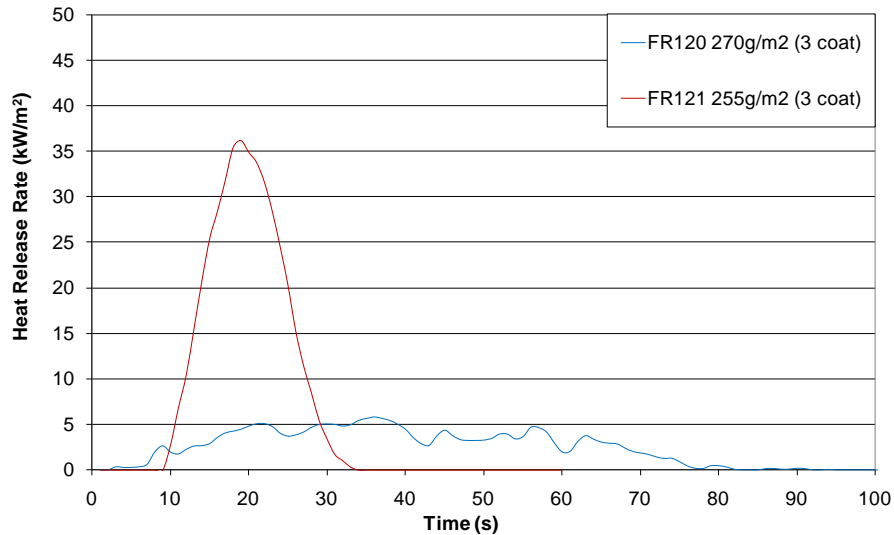
Figure 85 Average heat release curves for FR120 and FR121 samples

This comparison clearly demonstrates that the FR120 system was the least flammable protective coating as it was not ignited at any point during the test. Free radical release coincides with the early flame reactions and the barrier properties of the coating prevent ignition of the pyrolysis products that are produced. The FR121 system shows some fire retardant properties as its peak heat release is maintained at approximately 40 kW m^{-2} and burn time is reduced, however ignition was not prevented. A summary of all the flammability data collected during these experiments are shown in Table 20.

Table 20 FR120 and FR121 cone calorimeter properties

Sample	t_{ig} (s)	PHRR (kW m^{-2})	tPHRR (s)	THR (kW m^{-2})
FR120	0 ± 0	11.1 ± 2	338 ± 229	284 ± 67
FR121	3 ± 1	30.1 ± 12	130 ± 5	352 ± 144

4.1.4. Calculation of fire propagation index – BS 476: Part 6 (adapted)

The analysis carried out in accordance with BS 476: Part 6 for both fire retardant samples supports suggestions that protection is not only dependant on the level of intumescence or char production. Neither of the two systems analysed contain intumescent species or char promoting additives although the results in the Part 6 test show that reasonable improvements can be made using other methods. Table 21 shows the fire propagation index calculated from three repeat analyses of each sample, these are then compared to a reference sample which consists of a board coated with two layers of nitrocellulose paint.

Table 21 BS 476: Part 6 (adapted) analysis of commercial samples FR120 and FR121

Sample	s1 (0.5-3 min)	s2 (4-10 min)	s3 (11-20 min)	S (0-20 min)	Fire propagation index (L)	Pass/Fail
Nitrocellulose	23.79 19.61 16.89	4.36 4.39 3.17	0.66 0.63 0.54	28.81 24.63 20.6	24.22	Fail
Nitrocellulose + FR120	3.7 6.92 4.36	2.24 1.93 2.55	0.4 0.39 0.54	6.34 9.24 7.46	7.68	Fail
Nitrocellulose + FR121	3.78 5.84 1.84	3.62 3.54 3.68	0.55 0.6 0.38	7.95 9.98 5.9	7.95	Fail

The data clearly shows that the unprotected reference board has a very high fire propagation index, correlating to a 'Class 4' rated system. When the same reference board is over-coated with the FR120 and FR121 systems, the fire propagation index value is significantly reduced. The greatest improvement occurs in the early stages of the experiment as indicated by s1 values in Table 21. As the beginning of the analysis is the most heavily weighted portion and the most crucial period for the protection of painted surfaces, it is this portion of the test that should be targeted to gain the most optimised formulation.

These results show that the highly halogenated systems provided the more promising results. The halogen decomposition coincides with the initial flaming of the coating and substrate material therefore the flame is quenched to a certain degree and flaming is controlled in the initial stages. Within a thin film there is a limited supply of halogens however by the time these have been consumed the most crucial period of the test is over. Also by this time the nitrocellulose has decomposed and the majority of flammable products have been released without ignition.

Table 22 Char height analysis of commercial samples FR120 and FR121 recorded after BS 476: Part 6 experimentation

Sample	Min (mm)	Max (mm)	Average (mm)	Average (mm)
Nitrocellulose	0	0	0	0
	0	0	0	
	0	0	0	
Nitrocellulose + F120	0	0	0	0
	0	0	0	
	0	0	0	
Nitrocellulose + FR121	2	8	5	4.5
	0	6	3	
	3	8	5.5	

The major limitation of halogenated systems is their elevated corrosivity toxicity and smoke production. Their reduced ability to produce a protective char layer during combustion also reduces the protection afforded by these systems. Table 22 shows the char heights of the FR120 and FR121 systems after analysis in the Part 6 test. The data in Table 22 clearly shows that neither the reference nor the FR120 system produce any char during combustion, so that the paper layer of the plasterboard is lost during combustion. The FR121 sample leaves a small amount of residue behind and it can be seen from the data in Table 21 that this improves the fire propagation index for later periods of analysis (the s2 and l2 time periods) when compared to the FR121 and reference nitrocellulose samples. Halogenated coating systems are rarely used for bulk materials as they fail to prevent combustion in cases where the amount of fuel far outweighs the proportion of halogens in the coating.

4.1.5. Prediction of performance in BS 476: Part 6

The results of the screening methods correlate to performance in the BS 476: Part 6 in most cases, except in the data collected for char production. FR120 displays a lower heat release rate, prevents ignition and records the lower fire propagation index in the BS 476: Part 6 (adapted) however this system also displays the least char production. This is due to the halogenated mechanism of fire retardance. FR120 is a halogenated system providing protection by interrupting the flame reaction and hindering ignition. FR120 and FR121 do not promote char production suggesting that it is more than simply the amount of char produced that produces a good result in the BS 476: Part 6 apparatus.

4.2. Structural Steel Intumescent

The structural steel intumescent formulation is a commercial ammonium polyphosphate system similar to that reported in Table 4 but the exact formulation is unknown.

4.2.1. Assessment of fire retardant action

When coated onto a wooden splint and subjected to a Bunsen burner flame approximately 3 mm of intumescence was observed (Figure 86). Ignition occurred though no evidence of flame spread was seen and flames self-extinguish. Vapours were lost as intumescence fails; this may be due to the incomplete softening of the resin as the spumific decomposes or perhaps the spumific decomposes too rapidly and the vapours burst out of the resin matrix; both of these phenomena could be attributed to incorrect flame temperature and pyrolysis of substrate at low temperature for this specific formulation.
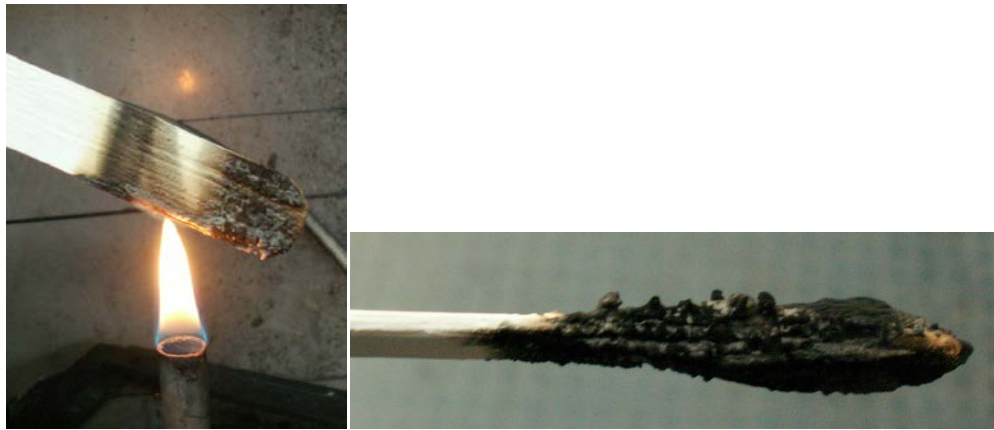
Figure 86 Images of Steel intumescent after exposure to Bunsen burner

4.2.2. Analysis of thermal decomposition – TGA analysis

The variation between decomposition mechanism in air and nitrogen atmosphere is clearly shown in Figure 87. Air decomposition takes place in two stages. The initial step is rapid and begins at approximately 300 °C leaving a residual mass of 70 %. The second step is slower and leaves a residual mass of 50 % at 500 °C which slowly oxidised until the conclusion of the analysis. Delayed initial decomposition and sustained residual char mass is believed to offer a high level of fire protection. The temperature ranges involved with the steel intumescent system are too high for protection of multilayer paint surfaces but do provide valuable information on successful intumescent systems. In the case of TGA in nitrogen the decomposition begins much earlier (around 50 °C) and continues in one slow step until 350 °C. Then a more rapid process reduces the residual mass from 80 % to 60 % which remains fairly stable until 900 °C, this is the residual char layer that would provide protection at higher temperatures.
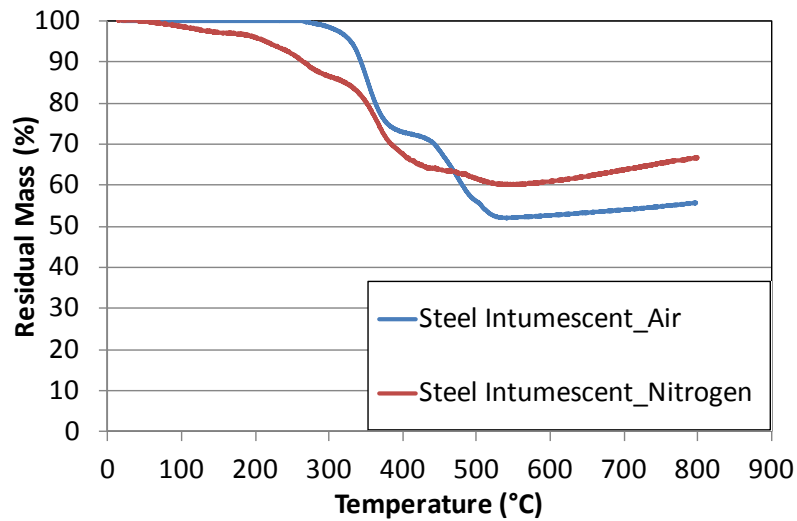
Figure 87 Decomposition curves for Steel intumescent in air and nitrogen; ambient to 900 °C, at a heating rate of 10 °C min-1

4.2.3. Assessment of cone calorimeter properties

The steel intumescent formulation was analysed (three coat thickness) on the plasterboard, coated with two coats of nitrocellulose (approximately 0.1 mm dry film thickness), substrate and embedded thermocouple alongside reference samples consisting of two coats of nitrocellulose on plasterboard substrate. Samples were subjected to the cone heater at an irradiance of 35 kW m^{-2}. The triplicate heat release curves were compared to the curve obtained from the nitrocellulose analysed in isolation. The results are shown below.
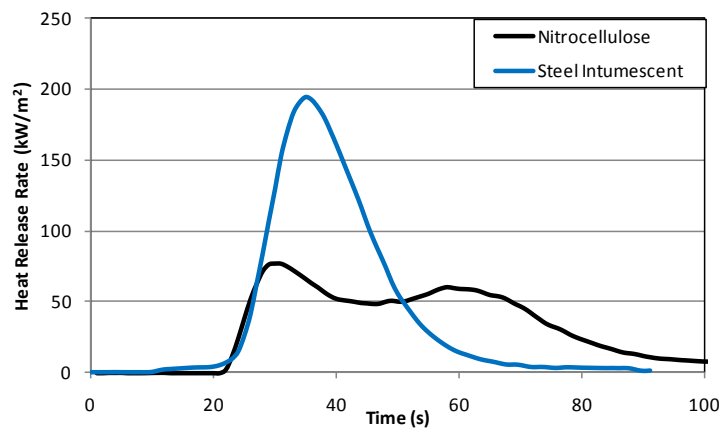
Figure 88 Comparison of average heat release rate curves from Steel intumescent and Nitrocellulose experiments.

Table 23 Steel intumescence sample cone calorimeter properties

Sample	t_{ig} (s)	PHRR (kW m^{-2})	tPHRR (s)	THR (kW m^{-2})
Nitrocellulose	10 ± 1	82 ± 16	36 ± 12	3403 ± 390
Steel intumescent on NC	23 ± 0	195 ± 25	35 ± 1	3756 ± 543

Results were collected in triplicate for each of the samples, cone properties are listed in Table 23 and average heat release curves depicted in Figure 88. Discrepancies were expected in the curves due to variations in the occurrence, level and position of intumescence. Time to ignition cannot be accurately determined from the heat release rate curves (in Figure 88) as explained previously. Instead the carbon dioxide production rate curves in Figure 89 more accurately depict the delay in ignition time for steel intumescent samples when compared to the nitrocellulose system. Peak heat release rate is higher for the steel intumescent samples; this is not surprising as the coating will contribute some fuel for combustion. Flammable vapours and pyrolysis products may become trapped in the voids in the coating and are stored, whereas the nitrocellulose is decomposed directly under the cone heater and pyrolysis products are free to mix with (and become diluted by) the atmosphere before meeting the ignition spark. This leads to a smaller flame but for an extended period of time until all of the combustible material is consumed. The total heat release for the nitrocellulose samples is less than that of the steel intumescent - approximately 3500 compared to approximately 3750 kW m^{-2} - (though this is likely to be an underestimate). Protection is achieved via two main mechanisms; firstly the coating prevents some of the nitrocellulose material decomposing as it is protected from the heat; secondly and more predominantly the pyrolysis products are forced to escape through weakness in the coating (at the edges of the sample board) which is away from the ignition spark, thus combustible material is able to escape and be diluted to a non-combustible concentration before ignition can occur.

The carbon dioxide production rate curves for the samples shown in Figure 89 depict a different situation. This is a more accurate representation of time to ignition and heat release rate curves. Nitrocellulose samples are exposed and so as soon as the required concentration of combustible products is obtained in the region of the ignition arm, ignition is achieved. It is expected that this be much later for the coated samples as they are protected to some degree from the heat source and therefore a flammable concentration takes longer to achieve.
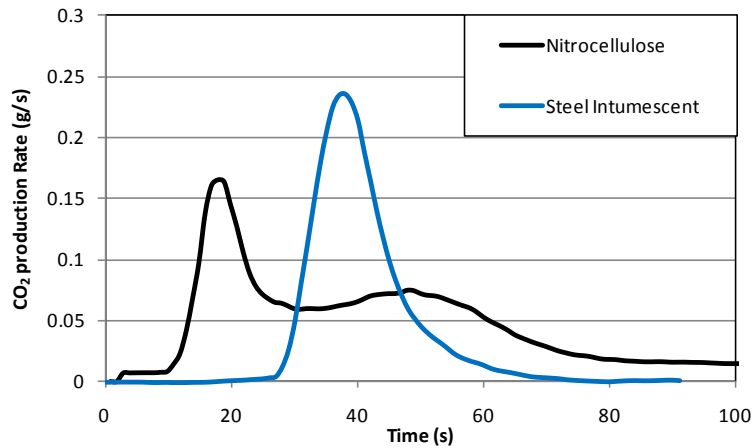
Figure 89 Comparison of average carbon dioxide production rate curves for Steel Intumescent and Nitrocellulose experiments.

The peak rate of carbon dioxide production is lower for nitrocellulose samples than steel intumescent samples (0.17 g s^{-1} compared to 0.2-0.26 g s^{-1}). Combustible gases are produced at a lower rate and are further diluted by the atmosphere thus combustion, and therefore carbon dioxide production rates, are maintained at much lower levels. Burn time is prolonged as a small flame is sustained until all combustible material is consumed. Conversely, for the steel intumescent samples, combustion rates are much higher and so production rates for carbon dioxide are also increased. Flaming is short-lived as thermal feedback is greater and the combustible material is consumed more rapidly. Flaming aids the expansion of the intumescent which acts to protect against further flaming. Repeatability for the steel intumescent systems is good with all the ignition times recorded at the same time. Variation in the heat release rate and carbon dioxide curves is attributed to variation in the level of intumescence seen and also the amount of combustible products that remain after the flameout time.

Temperature profiles collected from the thermocouple embedded within the cone samples are depicted in Figure 90. Triplicate records are not shown due to an error with one of the thermocouples. Both traces show identical temperature profiles in the early stages of the analysis. Variation occurs at approximately 50 seconds. The first trace shows a steadier increase but for an extended period of time, this continues until the termination of the experiment, whereas the second trace shows a more rapid temperature increase up to approximately 245 °C at which point the profile plateaus and temperature increase is prevented for the remainder of the experiment. This suggests that a higher level of intumescent was achieved in the second trace, particularly in the area directly above the thermocouple; this reduces the amount of heat able to be transmitted through the coating to the thermocouple and the nitrocellulose beneath.

132
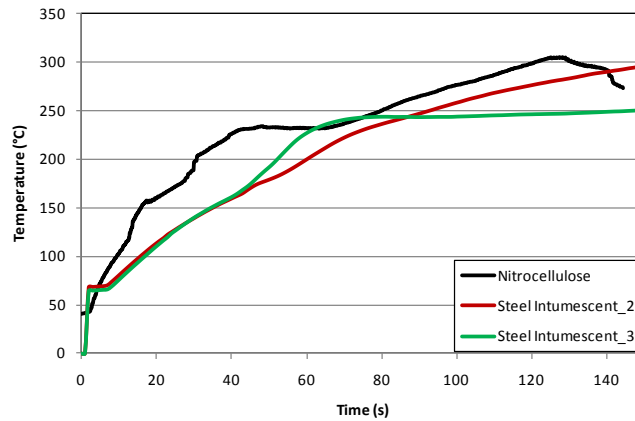
Figure 90 Comparison of thermocouple temperature profiles from the Steel intumescent and Nitrocellulose samples

When compared to the temperature profile collected from a sample with only nitrocellulose present, the initial temperature increase is far slower for steel intumescent samples. The initial temperature increase for both samples coincides with the ignition temperature for each of the samples (approximately 10 seconds for the nitrocellulose and 23 seconds for the steel intumescent sample). The rapid temperature increase observed in nitrocellulose samples between 0-40 seconds correlates to the initial peak heat release rate seen in Figure 88, after which the thermocouple remains exposed and continued heating occurs from the cone heater and the small sustained flame. Steel intumescent_2 shows initial reduction in temperature profile due to protection afforded by the expanded coating, and then it appears that the thermocouple becomes exposed as the temperature profile after 80 °C mirrors that of the nitrocellulose samples when further heating is due to the cone heater alone. Steel intumescent_3 shows the effect on temperature profile of a successful coating. The temperature is prevented from increasing above 250 °C suggesting that the intumescent char is perfectly positioned above the thermocouple and protects to higher temperatures.

4.2.4. Assessment of thermal conductivity - BS EN 367

Structural steel intumescent samples were subjected to BS EN 367 analysis to determine the thermal conductivity of these commercial intumescent systems. This would assess the temperature at which intumescence occurs and estimate the level of protection given. The temperature profile results are shown below in Figure 91.
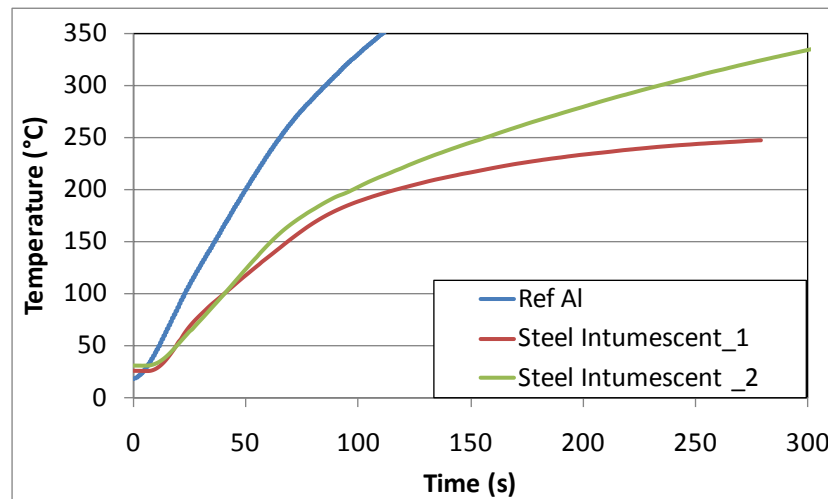
Figure 91 Temperature profiles of Steel Intumescent samples tested in the BS EN 367 within a heat flux range of 30-40 kW m^{-2}

Results collected show that intumescence does not occur until a temperature of 200 °C is reached. At this temperature the intumescent char formation is rapid producing a stable residue which provides protection at higher temperatures. The time to reach 150 °C (listed in Table 24) is not reduced by the use of the steel intumescent system when compared to the reference steel sample due to the high activation temperature of this intumescent. However, the thermal conductivity of the sample is significantly reduced above the activation temperature of 200 °C. Therefore if the temperature of activation can be lowered by altering the formulation (without compromising the speed and structure of the residual char) this provides strong evidence that intumescence is the optimum mechanism for reducing the heat transfer through the coating.

Table 24 Time to reach 150 °C and 350 °C for Steel Intumescence samples in the range of 30-40 kW m^{-2}

Sample	Time to reach 150 °C (s)	Time to reach 350 °C (s)
Reference Aluminium sheet	50 ± 2	122 ± 11
Steel Intumescent	44 ± 7	520 ± 35

4.2.5. Calculation of fire propagation index – BS 476: Part 6 (adapted)

Analysis of the steel intumescent system in the BS 476: Part 6 (adapted) test suggests that though the activation temperature of the system is high, protection performance is still good. This system passes the adapted test. The results are listed in Table 25.

.

134

Table 25 BS 476: Part 6 (adapted) analsyis of commercial steel intumescenct sample

Sample	s1 (0.5-3 min)	s2 (4-10 min)	s3 (11-20 min)	S (0-20 min)	Fire propagation index (L)	Pass/Fail
Nitrocellulose	23.79 19.61 16.89	4.36 4.39 3.17	0.66 0.63 0.54	28.81 24.63 20.6	24.22	Fail
Steel Intumescent	3.18 5.34 0.14	1.39 0.36 0.5	0.33 0.33 0.27	4.9 6.07 0.91	3.96	Pass

Observations of the char residue produced suggest it is highly stable and contains many voids. This sample produces intumescent char residue from the early stages if the test. As it is rapidly produced and stable to high temperatures the level of protection is high. The most significant values recorded are in the early stages of the analysis (which are more heavily penalised in the calculation of the fire propagation index value).

Though this sample passes this particular test it has been previously discussed that it is not suitable for the particular application that is the focus of this thesis due to the high temperatures required to achieve activation of the intumescence.

4.2.6. Prediction of performance in BS 476: Part 6

The steel intumescent system exhibits a high level of fire protection in all screening method analyses. The only drawback appears to be the high activation temperature of intumescence which means that temperature ranges are too high for multilayer paint protection. The residual char produced is rapid in formation, stable in structure and uniform producing a high level of protection in the BS 476: Part 6 apparatus. This mechanism also provides good performance in the cone calorimeter and BS EN 367.

4.3. MAGMA FIRESTOP SAMPLES

Magma Firestop produce commercial intumescent systems for use on wooden substrates and display lower activation temperatures for intumescence. Samples were provided and investigation was undertaken to determine how a lower activation temperature is achieved and the fire protection afforded in the screening methods.

Details of the samples obtained from Magma Firestop are tabulated in Table 26.

.

Table 26 Magma Firestop product information

Sample Name	Label on bottle	Website Information
Magma TG-3	Magma Firestop TG-3 Low-Intumescent <u>Clear</u> FR varnish (water-based)	Outdoor application. Not only penetrates wood surface but also forms a weather-tight adhesive bond
Magma Latex (white)	Magma Firestop Latex Non-intumescent <u>White</u> FR wall paint (water-based)	Fire retardant wall paint (latex) for interior usage
Magma Prime (Black)	Magma Firesheen Prime Med-Intumescent <u>Black</u> FR paint (water-based)	No mention on website
Magma Prime (Clear)	Magma Firesheen Prime High-Intumescent <u>Clear</u> FR paint	Intumescent prime coating for interior applications

4.3.1. Assessment of fire protection action

Initial flammability analysis was carried out on wooden splints to determine the nature and performance of these systems; whether they are halogenated or intumescent; the extent of intumescence; and behaviour when exposed to a small naked flame (Bunsen burner).

4.3.1.1. MAGMA FIRESTOP TG-3

Prior to heat exposure the coating produces an off-white smooth translucent film when dried. The sample burned but showed no signs of flame spread even when the splint was further tested in a vertical orientation. Bubbling of the coating occurred where the coating was applied in a thicker layer. The flame appeared yellow with a green base; perhaps suggesting the presence of copper. Charring of the wooden splint occurs and a white smoke is produced that pushes the flames outwards from the surface of the wood by the force of escaping vapours. Due to the nature of the coating it is able to soak into the wooden splint to some degree and so no loss of adhesion is observed during burning. There is little or no intumescence observed for this sample in this screening experiment at this thickness as can be seen in Figure 92.

Figure 92 Images of Magma TG-3 after exposure to Bunsen burner

4.3.1.2. MAGMA FIRESTOP LATEX

This sample produces a white coating which spreads thickly due to higher viscosity of the coating. The coating then turns from white to pale green when exposed to the flame and returns to white on cooling as shown in Figure 93. White smoke is evolved and minimal flame spread is observed even when the splint is tested in a vertical orientation. Charring of the wood occurs and the paint de-adheres from the splint, cracking off to expose the substrate. No intumescence is observed and ignition occurs, burning with a small yellow flame.

Figure 93 Images of Magma Latex (white) after exposure to Bunsen burner

4.3.1.3. MAGMA FIRESHEEN PRIME (BLACK)

This system is blue/black in appearance, drying to black. This is a low viscosity coating and soaking into the wood is observed but to a lesser extent than the TG-3. This sample showed some indication of moderate intumescence (Figure 94) in areas where the coating has been allowed to build-up. Ignition was observed and the flame was yellow with a blue/green base. Minimal flame spread is observed even with the splint in a vertical orientation. No peeling or loss of adhesion recorded. As the coating was destroyed and exposed the substrate the wooden splint ignited and supported sustained burning.

Figure 94 Images of Magma Prime (black) after exposure to Bunsen burner

4.3.1.4. MAGMA FIRESHEEN PRIME (CLEAR)

This was a viscous, cloudy, white coating, glue-like in appearance. The sample was sticky to the touch and displays good adhesion to the substrate. When tested on a splint, it is highly intumescent and swells to several times the initial coating thickness (Figure 95). The coating prevents ignition of the substrate, and does not itself ignite. A carbonaceous residue remains that protects the substrate from further attack from heat. Various sized bubbles are formed throughout the coating. There is evidence that some of these are lost as vapour however enough are captured in the resin which firms to form a spongy residue. There is no loss of adhesion between the coating and substrate. When exposed to more extreme heating, the residue blackens further, remains stable and does not diminish.

Figure 95 Images of Magma Prime (clear) after exposure to Bunsen burner

4.3.2. Assessment of thermal decomposition - Thermogravimetric (TGA) analysis

TGA analysis was carried out on all samples to characterise their thermal decomposition. A heating regime of 10 °C min^{-1} over a temperature range of 25-900 °C was adopted. These decomposition curves were collected in an air atmosphere and are depicted in Figure 96.
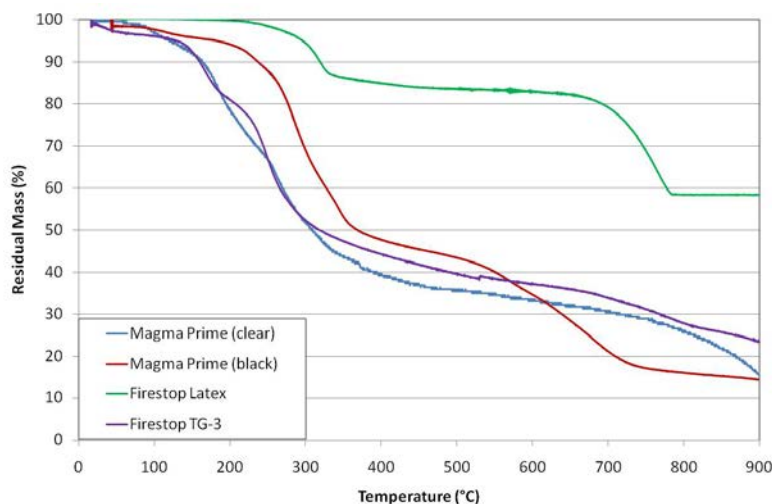
Figure 96 Decomposition curves for Magma samples in air; ambient to 900 °C at a heating rate of 10 °C min^{-1}

Firestop Latex shows the highest onset temperature of decomposition (just above 250 °C) as well as the highest percentage residual mass (58 %). The initial stage of decomposition finishes just above 300 °C leaving a stable residue of 85 % mass. This residue undergoes further decomposition at 700 °C at which point a second rapid stage is observed finishing at 775 °C with a residual mass of 58 %, this is due to the high loading level of inert additives (possibly chalk) in formulation. It was thought that this coating offers barrier protection as no intumescence was observed in the Bunsen burner experiments. Though the residue is stable above 900 °C protection performance on a molten and highly flammable substrate such as the blue board would not be expected. Magma prime (clear) and Firestop TG-3 display the lowest onset temperature of decomposition at approximately (150 °C) putting them within the range for protection of multilayer paint. Unfortunately these coatings also yield the lowest residual mass of only 15-25 %, at temperatures above 800 °C suggesting that protection may be limited to the lower temperatures only – unless this residue is in the form of an intumescent layer. TG-3 demonstrates a similar decomposition curve to the Magma Prime (clear) system, however it is not intumescent and therefore the residual mass is unlikely to provide the level of protection required. Magma Prime (black) begins decomposition at approximately 100 °C but this initial stage is far slower and finishes at approximately 225 °C. Then there are two more rapid decomposition stages. The first begins at around 250 °C and finishes at approximately 350 °C with 35 % residual mass of carbonaceous char remaining. The second is the oxidation of this

carbonaceous material which starts slowly but intensifies just before 600 °C and ends at 700 °C with a residual mass of only 27 %.

4.3.3. Assessment of cone calorimeter properties

Only three of the four Firestop samples were assessed in the Cone calorimeter with embedded thermocouple, as Firestop TG-3 displayed poor sample uniformity and coating properties when applied over the nitrocellulose substrate due to its low viscosity and pooling affects during drying.

Plasterboard plaques of size 10cm x 10cm were coated with two layers of nitrocellulose paint - to give a total dry thickness of approximately 0.1 mm. A thermocouple was then embedded into the centre of the plaque and three coats of the coating under test were applied. These were then exposed to a heat flux of 35 kW m^{-2}.

Table 27 Details of samples investigated

Sample Name	Coatings Mass (g)	Coating Thickness (mm)
Latex_1	5.33	0.23
Latex_2	5.66	0.2
Latex_3	5.48	0.26
Prime (black)_1	5.38	0.27
Prime (black)_2	5.4	0.23
Prime (black)_3	4.53	0.44
Prime (clear)_1	7.76	0.36
Prime (clear)_2	6.95	0.34
Prime (clear)_3	6.5	0.28

Heat release rate data collected from the samples is shown in Figure 97. The Magma Latex (white) samples displayed very short lived flames - perhaps due to the presence of a gas phase flame inhibitor. Ignition was observed (around 28 seconds) when the coating surface cracked, releasing the flammable vapours to the ignition source. These samples showed the highest peak heat release rates of all the samples analysed - approximately 100 Kw m^{-2}. Due to the lack of intumescence (0 mm residual char) this was the only sample for which the ignition arm could be successfully removed. The Magma Prime (black) samples also ignited under this heat flux (with time to ignition of 26 seconds) however some level of intumescence was observed prior to ignition which explains the variation in ignition times recorded. It appeared that the full level of intumescence was not obtained before the decomposition of the nitrocellulose began under these conditions. Bubbles were large, and formed prematurely, thus were not trapped by the resin, and instead lifted the coating from the substrate and allowed the

combustible nitrocellulose vapours to ignite. A peak heat release rate of approximately 58-70 kW m^{-2} was recorded. This sample showed some shrinking towards the centre of the plaque exposing the substrate around the edges of the sample and further disruption was caused in the area of the sample where the ignition arm was situated. The residual layer swelled to 2 cm thick however was very fragile and flaky.
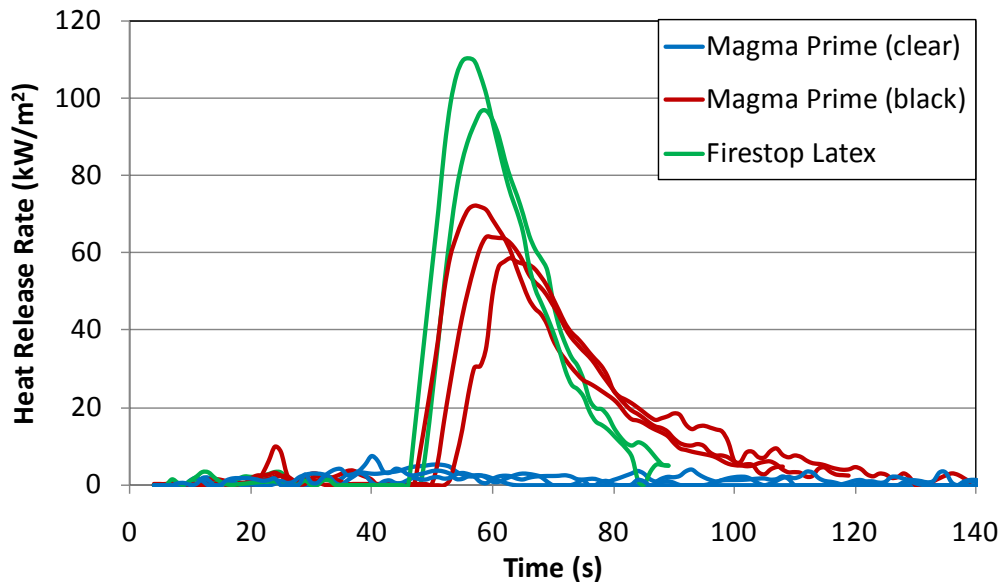
Figure 97 Heat release curves for Magma samples analysed at 35 kW m^{-2}

Finally, the Magma Prime (clear) sample showed an excellent level of intumescence that occurred around 130 °C prior to the decomposition of the nitrocellulose paint at around 150 °C. Magma Prime (clear) prevents ignition and maintained a heat release rate of less than 5 kW m^{-2}. This system displayed two stages of intumescence, one involving only the coating (in the form of worm-like structures) and the second, as the gases from the decomposing nitrocellulose became trapped which was uniform across entire plaque. The initial intumescence liberates small bubbles and produces a white residue layer. Later, intumescence causes blackening of the residual layer and a greater number of bubbles. The char layer reaches around 25-30 mm and relaxes back on cooling to around 20 mm. The char is spongy and light.

All heat release rate values above are likely to be underestimated by oxygen depletion calorimetry and so carbon dioxide production rate curves are reported below in Figure 98.
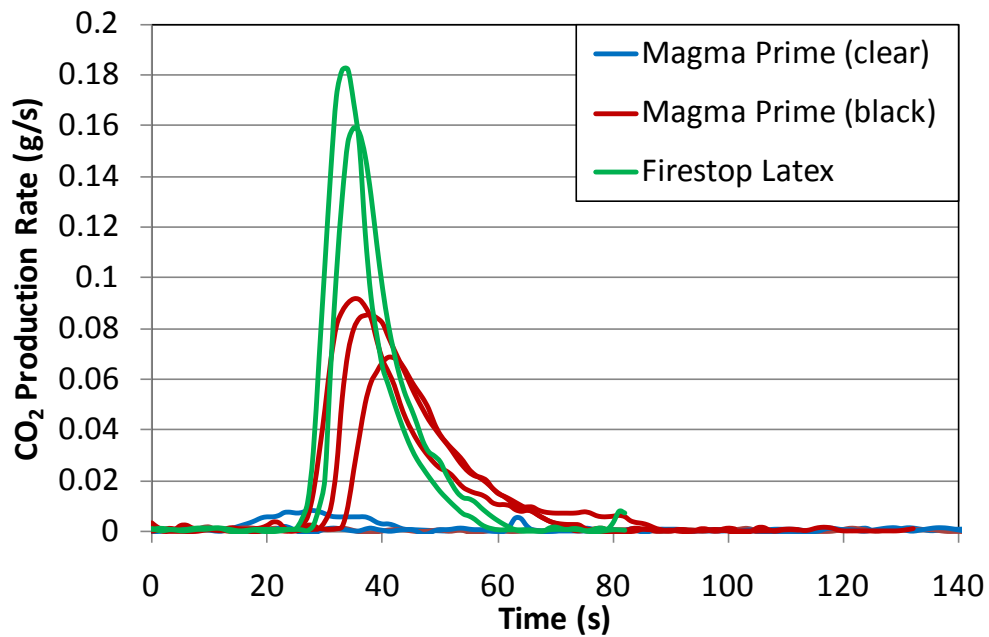
Figure 98 Carbon dioxide production rate curves for Magma samples analysed at 35 kW m^{-2}

The carbon dioxide production rate curves in Figure 98 follow the same trends as the heat release rate curves. However, they occur at 25-35 s, rather than at 45 – 55 s. This suggests that the majority of oxygen depleted from the atmosphere is used for the combustion of the coating and is transferred into carbon dioxide. The nitrocellulose paint is protected and even if its decomposition is possible, the combustible vapours are unable to escape and so the nitrocellulose fails to affect the results significantly in this case. The only noticeable variation in results is the extended burn time reported by the heat release rate curves, which are not depicted in the carbon dioxide production rate curves. This is because the carbon dioxide production rate is not prolonged by the combustion of the coating. The peak of production coincides with the decomposition of the nitrocellulose which is omitted from the heat release data due to the lack of depletion of atmospheric oxygen. Further flammability properties are listed in Table 28 below.

Table 28 Magma sample cone calorimeter properties

Sample	t_{ig} (s)	PHRR (kW m^{-2})	tPHRR (s)	THR (kW m^{-2})
Magma Prime (clear)	0 ± 0	8.6 ± 1	312 ± 124	323 ± 136
Magma Prime (black)	26 ± 2	65 ± 5	53 ± 2	1703 ± 54
Magma Prime (Latex)	24 ± 1	103 ± 7	50 ± 1	1963 ± 73
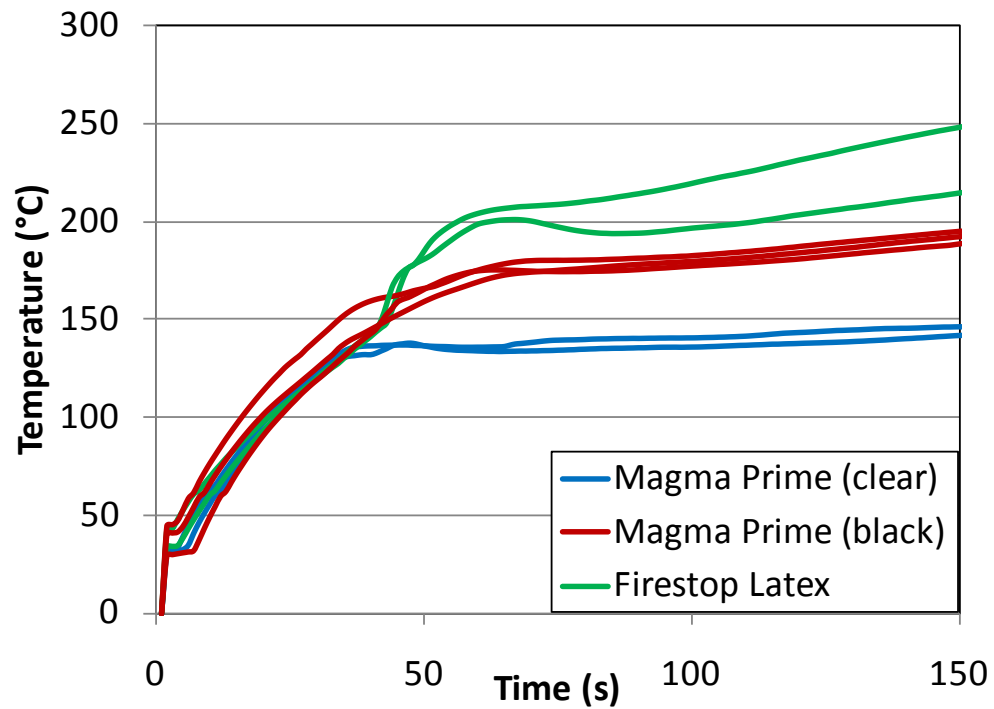
Figure 99 Thermocouple temperature profiles for Magma sample analysed at 35 kW m^{-2}

The temperature profiles collected from the thermocouple embedded in the sample plaques are shown above in Figure 99. The data clearly shows that the level of protection for all three coatings is the same up until approximately 40 seconds. At this point the Firestop Latex temperature increases rapidly as the coating is ruptured and the nitrocellulose ignites. The temperature then increases (though at a slower rate) until the end of the experiment, due to radiation from the cone calorimeter. The Magma Prime (black) temperature also continues to increase at a much slower rate. The rate of increase is reduced by the protection provided by the partially intumesced sample. The peak temperature observed is maintained at less than 200 °C. The optimum temperature profile is observed from the Magma Prime (clear) sample. The coating intumesces and maintains the temperature of the substrate below 150 °C. This reduces if not completely prevents the decomposition of the nitrocellulose substrate.

4.3.4. Assessment of thermal conductivity - BS EN 367

Firestop Latex, Magma Prime (black) and Magma Prime (clear) were coated onto aluminium sheets of size 140 mm x 140 mm and 2 mm thick. The samples were dried in an oven prior to exposure to the Mekker burner at a heat flux of approximately 30-40 kW m^{-2}.

Results are shown in Figure 100, Figure 101 and Table 29 below. Firestop Latex and Magma Prime (black) samples show the lowest level of protection in this experiment, displaying the most rapid temperature increase. The temperature increases observed are constant throughout the duration of the experiment and do not appear to be significantly hindered by

the coating. Magma Prime (black) samples do appear to provide a slightly higher level of protection at higher temperatures but this does not occur below 200 °C which is above the required temperature range for protection of nitrocellulose paint. The level of intumescence observed from this sample was reduced on the aluminium, when compared to the char residue yield, in cone calorimeter experiments. This may explain the reduced performance in this experiment and suggest a synergism between the coating and the cellulose in the cone calorimeter and Bunsen burner experiments. The Magma Prime (clear) system shows the greatest level of protection, maintaining the substrate temperature below 150 °C for approximately 110 seconds and reducing the rate of temperature increase thereafter. It achieves this by producing an intumescent layer of approximately 50 mm which is maintained throughout the experiment and relaxes on cooling to 45 mm. Residues from all samples are shown in Figure 101.
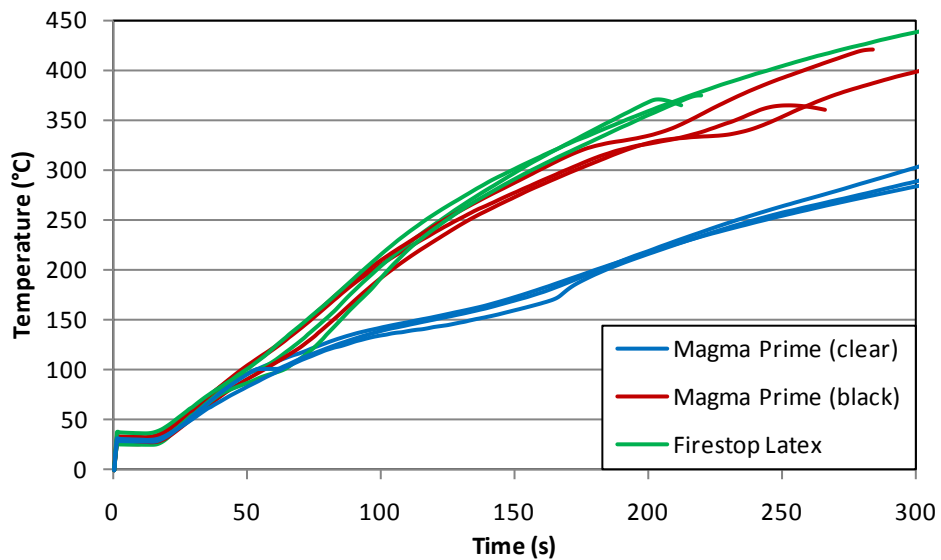
Figure 100 Temperature profiles of Magma samples tested in the BS EN 367 experiments

| Black | White | Clear |
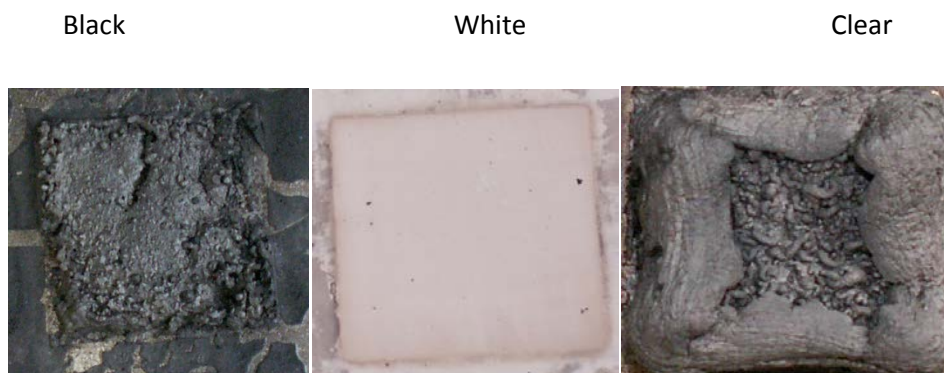
Figure 101 Images of char residues remaining after BS EN 367 experiments

Table 29 to reach 150 °C and 350 °C for Magma Firestop samples in the range of 30-40 kW m^{-2}

Sample	Time to reach 150 °C (s)	Time to reach 350 °C (s)
Reference Aluminium sheet	50 ± 2	122 ± 11
Magma Prime (clear)	121 ± 9	393 ± 21
Magma Prime (black)	75 ± 4	231 ± 13
Firestop Latex	78 ± 5	149 ± 55

4.3.5. Calculation of fire propagation index - BS 476: Part 6 (adapted)

Analysis in the BS 476: Part 6 (adapted) experiments predicts performance in standard fire tests and revealed some surprising results in this case, these are listed in Table 30.

Table 30 BS 476: Part 6 (adapted) analysis of commercial Magma Firestop samples

Sample	s1 (0.5-3 min)	s2 (4-10 min)	s3 (11-20 min)	S (0-20 min)	Fire propagation index (L)	Pass/Fail
Nitrocellulose	23.79 19.61 16.89	4.36 4.39 3.17	0.66 0.63 0.54	28.81 24.63 20.6	24.22	Fail
Magma Prime (clear)	7.04 2.69 4.32	3.76 1.94 1.98	1.12 1.01 0.48	11.93 5.63 6.78	8.11	Fail
Magma Prime (black)	10.47 11.15 8.77	3.11 2.78 2.5	0.78 0.76 1.03	14.37 14.69 12.31	13.79	Fail
Magma Latex (white)	21.24 11.38 6.53	5.35 2.16 1.41	0.8 0.08 0.02	27.39 13.61 7.96	16.32	Fail

Surprisingly all samples fail the BS 476: Part 6 (adapted) experiment. Though the Magma Prime (clear) sample produces a lot of char residue, observations reveal that it is slow to form (failing to provide the required protection in the initial stages of the analysis) and is less stable (the char has such low density that it falls off the substrate during prolonged heating). Magma Prime (black) and Firestop Latex show little or no intumescent activity. These systems predominantly provide protection by forming a barrier which prevents the escape of pyrolysis products and diffusion of oxygen until such a time as the barrier itself becomes damaged, which in the case of the Firestop samples occurs early in the test.

All of the results presented demonstrate that the Magma Prime (clear) is the most suitable coating which can be further improved for the protection of multilayer paint surfaces. The Magma Prime (black) does appear to have some fire retardant benefits however due it its reduced level of intumescence and dark colour it will not be pursued as an alternative at this time. The Firestop Latex and Magma TG-3 samples will also no longer be considered due to their poor protection and coating performance.

4.3.6. Prediction of performance in BS 476: Part 6

Magma Prime (clear) shows the highest level of performance of all Magma samples in all experiments and the same hierarchy is mirrored in the results recorded for the BS 476: Part 6 (adapted). This suggests that the screening methods provide good estimation of performance in the BS 476: Part 6 (adapted) with regard to intumescent samples. Surprisingly the performance of the Magma Prime (clear) sample in the BS 476: Part 6 (adapted) appears worse than the steel intumescent sample during comparison. Though the amount of residue maintained by the Magma Prime (clear) sample outweighs that produced by the steel intumescent, it could be the structure of the swollen residue which is vital to the level of protection given. As the steel intumescent sample residue is more robust, it may provide more protection to the flammable substrate therefore reducing the fire propagation index below that which was recorded for the Magma Prime (clear) sample. It could also be due to a delay in the formation of the Magma Prime (clear) residue layer or perhaps de-adhesion of the char at later periods of the experiment. This evidence further supports the suggestion that good results in the BS 476: Part 6 (adapted) rely on more than amount of intumescent production.

As Magma Prime (clear) is the most promising of the samples analysed at this time more work will be done to characterise the composition. This will enable reproduction of the sample and further improvements where necessary.

4.4. CHARACTERISATION OF MAGMA SAMPLES

4.4.1. Magma Prime (clear) – Sample preparation

2.05 g of Magma prime clear was dissolved in 50ml of water; the white precipitate that formed was then filtered off and dried in the oven (30 °C). The water portion was also dried in the oven to determine the resin content.

From 2.05 g of Magma clear, 0.395 g of solids remained after drying, this is roughly 20 % of the total sample content. 0.916 g of resin remained after the last of the water had dried off; this is approximately 45 % of the total mixture.

4.4.2. d-ATR

d-ATR was carried out on all samples to determine composition and functionality of the coatings.

Raw materials such as diammonium phosphate, pentaerythritol, precipitate collected from dissolving the Magma Prime (clear) in water and also the residue collected after the burning of the Magma Prime (clear) sample were analysed in powder form. Films were produced of the remaining Magma samples. Powder and film samples were dried in the oven at 30 °C for a few

days prior to scanning in the in dATR-FTIR. Spectra from each analysis were compared to determine which, if any, of the additives were present in the Magma samples.

4.4.2.1. MAGMA PRIME (BLACK)

When spectra from the Magma Prime (black) sample are compared with spectra from all reagents, results suggest the presence of Pentaerythritol. Comparison data is shown in Figure 102.
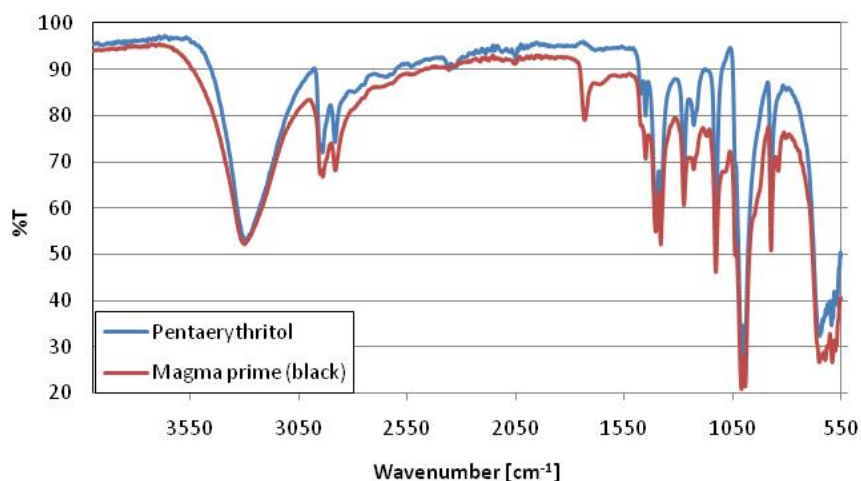
Figure 102 Comparison of ATR spectra collected from Magma prime (black) and Pentaerythritol samples

4.4.2.2. MAGMA FIRESTOP TG-3
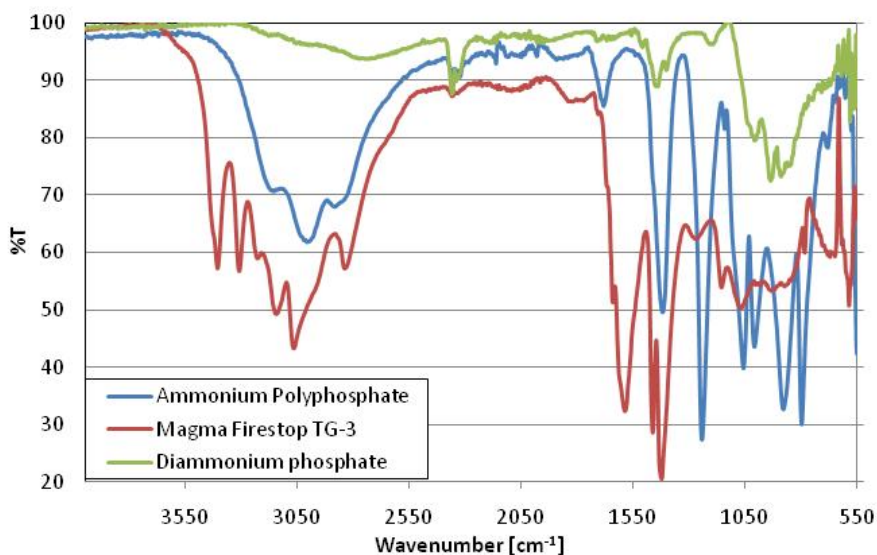
Figure 103 Comparison of ATR spectra collected from Magma Firestop TG-3, Diammonium phosphate and Ammonium polyphosphate

The spectra of Firestop TG-3, diammonium phosphate and ammonium polyphosphate are shown in Figure 103. All the spectra have some similar and potentially matching peaks

147

however these results are not conclusive. Further analysis - such as NMR – could be suitable for this sample.

4.4.2.3. MAGMA PRIME (CLEAR)

The Magma Prime (clear) sample was separated by filtering off the white precipitate and then evaporating the water off the resin portion, which were analysed by dATR-FTIR. The 'residue' sample was collected from a partially burnt sample of the Magma Prime (clear) which did not appear to be fully intumesced.
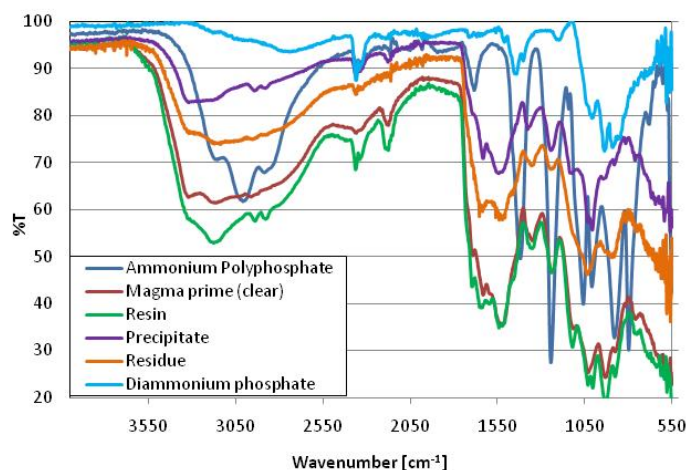
Figure 104 Comparison of ATR spectra collected from Magma Prime (clear), precipitate, resin, residue and compared to ammonium polyphosphate and diammonium phosphate samples

The peak at ~2360 cm^{-1} and the fingerprint region ~ 500-600 cm^{-1} (Figure 104) suggests a potential match for diammonium phosphate and the Magma Prime (clear) sample in particular the resin and the precipitate samples. There is less evidence to support the occurrence of ammonium phosphate within the sample however it cannot be completely ruled out due to the peaks in the 2050 – 2550 cm^{-1} region, the very strong and sharp peaks in the fingerprint region that are not apparent in the Magma Prime (clear) sample. The spectra suggest the presence of the same component in the Magma Prime (Clear), 'resin', 'residue' and 'precipitate'. Absorbancies above 3100 cm^{-1} suggest the presence of N-H or O-H bonds.

4.4.2.4. FIRESTOP LATEX

Analysis of the Firestop Latex sample shows no match with diammonium phosphate and only minimal similarities with the pentaerythritol spectra, Figure 105 and Figure 106 respectively.
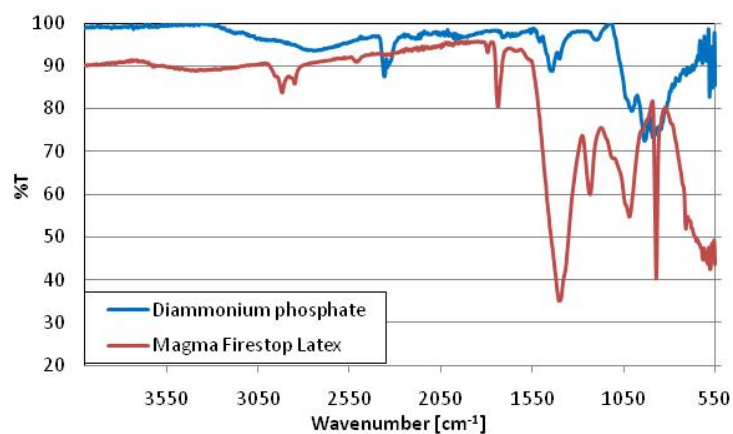
Figure 105 Comparison of ATR spectra collected from Firestop Latex and diammonium phosphate samples
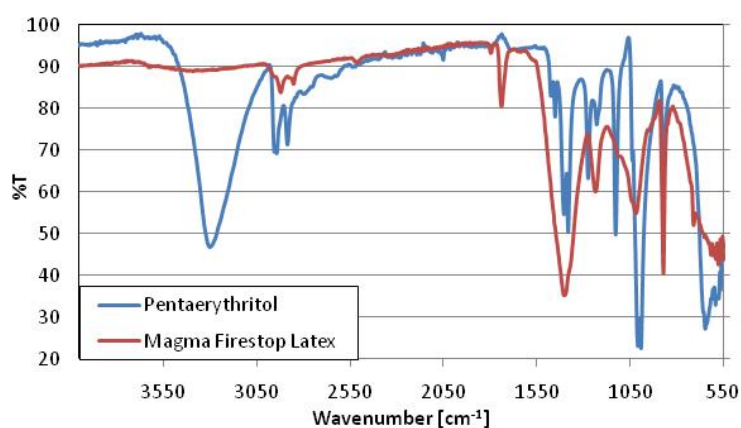
Figure 106 Comparison of ATR spectra collected from Firestop Latex and Pentaerythritol samples

Some peaks in the fingerprint region suggest there may be some similarities in the functional groups found in both samples however the absence of the large pentaerythritol peak at 3300 cm^{-1} almost certainly rules this additive out, unless the OH groups are lost (or substituted) in the formation of the sample.
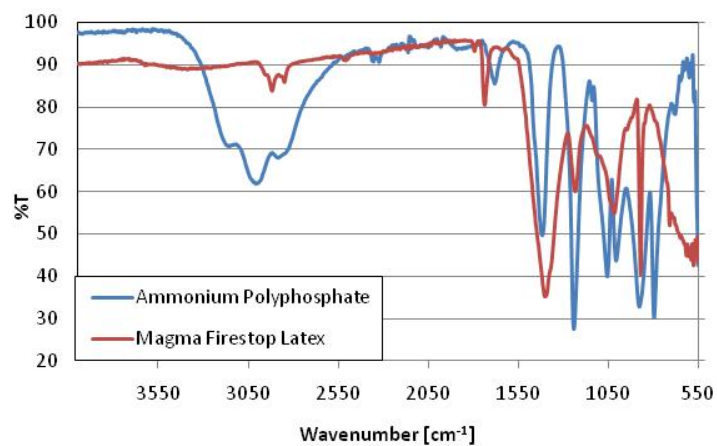
Figure 107 Comparison of ATR spectra from Firestop Latex and Ammonium polyphosphate samples

Further analysis includes comparisons with Ammonium polyphosphate. Few similarities are apparent as shown in Figure 107. Some peaks in the fingerprint region are similar however it is not conclusive as the large OH peak around 3000 cm^{-1} is not present in the Firestop Latex sample.

4.4.3. SEM-EDAX

SEM-EDAX was carried out on Magma Prime (clear) samples to help to determine the composition of the system. The complete system was analysed alongside the separated components and the results are shown below.

4.4.3.1. MAGMA PRIME (CLEAR) – FILM

Element	
C	28.06
N	25.92
O	30.67
Mg	0.29
Al	0.18
Si	1
P	13.89
Total	100
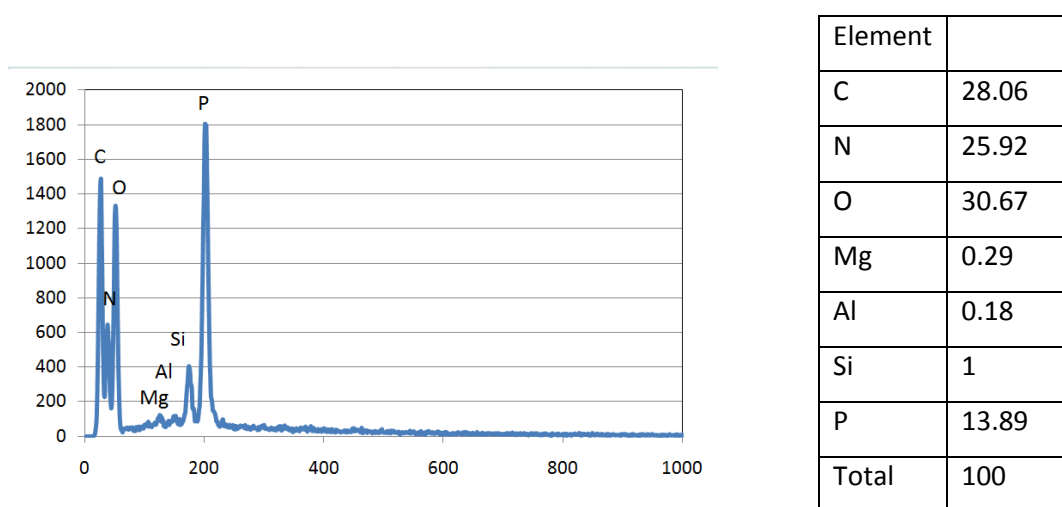
Figure 108 EDAX analysis graph and elemental quantification ratios for Magma Prime (clear) - film

Figure 108 shows the EDAX analysis results of Magma Prime (clear) film samples. The occurrence of phosphorus species in the formulation are clearly represented and make up approximately 14 % of the sample analysed; supporting the inference that diammonium phosphate may be present. Small traces of magnesium, aluminium and silica may suggest the presence of some form of clay (such as montmorillonite) however the inclusion of such a material would reduce the likelihood of the film drying to a cloudy clear colour, unless the particles were nanoscopic.
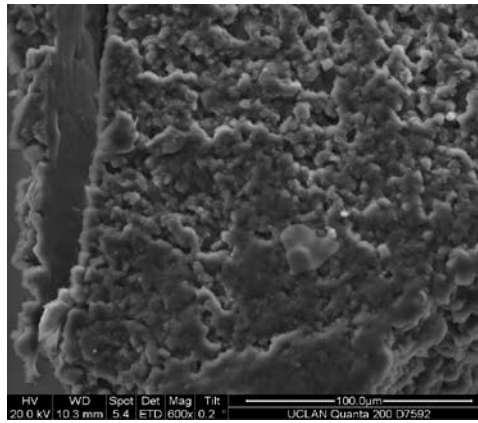
Figure 109 SEM image of Magma Prime (clear) - film at 600 times magnification

A SEM image recorded at 600 times magnification is shown in Figure 109 and indicates that fibres are not present in this formulation to stabilise the char residue.

4.4.3.2. MAGMA PRIME (CLEAR) – RESIN
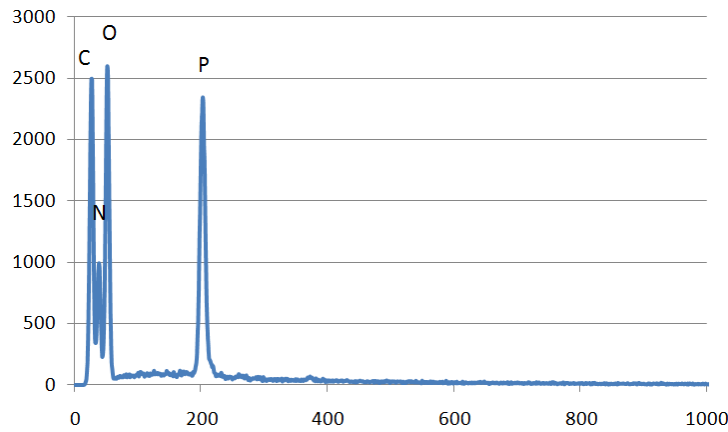
Element	
C	29.68
N	25.24
O	37.95
P	7.13
Total	100

Figure 110 EDAX analysis graph and elemental quantification ratios for Magma Prime (clear) – resin

Resin analysis, depicted in Figure 110, shows no presence of magnesium, aluminium or silica. This suggests that these species are contained in another fraction, more likely the precipitate due to insolubility in water.

4.4.3.3. MAGMA PRIME (CLEAR) – PRECIPITATE
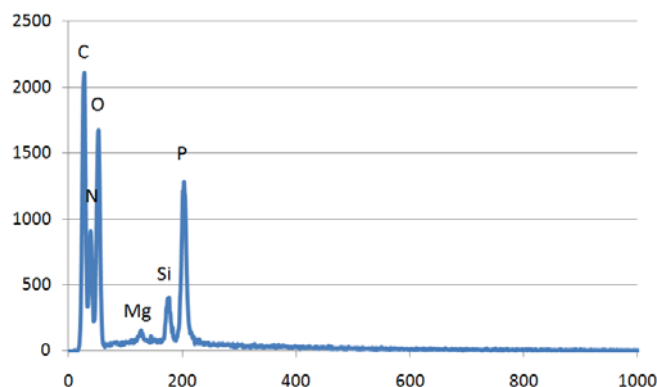
Element	
C	30.06
N	29.46
O	34.01
Mg	0.4
Si	1.17
P	4.9
Total	100

Figure 111 EDAX analysis graph and elemental quantification ratios for Magma Prime (clear) - precipitate

Analysis of the precipitate yields similar results (Figure 111) to the film sample (Figure 108) with similar elements being identified. However lower levels of phosphorus are recorded. When this ratio is combined with that found in the resin fraction, however, the total is similar to that recorded in the complete film analysis. Traces of silica may suggest the use of silicone-coated or encapsulated DAP species.

4.4.3.4. MAGMA PRIME (CLEAR) – RESIDUE
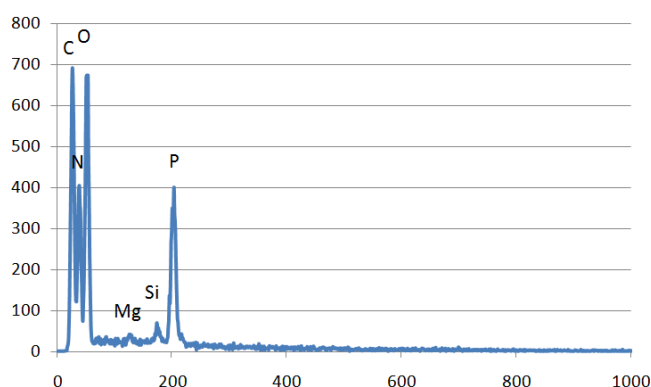
Element	
C	23.8
N	29.78
O	35.09
Mg	0.32
Si	0.24
P	6.76
Total	100

Figure 112 EDAX analysis and elemental quantification ratios for Magma Prime (clear) – residue

The residue was collected after moderate heating of the dried film prior to combustion or blackening of the sample. Figure 112 shows the remaining elemental species present in this case. The phosphorus content is far lower than in previous samples suggesting the loss of phosphorus species during heating. The aluminium is also no longer detectable suggesting it also lost in the decomposition of the film.

4.4.3.5. MAGMA PRIME (CLEAR) – CHAR
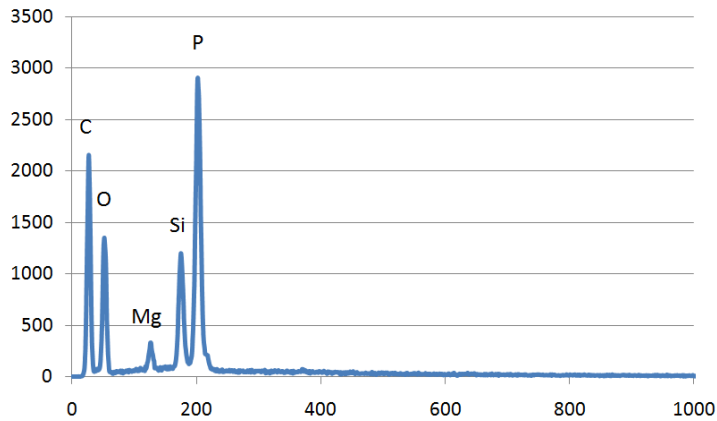
Element	
C	53.23
O	29.75
Mg	1.24
Si	3.97
P	11.8
Total	100

Figure 113 EDAX analysis and elemental quantification for Magma Prime (clear) – Char

Analysis of the residue collected after exposure to the BS EN 367 experiment yielded the results shown in Figure 113. The loss of the aluminium peak supports the conclusion that this takes part in the early stages of the decomposition and the large silica and magnesium peaks suggest that their action is in the condensed phase as they are maintained in the residue and the ratios increase due to the loss of some of the carbon and oxygen from the structure.
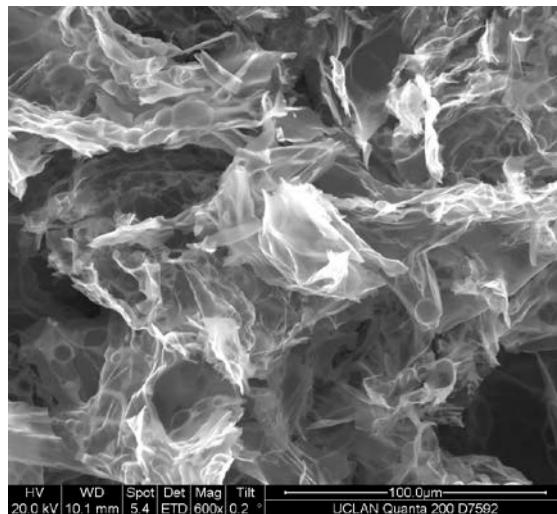
Figure 114 SEM image of the Magma Prime (clear) - char at 600 times magnification

The SEM image in Figure 114 shows the char structure and aids explanation of the physical properties of the residual foam. The thin, plate-like structure allows vast scope for expansion as the vapours become trapped and held within the structure. Many voids ensure the char is robust and able to withstand high temperatures whilst being light and spongy, capable of reducing the thermal conductivity of the coating significantly.

4.4.4. NMR

NMR analysis was carried out on Magma Prime (clear) samples to establish the presence of functional groups within the formulation. The results are shown below in Table 31 and Table 32.

4.4.4.1. MAGMA PRIME (CLEAR) – RESIN

The species located using this technique and listed in Table 31. The peak at 155ppm suggests the presence of a C=O group, either an ester or an amide, most likely urea. The group of peaks clustered around 40-70ppm indicate the presence of CH-O and CH-N groups, again supporting the inference that urea is present. Higher carbon and oxygen, and lower nitrogen ratios would be expected in cases using urea however, the incorporation of pentaerythritol may explain the imbalance in ratios observed in this case.

Table 31 NMR spectra results from Magma resin sample

Ca. 15 ppm	Spinning sideband (artefact)
40 - 70 ppm	CH-O?, CH-N? (sharp peaks are probably organic liquid fractions)
Ca. 85 ppm	Spinning sideband (artefact)
Ca. 155 ppm	C=O of ester or amide
Ca. 225 ppm	Spinning sideband (artefact)

Urea phosphates are widely used in fire retardant wood treatment due to the reduction in viscosity coinciding with the decomposition of DAP producing a foamed residue. Phosphoric acid may also be incorporated to aid curing of urea formaldehyde resins in the formulation.

4.4.4.2. MAGMA PRIME (CLEAR) – RESIDUE

The species listed in were identified in Table 32

 Magma residue samples subjected to 13C NMR. The most significant factor in these results is the absence of any conventional aliphatic groups such as CH_2 and CH_3. This supports the presence of pentaerythritol within this formulation.

Table 32 NMR spectra results from Magma residue sample

Ca. 15 ppm	Spinning sideband (artefact)
40 - 70 ppm	CH-O?, CH-N?
Ca. 85 ppm	Spinning sideband (artefact)
Ca. 100 ppm	C=C (olefinic)?
Ca. 155 ppm	C=O of ester or amide
Ca. 225 ppm	Spinning sideband (artefact)

The results shown above should be interpreted with caution as the sample preparation was not optimum in this case. Dissolution was not complete and the nature of the sample made analysis complex and increased the likelihood of error in the results.

4.4.5. ICP-MS

The sample was prepared as described previously (section 2.2.6.). 0.093g of Magma Prime (clear) was added to 10ml of nitric acid and digested in a microwave for about half an hour. After an hour the cooled acid mixture was placed into the auto sampler tube for the ICP-MS. A blank of only nitric acid was also run for comparison purposes.

The ICP-MS spectrum obtained is shown below (Figure 115).
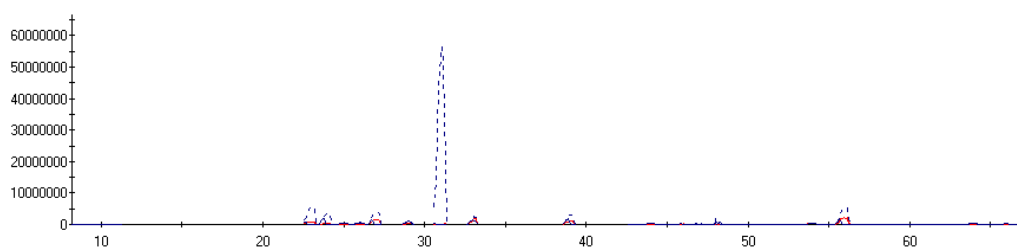
Figure 115 ICP-MS spectra of Magma prime (clear)

The only peak of interest is the large phosphorus peak shown just above 30. As this sample was run in water it is apparent that most of the other analytes are part of the water fraction of the sample. Aluminium, magnesium, silicon and sodium peaks are also present however the amount of each is only negligibly more than the blank. Even when zooming in to various sections of the graph it is clear that the sample is predominantly phosphorus with little else to

report (with confidence) on the composition of the sample. This data can also be quantified however in this instance the calibration was not carried out and so this data is only qualitative.

4.4.6. HUMIDITY EXPERIMENTS

Humidity experiments were carried out to determine the extent to which a coating will absorb or lose water depending on the environment in which it is found. This is of particular importance to coatings used on external surfaces where they are exposed to varying weather conditions. Coatings that take on a lot of water are subject to leaching, and de-adhesion may occur as well as the potential for changing the properties of the final surface finish for example; gloss or matt, rough or smooth etc.

Samples of a single coat of Magma prime clear were prepared on aluminium sheet substrate and exposed to various environments to determine if the samples take on or lose water in different conditions. Dry conditions were obtained by using a low temperature oven at 30-40°C. Humid conditions were achieved by placing samples in a desiccator containing saturated NaCl in the base. The initial mass of each sample was recorded and then samples were exposed to the humid environment until a steady mass reading was achieved the samples were then moved to the dry environment and then back. The experimental regime is listed in Table 33.

Table 33 Exposure regime

Day	Condition
0	Initial
0.5	Humid
1	Humid
1.5	Humid
4	Humid
4.5	Humid
5	Dry
5.5	Dry
6	Dry
8	Dry
13	Humid
14	Humid
20	Dry

The graph in Figure 116 depicts the fluctuations in mass of both samples in the two conditions.
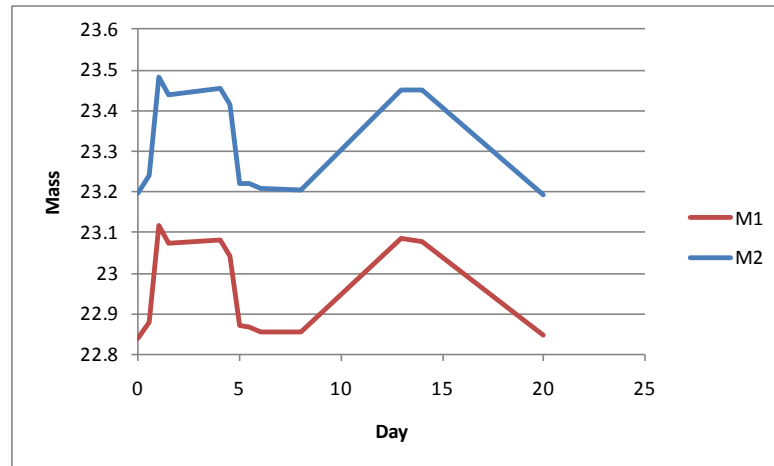
Figure 116 Mass fluctuations of samples exposed to humid and dry conditions

The results show good repeatability as the same trend is seen for both samples; the amount of increase or decrease in mass for the two samples is equal. This suggests that the amount of water absorbed/desorbed is a factor of surface area and possibly thickness, though this is not tested here. In each case the mass of sample returns to the same stable mass in wet conditions and the same stable mass in dry conditions suggesting that the number of times the samples is exposed to each environment does not affect the mass of water absorbed or desorbed. After the first introduction of the sample to the humid atmosphere the sample surface became rough; tiny bubbles appeared in the surface of the coating. These were maintained during drying however they became no worse during the second exposure to the humid atmosphere. This suggests that the water is changing or damaging the samples surface however is dependent on the extent of wetting. As the humidity of the atmosphere was maintained and became no worse neither did the extent of bubbling. However, if water were to be dripped onto the surface (as would happen in the rain) or if the sample were to be submerged it would become further deteriorated or even washed away.

Conclusions drawn from this work include that the amount of water absorbed/de-absorbed is dependent on the surface area of the sample exposed, as well as the humidity or drying temperature. Damage incurred to the sample surface is also dependent on the extent of 'wetting'.

4.4.7. MAGMA AND RESIN ANALYSIS

As replicated samples produced were unstable and gave poor coating properties, Magma samples were mixed with various other resins used in this research to determine if a more stable mixture could be obtained. The results are shown in Table 34.

Table 34 Compatibility details of Magma samples combined with various resins

Magma prime clear 1.23g, plus 1.45g PVDC resin.	Magma prime clear 1.25g, plus 1.36g acrylic resin.
Blends well. Maintains viscosity. No apparent lumps or granules. Suitable for further testing. Dries to form a complete yet 'crazed' film, that is translucent and 'off white' in colour.	Does not blend. Creates a white grainy paste-like material. Unsuitable for further testing.
Magma prime black 1.37g plus 1.37g of PVDC resin.	Magma prime black 1.29g plus 1.33g of acrylic resin.
Blends well. Slight colour change from dark blue/black to slightly lighter colour. No apparent lumps or granules. Suitable for further testing. Dries to form a matt black film, interrupted by the presence of bubbles in the surface of the film.	Blends well. Slight colour change from dark blue/ black to slightly lighter colour. No apparent lumps or granules. Suitable for further testing. Forms a matt black film on drying, due to its pooling some creasing is noted in the surface of the film, though it is otherwise largely un-textured.
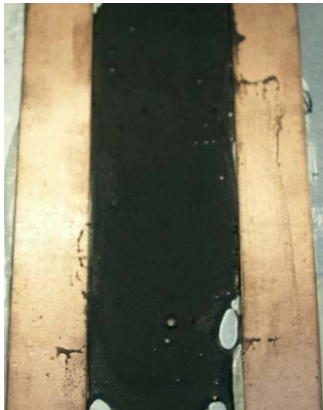
The "Doctor blade" method was utilised to produce a thin and continuous film from the sample mixtures. However, due to the low viscosity, some samples were susceptible to pooling. This method did not in all cases produce a uniform continuous film. Magma prime clear plus acrylic resin did not mix well and appears to cross-link to form a paste-like material.

Samples were then exposed to heat to determine if the intumescent action was equal to that of the unchanged Magma prime (clear) sample.

Samples in PVDC resin:

Magma prime (clear) and PVDC resin mixtures produce small bubbles and white fumes when heated. Bubbles increase in size as the reaction progresses. Discolouration occurs at the edges of the sample. The residue formed is very flimsy and a thin sticky skin is produced which is significantly different from observations of that collected from Magma prime (clear) samples in previous flammability tests. The maximum residue thickness achieved was 7 mm, which firms on cooling.

Magma Prime (black) combined with PVDC resin produces some small bubbles at low temperatures. A single skin forms over a single large bubble which deflates on bursting. The maximum height obtained is 7 mm but a stable residue was only 3.5 mm thick.

Samples in Acrylic resin:

Magma Prime (clear) in combination with acrylic resin formed dried clumps and appears to turn yellow/green during heating. Further discolouration occurs as heating continues however no intumescence is observed. Softening of the residue occurs but the overall dimensions of the sample remain the same as no intumescence is recorded.

Magma Prime (black) mixed with acrylic resin leads to bubbling causing the sample to thicken. A thin rubbery skin is formed which appears robust however not as substantial as the spongy Magma Prime (clear) char residue. The maximum residue height was 4 mm.

Samples in Vinyl resin:

Magma Prime (clear) in combination with vinyl resin forms bubbles of various sizes and discolouration occurs during heating. The residue is very sticky and the maximum height was 4 mm.

PVDC resin appears to be the most suitable for introduction of these additives, however, even this is unstable; perhaps different ratios may enable mixes to be more effective.

SUMMARY

This chapter investigates current commercial formulations to determine their composition and burning behaviour. Screening test methods were undertaken to estimate the level of protection offered by commercial coatings and further investigate formulation factors affecting performance, such as selection of the appropriate fire retardant mechanism, stability of formulations and interactions of components leading to poor coating performance. Results suggest that an intumescent coating will most significantly reduce the thermal conductivity of

a coating whereas a halogenated system will provide the highest level of protection against ignition. Cellulosic systems activate at lower temperatures than their steel intumescent counterparts and use intumescent additives such as DAP to reduce the onset temperature of intumescence. The fire propagation test shows that it is not only intumescence that is effective for passing the fire tests. However, factors such as residue stability and structure should also be considered to enable optimum protection to be achieved. Though characterisation of the existing formulations was not conclusive, some valuable information was gathered as to the formulations used to achieve various fire retardant mechanisms within specified heating ranges. Physical properties were also investigated which highlighted the need for water-proof formulations for exterior applications.

CHAPTER 5. NOVEL FORMULATIONS

The next stage of research was aimed at formulating a novel system tailored for application over multilayer paint using criteria outlined in previous chapters. This took a two pronged approach; firstly, to add various fire retardant additives to base resins to screen for promising and effective additives; secondly, to attempt to replicate the commercial systems characterised in the previous chapter and tailor them to our specific requirements. These were subjected to the screening test methods to establish their performance and also to determine which screening method best replicates results gained in the standard test method, the BS 476 Part 6: propagation of flame.

Samples were prepared on plasterboard substrate coated with two layers of nitrocellulose paint. A thermocouple was embedded in the centre of the sample at the interface between the nitrocellulose and coating as shown in Figure 44. The radiant heater in the cone calorimeter was set to give a heat flux of 30 kW m^{-2} for analysis.

5.1. FIRE RETARDANT ADDITIVES IN PVDC RESIN

Initially experiments were performed to establish the effect of some intumescent and fire retardant additives on the fire retardancy of base resins. PVDC was the resin of choice for the first stage of these experiments as it is inherently fire retardant due to the presence of chlorine. This is a relatively stable resin that is compatible with most other additives and will be resilient to changes when the additives are incorporated. This will ensure a feasible paint system after the formulations are complete. Details of the formulations are described in section 2.1.2.1.

5.1.1. Assessment of cone calorimeter properties
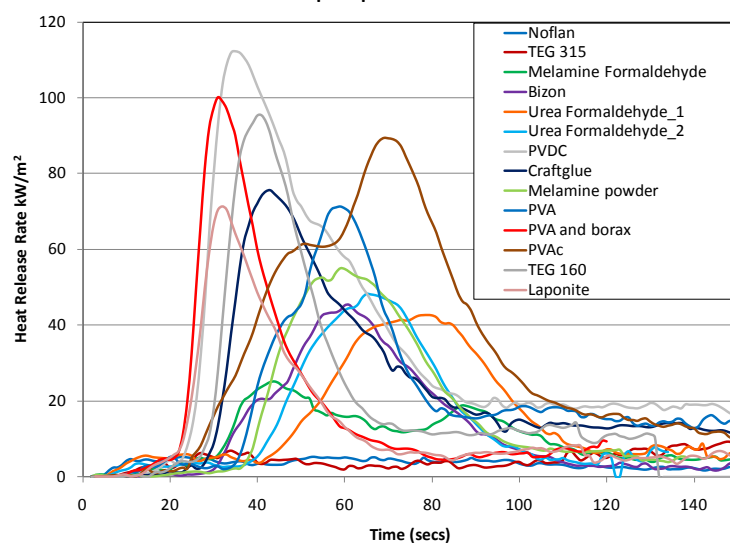
Figure 117 Heat release rate curves for various additives in PVDC resin at 30 kW m^{-2}

Average heat release rate curves for all samples are shown together in Figure 117. There is a wide scatter in results when considering peak and total heat release. All additives were incorporated to reduce the peak heat release rate of the reference PVDC resin. Two samples failed to ignite when exposed to the cone calorimeter at a heat flux of 30 kW m^{-2}; these were the Noflan and TEG315 samples.
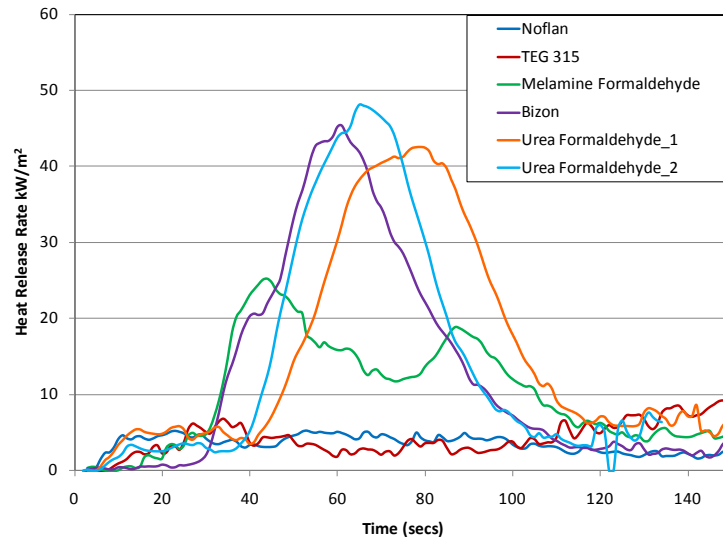
Figure 118 Heat release rate curves for samples below 50 kW m-2 in PVDC resin

The best performing samples with a peak heat release rate less than 50 kW m^{-2} are shown in Figure 118. These six specimens can be split into two groups; the first group fails to ignite at all, displaying heat release curves maintained below 10 kW m^{-2}, and the second all have peak heat release rates between 40 and 50 kW m^{-2}. These include Melamine, Urea Formaldehyde, and Bizon samples. As all samples were incorporated into identical resin systems, the changes in behaviour observed in Figure 118 are attributed to the additives incorporated.
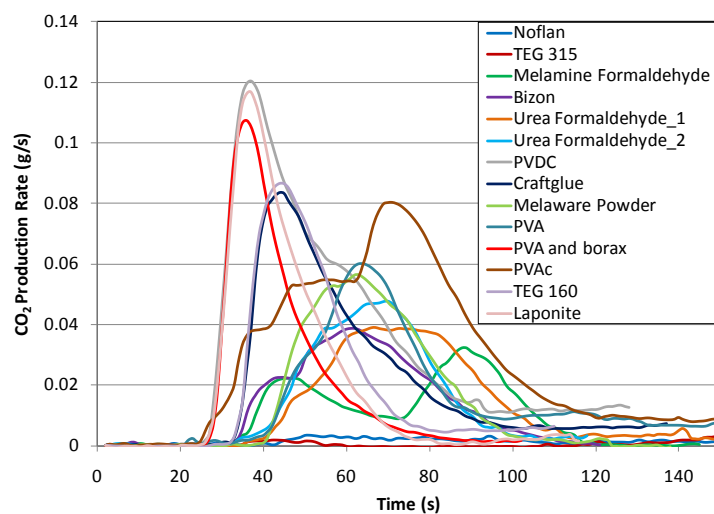
Figure 119 Carbon dioxide production rate curves for various additives in PVDC resin

The carbon dioxide production rate curves follow a similar pattern to the heat release rate curves. The peak of production rate is highest for the unchanged resin, closely followed by the Laponite and TEG 315 samples; this could be due to the activation temperature of these additives being a lot higher than that provided by the cone calorimeter. The decomposition of nitrocellulose occurs prior to the intumescence of the protective coating and therefore combustion occurs. This leads to an increase in thermal feedback to the coating providing the heat needed to allow the complete intumescence to develop. This high temperature intumescence is then too late to protect any of the substrate from combustion. The samples displaying the highest carbon dioxide production rate were not investigated further, while the six samples with the lowest curves are shown in Figure 120.
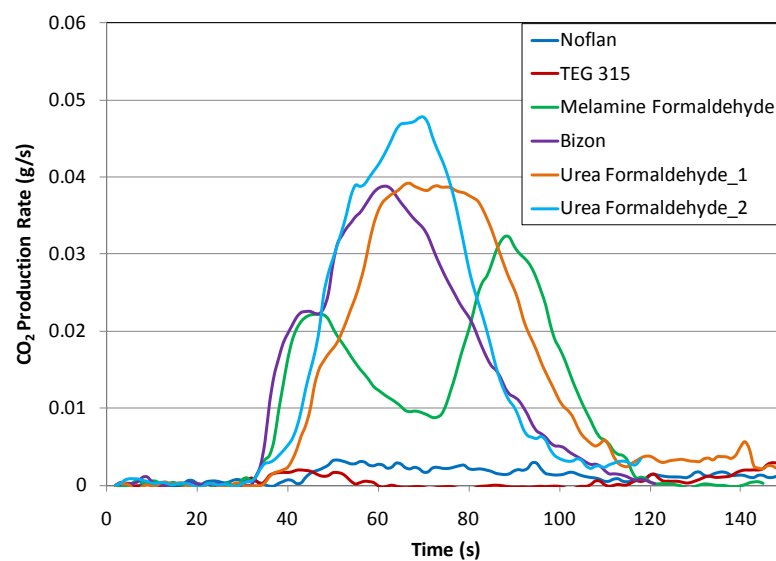
Figure 120 Carbon dioxide production rate curves for samples below 50 kW m^{-2} in PVDC resin

The similarity between the heat release rate and carbon dioxide production curves indicates that all coatings have been effective in preventing ignition of the nitrocellulose. The CO_2 production rate for the Noflan and TEG 315 samples is negligible as would be expected from samples which fail to ignite. The two peaks shown by the Melamine formaldehyde system is attributed to the small but sustained flame that re-ignites decomposition products later in the experiment, giving a second, larger peak of heat release. The two urea formaldehyde samples show fairly good repeatability but do highlight the problems of using laboratory prepared additives which are not monitored or quality controlled. As the sample preparation and experimental parameters are kept constant, the difference in the data collected of the two urea formaldehyde samples is likely to come from variation in the resin itself. As this was produced in the laboratory it is possible that the concentrations will be varied. The peak of carbon dioxide production rate is lower than estimated by the heat release rate curve but is prolonged. The cone calorimeter properties are listed in Table 35.

Table 35 PVDC plus additives cone calorimeter properties

Sample	t_{ig} (s)	PHRR (kW m^{-2})	tPHRR (s)	THR (kW m^{-2})
PVDC	24 ± 1	116 ± 12	30 ± 4	4753 ± 384
TEG 315	0 ± 0	14 ± 1	208 ± 20	3126 ± 485
TEG 160	30 ± 1	99 ± 8	37 ± 2	2715 ± 52
Laponite	26 ± 1	115 ± 13	29 ± 1	2461 ± 239
PVA flakes	43 ± 6	88 ± 4	53 ± 6	3474 ± 186
PVA plus Borax	24 ± 1	101 ± 14	28 ± 1	2371 ± 380
Craftglue	30 ± 4	85 ± 15	40 ± 4	3380 ± 654
Bizon	43 ± 13	66 ± 22	59 ± 14	1869 ± 656
UF1	48 ± 12	66 ± 7	71 ± 12	1870 ± 807
UF2	42 ± 5	65 ± 10	62 ± 9	1842 ± 419
Noflan	0 ± 0	8 ± 1	126 ± 75	981 ± 304
Melamine Powder	45 ± 9	90 ± 16	58 ± 10	2246 ± 471
MF	57 ± 21	55 ± 15	69 ± 21	2069 ± 670
PVAc	38 ± 16	106 ± 13	55 ± 13	4714 ± 573
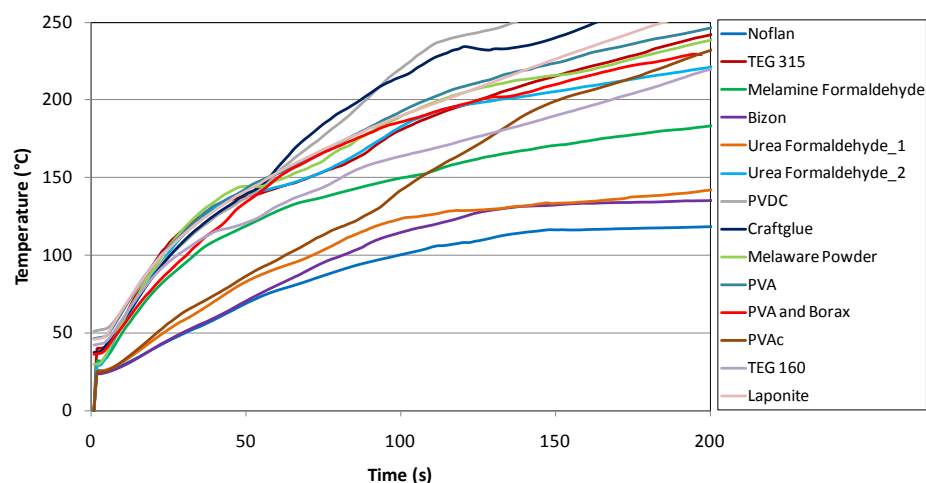
Figure 121 Thermocouple temperature profile for various additives in PVDC resin

Results from the thermocouples embedded in the plasterboard are compared in Figure 121 and clearly fall into two groups. The majority of samples cross the 150 °C temperature threshold between 20-30 seconds, however the three samples offering the best protection: Noflan, Bizon and Urea Formaldehyde_1 do not cross the 150 °C for the entire duration of the 200 seconds analysis.
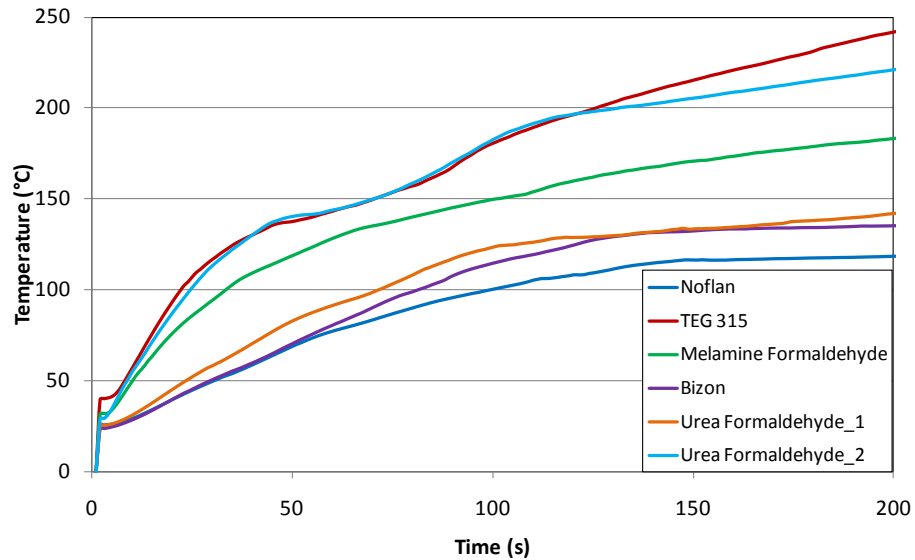
Figure 122 Thermocouple temperature profile for Noflan, TEG 315, Bizon, MF, UF_2 and UF_2 samples at 35 kW m^{-2}

When the samples with the lowest heat release rate are shown on smaller scale axes it is clear that there is a large difference in performance within this group. Three samples prevent temperature increase above 150 °C for the duration of the experiment (200 seconds), these were: Noflan, Bizon and Urea Formaldehyde_1. The other three samples (Melamine Formaldehyde, TEG 315 and Urea Formaldehyde_2) show very little difference from the remainder of samples analysed. This supports the suggestion that the samples with the lowest heat release rate or carbon dioxide production rate do not always have the best properties as far as protection from heat are concerned. Instead protection is dependent on the position, extent and structure of any char residue, particularly intumescence. Coating barrier properties are also dependent on structure, heat re-radiation and thermal conductivity.

All of the screening methods used caused problems distinguishing between various systems; in this batch due to the similarities in type and performance. None of the samples were particularly effective intumescents so there was little to distinguish one sample from another in terms of thermal conductivity. The use of identical resin systems means that incompatibility was a factor for many systems. Two or three of the additives were effective through alternative fire retardant mechanisms. Noflan is investigated later in this thesis.

Poor coating properties such as: inadequate dissolution or dispersion of additives, low viscosity causing pooling, and inadequate flow, rules out many of the formulations at this stage. Lack of dissolution of the PVA solids within formulation increase the surface area of the sample exposed to the heat flux and therefore increases the temperature of the system. Expandable graphite settles after mixing. Although thorough mixing takes place prior to coating, the

additives are poorly dispersed reducing fire retardant activity. Many of the additives become disproportionately trapped in the fibres of the roller or brush during application thus reducing the concentration of fire retardant additives within the dried coating at the time of testing.

As this approach had limited success, it was drawn to a close at this point in preference for the more guided approach of simulating previous successful formulations with adaptations aimed at lowering the activation temperature.

5.2. STANDARD INTUMESCENT FORMULATIONS

Novel formulations were produced based on standard intumescent systems and subjected to the same screening experiments to determine the optimum for protection. Various resin systems were also investigated based on the findings from the characterisation of commercial intumescent systems. The lower temperature activation intumescent systems (such as Firestop Magma samples) are reported to be developed in vinyl copolymer systems. For this reason the base resins chosen for the novel formulations include: Dulux Vinyl silk - a vinyl copolymer resin (Vs), Vinyl resin - a base vinyl resin containing no copolymers filler or additives (Vr), and finally Wickes Vinyl silk emulsion – a vinyl copolymer emulsion (W). Formulations are described in section 2.1.2.2.

5.2.1. Assessment of fire retardant action

Initial analysis suggests that DAP systems produce more swelling than their APP counterparts when applied to a cellulose substrate such as the wooden splint. This effect is independent of the resin system used. Evidence of this can be observed in the images shown in Figure 123.

VsAUP   VrAMP   VrDUP

VsAMP   VsDMP   VsDUP

WAMP   WDUP   WDMP   WAUP
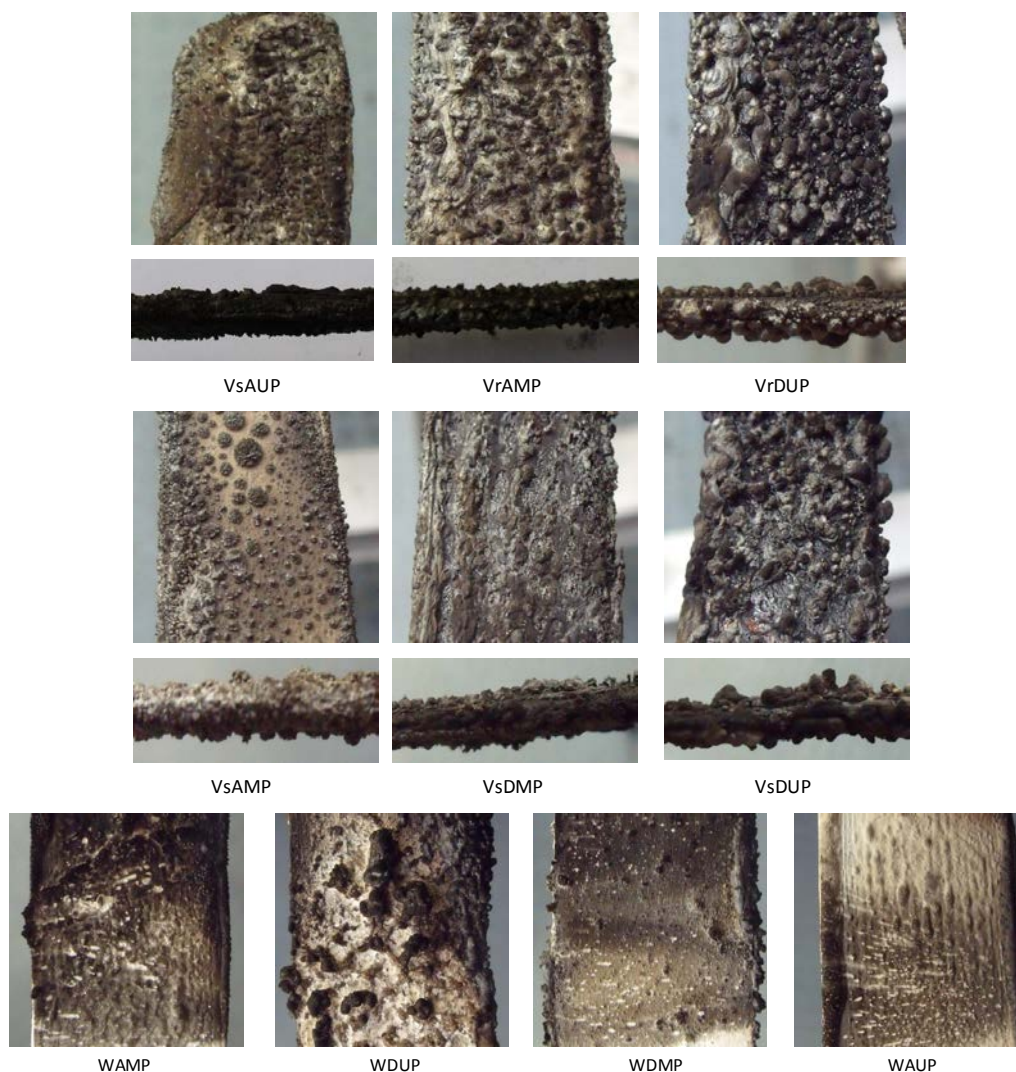
Figure 123 DAP or APP, Melamine or Urea and Pentaerythritol systems after exposure to the Bunsen burner

DAP systems not only intumesce to a greater degree but the residue also forms more rapidly than observed with APP samples. This could be due to the action of the diammonium phosphate lowering the pyrolysis temperature of the cellulosic material. Heating of DAP at approximately 160°C (below the decomposition of cellulose) leads to the formation of phosphoric acid and ammonia. The phosphoric acid may phosphorylate the primary hydroxyl group of nitrocellulose to form a phosphorus ester. These esters catalyse dehydration of the nitrocellulose, promoting the formation of char and water.[121] The acid may also cross-link with the cellulose, changing the pathway of pyrolysis to yield less flammable products.[122]

$$(NH_4)_2HPO_4 = 2NH_4^+ + HPO_4^{-2} = 2NH_{3(g)} + 3H^+_{(aq)} + PO_4^{-3}_{(aq)}$$
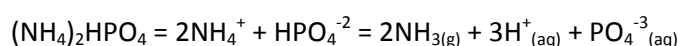
Spongy residue made up of many small voids are formed as opposed to the brittle residue formed by the APP specimens. Limitations include the poor dispersion of DAP within the

167

formulation leading to increased intumescence in the areas where clumps of the additive have formed and poor coating appearance prior to exposure to the flame.

5.2.2. Assessment of thermal decomposition - Thermogravimetric (TGA) analysis

TGA analysis was carried out in both air and nitrogen atmospheres to determine the effect of different additives on the formulation.
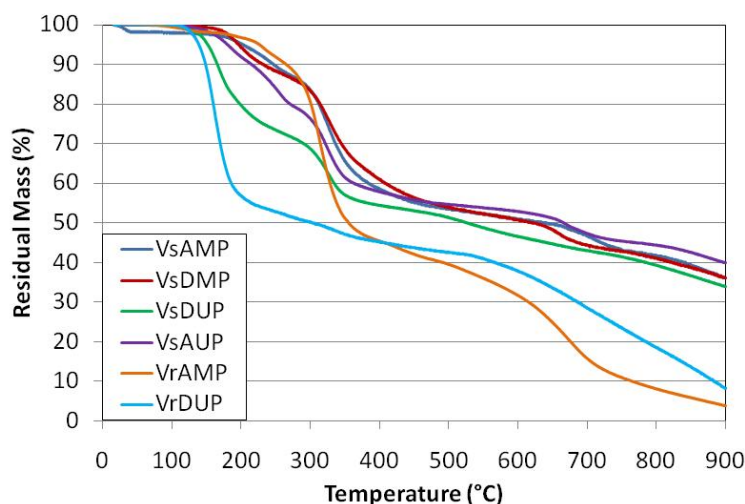
Figure 124 Decomposition curves for DAP and APP formulations in air; ambient to 900 °C at a heating rate of 10 °C min^{-1}

Vinyl silk (Vs) resin samples sustain the most residual mass (30-40 %) at higher temperatures when compared to the vinyl resin (Vr) alternatives (0-10 %). This could in part be attributed to the filler and pigment loadings present in the Vs samples which are absent in the Vr samples. With the exception of only the VsDMP sample, the DAP species display an approximate decomposition temperature of 150 °C whereas the APP samples do not begin decomposition until 220 °C. Melamine also appears to stabilise the sample to a higher temperature than urea. The predominant factor in altering the decomposition curve is the choice of resin system used.
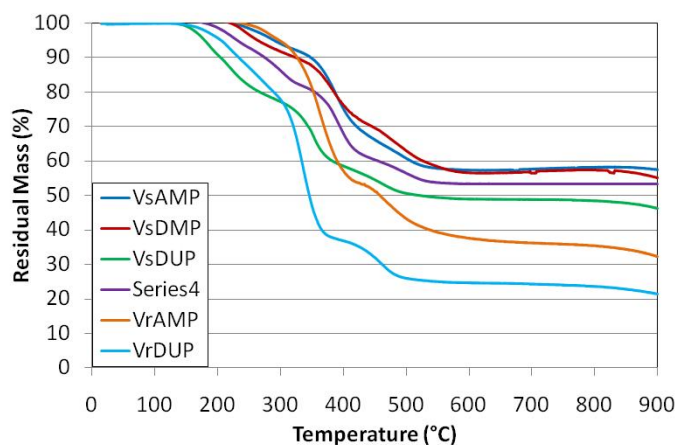
Figure 125 Decomposition curves for DAP and APP formulations in nitrogen; ambient to 900 °C at a heating rate of 10 °C min^{-1}

TGA analysis in nitrogen, shown in Figure 125 follows a similar trend with no significant change in the number of decomposition steps observed. Again vinyl resin samples decompose to a reduced residual mass at higher temperatures whereas the vinyl resin samples maintain a residual mass of 50-60 %. The onset temperature of decomposition recorded for DAP samples is below 200 °C, in contrast to 250 °C, recorded for APP samples.

When results from both air and nitrogen atmospheres are compared, as shown in Table 36, it can be observed that the incorporation of melamine into the formulation has the effect of preserving a portion of the polymer in the nitrogen analyses.

Table 36 Polymer preservation analysis in air and nitrogen atmospheres – Vinyl silk and Vinyl resin samples

Sample	Residual Mass in air (%)	Residual Mass in nitrogen (%)	Amount of polymer preserved (%)
VsAMP	37	57	10
VsDMP	37	55	8
VsDUP	34	47	3
VsAUP	40	52	2
VrAMP	5	32	17
VrDUP	9	21	2

Melamine and urea will oxidise in the presence of oxygen and therefore decompose in air atmosphere. Comparison of the residual mass formed in nitrogen atmospheres with those decomposed in air atmosphere display an increased in mass in excess of 10 %. As a loading of 10 % of urea or melamine was added, a 10 % residue increase is expected due to the presence of the un-oxidised melamine or urea. However, in cases where the value is in excess of 10 %

the additional residue is due to preservation of the polymer. This phenomenon is most prominent in the melamine samples though it is seen to a lesser extent in the urea counterparts. Melamine decomposition occurs at approximately 280°C, above the temperature of nitrocellulose decomposition whereas urea decomposition occurs from 175°C suggesting it may occur alongside nitrocellulose decomposition. This suggests that melamine may be preferable in the final formulation to protect the substrate from decomposition in oxygen depleted atmospheres such as in a fire.
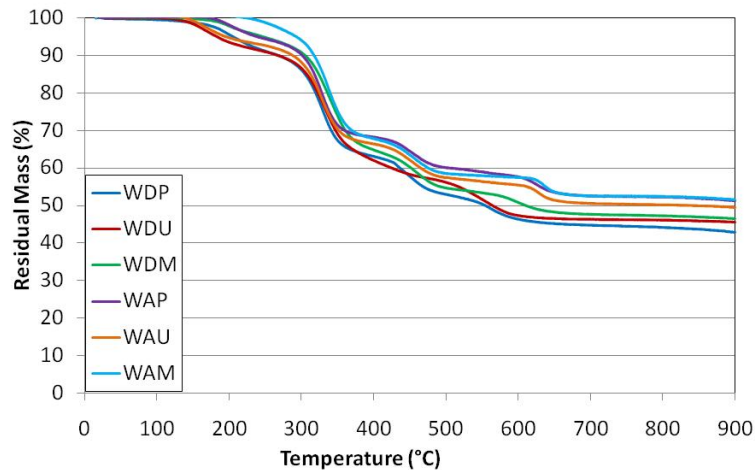
Figure 126 Decomposition curves for Wickes resin formulations in air; ambient to 900 °C at a heating rate of 10 °C min^{-1}

Figure 126 clearly shows that samples containing DAP and Urea begin decomposition at a lower temperature (150 °C) than species containing both APP and melamine (250 °C). All samples sustain a residual mass in excess of 40 % even at 900 °C.
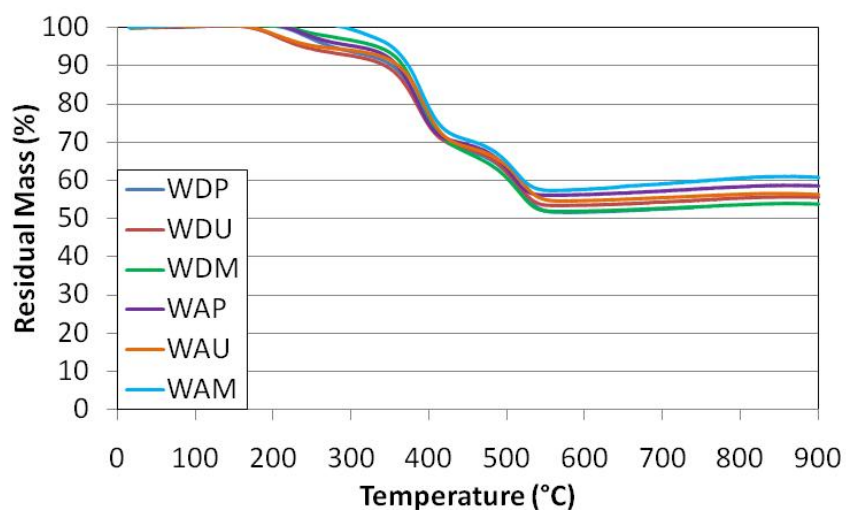
Figure 127 Decomposition curves for Wickes resin formulations in nitrogen; ambient to 900 °C at a heating rate of 10 °C min^{-1}

In nitrogen atmosphere the decomposition curve variation is even further diminished. These results provide further support for the melamine stabilising samples to higher temperatures whereas urea containing samples have a lower temperature of decomposition. The residual mass in all cases in excess of 50 %.

5.2.3. Assessment of burning behaviour using the cone calorimeter

All formulations improve the heat release rates of the original resin samples as shown in Figure 128 and Figure 129.

Figure 128 Heat release rate curves for DAP or APP, Melamine or Urea and Pentaerythritol in vinyl resin and vinyl silk systems
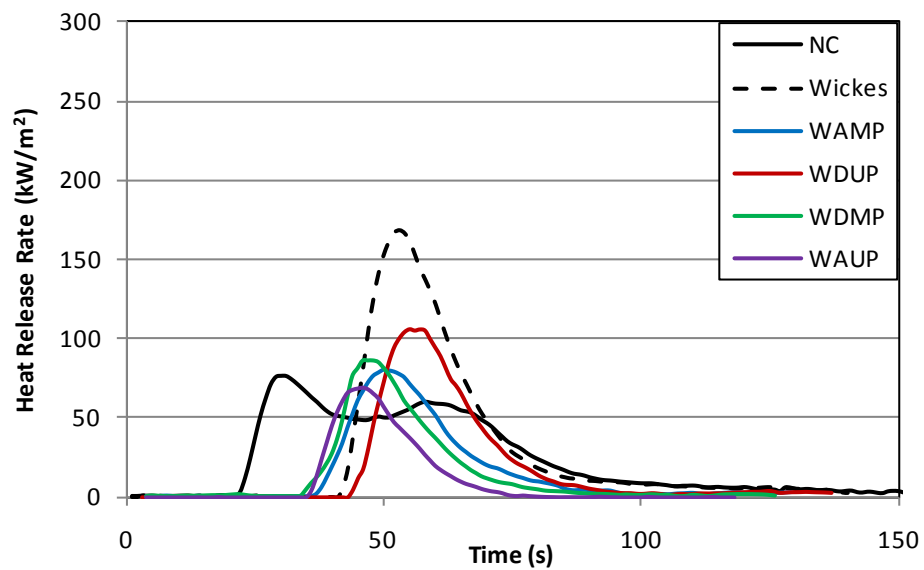
Figure 129 Heat release rate curves for DAP or APP, Melamine or Urea and Pentaerythritol in Wickes vinyl emulsion systems

Vinyl resin and Wickes Vinyl silk emulsion samples show similar peak heat release rate values as the initial peak in the nitrocellulose heat release rate curve however peaks are delayed; in the case of the vinyl resin samples by as much as 50 seconds and 15-20 seconds for Wickes vinyl silk emulsion samples. Dulux vinyl silk samples display a reduced peak of heat release rate due to the additional fillers and pigments within formulation however all heat release data is skewed by the nitrocellulose substrate so carbon dioxide rate curves should also be considered. These are shown in Figure 130 and Figure 131 respectively.

Figure 130 Carbon dioxide production rate curves for DAP or APP, Melamine or Urea and Pentaerythritol in vinyl resin and vinyl silk systems
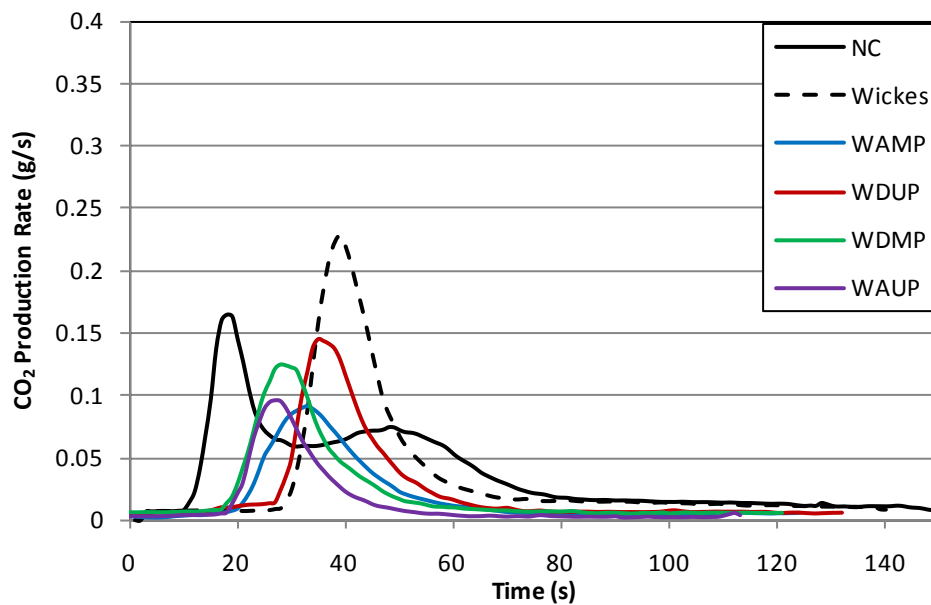
Figure 131 Carbon dioxide production rate curves for DAP or APP, Melamine or Urea and Pentaerythritol in Wickes vinyl emulsion systems

Trends observed in heat release rate curves data shown Figure 128 and Figure 129 are mirrored in carbon dioxide production rate curves shown in Figure 130 and Figure 131. In these graphs improvements to the original resin systems are more easily seen. The peak heat release rate of nitrocellulose combustion is reported in both graphs however in the case of the Vinyl silk and Vinyl resin samples the time to ignition is delayed and peak carbon dioxide production rate is significantly reduced. The initial peak attributed to the nitrocellulose combustion at approximately 18 seconds is no longer observed. Instead the combustion of the coating is recorded at approximately 40-60 seconds. This suggests that coatings are able to prevent ignition of the highly flammable nitrocellulose pyrolysis products and furthermore reduce the flammability of the reference base resin sample. This is more prominent in Vinyl silk samples than vinyl resin specimens however this is due to the addition of fillers and pigments which are not present in vinyl resin systems.

In contrast the Wickes Vinyl silk samples suggest the combustion of nitrocellulose is delayed but not prevented. This is particularly evident in WDUP and WDMP results. Carbon dioxide production rate peak is reduced however ignition occurs earlier due to the ignition of the nitrocellulose decomposition products.

Table 37 Cone calorimeter properties of DAP or APP, Melamine or Urea and Pentaerythritol in various vinyl resin systems, at 35 kW m^{-2}

Sample	t_{ig} (s)	PHRR (kW m^{-2})	tPHRR (s)	THR (kW m^{-2})
VsAMP	40 ± 6	21 ± 9	73 ± 7	888 ± 626
VsDMP	29 ± 7	27 ± 17	74 ± 27	609 ± 425
VsDUP	34 ± 3	48 ± 12	70 ± 4	1337 ± 207
VsAUP	24 ± 5	62 ± 5	67 ± 5	2042 ± 930
VrAMP	26 ± 2	82 ± 6	69 ± 6	3277 ± 508
VrDUP	33 ± 2	79 ± 3	69 ± 2	3020 ± 322
WAMP	30 ± 13	74 ± 24	46 ± 6	1737 ± 650
WAUP	20 ± 5	66 ± 8	43 ± 5	1189 ± 145
WDMP	21 ± 4	86 ± 17	43 ± 5	1602 ± 284
WDUP	27 ± 4	89 ± 27	52 ± 5	2026 ± 494

The cone calorimeter properties are listed in Table 37 and show that Vinyl resin samples give the highest recorded value for total heat release (THR) in the cone calorimeter; this may be due to the lack of pigment and chalk within these samples which are present in the vinyl silk and Wickes vinyl emulsion samples producing the white colour.

Temperature profiles collected from thermocouple embedded in the cone calorimeter plaques are shown in Figure 132 and Figure 133.
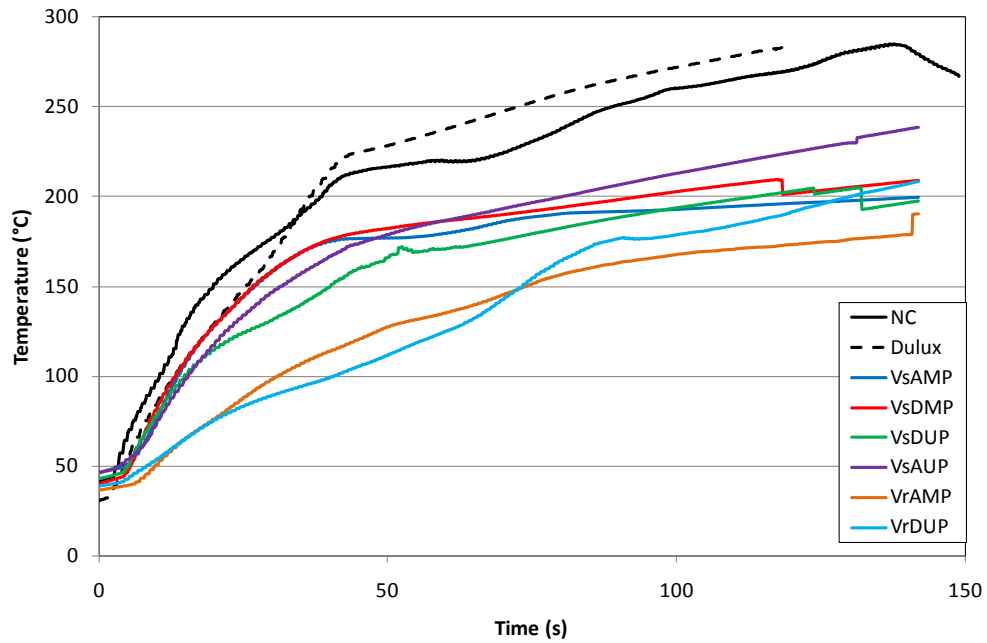
Figure 132 Thermocouple temperature profiles for DAP or APP, Melamine or Urea and Pentaerythritol in vinyl resin and vinyl silk systems

Figure 132 clearly shows that the optimum performance is shown by the VrAMP and VrDUP samples as the temperature is maintained significantly lower in these samples compared to any other. This suggests that the vinyl resin softens at the optimum time to trap the decomposition gases and intumesce as well as preventing the ignition of the resultant vapours.

Figure 133 Thermocouple temperature profiles for DAP or APP, Melamine or Urea and Pentaerythritol in Wickes vinyl emulsion systems

The majority of systems show improvement when compared to the nitrocellulose, Wickes and Dulux reference samples, most prominently at higher temperatures (in excess of 200 °C). This

suggests that the additives reduce the thermal conductivity of the reference samples and increase the level of intumescence.

The residue resulting after the cone calorimetry was measured to determine the height. As this was often not of uniform thickness, a minimum, maximum and average value were calculated, these are shown in Table 38.

Table 38 Residue height for DAP or APP, Melamine or Urea and Pentaerythritol in various vinyl resin systems, 35 kW m^{-2}

Sample	Residue height (mm) – 35 kW m^{-2}		
	Minimum	Maximum	Average
VsAMP	21	32	26.5
VsAUP	11	18	15.4
VsDMP	5	11	8
VsDUP	3	6	4.5
VrAMP	1	8	3.5
VrDUP	2	5	2.5
WAMP	1	11	6
WAUP	0	18	9
WDMP	0	9	4.5
WDUP	1	7	4

The maximum residue height is recorded for the VsAMP sample, suggesting that the decomposition of this sample is optimum for the production of residue. However, in many cases though the measured residue height was significant the residue itself was not optimised to reduce thermal conduction. For example much of the residue formed in these systems compromised of only one large chamber of trapped vapours rather than the smaller chambers found in the Magma clear sample and other successful intumescent systems. Should this large bubble be disrupted then all of the residue collapses leaving very little protection for the remaining material. Conversely should the coating be made up of many smaller bubbles, if one is destroyed then there are many others to maintain the level of protection. This supports the suggestion that it is the physical properties of the residue and not only the amount of char present that reduces thermal conductivity and therefore provides protection.

5.2.4. Assessment of thermal conductivity - BS EN 367

The same samples were subjected to the BS EN 367 procedure (outlined in 2.3.3.) to assess the level of thermal conduction of each sample.
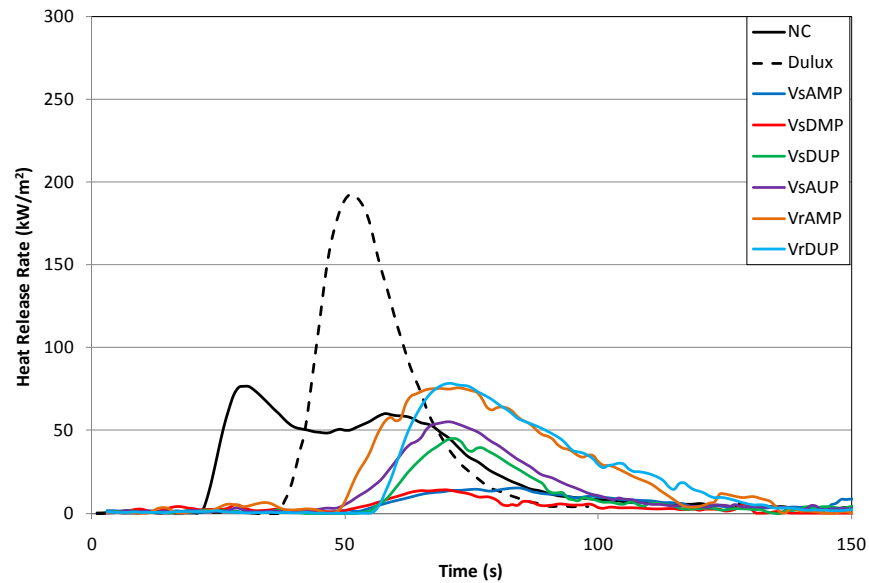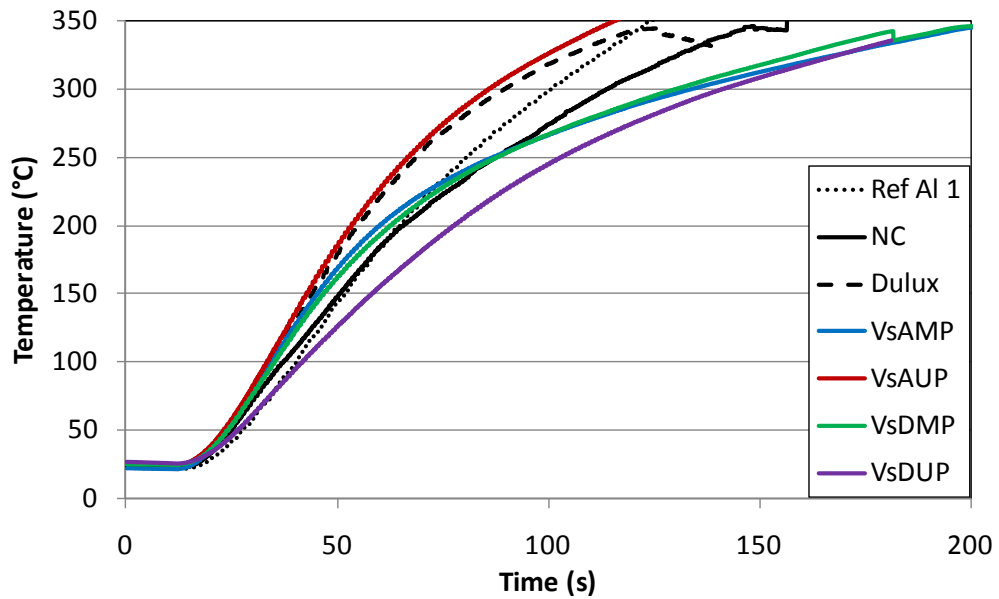

Figure 134 BSEN 367 temperature profile curves for DAP or APP, Melamine or Urea and Pentaerythritol in vinyl resin and vinyl silk systems
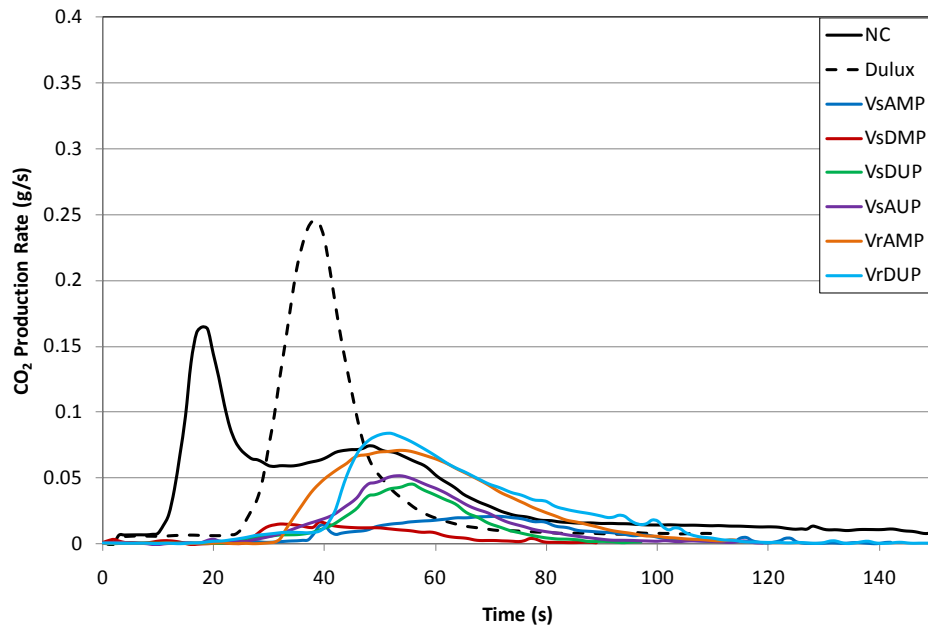

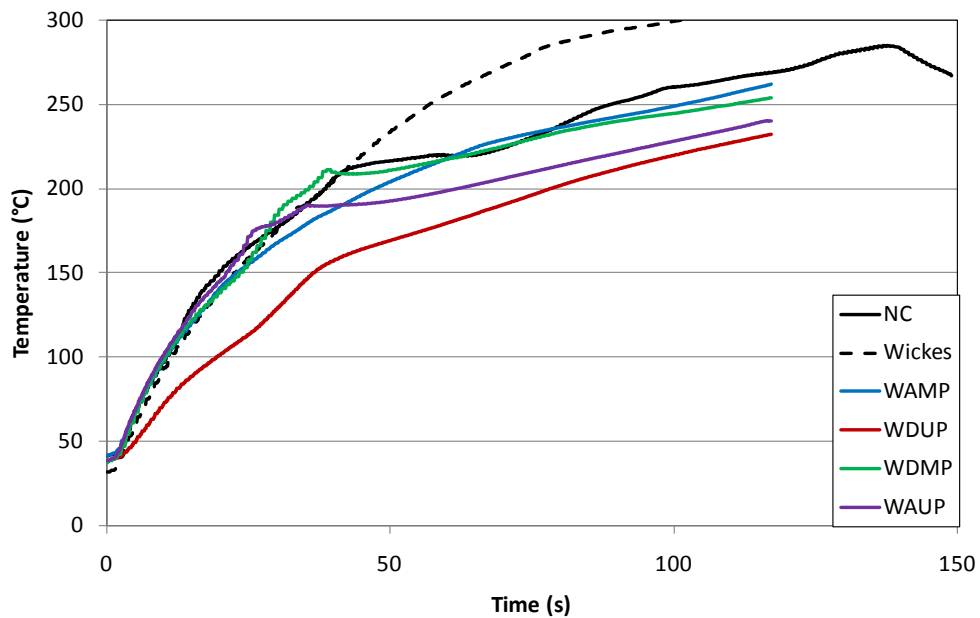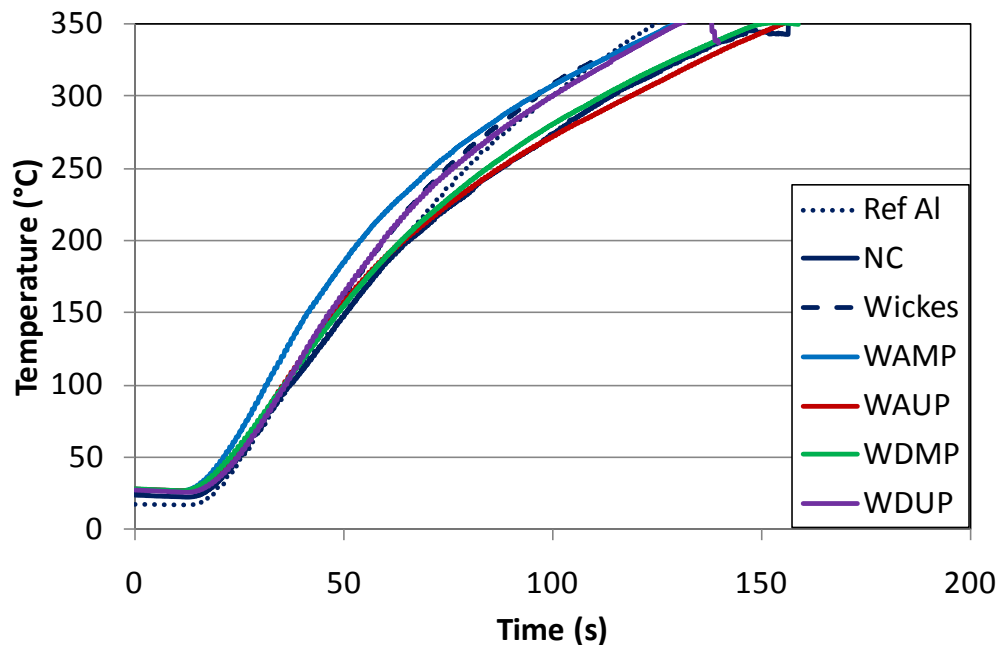Figure 135 BSEN 367 temperature profile curves for DAP or APP, Melamine or Urea and Pentaerythritol in Wickes vinyl emulsion systems

The temperature profiles shown in Figure 134 and Figure 135 respectively show that the VsDUP, VsDMP, VrDUP and VsAMP samples have the lowest thermal conductivity as outlined by this experiment. The majority are DAP based samples suggesting that the activation of the

DAP is early enough to have an intumescent effect in time for it to successfully prevent the transmission of heat through the coating and into the aluminium substrate. This is supported by the residue height analysis listed in Table 40 which also shows that the DAP systems displayed a greater residue yield that the APP systems in this method.

Time to reach 150 °C and 350 °C are listed below in Table 39. Vinyl silk appear to take longer to reach 350 °C, this is perhaps due to the presence of intumescence at higher temperatures. It could also be explained by the additional barrier protection afforded by the pigmented systems rather than the vinyl resin systems which at this stage have no titanium dioxide or chalk in the formulation.

Table 39 Time to reach 150 °C and 350 °C for various vinyl resin systems in the BS EN 367 within the range 30-40 kW m^{-2}

Sample	Time to reach 150 °C (s)	Time to reach 350 °C (s)
Reference Aluminium sheet	50 ± 2	122 ± 11
VsAMP	45 ± 1	208 ± 11
VsAUP	44 ± 3	124 ± 12
VsDMP	47 ± 3	195 ± 20
VsDUP	55 ± 8	191 ± 14
VrAMP	42 ± 3	175 ± 2
VrDUP	51 ± 7	169 ± 11
WAMP	41 ± 1	129 ± 4
WAUP	46 ± 2	150 ± 8
WDMP	49 ± 6	150 ± 6
WDUP	47 ± 2	131 ± 5

Surprisingly in some cases the time to reach 150 °C does not correlate to the amount of residue recorded in Table 40. An explanation for this could be that the residue layer does not evolve until after the substrate material has surpassed the 150 °C threshold. Some systems required a large amount of energy (or a high temperature) in order for the intumescent additives to activate. This looks to be the case for the APP samples, in particular the VsAMP and WAUP samples, which had some of the largest residue heights recorded however also some of the quickest recorded times to reach 150 °C.

Residue height does appear to be affected by substrate type, the residue height recorded from samples on a nitrocellulose substrate vary a significant amount from the residue heights recorded on the aluminium substrate. An explanation for this might be that in the case of the cone calorimeter samples, the resin softens at a temperature which may or may not coincide with the decomposition of the nitrocellulose, thus trapping any vapours produced during this process. Rapid decomposition of the nitrocellulose may lead to a large amount of decomposition vapours being evolved which may burst any bubbles made in the resin

(reducing residue yield). However, in the case of the BS EN 367 samples, there is no nitrocellulose to decompose and provide vapours to aid intumescence. These samples rely entirely on the vapours produced from the decomposing film, which may coincide with the softening of the resin and thus determine the level of intumescence observed.

Table 40 Residue height for DAP or APP, Melamine or Urea and Pentaerythritol in various vinyl resin systems in the BS EN 367 experiment

Sample	Residue height (mm) – BS EN 367		
	Minimum	Maximum	Average
VsAMP	1	5	3
VsAUP	0	0	0
VsDMP	0	5	2.5
VsDUP	0	4	2
WAMP	0	0	0
WAUP	0	7	3.5
WDMP	0	5	2.5
WDUP	0	3	1.5
VrAMP	0	0	0
VrDUP	0	6	3

This analysis method is efficient for the determination of thermal conductivity and provides a value which can be compared with other samples subjected to the same regime however, limitations include being unable to determine exactly which components are working well together and which are failing to provide improvement, also a system which performs well under the parameters of this analysis may not perform so well on the nitrocellulose substrate and so further testing is required.

5.2.5. Calculation of fire propagation index – BS 476: Part 6 (adapted)

Samples were then subjected to the adapted BS476: Part 6 (procedure outlined in 1.9.3.) to assess the key parameters to be address to produce a successful coating formulation and the results are shown in Table 41.

Table 41 BS 476: Part 6 (adapted) analysis of commercial various vinyl resin systems

Sample	s1 (0.5-3 min)	s2 (4-10 min)	s3 (11-20 min)	S (0-20 min)	Fire propagation index (L)	Pass/Fail
Nitrocellulose	23.79	4.36	0.66	28.81	24.22	Fail
	19.61	4.39	0.63	24.63		
	16.89	3.17	0.54	20.6		
VsAMP	2.06	2.28	0.45	4.79	4.72	Pass
	5.75	3.13	0.51	9.38		
	0	0	0	0		
VsAUP	0.09	1.44	0.27	1.8	3.29	Pass
	3.06	0.54	0.07	3.67		
	0.72	3.34	0.34	4.4		
VsDMP	3.38	1.97	0.44	5.78	5.86	Pass
	2.29	1.35	0.12	3.77		
	4.99	2.59	0.44	8.03		
VsDUP	3.68	1.7	0.37	5.75	4.48	Pass
	2.4	0.54	0.27	3.21		
	3.15	1.14	0.2	4.49		
WAMP	6.03	3.73	0.49	10.26	7.62	Fail
	2.3	3.7	0.38	6.38		
	3.13	2.67	0.41	6.21		
WAUP	1.86	2.17	0.2	4.24	4.73	Pass
	0.55	2.2	0.14	2.89		
	2.17	4.48	0.41	7.06		
WDMP	5.1	3.11	0.26	8.47	8.3	Fail
	2.92	1.99	0.23	5.15		
	7.36	3.42	0.52	11.3		
WDUP	4.58	3.77	0.6	8.95	10.58	Fail
	7.13	4.0	0.44	11.57		
	8.14	2.87	0.21	11.21		

These results clearly show that coating performance is not only reliant on physical properties and amount of residue. The vinyl silk (acrylic copolymer emulsion) samples appear to provide the highest level of protection in this experiment.   The DAP based systems perform significantly worse in the first portion of the experiment (s1) which is also the most heavily penalised, thus increasing the overall fire propagation index.

Table 42 Char height for DAP or APP, Melamine or Urea and Pentaerythritol in various vinyl resin systems in the BS 476: Part 6 (adapted) experiment

Sample	Char Height (mm) – BS 476: Part 6 (adapted)				
	Minimum	Maximum	Lifting	Average	
NC	0	0	0	0	
	0	0	0	0	0±0
	0	0	0	0	
VsAMP	15	45	None	30	
	10	47	None	28.5	27±4
	5	40	None	22.5	
VsAUP	3	25	De-adhered	14	
	4	35	None	19.5	19±4
	5	40	None	22.5	
VsDMP	7	13	De-adhered - 25	10	
	3	15	De-adhered - 20	9	12±3
	4	25	None	14.5	
VsDUP	2	20	30	11	
	3	22.5	30	12.75	12±1
	2	22	34	12	
WAMP	5	23	N/A	14	
	4	25	N/A	14.5	14±1
	5	24	N/A	14.5	
WAUP	3	28	N/A	15.5	
	4	40	N/A	22	18±3
	3	32	N/A	17.5	
WDMP	9	15	De-adhered	12	
	10	20	De-adhered	15	14±2
	9	22	De-adhered	15.5	
WDUP	5	22	60	13.5	
	4	19	30	11.5	12±1
	3				

In this experiment the APP systems have produced the greatest amount of residue as shown in Table 42. However as shown in previous results (Table 38 and Table 40) residue height is not the only factor to be considered in order to perform well in this experiment.

5.2.6. Prediction of performance in the BS 476: Part 6

Results collected from the screening test methods provide mixed and often conflicting evidence for estimation of performance in the BS 476: Part 6 with regard to water-based novel formulations. This again supports the suggestion that there are more factors involved than merely the occurrence and extent of intumescence. In the case of many of the water-based novel formulations, the residue de-adhered from the substrate or cracks formed revealing the underlying material.

Intumescence in the BS EN 367 analysis was minimal; this could be due to the orientation of the sample, inadequate heating regime, substrate type or lack of nitrocellulose material in the

substrate layer, meaning a reduced amount of vapours to trap in the intumescent char layer. This meant that thermal conductivity measured were made of the un-expanded coating which is not indicative of its state other test situations (in both the cone and BS 476: Part 6 analyses the coatings were all swollen to a greater or lesser extent). The BS EN 367 analysis is only really useful at distinguishing between intumescent coatings with a significant variation in extent and amount of intumescence.

In some of the most successful cases the coating did not intumesce to a great degree but instead formed a barrier preventing escape of combustible gases and diffusion of oxygen through to the substrate. This is particularly effective in the earlier stages of the analysis, before the intumescence has time to occur. However the most effective coatings, those with the lowest fire propagation index values in the BS 476: Part 6, did also display the greatest amount of char production during the analysis.

5.3. OIL AND SOLVENT BASED

Oil and solvent based samples were produced to investigate several factors; firstly to improve the compatibility and stability of DAP samples which destabilise after less than 24 hours in water-based systems; secondly to monitor the suitability of the outlined screening test methods to assess the performance of non water-based systems and finally to assess the impact on level of protection provided when considering a solvent or oil based system as opposed to a water-based one. Formulations are detailed in section 2.1.2.3.

5.3.1. Assessment of fire retardant action

Bunsen burner tests on wooden splints, shown in Figure 136, immediately determined the poor performance of the gloss based systems which did not intumesce, while forming burning droplets potentially contributing to downward spread of flame in a real fire.

GDP   GDU   GDM

VDP   VDU   VDM
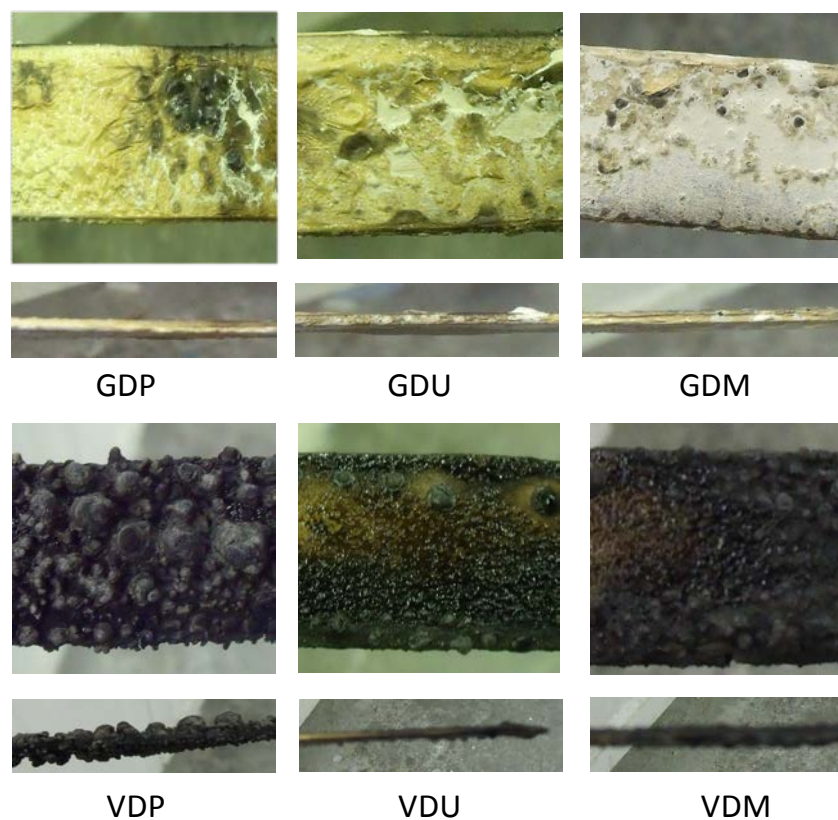
Figure 136 Images of Oil and Solvent based samples after exposure to Bunsen burner

Conversely the oil based systems appeared to show a promising level of intumescence particularly when combined with the DAP and Pentaerythritol ingredients.

5.3.2. Assessment of thermal decomposition – Thermogravimetric (TGA) analysis

Thermogravimetric analysis of all samples clearly outlined the difference in decomposition made by the resin chosen for particular samples.
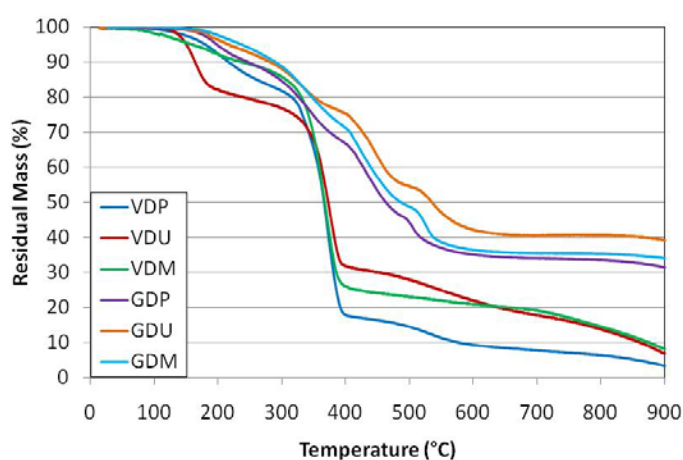
Figure 137 Decomposition curves of oil and solvent based formulations in air; ambient to 900 °C at a heating rate of 10°C min^{-1}

In air atmosphere all samples display similar decomposition rates, all beginning at approximately 200 °C however; the varnish samples have a far more rapid decomposition stage taking place just below 400 °C which is not observed in gloss samples. Gloss samples also maintain a residual mass of approximately 30-40 % due to the higher loadings of pigments and filler.
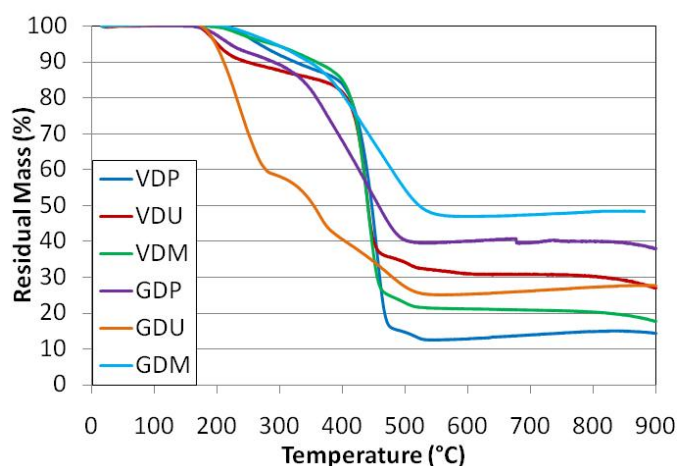
Figure 138 Decomposition curves of oil and solvent based formulations in nitrogen; ambient to 900 °C at a heating rate of 10 °C min^{-1}

TGA analysis in nitrogen separates the samples with regard to their residual mass at higher temperatures. Again the varnish samples demonstrate the lowest residual mass up to 900 °C whereas gloss samples in some cases (GDM) maintain a residual mass of almost 50 % between 550 °C and 900 °C.

Table 43 Polymer preservation analysis in air and nitrogen atmospheres – oil and solvent based samples

Sample	Residual Mass in air (%)	Residual Mass in nitrogen (%)	Amount of polymer preserved (%)
VDU	7	28	21
VDM	35	48	13
GDU	40	28	-12
GDM	7	20	13

Table 43 lists the polymer preservation observations when melamine is present in formulation. It appears that melamine acts to preserve the polymer independently of the resin system used.

5.3.3. Assessment of burning behaviour in the cone calorimeter

Figure 139 shows the unexpectedly low heat release rate measurements for the nitrocellulose reference sample this is partially explained by the issues of using oxygen depletion calorimetry

to determine the heat release rate for oxygen containing species (explained in 3.5.2.) however a lower carbon dioxide production rate is also shown in

Figure 140. This is explained by the small flame which is sustained and combusts the decomposition products at a fairly constant rate as they are produced by the heat radiating from the cone heater.
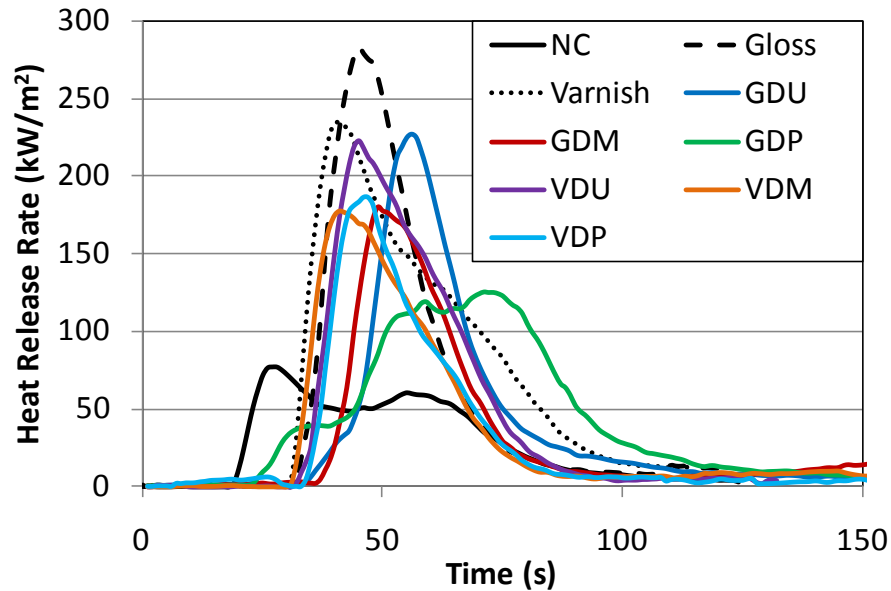
Figure 139 Heat release rate curves for oil and solvent based DAP systems

In the case of these samples there seems to be no correlation between components added and peak of heat release rate or time to ignition. These results would tell more of the interactions between components had the pentaerythritol been incorporated alongside the melamine and urea in the gloss and varnish resins.

All of the carbon dioxide production rates recorded for solvent and oil based samples have a similar peak rate of 0.25 g s^{-1} as shown in

Figure 140 with the exception of the GDP sample with a peak of only 0.17 g s^{-1}. This sample also combusts steadily with a small sustained flame as opposed to the other samples in this group which combust rapidly with large flames which are short-lived.
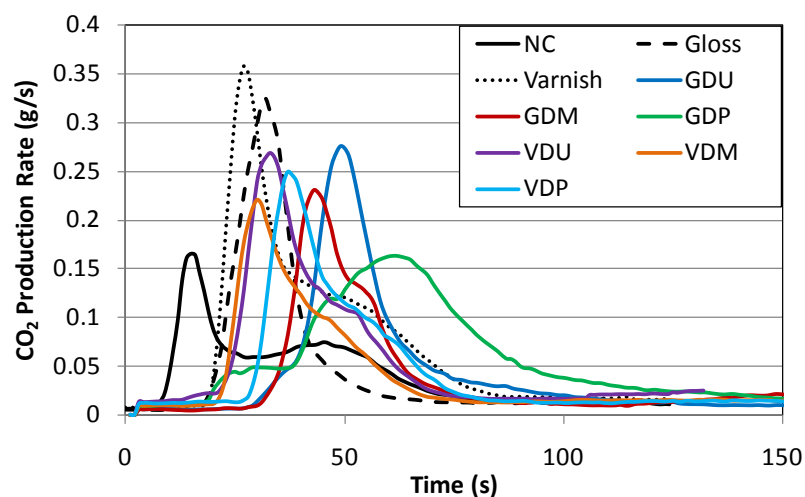
Figure 140 Carbon dioxide production rate curves for oil and solvent based DAP systems

The peak of carbon dioxide production is earlier for varnish samples (30-40 s) than for gloss specimens (45-60 s) though not significantly higher, all falling between 0.2 and 0.27 g s^{-1} this is explained by the presence of inert fillers and pigments in the gloss sample reducing the concentration of flammable materials in the gloss samples. Samples have shown ability to reduce peak heat release rate of reference base resin systems as well as increasing the time to ignition for all reference and nitrocellulose samples. Improvements are not as prominent as observed for water-based samples previously reported.

Table 44 Oil and solvent samples cone calorimeter properties

Sample	t_{ig} (s)	PHRR (kW m^{-2})	tPHRR (s)	THR (kW m^{-2})
GDU	29 ± 6	263 ± 28	52 ± 4	5751 ± 759
GDM	27 ± 5	254 ± 33	49 ± 5	4916 ± 983
GDP	28 ± 10	184 ± 13	63 ± 12	6459 ± 1607
VDU	21 ± 3	226 ± 11	43 ± 2	6048 ± 349
VDM	19 ± 2	178 ± 10	39 ± 2	3839 ± 308
VDP	25 ± 2	196 ± 39	42 ± 2	4606 ± 683

Gloss samples have a longer time to ignition as shown in Table 44. This is because gloss samples have a higher reflectivity (=1/Emissivity) and thermal conductivity, and heat is more

rapidly transferred through the coating to the substrate layer which is more insulating, causing the ignition temperature to be reached later once all of the coating layers and substrate have reached ignition temperature. This induces a higher peak heat release rate as all of the fuel in combusted simultaneously. Varnish samples have a more rapid time to ignition as the thermal conductivity is lower; heat transfer through the layer is significantly slower. A temperature gradient is formed within the thickness of the coating; the upper layers reach ignition point and ignite before the underlying layers have reached an adequate temperature for ignition. This results in a quicker time to ignition but a lower peak of heat release rate as shown in Figure 139 and Figure 140 respectively.
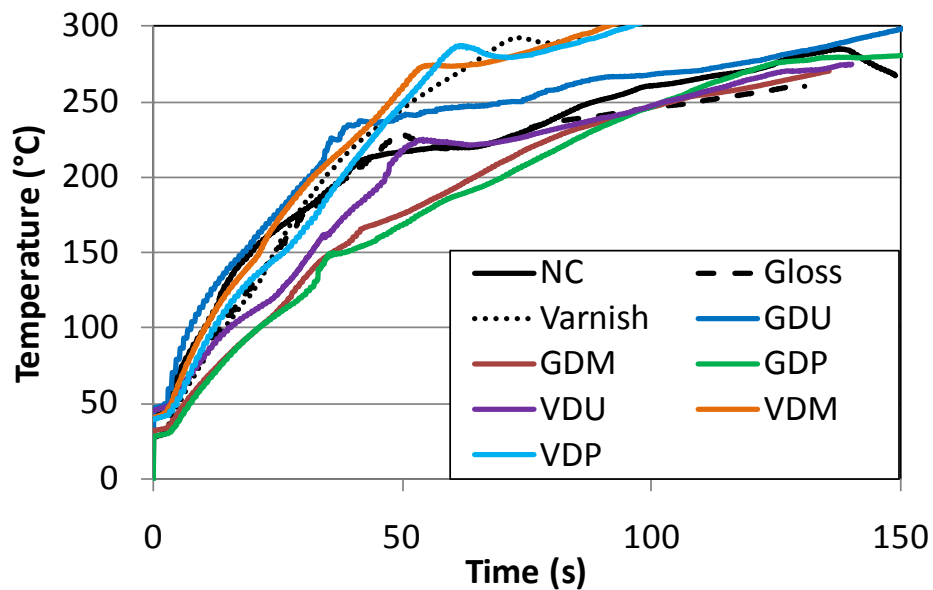
Figure 141 Thermocouple temperature profiles for oil and solvent based DAP systems

Thermocouples embedded within the cone plaque sample record the temperature profile at the coating, substrate interface. Temperature at this interface will be affected by the thermal conductivity of any coating or char above the thermocouple or heat evolved from the combustion of the coating or substrate during experimentation. The longer the temperature is maintained as low as possible the more of the substrate will be protected and the less risk is posed. Figure 141 shows that the lowest temperature was maintained for the longest time by the GDP, GDM and VDU systems.

Table 45 Residue height for oil and solvent based DAP systems, 35 kW m^{-2}

Sample	Residue height (mm) – 35 kW m^{-2}		
	Minimum	Maximum	Average
VDP	1	6	3.5
VDU	1	3	2
VDM	1	4	2.5
GDP	1	10	5.5
GDU	1	5	3
GDM	1	8	4.5

Table 45 tabulates all residue heights recorded for samples after exposure to the radiant heater in the cone calorimeter. There does not appear to be a significant variation in residue height between samples; varnish samples produce only slightly reduced average residue heights in comparison to the gloss samples. One suggestion for the increase in residue yield from cone samples in comparison to the Bunsen burner samples is the trapping of the decomposition vapours of the nitrocellulose substrate during intumescence whereas none of these gases are present during the expansion in the Bunsen burner tests and so less intumescence is observed. Another explanation could be that due to the reduced thermal conductivity of the varnish samples, top layers soften and decompose prior to the softening and decomposition of lower layers. Many of the vapours are lost prior to expansion thus expansion relies on the decomposition vapours of the lower level material only. Either that or the decomposition is so vigorous that the bubbles formed are burst due to the rapid formation of gases which cannot be contained by the resin.

5.3.3. Assessment of thermal conductivity - BS EN 367
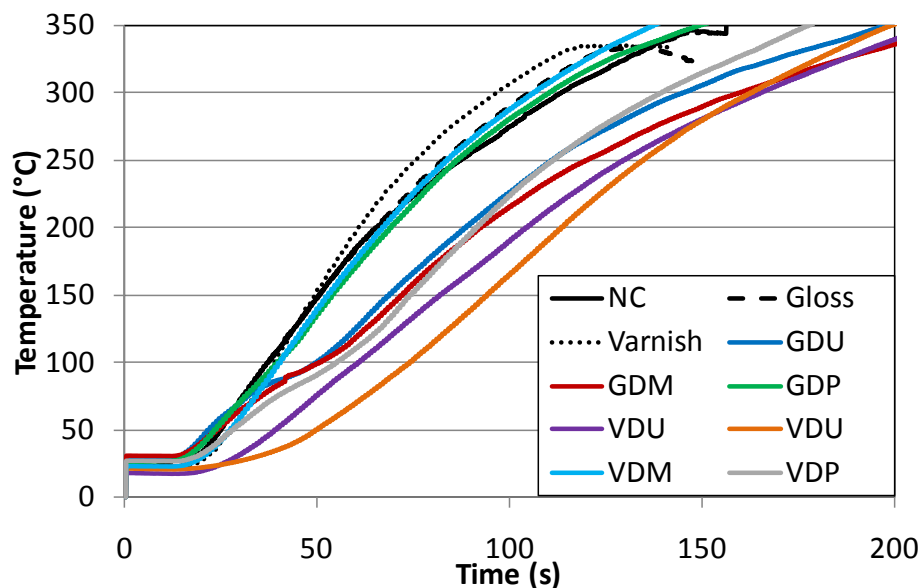
Figure 142 BS EN 367 temperature profile curves for oil and solvent based DAP systems

The graph in Figure 142 clearly shows an improvement in protection from the varnish samples when compared to the gloss. The critical time to reach 150 °C is far longer for varnish samples due to the reduced thermal conductivity of the coatings. Conversely the gloss samples displaying a higher thermal conductivity need far less time to reach the critical temperature of 150 °C. This is the opposite of results expected when considering the char heights recorded from the cone calorimeter experiments. This could be explained if the residue from gloss samples was produced at a later period in combustion, after the temperature had exceeded 150 °C. When this residue layer is compromised it leads to ignition due to the trapping of the flammable decomposition products collected after the deterioration of the nitrocellulose substrate material.

Table 46 Residue height for oil and solvent based DAP systems in the BS EN 367 experiment

Sample	Residue height (mm) – BS EN 367		
	Minimum	Maximum	Average
VDP	0	2	1
VDU	0	2	1
VDM	0	2	1
GDP	0	6	3
GDU	0	4	2
GDM	0	6	3

Residue height analysis of the BS EN 367 samples is listed in Table 46. The minimum residue height is all cases is 0 where either the bubbles were ruptured due to the rapid formation of decomposition vapours or the release of the vapours failed to coincide with the softening of the resin. The location of this reduced residue yield will affect the temperature profiles shown in Figure 142, in most cases it was at the edges of the sample plaques. However, as the residue breaks down (with extending heating) in the centre of the plaque the sample becomes more vulnerable to attack by heat, thus more rapidly increasing the temperature of the substrate material. As with the cone calorimeter samples, the greatest maximum residue height was observed for gloss samples. All varnish samples produced the same low level of residue production whereas the gloss samples are less uniform with more peaks, increasing the surface area for the heat to attack. Gloss samples yield significantly more residue when applied to the aluminium and plasterboard substrates compared to the wooden splint in the Bunsen burner analysis. This could be due to the optimised heating regime of the aluminium substrate; the trapping of the nitrocellulose decomposition products in the intumescence of the cone calorimeter samples; and the lack of drying time for Bunsen burner samples meaning a high solvent content in these samples at the time of testing.

Table 47 Time to reach 150 °C and 350 °C for oil and solvent systems in the BS EN 367 within the range 30-40 kW m^{-2}

Sample	Time to reach 150 °C (s)	Time to reach 350 °C (s)
Reference Aluminium sheet	50 ± 2	122 ± 11
GDU	51 ± 15	175 ± 21
GDM	55 ± 15	173 ± 35
GDP	55 ± 15	166 ± 18
VDU	86 ± 7	202 ± 6
VDM	65 ± 18	157 ± 19
VDP	59 ± 14	171 ± 9

Gloss samples even reduce the time to reach 150 °C (Table 47) compared to the reference aluminium sample. This suggests that flaming combustion or exothermic decomposition reactions are taking place which outweigh the improvements made by reducing the thermal conductivity of the substrate by adding the coating, overall increasing the temperature of the substrate at a faster rate than observed in the reference sample. The varnish samples greatly increase the time taken to reach 150 °C. Reduction in thermal conductivity by adding the coating coupled with endothermic decomposition reactions, increase the time taken for the substrate material to heat up.

As none of the oil and solvent based coatings performed as well as the water-based coatings in any of the analyses, they were not submitted for BS 476: Part 6 testing.

5.3.4. Prediction of performance in the BS 476: part 6 (adapted)

When analysed on steel substrates intumescent activity was interrupted and therefore no significant variation in thermal conductivity of samples could be determined. This prevented prediction of the performance in the BS 476: Part 6 (adapted) with regard to thermal conductivity. Some results were collected from the cone calorimeter and Bunsen burner experiments, and though these did not reliably produce a hierarchy within results collected from samples of the same resin type, it did outline the increase in fire protection offered by water-based, as opposed to oil or solvent based, samples.

SUMMARY

This chapter outlines the importance of stability and compatibility of components during formulation. This is a significant concern for coating developers. A very successful product loses its value if stability cannot be assured. Products with poor dispersion or coating properties do not perform as well in fire tests. Lack of dispersion causes a reduction in surface area of the active fire retardant ingredient, in turn reducing the possibility of a reaction, reducing protection. Poor coating properties, such as textured finish, increase flammability by allowing hot spots to occur promoting ignition. Lean coating areas are vulnerable to the attack of heat and the dispersion of pyrolysis products into the flame zone.

A range of fire retardant additives were investigated and screened. DAP gives optimum protection on cellulose substrates when compared to steel substrate, and APP on either cellulose or steel. Water-based systems are found to give the optimal fire protection but reduced stability. Oil and solvent based systems did not increase stability but did reduce performance. On-site mixing of a two pack system is an option to minimise the affect of instability. Vinyl resin systems are found to produce the optimal protection properties. APP and DAP produce significantly different results, but the optimum depends on the test undertaken and the flammability parameter recorded. Melamine is shown to increase the polymer retention in the condensed phase, in inert atmospheres, over urea in TGA analyses, thus maintaining a higher percentage of protective residue at higher temperatures.

Screening test methods analyse individual factors of flammability but none in isolation estimate product performance in the BS 476: Part 6, as flammability is a complex combination of many parameters some of which are test dependant.

6. CONCLUSIONS

In this thesis a new understanding of the fire protection of multilayer paint build-up using various commercial and novel fire retardant coatings has been described through analysis of thermal decomposition behaviour and fire protection screening methods. A large number of flammability test methods have been reported in the literature and by standardisation bodies however none are concerned with low activation temperature fire retardant coatings, for application over a flammable substrate (such as multilayer or nitrocellulose paint). This work has focused the development of a range of screening methods which assess relevant flammability parameters and predict fire protection performance in the standard fire tests in order to provide the tools necessary for development of such protective coatings, and to test those tools on a variety of such coatings.

Factors affecting coating performance have been investigated with regard to both test and coating variables, and evidence is presented which indicates that factors such as coating type and thickness, substrate composition, thickness and thermal properties, fire retardant mechanism, and heat flux of exposure and other fire conditions all affect the burning behaviour of paint and protective coating systems. Results reported suggest that paint and coating thickness (or area density) significantly affects burning behaviour (more prominently in non-fire retardant systems) by increasing heat release rate and shortening time to ignition. This is due to an increased amount of fuel available to support combustion, and insulating thermal properties of the substrate (multiple painted layers) preventing dissipation of heat. Applied heat flux increases heat release rates, decrease time to ignition and reduces scatter in data. A temperature range for analysis is specified which balances burn time and analysis detail with discrimination between good fire protective coatings and those requiring more development. Rheological properties reported also suggest that vinyl acetate resin systems exhibit optimum softening properties and complex viscosity behaviours for development of intumescent systems. Findings correlating to coating factors effecting protection performance are reported in CHAPTER 3. but results suggest that the most significant is the substrate to which the coating is applied.

Warrington blue board (WBB) is reported as being the substrate on which all products should be assessed as this provides a 'worst case scenario'. Although when tested this substrate falls into the 'class 4' rating of severe flame spread hazard results reported suggest it is not representative of a real multilayer paint build-up substrate in relation to adhesion and other physical and combustion properties. WBB displays good adhesion whereas multilayer paint often delaminates and de-adheres increasing the fire risk, it melts before ignition, and provides

its own oxygen for combustion! Investigation of the composition of the Warrington blue boards suggest differences depending on the fire test method to be used. Results provide strong evidence that the BS 476: Part 6 substrate is 'more flammable' displaying earlier time to ignition, greater heat release rate and total heat release rate values by virtue of a higher nitrocellulose content. It is therefore conceivable that this substrate may require a higher level of protection than it BS 476: Part 7 counterpart. Both substrates are found to contain nitrocellulose paint layers (though in differing amounts). This results in a substrate material which decomposes at 170 °C and melts at even lower temperatures providing a molten, highly flammable and vigorously burning material for protection. Decomposition vapours require only the presence of a spark to ensure ignition as the structure contains nitro groups which decompose to release molecular oxygen and nitrogen gas (N_2); leaving reactive oxygen available for the combustion of hydrocarbons into carbon dioxide and water without the need for oxygen to diffuse in from the atmosphere. This also leads to problems measuring the heat release rate using oxygen depletion calorimetry; the methods employed by the cone calorimeter. Components of both boards were analysed and results suggest that there is no interaction between components. However, decomposition is a function of the individual layered components, and not as a bulk material due to the temperature gradients occurring during thermal decomposition.

A range of additives have been screened and intumescent coatings have been suggested as the favourable method of protection for such flammable substrates. The thermal conductivity of the coating is reduced following swelling, inhibiting the transfer of heat from and diffusion of gases into, the combustion zone. Halogenated systems also provide efficient fire retardant coatings, but fail when used as thin film coatings when the amount of halogens present is insufficient to protect the bulk present in a polymer or thicker flammable substrate - as with the Warrington blue board. Halogenated systems also produce toxic and corrosive combustion products and large quantities of smoke which could add to the fire hazard by hindering escape.

Characterisation and flammability testing of existing formulations shows that though ammonia polyphosphate (APP) compositions provide a good level of intumescent protection with a well structured char, the activation temperature is too high for protection of paint build-up. Timber product fire retardant systems display lower activation temperatures due to the incorporation of diammonium phosphate (DAP) into the formulation.

Magma Prime (clear) displays excellent results in the screening test methods however it fails to provide protection in the BS 476: Part 6 test method. This is most likely due to the heating regime used, and the volume of the residue pulling it off the substrate material when in a

vertical orientation. Characterisation was carried out with some success, and replication of the formulation lead to some interesting advancements in formulation, although stability in the can remained a problem. Formulations can be optimised for specific heating regimes and this should be investigated further should this work continue.

Novel formulations were developed. Diammonium phosphate was investigated as an alternative low temperature intumescent additive, though results suggest that optimum performance was gained when assessed directly after mixing due to the stability and compatibility problems reported. These leave DAP undispersed in these formulations. Solutions include on-site mixing, emulsification or microencapsulation of the DAP. Various resin systems have been utilised (vinyl silk, vinyl resin and Wickes vinyl emulsion) to investigate compatibility. Results show that vinyl silk formulations exhibit the lowest heat release rate and longest time to ignition in the cone calorimeter, but this is most likely due to the higher level of inert fillers and pigments present, which if incorporated into the vinyl resin, would improve the protection provided by these formulations too. Protection is not so evident in the thermal conductivity analyses, as samples fail to intumesce in the BS EN 367 apparatus. This may be due to orientation, or heating of the sample, but is most likely due to the properties of the substrate material. The biggest limitation of these coatings is that intumescent barriers are made up of singular large voids which deflate once ruptured, leaving the substrate exposed. Research should continue to develop residues with more, smaller voids, to produce a more stable char that will protect to higher temperatures.

Melamine is shown to improve the retention of polymer residue in the condensed phase, compared to urea, or in the absence of both. Thermal decomposition, investigated using thermogravimetric (TGA) analyses, show an increase in residue in melamine containing species, over and above the melamine loading itself.

Oil and solvent based systems were investigated as a potential alternative to the unstable water-based systems described. These proved particularly vulnerable to incompatibility, due to interactions within the formulation. Results show that though the coatings are able to reduce peak heat release rates and delay the ignition times of reference samples (base resin and nitrocellulose) the improvement is not as prominent as observed with the water-based systems, and coating stability is not improved.

Though the screening test methods developed in this work provide a good indication of individual parameters of product performance (such as time to ignition, heat release rate, level of intumescence and thermal conductivity), the complexity of the combination of all of these factors means that no single method can accurately predict the performance in the BS 476:

Part 6 standard test method in isolation. Methods are able to distinguish between systems with varying fire retardant mechanisms and amount of intumescence, but remain relatively crude; lacking the detail required distinguishing between coatings offering a similar level of protection. However, the screening methods do provide more information on the level of protection provided prior to assessment in an expensive certified test, and are therefore a valuable tool for the development of novel formulations. Levels of intumescence are most clearly observed during exposure to the Bunsen burner flame, while intumescent action is minimised on the aluminium substrate used in the BS EN 367, thus underestimating thermal protection by the coatings. Contribution of the coating to the fire load is assessed using the cone calorimeter and thermal conductivity of the coating is primarily assessed using analysis of the thermocouple temperature profiles at the substrate-coatings interface within cone calorimeter samples.

6.1. Future Work

Availability of standard resins and knowledge of more coatings formulation chemistry is an essential component for future work. Investigation of rheological properties of a wider range of resin systems would quantify characteristics such as softening temperature and flow properties. This was not feasible during this work due to the unavailability of materials and equipment, until near the end of this programme. Analysis of this kind allows selection of a resin which remains solid, but softens before the spumific component of the intumescent formulation evolves gas (around 100-150 °C for DAP) while maintaining adhesion to the Warrington blue board substrate and trapping decomposition products from the substrate and coating as intumescence occurs around 170-200 °C. The foamed resin should then stiffen maintaining the multi-cellular structure and remain stable to higher temperatures without yielding under its own weight. Properties such as dispersion of additives, flow and coating stability may also be assessed using various rheological methods, using the same apparatus.

Further development of formulations should consider the use of different intumescent additives, char stabilisers (such as fibres) and fire retardants such as nesquehonite. Nesquehonite, $Mg(HCO_3)(OH) \cdot 2H_2O$ or $MgCO_3 \cdot 3H_2O$, can be easily synthesised using various methods outlined by Kloprogge et el. [123] and Ferrini et el. [124] and has an onset of decomposition temperature of 70-100 °C. Decomposition occurs via endothermic reactions evolving water which are important properties of a fire retardant additive making it worthy of further investigation for use in this particular application.

Optical and SEM images of the residues would also give information of the structure of the residual char and this could be correlated to performance in the fire tests as well as aiding

development of multi-cellular foam structures rather than the brittle, large void structures seen in this work.

As previously mentioned diammonium phosphate (DAP) stability in the can is a major issue in the formulations discussed in this work. Therefore future work should consider new systems or methods of incorporation that reduce such adverse interactions. This may include on-site mixing of two pack products or microencapsulation of the specific additive in question.

REFERENCES

[1] Eagar, T. W. and Musso, C. (2001) Why did the World Trade Centre Collapse? Science, Engineering and Speculation. Journal of Operations Management. Vol. 53. Issue 12. pp. 8-11.

[2] Lake, P. (1999) Paint Finishes - Flaming Hazard? The Journal of the Institute of Maintenance and Building Management.

[3] UK Fire Statistics 2007. Accessed at
http://www.communities.gov.uk/fire/researchandstatistics/firestatistics/firestatisticsuk/

[4] Pickard, R. W. (1954) The Fire Hazard of Surface Coatings. Paint Journal. pp. 426-430.

[5] Rawlings, P. (1995) Paint Flammability. Fire Engineers Journal. pp. 31-35.

[6] Approved Document B, Volume 2: Buildings Other Than Dwelling Houses. The Building Regulations 2000 Fire Safety. (2007) RISA Publishers, London.

[7] Regulatory Reform, England and Wales. The Regulatory Reform (Fire Safety) Order 2005. Statutory Instruments. No 1541. Accessed at
http://www.legislation.gov.uk/uksi/2005/1541/pdfs/uksi_20051541_en.pdf on 03/05/2011.

[8] Buszard, D. L. (1998) The Role of Fire Retardants in Reducing Fire Hazards. In Flame Retardants '98. pp. 45-54, Interscience Communications, London.

[9] DeHaan, J. D. (2007) Kirk's Fire Investigation. 6th Edition. Pearson Prentice Hall. New Jersey.

[10] Staggs, J.E.J. and Phylaktou, H.N. (2008) The effects of emissivity on the performance of steel in furnace tests. Fire Safety Journal. Vol. 43 pp. 1-10.

[11] Berdahl, P. (1995) Pigments to reflect the infrared radiation from fire. Journal of Heat Transfer. American society of Chemical engineers. Vol. 117 pp. 335-338.

[12] Athey, R. J. Jr. and Shaw, P. A. (1999) The Problem with Fire. European Coatings Journal Vol. 10. pp. 68-74.

[13] Author Unknown. (2005) Covering Hospital Safety. Wilmington Publishing Ltd. ProQuest Information and learning company. Accessed at
http://findarticles.com/p/articles/mi_qa4028/is/ai_n13511236/?tag=content;coll.

[14] Lyons, J. W. (1970) The Chemistry and Uses of fire-retardants. John Wiley & Sons, Inc, London.

[15] Xing, W.Y., Song, L., Hu, Y., Lv, X. and Wang, X. (2010) Combustion and thermal behaviours of the novel UV-cured intumescent flame retardant coatings containing phosphorus and nitrogen. E-Polymers. Accessed at http://e-polymers.org

[16] Madorsky, S. L. (1964) Thermal Degradation of Organic Polymers. Interscience, New York.

[17] Allen, N.S and Edge, M. (1992) Chapter 1: Polymer structure and stability. Fundamentals of Polymer Degradation and Stabilisation. Elsevier Applied Science, Cambridge.

[18] Martin, S. R. W., and Tawn, A. R. H. (1962) The Chemistry of Resin Formation and Resin Properties. In The Science of Surface Coatings. Ernest Benn Limited, London

[19] Paul, S. (1996) Surface Coatings, Science & Technology. Second Edition. John Wiley & sons, Chichester.

[20] Hirschler, M. M. (2008) Chemical Aspects of Thermal Decomposition of Polymeric Materials. In Fire Retardancy of Polymeric Materials. Edited by Grand, A. F., and Wilkie, C. A. Marcel Dekker Inc, New York.

[21] Bentley, J. and Turner, G. P. A. (1967) Chapter Fourteen: Epoxy Coatings. In Introduction to Paint Chemistry. Chapman and Hall Ltd., London.

[22] Epoxy resin curing process. Last accessed 12-09-2011 at http://pslc.ws/macrog/lab/images/image23.gif

[23] Deanin, R. D. (1972) Chemical Composition. In Polymer Structure, Properties & Applications. Cahners Publishing Company, Inc., USA.

[24] Luda, M. P., Balabanovich, A. I., and Camino, G. (2002) Thermal Decomposition of Fire Retardant Brominated Epoxy Resins. Journal of Analytical and Applied Pyrolysis. Vol. 65. Issue 1. pp. 25-40.

[25] Erickson, K. L. (2007) Thermal Decomposition Mechanisms Common to Polyurethane, Epoxy, Poly(Diallyl Phthalate), Polycarbonate and Poly(Phenylene Sulfide). Journal of Thermal Analysis and Calorimetry. Vol. 89. Issue. 2, pp. 427-440.

[26] Ebdon, J. R., and Ebdon, P. J. (2008) Recent developments in flame-retarding thermoplastics and thermosets. In Fire Retardant Materials. Edited by A. R. Horrocks and D. Price. Woodhead Publishing Limited., Cambridge.

[27] Thiele, L. and Becker, R. (1993) Catalytic Mechanism of Polyurethane Formation. In Advances in Urethane Science and Technology: Science & Technology. Edited by K. C. Frisch and D. Klemper. CRC Press, USA.

[28] Hull, T.R. Chapter 11. Challenges in fire testing: reaction to fire tests and assessment of fire toxicity. Edited by A. R. Horrocks, and D. Price. Woodhead Publishing Ltd, Cambridge, UK.

[29] BS 476: Part 6: 1989. Fire tests on building materials and structures – Part 6: Method of test for fire propagation for products.

[30] BS 476: Part 7: 1997. Fire tests on building materials and structures – Part 7: Method of test to determine the classification of the surface spread of flame of products.

[31] Hull, T. R. and Stec, A. A. (2009) Introduction - Polymers and Fire. In Fire Retardancy of Polymers: New Strategies and Mechanisms. Edited by T.R Hull and B. K Kandola. RSC Publishing, Cambridge.

[32] Pal, G. and Mackasy, R. (1991) Plastics: Their behaviour if fires. Elsevier, New York.

[33] Zhang, H. (2004) Fire-Safe Polymers and Polymer Composites. US Department Of Transport. Report Number: DOT/FAA/AR-04/11. Federal Aviation Administration.

[34] Aoutid, F., Bonnaud, L., Alexandre, M., Lopez-Cuesta, J.-M. and Dubois, P.H. (2009) New prospects in flames retardant materials: From fundamentals to nanocomposites. Materials Science and Engineering. Vol. 63. pp. 100-125.

[35] Drysdale, D. (1998) An Introduction to Fire Dynamics. Second Edition. John Wiley & Sons, Colchester, UK.

[36] Quintiere, J. G. (1998) Principles of Fire Behaviour. Delmar Publishers, USA.

[37] Nelson, M. I. and Brindley, J. (1999) Polymer Combustion: Effects of Flame Emissivity. Philosophical Transactions: Mathematical, Physical and Engineering Sciences. Vol. 357. No. 1764. pp. 3655-3673. The Royal Society.

[38] Babrauskas, V. (2000) Fire Test Methods for Evaluation of Fire-Retardant Efficacy in Polymeric materials. Chapter 3. In Grand, A. F and Wilkie, C. A, Fire Retardancy of Polymeric Materials. CRC Press, New York, USA.

[39] Unpublished work. Lindhol, J. Brink. A. and Hupa, M. Cone calorimeter – A tool for measuring heat release rate. Accessed at
http://www.tut.fi/units/me/ener/IFRF/FinSweFlameDays09/4B/LindholmPaper.pdf

[40] Friedman, R., Friedman. J. and Linville, L. (2003) Principles of Fire Protection Chemistry and Physics: Part II – Fire Protection Chemistry and Physics. Chapter 10 – Fire Characteristics: Solid Combustibles. 3rd Ed. Jones and Bartlett Publishers, London, UK.

[41] Babrauskas, V and Peacock, R. D. (1992) Heat Release Rate: The Single Most Important Variable in Fire Hazard. Fire Safety Journal. Vol. 18, Issue 3. pp. 255-272.

[42] Schartel, B and Hull T. R. (2007) Development of fire-retarded materials – Interpretation of cone calorimeter data. Fire and Materials. Vol. 31 Issue 5. pp. 327-354.

[43] Huggett, C. (1980) Estimation of Rate of Heat Release by Means of Oxygen Consumption Measurements. Fire and Materials. Vol. 4. pp. 61-65.

[44] Karlsson, B and Quintiere, J.G (2000) Enclosure Fire Dynamics. 2nd Ed. John Wiley & Sons, Colchester, UK.

[45] ISO 5560-1:1993. Fire Tests on Building Materials and Structures. Part 15 – Method for Measuring the rate of Heat Release of Products.

[46] Carpenter, K. and Janssens, M. (2005) Using Heat Release Rate to Assess Combustibility of Building Products in the Cone Calorimeter. Fire Technology. Vol. 41, No. 2 pp.79-92.

[47] Staggs, J.E.J. (2009) Convection heat transfer in the cone calorimeter. Fire Safety Journal. Vol. 44. pp. 469-474.

[48] ENV 13381-4. (2002). Test Methods for Determining the Contribution of the Fire Resistance of Structural members – Part 4: Applied Protection to Steel Members. European Committee for Standardisation (CEN): Brussels.

[49] Ellis, W. (1995) ASTM Method D 1360. Chapter 56 – Testing Coatings for Heat Resistance and Flame Retardance. Paint and Coatings Testing Manual. Koleske, J. V Ed. Fourteenth Edition of the Gardner-Sward Handbook. American Society for Testing and Materials, Philadelphia.

[50] Bartholmai, M., Schriver, R. and Schartel, B. (2003) Influence of external heat flux and coatings thickness on the thermal insulation properties of two different intumescent coatings using cone calorimeter and numerical analysis. Fire and Materials. Vol. 27 pp. 151-162. John Wiley and Sons, Chichester.

[51] Omrane, A., Wang, Y. C., Goransson, U., Holstedt, G. and Alden, M. (2007) Intumescent coating surface temperature measurement in a cone calorimeter using laser-induced phosphorescence. Fire Safety Journal. Vol. 42 pp. 68-74. Elsevier Ltd, Cambridge.

[52] Engineering Fundamentals, general properties of steel. Last access at
http://www.efunda.com/materials/alloys/alloy_home/steel_properties.cfm

[53] Purkiss, S. A. (2007) Fire Safety Engineering: design of structures. Elsevier/Butterworth-Heinemann, Oxford.

[54] Jimenez, M., Duquesne, S. and Bourbigot, S. (2006) High throughput fire testing for intumescent coatings. Industrial & Engineering Chemistry Research. Vol. 45. Issue 22. pp.7475-7481. American Chemical Society, London.

[55] ISO 5658-2:2006. Reaction to Fire Tests – Spread of Flame. Part 2 – Lateral Spread on Building and Transport Products in Vertical Configuration.

[56] BS EN 13823:2002 Reaction to fire tests for building products – Building products excluding floorings exposed to the thermal attack by a single burning item.

[57] Van Hees, P. and Axelsson, J. (2007) Chapter 12: Modelling of Euroclass Test Results by Means of the Cone Calorimeter. In Multifunctional Barriers for Flexible Structure. Springer Series in materials Science, New York. pp. 215-226.

[58] Accessed at www.insulation.kingspan.com/uk/Euroclass.pdf on 10/04/2011.

[59] Troitzsch, J. (2004) Section 10.4 – European Union. Plastics flammability handbook: principles, regulations, testing and approval. 3rd Edition. Hanser, Munich. pp. 275.

[60] Price, D., Cunliffe, L.K., Bullet. K.L., Hull, T. R., Milnes, G. J., Ebdon, J. R., Hunt, B. J. and Joseph, P. (2007) Thermal Behaviour of Covalently Bonded Phosphate and Phosphonate Flame Retardant Polystyrene Systems. Polymer Degradation and Stability. Vol. 92. pp 1101-1114.

[61] Sargent, P. (1998) Multi-Layer Paint: The Fire Problem. Pigment & Resin Technology. Vol. 27. No. 6. pp.361-363.

[62] Thomas, P.H. and Bullen, M. L. (1979) On the role of KρC of room lining materials in the growth of room fires. Fire and Materials. Vol. 3. Issue 2. pp. 68-73.

[63] Murrell, J. and Rawling, P. (1995) Fire Hazard of Multi-Layer Paint Surfaces. Proceedings of the International Fire and Materials Conference. pp. 329-338.

[64] Mower, F. W. (2001) The Effect of "Blistering" on the Ignition and Flammability of Painted Gypsum Wallboard. Building and Fire Research Laboratory of the National Institute of Standards and Technology. pp. 1-12.

[65] BS3900 part E6. (2009) Cross Hatch Adhesion Test. BS3900 part E6.

[66] Muncaster, R. (1981) Thermal A-Level Physics. pp. 204-243. Stanley Thornes Ltd, Cheltenham.

[67] Lienhard, J.H. IV and Lienhard, J.H. V. (2011) A Heat Transfer Textbook. 4th edition. Prentice –Hall, Englewood Cliffs.

[68] Rabash, D., Ramachandran, G., Kandola, B., Watts. J. and Law. M. (2004) Circumstances Favourable to Rapid fire spread. In Evaluation of fire safety. pp.106. John Wiley and Son, Chichester.

[69] Ohlemiller, T. and Shield, J. One- and Two-Sided Burning of Thermally Thin Materials. Fire and Materials (1993) Vol. 17. pp.103-110.

[70] Shaw, R. J. (1989) The use of flame-retardant coatings on walls and ceilings. Journal of the Oil and Colour Chemists Association. Vol. 72 pp. 176-180.

[71] Whittingstall, P. Paint Evaluation Using Rheology. Accessed online at: www.tainst.com on 7th July 2011.

[72] Franck, A.J. (2011) Paints and Coatings. Accessed at www.tainst.com

[73] Franck, A.J. (2011) Understanding Rheology of Structured Fluids. Accessed at www.tainst.com

[74] Mezger, T. G. (2006) The Rheology Handbook. 2nd Edition. Vincentz Network, Hannover.

[75] Warrington Fire, State of the art report. Fire Hazard of Multi-Layer Paint surfaces. pp.1-41.

[76] Tarran-Jones, M. (1986) Tests show paint plays a major role in rate of flame spread. FIRE, Vol. 39.

[77] Goldsmith, N. Residential Flats 53-66 Chelsea Gardens London SW1 (2007) London Fire Brigade Fire Investigation Group New Cross. pp. 1-19.

[78] Author Unknown. Flammability of Paint Films. (1992) 'Dear Chief Officer'

[79] Stauffer, E., Dolan, J.A. and Newman, R. (2008) Chapter 12: Interpretation of Ignitable Liquid Residues Extracted from Fire Debris. Materials constituting Substrates: Wall Coverings. Fire Debris Analysis. London. pp. 449.

[80] Williams, A. (1981) Fire at a Nurses Home, Victoria Hospital, Kirkcaldy, Fife.

[81] Morgan, P. (1994) Multiple Layer Paint Fire if Flats in Kings Norton. (FSIS REF 22/94) Building Research Establishment.

[82] Author Unknown. Shropshire House, Capper Street WC1. 9th September 1994. London Fire Brigade: Fires of Special Interest.

[83] Marshal, F. (2000) Sub article 9. Fire Safety: Construction and Operation of Local Detention Facilities.

[84] Arnold, J. Large Building Fires and Subsequent Code Changes (2005). Clark County Department of Development Services Building Division. pp. 13.

[85] McFee, W. (1949) The Peculiar Fate of the Morrow Castle Penguin Books, New York. pp. 344.

[86] Cochran, J. (2003) Lessons not learned: Life Safety issues from The Cocoanut Grove to The Station...

[87] Warrington Fire Ltd. Fire Hazard of Multi-layer Paint surfaces. Summary Report. WARRES NO. 61216.

[88] Mehaffey, J. R. (1987) Flammability of building Materials and Fire Growth. Designing for Fire Safety: The Science and its Application to Building Codes.

[89] Vandersall, H.L. (1971) Intumescent coating systems, their development and chemistry. Fire Flammability. Vol. 2. pp. 97-140.

[90] Le Bras, M., Camino, G., Bourbigot, S. and Delobel, R. (1988) Fire Retardancy of Polymers the Use of Intumescence. Special Publication 224. The Royal Society of Chemistry, Cambridge.

[91] Wang, D.Y., Liu, Y., Wang, Y.Z., Artiles, C.P., Hull, T.R. and Price, D. (2007) Fire retardancy of a reactively extruded intumescent flame retardant polyethylene system enhanced by metal chelates. Polymer Degradation and Stability. Vol. 92 pp. 1592-1598.

[92] Harmathy, T.Z. and Stanzak, W.W. (1970) Elevated Temperature Tensile and Creep Properties of Some Structural and Pre-stressing Steels. Special Technical Publication 464 on Fire Testing Performance. American Society for Testing and Materials, Philadelphia. pp. 186-208.

[93] Cote, A.E. and Linville, J.L. (1986) Fire Protection Handbook 16th Edition. Fire Safety in Building Design and Construction. National Fire Protection Association: Quincy. pp. 7-108.

[94] Shelton, J. A. and Brook, M. G. (1984) Tailored Polymers: Intumescent Coatings. Materials and Design. Vol. 5. Elseiver, Cambridge.

[95] Pappa, A. A., Tzamtzis, N.E., Statheropoulos, M.K., Liodakis, S.E and Parissakis, G. K. (1995) A comparative study of the effects of fire retardants on the pyrolysis of cellulose and Pinus halepensis pine-needles. Journal of Analytical and Applied Pyrolysis. pp. 3185-100.

[96] Agueda, A., Pastor, E. and Planas, E. (2008) Different scales for studying the effectiveness of long-term forest fire retardants. Progress in Energy and Combustion Science. Vol. 34 pp. 782-796.

[97] Vroman, I., Giraud, S., Salaun, F and Bourbigot, S. (2010) Polypropylene fabrics padded with microencapsulated ammonium phosphate: Effect of the shell structure on the thermal stability and fire performance. Polymer Degradation and Stability Vol. 95 pp. 1716-1720.

[98] Grexa, O., Horvathova, E., Besinova, O and Lehocky, P. (1999) Flame retardant treated plywood. Polymer Degradation and Stability. Vol. 64 pp. 529-533.

[99] Hamdani, S., Longuet, C., Perrin D., Lopez-cuesta, J-M and Ganachaud, F. (2009) Flame Retardancy of silicone-based materials. Polymer Degradation and Stability. Vol. 94 pp. 465-495.

[100] Pape, P.G. and Romenesko, D.J. (1997) The role of silicone powders in reducing the heat release rate and evolution of smoke in flame retardant thermoplastics. Journal of Vinyl Additition Technology Vol. 3 pp. 225–32.

[101] Schmauks, G., Friede, B., Schreiner, H. And Roszinski, J. O. (2009) Amorphous Silicon Dioxide as Additive to Improve the Fire Retardancy of Polyamides. In Fire Retardancy of Polymers New Strategies and Mechanisms. pp. 35-48. Edited by T.R. Hull and B.K. Kandola. Royal Society of Chemistry, Cambridge.

[102] Gardelle, B., Duquesne, S., Vu, C., and Bourbigot, S. (2011) Thermal Degradation and Fire Performance of Polysilazane-based Coatings. Thermochimica, Acta. Vol. 519. Issue 1-2. pp. 1-10.

[103] Green, J. (2006) Fire-Retardants/Fire resistive Coatings. In coatings Technology handbook. CRC Press, USA.

[104] Ashton, H. C. (2005) Fire retardants. In functional Fillers for Plastics (Xanthos, M. Ed) Wiley-VCH Verlag GmbH & co KGaA. pp. 285-315.

[105] Horacek, H. and Grabner, R. (1996) Advantages of flame retardants based on nitrogen compounds. Polymer Degradation and Stability. Vol. 54 pp. 205-215.

[106] Hollingbery, L. A. and Hull, T. R. (2010) The fire retardant behaviour of huntite and hydromagnesite – A review. Polymer Degradation and Stability. Vol. 95. pp. 2213-2225.

[107] Rothon, R. N. (2003) Effects of particulate fillers on flame retardant properties of composites. In: Rothon RN, editor. Particulate filled polymer composites. Shrewsbury: Rapra Technology Ltd. pp. 263-302.

[108] Hull, T.R., Witkowski. A. and Hollingbery. L. (2011) Fire retardant action of mineral fillers. Polymer Degradation and Stability. Vol . 96. Issue 8. pp. 1462-1469.

[109] Whitford, M. J. (1992) Getting rid of Graffiti: A Practical Guide to Graffiti removal and Anti-Graffiti Protection. E & FN, London.

[110] Deanin, R. D. (1972) Commercial Polymers: Their Properties and Applications. pp. 454.

[111] Duquesnce, S., Magnet, S., Jama, C. and Delobel. R. (2004) Intumescent paints: fire protective coatings for metallic substrates. Surface and Coatings Technology 180-181. pp. 302-307.

[112] Malucelli, G., Han, Z., Fina, A. and G. Camino. (2010) Intumescent coating for the protection of steel structures: State of the art perspectives. European Coatings Conference, Berlin.

[113] Patel, P. PhD Thesis: Investigation of the Fire Behaviour of PEEK-based Polymers and Compounds. pp. 45.

[114] BS EN 367: 1992. Protective clothing – Protection against heat and flames – Test Method: Determination of the heat transmission on exposure to flame.

[115] Parker, W.J. (1985) Calculations of the heat release rate by oxygen consumption for various applications. Journal of Fire Sciences. Vol. 2 pp. 380-395.

[116] Biteau, H., Steinhaus, T., Schemel, C., Simeoni, A., Marlair, G., Bal, N. and Torero. J.L. (2008) Calculation Methods for the Heat Release Rate of Materials of Unknown Composition. International Association for Fire Safety Science, BRE.

[117] Abe, T., Tobisawa, S. and Nomura, Y. (1958) Studies of the Thermal Decomposition of Cellulose Nitrate by Means of the Recording Thermal Balance. Department of Chemistry Defense Academy. Vol. 31. No 9. pp. 1041-1044.

[118] Dauerman, L. and Tajikm, Y.A. Thermal Decomposition and Combustion of Nitrocellulose. American Institute of Aeronautics and Astronautics Journal. Vol. 6. No 8. pp. 1468.

[119] Huwei, L. and Ruonong, F. (1988) Studies on Thermal Decomposition of Nitrocellulose by Pyrolysis-Gas Chromatography. Journal of Analytical and Applied Pyrolysis. Vol. 14. Issue 2-3. pp. 163-169.

[120] Warrington Fire Ltd. Code of Practice – Refurbishment of Communal Buildings and The Fire Risk of Multilayer Paints. October 2005.

[121] Suardana, N. P. G., Ku, M.S. and Lim, J.K. (2011) Effects of diammonium phosphate on the flammability and mechanical properties of bio-composites. Materials and Design. pp. 1990-1999

[122] Chapple, S. and Ansndjiwala, R. (2010) Flammability of natural fibre-reinforced composites and strategies for fire retardancy.: A review. Journal of Thermoplastic Composite Materials. Vol.23. pp. 871-893

[123] Kloprogge, J.T., Martens, W. N., Nothdurft, L., Duong, L.V. and Webb, G.E. (2003) Low temperature synthesis and characterisation of nesquehonite. Journal of Materials Science Letters. Vol. 22 pp. 825-829.

[124] Ferrini, V., De Vito, C. and Mignardi, S. (2009) Synthesis of nesquehonite by reaction of gaseous CO_2 with Mg chloride solution: Its potential role in the sequestration of carbon dioxide. Journal of Hazardous Materials. Vol. 168 pp. 832-837.